Determination of antibiotic susceptibility of the bacteria causing urinary tract infections using a novel lab-on-a-chip design

Benjamin Crane

2022

Determination of antibiotic susceptibility of the bacteria causing urinary tract infections using a novel lab-on-a-chip design

A thesis submitted in partial fulfilment of the requirements of Manchester Metropolitan University for the degree of Doctor of Philosophy

Benjamin Crane

Faculty of Science and Engineering

2022

Abstract

Urinary tract infections (UTIs) are one of the most common types of bacterial infection in the UK, and also are expensive to treat costing the National Health Service ~£54 million between 2016 and 2017. Culture-based antibiotic susceptibility testing (AST) is used to identify an antibiotic to treat drug-resistant urinary tract infections and takes 48 hours to complete. Faster prescription of effective antibiotics should reduce the risk of sepsis and poor clinical outcomes. To address this need, we developed a Lab-on-a-Chip (LOC) based method to conduct electrochemical AST using screen-printed macroelectrodes (SPEs) and antibiotic-loaded hydrogels. SPEs were fabricated using carbon-graphite based inks, with resazurin bulk modified SPEs (R-SPEs) being fabricated through modification of the SPEs WE. Polyvinyl alcohol (PVA) based hydrogels were loaded with the following antibiotics were used; cephalexin, ceftriaxone, colistin, gentamicin, piperacillin, trimethoprim and vancomycin as well as an antibiotic-free control. LOC devices were then designed to encapsulate both the R-SPEs and the antibiotic hydrogels to enable multiplexed electrochemical AST to occur on a single device.

In the initial testing of the R-SPEs and the antibiotic hydrogels independently of a LOC device, antibiotic susceptibility could be determined in 90 minutes for *E. coli*. After the preliminary work, eight chambered LOC devices were spiked with simulated UTI samples. Each chamber contained an R-SPE and an antibiotic hydrogel. After an incubation step, susceptibility of *Escherichia coli* and *Klebsiella pneumoniae* could be established in 85 minutes of testing which is significantly faster than the 48 hours required for conventional culture-based AST.

The sensitive detection of resazurin afforded by using the electrochemical detection methodology incorporated onto a LOC device described here offers an inexpensive and simple method for the determination of antibiotic susceptibility that is faster than using a culture-based approach.

Declaration

No part of this project has been submitted in support of an application for any other degree or qualification at this or any other institute of learning. Apart from those parts of the project containing citations to the work of others, this project is my own unaided work. This work has been carried out in accordance with the Manchester Metropolitan University research ethics procedures and has received ethical approval number (2021-1838-29007).

Signed:

Date:

Acknowledgements

I would like to sincerely thank all of my supervisory team, Dr Kirsty Shaw, Dr Patricia Linton, Dr Mamun Rashid, Dr Alex Iles and Prof. Craig Bank for their help and insight during PhD project.

I would like to thank Samuel Rowley-Neale for his help in teaching me the fundamentals of electrochemistry. As well as thanks to Jack Hughes and Dr Alejandro Garcia-Miranda Ferrari for producing all the SPEs and R-SPEs used in the project as well as for helping design the second-generation R-SPEs.

I would also like to thank the Manchester Metropolitan University technical staff for their help over the past few years.

Lastly, I would like to thank my fellow postgraduate researchers and my friends and family for their support during my PhD studies.

Abbreviations

A. baumannii – Acinetobacter baumannii

Ag-SPEs – Ag|AgCl referenced screen-printed macroelectrodes

AST – Antibiotic susceptibility testing

ATCC – American type culture collection

BSES – Buffered supporting electrolyte solution

B. pseudomallei – Burkholderia pseudomallei

C. albicans – Candida albicans

C-SPEs – Carbon-graphite referenced screen-printed macroelectrodes

CE – Counter electrode

C. freundii – Citrobacter freundii

E. faecalis – Enterococcus faecalis

E. coli – Escherichia coli

Ep – Electrochemical reduction or oxidation peak position

GC – Glassy carbon

Ip – Electrochemical reduction or oxidation peak height

Ipc – Cathodic electrochemical reduction peak height

K. pneumoniae – Klebsiella pneumoniae

LOC – Lab-on-a-Chip

MRSA – Methicillin resistant *Staphylococcus aureus*

MDR – Multidrug-resistant

NCTC – National Collection of Type Cultures

NHS – National Health Service

NADH – Nicotinamide adenine dinucleotide

OD – Optical density

OM – Outer membrane

ONC – Overnight culture

PBS – Phosphate buffered saline

P. mirabilis - Proteus mirabilis

P. aeruginosa – Pseudomonas aeruginosa

PVA – polyvinyl alcohol

RE – Reference electrode

R-SPEs - Resazurin bulk modified screen-printed macroelectrodes

S. typhimurium – Salmonella typhimurium

S. gallinarum – Salmonella gallinarum

SDC – Sample drop coverage

S. aureus –Staphylococcus aureus

S. saprophyticus – Staphylococcus saprophyticus

S. haemolyticus – Staphylococcus haemolyticus

UV – Ultraviolet

w/v – Weight by volume ratio

WE – Working electrode

Contents

Contents

1. Chapter 1: Literature Review

A systematic review was conducted as part of this thesis chapter entitled 'Lab on a Chip devices for Urinary Tract Infection diagnostics' and submitted to the Journal of Medical Microbiology in February 2022 (MIC-D-22-00042).

1.1 Bacteria and antibiotic resistance

Antibiotic resistance is one of the largest threats to global health and if left unchecked will result in increasingly severe clinical problems when treating bacterial infections, as a result of antibiotics being rendered ineffective. When first introduced, antibiotics were highly effective and revolutionised the treatment of bacterial infections. Alexander Fleming is credited as discovering one of the most well known antibiotics, penicillin, in 1928 [1], and by 1945 antibiotics, including penicillin, were being mass-produced and distributed to clinical settings [2]. The 1950s to 1970s were heralded as the golden era of antibiotics as new classes and types were discovered and implemented. However, post-1970s the discovery of new antibiotics has decreased, which in turn has reduced the number of therapeutic options for infections caused by bacteria which exhibit antibiotic resistance [3].

A timeline for the inception of antibiotics versus the detection of antibiotic resistance is shown in **Figure 1.1**. The speed at which antibiotic resistance can develop is best exemplified by penicillin, as in as little as five years post inception antibiotic resistance was first detected. Antibiotic resistance develops after an average of 13.8 years post-introduction (Value derived from the average time for bacteria to develop resistance for the following antibiotics; aminoglycosides [4], penicillin, sulphonamides, methicillin, tetracyclines [5, 6], sulphones [7], streptogramins [8], cycloserine [9], quinolones [10], azole [11], phenazine [12], diaminopyrimidine [13], gentamicin [4], vancomycin [5, 6], carbapenem [14], mupirocin [15], imipenem, ceftazidime, levofloxacin, linezolid [5, 6], daptomycin [16], ceftriaxone [17] and ceftaroline [5, 6]).

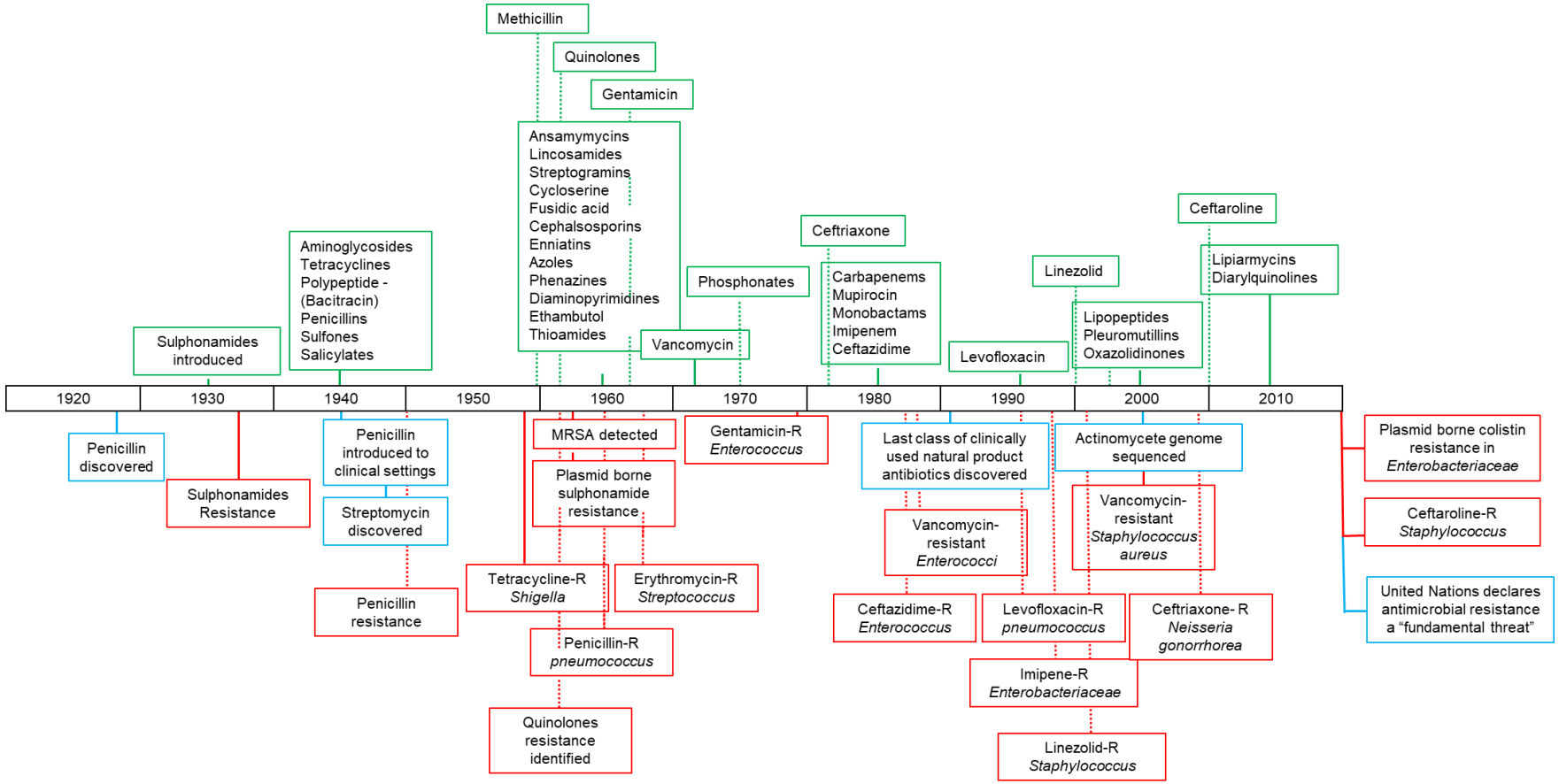

Figure 1.1. Timeline of the introduction of antibiotics into clinical settings (green), the development of antibiotic resistance (red) and significant antibiotic-related historical discoveries (blue). R = resistant, MRSA = methicillin resistance *Staphylococcus aureus*. Timeline comprised of information taken from reviews by Ventola. 2015 and Hutchings *et al*. 2019, in addition to individual sources [6, 18, 19].

Although the development of antibiotic resistance by a bacterial strain does not make all antibiotics redundant, the effectivity of antibiotics decreases considerably with each instance of resistance that occurs.

Single-drug resistant bacteria can be treated by identifying and then using an alternative antibiotic that has a mechanism of action to which the bacterium has no defence. Multidrug-resistant (MDR) bacteria, however, are much more difficult to treat due to the limited number of antibiotics than can be effectively implemented. The clinical definition of MDR is that an organism has acquired “non-susceptibility to at least one agent in three or more antimicrobial categories” [20]. An example of a bacteria that meets these criteria is Gram-positive methicillin-resistant *Staphylococcus aureus* (MRSA). MRSA has developed resistance to many of the commonly used antibiotic groups including aminoglycosides, fluoroquinolones, macrolides and the antibiotics tetracycline and chloramphenicol [21]. MDR behaviour is also exhibited by Gram-negative bacteria such as *Escherichia coli* (*E. coli)* [22] which demonstrates one of the highest resistances to both modern, and older antibiotics [23]. These are just two examples of the more commonly known bacteria; many other bacteria also exhibit singular and MDR behaviour. The introduction of new antibiotics into clinical settings has partially alleviated the issue of treating drug-resistant bacterial infections by providing alternative antibiotic treatment options. However, given that it is now well established that the overuse of antibiotics leads to the development of antibiotic resistance, steps must be taken to ensure the longevity of any currently used antibiotics to maximise the time they can be effectively used within clinical settings.

Antibiotic stewardship is an essential element in preventing antibiotic resistance from developing rapidly as well as extending the lifespan of the antibiotics that have seen prolonged use in the clinical settings. The UK has taken steps in recent years to reduce the use of antimicrobials. **Figure 1.2** shows the prescription of antibiotics in clinical settings within the UK wherein the general trend shows that there is a steady decrease in the prescription of antimicrobial agents over time demonstrating that the stewardship schemes do function as intended.

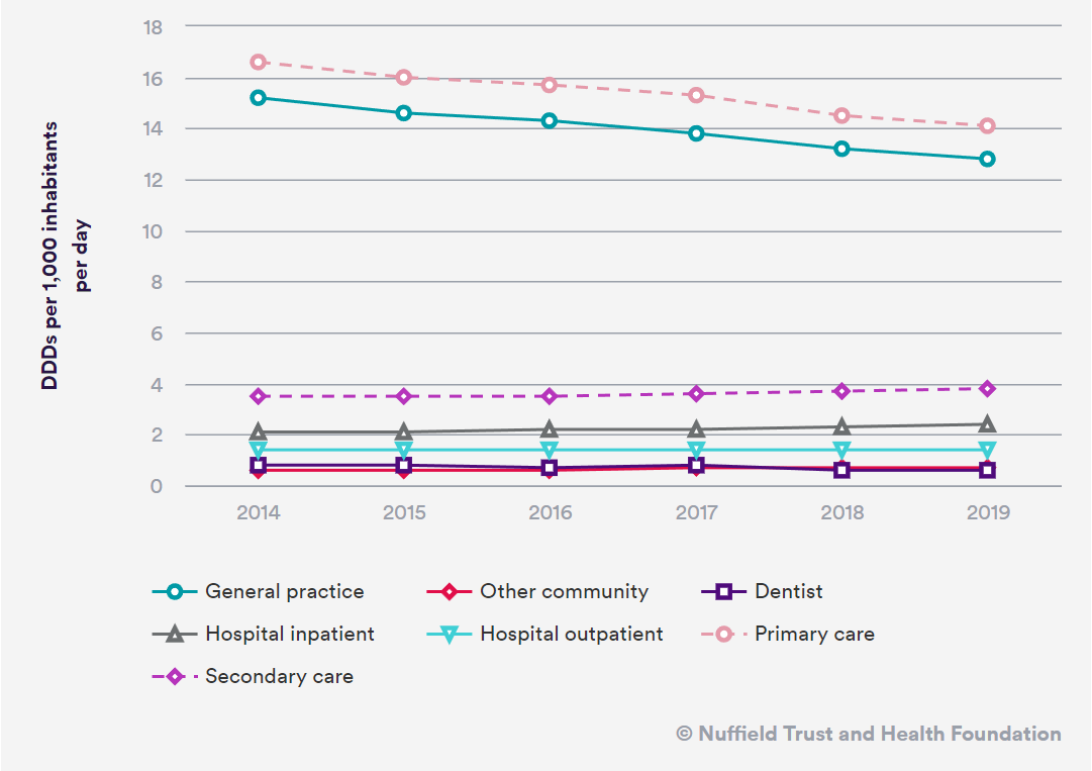

Figure 1.2 Shows the change in daily defined doses (DDDs) of antibiotics between 2014 to 2019 in the UK. Figure courtesy of the Nuffield Trust and Health foundation [24], data from the Public Health England, English surveillance programme for antimicrobial utilisation and resistance (ESPAUR) report [25]

Education about the current antimicrobial resistance situation is being conducted at the professional and public level to ensure people understand the issues that are currently being faced regarding antibiotic resistance. As part of the overall stewardship scheme, a document was published in 2015 by the National Institute for Health and Care Excellence (NICE). The purpose of the document was to educate health and social care practitioners, the organisations that commission and provide care, and the people taking antimicrobials on how antimicrobial agents can be used effectively [26]. Overall, the UK government aims to reduce the use of antibiotics by 15% by 2024 from 2019 as part of the five-year national action plan [27].

More recent government publications like “What is antimicrobial resistance and why do we need to take action against it?” published in 2021 by Ashiru-Oredope are more designed for public education about antimicrobial resistance and what the public can do to help prevent it [28]. These types of schemes are a step in the right direction for current and future antimicrobial

stewardship, however independently they are insufficient for sustainable long term antibiotic use. Two considerations must be met to ensure the longevity and effectiveness of any currently used antibiotics or antibiotics that are discovered in the future. Firstly, the use of broad-spectrum antibiotics for non-time-sensitive illnesses should be reduced. This would help reduce the rates of the development of antibiotic resistance as there is a known correlation between the overuse of an antibiotic and the development of antibiotic resistance in bacterial organisms [29-31]. Secondly, antibiotic prescriptions must be conducted more efficiently. When a patient is diagnosed with a bacterial infection that requires antibiotic treatment, the most effective antibiotic should be identified rapidly, and then prescribed to maximise the chances of effectively treating the infections with minimal chance for recurring bacterial infection by the causative pathogen.

Antibiotic resistance development is caused by the acquisition of genes which confer antibiotic resistance the process of which is both polyfactorial and complex. Bacterial genetics are complicated, with an estimated 20,000 potential resistance genes, fortunately, few of these genes alone grant functional resistance [32]. It is of note that resistance to one antimicrobial agent can be achieved through the presence of one or several different mechanisms as shown in **Figure 1.3**, therefore, a bacterium may have just one, or many of resistance enabling genes in its genome [33]. All these mechanisms decrease the likelihood of an antibiotic successfully binding to a target site, thereby allowing the bacteria to survive [33]. Antibiotic resistance can be innate, acquired or occur via mutation [34]. Innate resistance is where a resistance trait is always expressed within the bacterial species which is present independently of antibiotic exposure and horizontal gene transfer (HGT) [35]. This type of innate resistance is enabled by the lipopolysaccharides of the outer membrane which gives the membrane a low permeability to antibiotics, as well as in efflux pumps that can remove any antibiotics that permeate the membrane [36, 37]. Acquired resistance requires the addition of new genetic material to the genome of a bacterium, e.g. bacteria can acquire new genetic material via HGT.

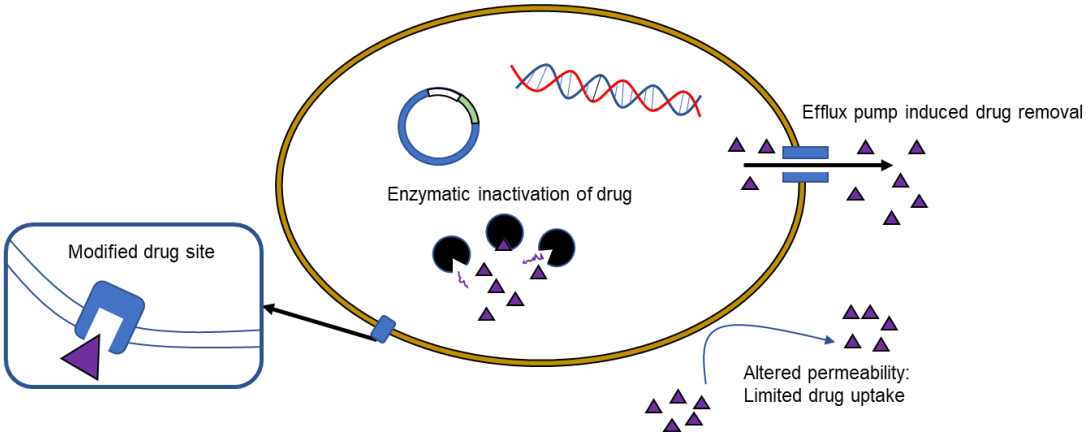

Figure 1.3. Schematic showing antibiotic resistance mechanisms that protect bacteria from antimicrobial agents; 1) modification of the drug target site to prevent the binding of the antibiotic with cell elements; 2) drug inactivation, such as enzymes that chemically alter or break down antibiotics; 3) active drug efflux, such as efflux pumps to prevent accumulation of antibiotic inside of the membrane; 4) limiting the uptake of a drug, such as changes in the membrane bacteria can reduce their permeability to antibiotics.

This enables the transfer of segments of plasmid DNA along a pilus to another bacterial cell and this donated genetic material is then integrated into the recipient cells genome forming recombinant DNA [38]. This form of gene transfer is non-specific, but it can enable the transfer of effective antibiotic resistance genes. The other limiting factor of HGT is that as a cell-mediated process not all bacterial cells are compatible due to surface occlusions, this has been observed in both Gram-positive [39] and Gram-negative bacteria [40]. An example of the impact of HGT is the development of resistance to the antibiotic colistin which was initially used as a backup antibiotic for use with critically ill patients in the event of infection with MDR Gram-negative bacteria. Colistin is a polymyxin type antibiotic which functions by binding to the lipopolysaccharides and phospholipids bound to the outer membrane of the Gram-negative microorganism [41]. Resistance to colistin develops in the form of the transferable gene mcr-1 which causes changes in the target site structure which, in turn, causes a reduction in the affinity of the antibiotics active site to the external nodule on the Gram-negative bacterial outer membrane [41, 42]. The mcr-1 gene has now been reported in *E. coli* isolates in China, Denmark, Germany and the UK [42].

Mutations can also change the bacterial genome. Bacteria have an average probability of a mutation occurring in a cell of between of 1×10^{-6} to

1×10^{-9} with most of the mutations being deleterious for the cells [32, 43]. However, in response to certain selection pressures, bacteria can alter their mutation rates by modifying interactions between allelic elements that are responsible for DNA repair and replication processes to increase the probability of a mutation occurring [44]. This innate ability is balanced by the rate at which beneficial and deleterious mutations occur within a cell that undergoes a mutation with a probability of 2×10^{-9} [45] and 2×10^{-4} to 8×10^{-4} respectively when looking at an *E. coli* K-12 model [46]. This process is what enables bacteria to develop methods of coping with natural selection pressures such as the introduction of antibiotics [44]. Provided acceptable conditions are presented bacteria can replicate at a rate that is significantly faster than that of larger organisms [47] with an example being *E.coli* which can replicate every 20 - 40 minutes under optimal conditions [48]. Coupled with the large size of bacterial populations, this fast replication time offsets the low probability of the beneficial mutations and enables them to occur at a rate unseen in organisms with slower replication cycles. Mutations that are beneficial to the bacteria and pertain to antibiotic resistance occur in only a handful of genes which encode antibiotic modifying enzymes, drug targets, drug transporters and regulators that control drug transportation [35]. Mutations that change genes to enable antibiotic resistance that do not result in cell death will then be passed on to successive generations of daughter cells resulting in a new population of antibiotic-resistant bacteria.

1.2 Gram-negative and Gram-positive bacteria

Bacteria are split into two distinct groups by differences in the structure of the cell walls. Gram-negative bacteria have an “envelope” which consists mainly of three distinct parts; the outer membrane which contains the lipopolysaccharides/endotoxins, the cell wall derived from peptidoglycan, and the inner membrane or cytoplasmic membrane [49]. Although technically porous due to the inclusion of many transmembrane proteins [50], the glycolipid derived outer membrane (OM) [51], serves as a very strong protective barrier for the cell as it prevents the uptake of harmful substances [52]. Additionally, there is a layer called the periplasm which is located

between the OM and inner membrane The periplasm is significantly more viscous than the cytoplasm due to the periplasm's high density of proteins [53]. Gram-negative bacteria can use the periplasm to isolate potentially harmful enzymes to prevent them from reaching the cytoplasm [54]. The properties of the OM and the periplasm confer antibiotic resistance properties. Due to this, Gram-negative bacteria are generally considered to be more innately antibiotic-resistant than Gram-positive bacteria due to the properties of the bacterial envelope [52]. The higher antibiotic resistance rate demonstrated by of Gram-negative bacteria has led to the World Health Organisation classifying Gram-negative bacteria as critical priority, versus the high priority of Gram-positive bacteria, which demonstrates the threat posed by antibiotic resistant Gram-negative bacteria [55]. An example of this is the study by Abbas *et al.* 2020, wherein it discussed that of the Gram-negative isolates taken from a tertiary care hospital, 64% were extensively drug resistant [56]. There are several Gram-negative bacteria strain types which are classified as medically important due to this innate antibiotic resistance including *Acinetobacter spp*., *Campylobacter* spp., *Enterobacteriaceae*, *Legionella pneumophila*, *Pseudomonas aeruginosa* and *Vibrio cholera*. Gram-negative bacteria can be single drug resistant or MDR to a range of aminoglycosides, carbapenems, fluroquinolones, polymyxins, sulphonamides, tetracyclines, third or fourth generation cephalosporins and/or ureidopenicillins [49].

Unlike Gram-negative bacteria, Gram-positive bacteria do not have an OM to enable innate antibiotic resistance and cell protection [52]. Instead, Gram-positive bacteria also have a thicker peptidoglycan cell wall to protect against pressure generated by the external and internal sources, this cell wall is reinforced with teichoic acids that form strands that run through the wall structure. These polymers make up 60% of the cell wall mass marking them as having intrinsic importance to the function of the cell wall [52], with the remaining 40% being made up of peptidoglycan [57]. Although the Gram-negative and Gram-positive peptidoglycan are structurally very similar, the Gram-negative peptidoglycan strands are roughly a few nM thick whereas the Gram-positive strands are 30-100 nM thick and are layered more densely than their Gram-negative counterparts [58, 59]. The type of crosslinking that occurs

is also different [60, 61]. Functionally, the crosslinking of the peptidoglycan cell wall of some Gram-positive bacteria infers a degree of antibiotic resistance due to the use of transpeptidase crosslinking enzymes which are not recognised by the active site of certain beta-lactamase antibiotics [61, 62]. These intrinsic differences alter the kinds of antibiotic that are effective against each of the Gram types, requiring some differences in how antibiotics are prescribed to treat Gram-negative and Gram-positive bacteria.

1.3 Urinary tract infections

Urinary tract infections (UTIs) are one of the most common types of bacterial infection in the world and due to their commonality, are one of the most expensive to treat. In the UK, UTIs accounted for 224,670 hospitalisations in 2014 [63] with catheter-associated UTIs costing the National Health service (NHS) ~£54.4 million between 2016 and 2017 [64]. UTIs are categorized as either: 1) Uncomplicated, which are characterised by a person having no structural or neurological issues of the urinary tract and are otherwise healthy [65] or 2) Complicated, which are characterised by a person having structural or neurological issues, immunosuppression and other associated immunological disorders or otherwise being compromised [66].

UTIs are precipitated by the colonization of the urethra followed by migration of the bacteria up the urinary tract to the bladder [67], usually initiated the contamination of the periurethral tract by a gut dwelling uropathogen [67]. The urinary tract, and by extension the bladder, are largely covered by the uroepithelium which is comprised of the umbrella, intermediate and basal layers which serve to provide effective protection from pathogens, toxins, and urine. This protection is polyfactorial with membrane lipids, surface glycans, and other uroepithelial cell constituent elements all providing a measure of protection against bacterial colonisation [67, 68].

Due to the environment being nutritionally deficient, uropathogens will attack the host cell lining of the urinary tract, damaging the cells to release the nutrients contained in the cytoplasm which also provides a niche microenvironment for bacterial growth [67]. Health complications can arise from complicated UTIs due to further bacterial colonisation from the bladder to

the epithelium in the kidneys. From here, bacteria can migrate across the tubular epithelial barrier and enter the bloodstream causing bacteraemia [69]. Bacteraemia results in urosepsis which make up 25% of sepsis cases in adults with an associated mortality rate of 25% to 60% [70]. This is further exacerbated by the fact that hospitals often use indwelling catheters for vulnerable persons who may have prolonged stays. Indwelling catheters are involved in 70-80% of confirmed complicated UTIs [71], and given that improperly treated complicated UTIs can develop into bacteraemia this demonstrates the significant health risk to vulnerable persons. The serious risk posed by UTI migration up the urinary tract illustrates the importance in the prescription of an effective antibiotic to treat UTIs, especially complicated UTIs.

UTIs are caused by a spectrum of different bacterial organisms which is shown in **Figure 1.4**. As previously discussed, drug resistance occurs in both Gram-negative and Gram-positive bacteria although in the past decade there has been an increase in MDR Gram-negative bacteria [49]. This, in conjunction with the fact that the majority of UTIs are caused by Gram-negative bacteria, in uncomplicated and complicated UTIs at 84% and 77% respectively [67, 72-77], means that UTIs could become especially difficult to treat over time.

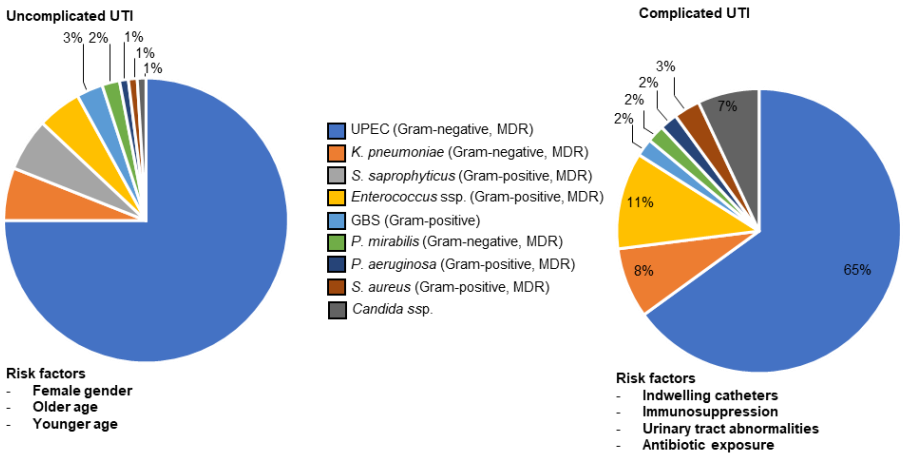

Figure 1.4. Predominant causes of uncomplicated, and complicated UTIs in addition to the associated risk factors. Taken from Flores-Mirales *et al*. 2015 [67]. UTI causative bacteria that can be MDR include; UPEC [78], *K. pneumoniae* [79], *S. saprophyticus* [80], *Enterococcus* ssp [81], *P. mirabilis* [82], *P. aeruginosa [83]*, and *S. aureus* [84].

This could potentially lead to increasingly poor patient prognosis for vulnerable patients.

Uropathogenic *E. coli* (UPEC) can migrate into the cytoplasm of the epithelial cells wherein it multiplies rapidly, forming a short-lived intracellular bacterial community similar to a biofilm. This film production and cytoplasm invasion give UPEC an innate ability to circumvent the patient's exocytosis defence [85, 86]. The formation of an intracellular bacterial community also allows UPEC to survive the tight bottlenecks that can occur with urinary tract invasion such as; ascension to the kidneys, inflammation, toll-like receptor 4 mediated expulsion, umbrella cell exfoliation and urination [87, 88]. UPEC driven UTIs can also reoccur due to bacteria stored inside intracellular reservoirs. These reservoirs are made up of between 4 and 10 cells which remain sequestered and viable for up to months post-infection before proliferating to cause a reoccurring UTI [87].

Klebsiella pneumoniae (*K. pneumoniae*), the second most common causative agent of UTIs, shares a similar infection pathway to *E. coli* using pili to facilitate biofilm formation and colonisation of the bladder [89] but develops fewer intracellular colonies compared to *E. coli* as the binding is comparatively weaker [90, 91]. The combination of the persistence of UTIs, the potential for reoccurring UTIs and the MDR characteristics shown by Gram-negative bacteria indicate that UTIs will become increasingly difficult to treat over time. This is compounded by the fact that UTIs make up a large proportion of all bacterial infections and the fact that improperly treated UTIs can cause serious health issues, further highlighting the importance of developing accurate and rapid methods of determining antibiotic susceptibility of uropathogens to efficiently treat UTIs and prevent recurring infections.

1.4 Current methods of UTI determination

The determination of the presence of a UTI is carried out using the identification of clinical symptoms [92] or the use of a dipstick [93]. The presentation of clinical symptoms varies slightly depending on the urological area to which bacteria had migrated to, with a bladder infection presenting as pungent or cloudy urine, lower abdominal or urethral pain, urine contaminated

with blood, frequent urination and pain when passing urine. Infection of the kidneys however presents as pain in the flanks, fever, rigours and chills.

Dipsticks contain reagents to enable the detection of nitrites, leukocyte esterase, proteins and blood the presence of which can be used to identify a UTI as the confirmation of these biomarkers indicate that there are bacteria present in a urine sample [93]. Medical history is also taken into consideration as there are numerous factors which contribute to a patient's susceptibility to UTI infection, including but not limited to; dysuria, nycturia, pollakiuria, prior infections, turbid urine, present or increased incontinence, suprapubic pain [94] and antibiotic exposure within the last two to four weeks [95].

After the presentation of symptoms or a positive dipstick test, a broad-spectrum antibiotic is often prescribed until the results from cultured based AST are made available [96], however, this practice presents two major issues. Firstly, if the pathogenic bacteria are resistant to the action of the antibiotics, then there will be no effect on the pathogen, and the non-pathogenic bacteria that inhabit the gastrointestinal tract may be negatively impacted, which in combination may cause a detrimental effect on the health of the person involved [97]. Secondly, the prescription of broad-spectrum antibiotics for a bacterial infection that is antibiotic-resistant is a major contributor to the further development of antibiotic resistance in pathogenic bacteria which reduces the longevity of frequently used broad-spectrum antibiotics [23, 98].

The reason for this reactionary antibiotic prescription is that bacterial identification and culture-based AST take time. The process starts with midstream urine capture followed by agar-based culture to facilitate pathogen isolation and identification [93]. The identification of bacteria is conducted using chromogenic agar which can be used to identify Gram-negative *E. coli* as well as Gram-positive *Staphylococcus saprophyticus* and *Enterococcus* species [99] with the time to identification being between 18-30 hours after urine collection [100]. If the colony forming unit (CFU) count from the urine sample is $\geq 10^4$ CFU/ml and contains a singular or one of the prominent types of uropathogenic bacteria then the urine sample is considered positive for a UTI [101]. A variety of factors affect the next step in the treatment process.

Men, pregnant women, and children under 16 years will have urine samples collected, and culture-based AST will be conducted to identify a narrow-spectrum antibiotic which is effective. Women who are not pregnant may be prescribed an immediate antibiotic after presentation of clinical symptoms if the symptoms are severe enough to warrant immediate treatment. A backup antibiotic may be used if the patient's symptoms become worse. If patients who are undergoing antibiotic treatment see their conditions worsen the antibiotic treatment may be reassessed. Additionally, patients will be referred to hospital if they show signs of serious illness or conditions that arise from complications such as sepsis [102].

After isolation of the bacteria, and after determining that an antibiotic is required to treat the UTI, culture-based AST is carried out. The current gold standard method for AST is the disk diffusion assay. This phenotypic based method first requires the isolation and growth of bacteria to sufficiently large population [103] before observation of zones of inhibited bacterial growth on nutrient agar around disks loaded with antibiotics. This type of assay produces a result within 16-24 hours after isolation of the pathogen [104, 105]. When an antibiotic is required due to either severe symptoms, or the immediate antibiotic is ineffective it can take upwards of 72 hours for an effective antibiotic to be prescribed in which time the health of a patient could deteriorate.

Genotypic based testing offers an alternative to disk diffusion assays which can be completed in less time [106, 107]. Molecular methods such as the polymerase chain reaction (PCR) can be used to identify resistance genes in the pathogen which can enable the identification of which antibiotics the bacteria may be resistant to [108, 109] within 10-16 hours [110, 111]. The benefit of the reduced time to analysis is offset by the following disadvantages: 1) high equipment costs [104, 105]; 2) the requirement for a preincubation step [112]; 3) the potential for multiple resistance genes [113]; and 4) that some resistance genes do not confer phenotypic resistance [32].

A more rapid method of conducting AST would enable the identification of the most effective antibiotic to treat a bacterial infection, ideally within the timeframe of a visit to the doctors. This would eliminate the need for the

prescription of a broad-spectrum antibiotic and help to extend the longevity of any antibiotics currently used in clinical settings.

1.5 Systematic review methodology

A systematic review was conducted following the Preferred Reporting Items for Systematic reviews and Meta-Analyses format (PRISMA) [114]. Scopus and PubMed were used as the literature sources with the following keyword combinations being used to conduct the literature search for articles: 1) Microfluidic AND urinary tract infection; 2) Microfluidic AND UTI; 3) “Lab on a chip” AND urinary tract infection; 4) Lab on a chip AND UTI. Articles published between January 2006 to June 2022 were included with the language criteria being English (UK and American) or translated papers. Articles were then screened independently, and any articles were excluded if they were: 1) Duplicated articles; 2) The article was a continuation of previous work that built upon a previously published method; 3) The title and abstract did not pertain to LOC devices for UTI based applications; or 4) Any of the analytical processes took place off the LOC or microfluidic device. Grey literature was also not included to keep the quality of the studies articles high. From a preliminary 140 identified articles during the vetting process, a further 95 articles were removed from consideration leaving 45 articles for the purposes of data extraction for the meta-analysis.

A broad spectrum of analytical methods was found in the literature identified, and as such the different methods were broadly grouped to simplify the data collection. The groups included molecular methods, direct quantification of bacterial growth, immunoassay, colorimetric, bioluminescence and Raman spectroscopy methods. Direct quantification of bacterial growth is defined as approaches that rely on methods such as single cell imaging which is used to directly monitor the lengthening and growth of bacteria [115] or the use of fluorescent markers and microscopy techniques to visually identify bacterial growth by identifying binary fission [116].

Time to analysis values were converted to minutes, if the time to analysis was not clearly stated in the literature, the timings outlined in the methodologies were used to estimate the time to analysis. When discussing

costs, any monetary values were converted to the United States Dollars. In the search criteria one of the variables was “sample type” which was classified as either as an “artificially constructed sample” or a “real clinical sample”. Artificially constructed samples were defined as all bacterial samples that were not clinically acquired UTI urine samples.

Real clinical samples were defined as clinical urine samples acquired from a hospital or other official medical organisations. When reporting the bacteria tested, where possible the strain types were converted to the American type culture collection (ATCC) reference number. Antibiotics were grouped the following format to simplify the data extraction and presentation “Antibiotic class (Antibiotic type)”. When extracting the data for the upper and lower limits of detection if the values were not outright stated the upper and lower limits of detection were taken as the upper and lower concentration of bacteria that was tested in colony forming units (CFU). If there was a different lower limit of detection depending on the type of bacteria used the highest CFU/ml lower limit of detection was used for the statistical analysis to represent the method.

Statistical analysis was conducted using R and R Studio addon (Version 4.0.5). Shapiro tests were used to establish normality within a data set. Correlation was established using Spearman correlation for non-normal data and Pearson correlation for normal datasets. Multiple groups were analysed using Kruskal-Wallis test using a pairwise Wilcoxon post hoc test for non-normal data. For normal data, an ANOVA with a post hoc Tukey test was used for normal data sets.

1.6 Systematic review of Lab-on-a-Chip devices for UTI diagnostics

Lab-on-a-Chip (LOC) devices offer an alternative method of conducting analytical procedures in a clinical setting. LOC devices use microfluidics to enable the miniaturization of both novel and existing techniques into devices that contain micrometer sized channels. The miniaturisation process means that LOC devices are compatible with reagent volumes down to the picolitre range [117], which enables LOC based methodologies to have smaller material and reagent requirements and offer advantages in terms of portability,

low-cost, and rapid analysis times compared to their macroscale counterparts. The methods employed in combination with LOC devices are often automated and enable parallel testing on a singular device which removes human error from the analysis process [118]. LOC devices can be used for a variety of different biomedical analytical purposes including the detection of pathogens [119], hormones [120], analysis of DNA, and proteins [121]. Herein we discuss the use of LOC devices with applications for UTIs to determine the current trends.

A variety of different methodological approaches in LOC devices designed for UTIs have been documented which is shown in **Figure 1.5 A**. The number of publications per year has seen a significant linear increase (Regression, p-value = 0.040) which would indicate that there is a growing interest in UTI-specific LOC devices. The purpose of the LOC devices described in the articles was to conduct UTI diagnosis, the AST of the bacteria causing a UTI or to conduct AMR as shown in **Figure 1.5 B**.

Overall, eight different methodological approaches were taken in the reviewed literature: 1) Molecular, defined by methods using the manipulation of DNA, RNA, proteins or other genetic material; 2) Direct quantification of bacterial growth, defined as methods that use microscopy or other imaging techniques to detect bacterial elongation, or other methods that enable the direct detection of bacterial growth using a cell viability indicator such as a dye; 3) Electrochemical, defined as methods which use the detection of changes in an electrical circuit such as current, or resistance, or the detection of a cell viability indicator via electrochemical means as the detection methodology; 4) Colorimetric, defined as methods that use the visual identification of colour changes that infer binary yes or no type information; 5) Immunoassay, defined as methods that use the detection of specific proteins or antigens using capture antibodies as the basis of the method; 6) chemiluminescent detection, defined as the detection and quantification of light produced during biological processes; 7) Raman spectroscopy, a unique method in the publications which is a non-destructive chemical analysis type method; and 8) Dual purpose devices, these were defined as a methodological approach which used two of

the previously defined method types on one LOC device to conduct both bacterial identification and AST.

1.6.1 LOC methodologies

Of the published articles, 9/45 used a purely **molecular based method.** Molecular based methods have well-established theory and methodologies [122-124] which may contribute to the frequent and growing use of such methods, as they were used the most frequently in the identified articles. A summary of the methods used, and their application can be found in **Table 1.1**. Three different types of amplification-based methods were used including PCR, both standard and real-time, as well as isothermal techniques, namely recombinant polymerase amplification (RPA) and loop-mediated isothermal amplification (LAMP). The latter isothermal techniques offer advantages in terms of not requiring accurate thermal cycling and so can be more easily deployed in resource-limited areas [125].

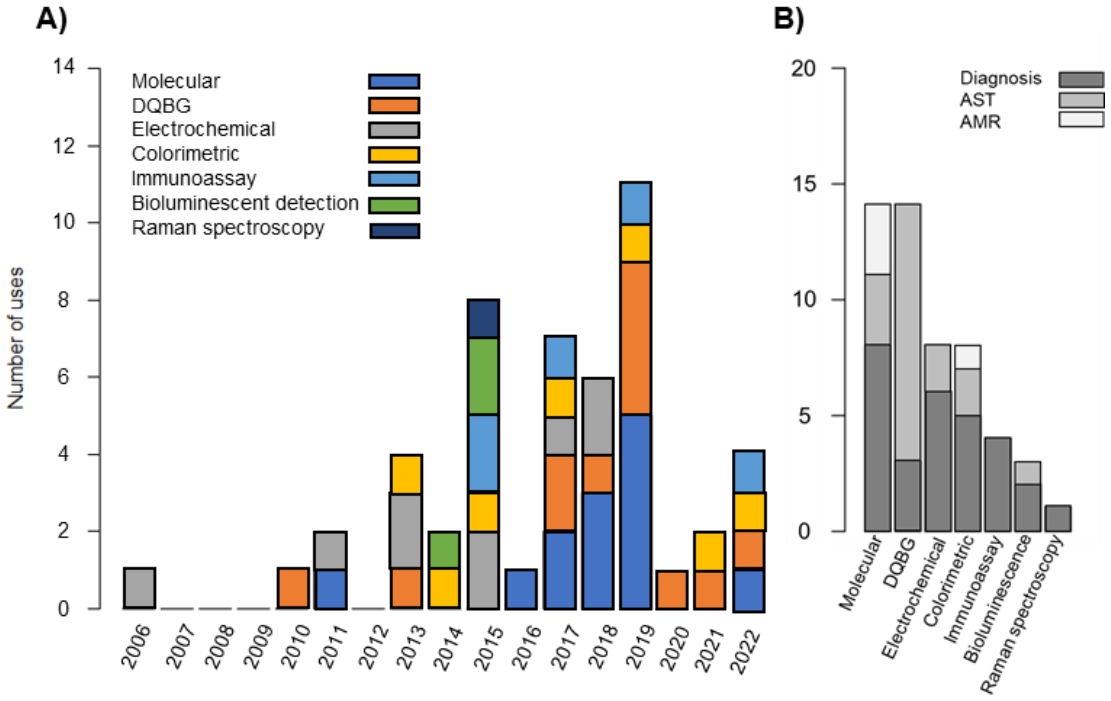

Figure 1.5: A) Shows the total number of the uses for each of the methodological approaches per year between 2006 and 2022. Direct quantification of bacterial growth is abbreviated to DQBG. **B)** Shows different methods used in bacterial identification, antibiotic susceptibility testing and antimicrobial resistance.

A consideration with molecular-based methods is that contamination in the form of other genetic material can be an issue. This could potentially result in a false-positive or otherwise negatively impact the results of the method. However, a high degree of specificity can be achieved through the design of primers and probes against specific known gene sequences using databases such as the National Center for Biotechnology Information [126]. This was addressed in several of the articles as each specifically targeted conserved regions of the bacterial genome to prevent this issue [127].

Methods that used the **direct quantification of bacterial** growth were presented in 7/45 articles, with a spectrum of different methodological approaches being used. However, it could be said that the diversity could indicate a lack of consensus on the most effective analytical methods. The direct quantification of bacterial growth works well in conjunction with the rapid doubling time of bacterial organisms [116] enabling rapid and simple AST that does not require a prolonged overnight culture to assess antibiotic susceptibility. A key limitation of this approach is the reliance on the bacteria undergoing binary fission and splitting to form new cells. In cases where the bacteria remain in the lag phase of growth wherein bacteria are not actively splitting [128], the time to analysis could increase.

Simpler diagnostic platforms in the form of **Colorimetric methods** made up a further 8/45 of the articles. Colorimetric based methods are simple to execute and do not require a high level of scientific training to use, in combination with the binary “yes” or “no” outputs colorimetric based devices fit well into environments where equipment is limited [129-133]. The limitation of colorimetric detection-based methods is that mechanisms of detection which rely on specific biological process such as catalase positive organisms to drive the chips detection method will miss any bacterial organisms that use different metabolic processes [129] e.g. bacteria which do not produce nitrites [134]. Colorimetric devices can produce false negatives as if the pathogenic bacteria are present at a low concentration the colorimetric response may not be triggered due to the bacteria producing insufficient secretions required to trigger the device.

Table 1.1 Summary of research papers identified indicating detection method, function, brief description, LOC device material and limit of detection.

Detection Method	Function	Description	LOC Device Material	Limit of Detection (CFU /mL)	Ref.
Molecular	ID	Cell enrichment via gold coated nanoporous membrane, cell lysis, followed by polymerase chain reaction (PCR) targeting 16S rRNA with reagent storage	Poly(methyl methacrylate) (PMMA)	1×10^3	[135]
		Centrifugal device design with cell lysis, multiplex recombinase polymerase amplification (RPA) of DNA and bacterial specific DNA fluorescent probes with reagent storage	PMMA	1×10^3	[136]
		Cell enrichment via ConA cell binding, multiplex RPA of DNA	Polydimethyl siloxane (PDMS)/Glass	5	[137]
		Isotachophoresis driven rRNA extraction, concentration, and probe hybridization, conjugation of 16S rRNA with fluorescent beacons	Borosilicate	1×10^6	[138]
	AST	Digital real-time loop-mediated isothermal amplification (LAMP) targeting the 23s ribosomal gene using commercial PCR Chit Kit containing 20,000 reaction chambers	Silicone	5×10^5	[139]
		Digital real-time LAMP targeting the 23s ribosomal gene using commercial PCR Chit Kit containing 1,280 electrode chambers	Glass	5×10^4	[140]
	AMR	DNA capture, then transfer to electrode chamber for real-time RPA of the blaCTXM-15 gene	Glass/indium tin oxide	1×10^3	[141]
		Bacterial capture via magnetic beads, followed by transfer to electrode chamber for real-time RPA of the blaCTXM-15 gene	PMMA	1×10^3	[142]
		DNA extraction, then LAMP of bacterial DNA	Polycarbonate	1×10^4	[143]
Direct quantification of bacterial growth	AST	Instrument-free gradient droplet formation, and bacterial exposure to a gradient concentration of nitrofurantoin followed by bright field microscopy	Tetradecane	1×10^5	[144]
		Bacterial capture in 2000 microfluidic channels followed by phase contrast microscopy	PDMS/Glass	1×10^4	[115]
		Centrifugal device for cell lysis and quantitative using phase contrast microscopy and absorbance spectroscopy	PDMS/Glass	N/A	[145]
		4 x 12 microfluidic array for fluorescent microscopy	Polymer/Glass	N/A	[116]
		Bacterial droplet packaging and docking array entrapment with fluorescent microscopy	PDMS	5×10^4	[146]
		Bacterial entrapment in one of four docking sites of 8000 wells with time-lapse imaging	PDMS/Glass	1×10^7	[147]
		Resazurin assay in LOC device housing 200 reaction wells containing antibiotics	PDMS/Glass	5×10^5	[148]
Colourimetric	ID	Bacterial capture on a dipstick type LOC device with 20 capillaries followed by colorimetric detection of resazurin	Fluorinated ethylene propylene	10	[149]
		Bacterial capture via nanoparticles, electrode chamber (conversion of hydrogen peroxide to water by catalase positive organisms), and visual ink chart	Polymer, glass and polyvinyl chloride tape	1	[129]
		Colorimetric reaction pads for detection of glucose, protein, occult blood, and nitrites	PMMA and paper (various)	N/A	[131]
		Colourimetric reaction pads for the detection of nitrites	Wax and paper (various)	N/A	[132]
		Heating unit combined with three LOC devices each with 15 testing chambers in series and chromogenic media	Aluminum, PDMS and glass	10	[130]
		Bacterial sequestration in chromogenic agar	PMMA	253	[150]
	AST	Colorimetric analysis analyses using absorbance in a 4x4 microwell array	PDMS	15	[133]
	AMR	Smartphone enabled detection of chromogenic cephalosporin substrate colour changes	Nitrocellulose paper and wax	1×10^4	[151]
Electrochemical	ID	Bacterial capture using magnetic nanoparticles, impedance spectrometry detection of 16S rRNA using sequence specific molecular beacons	PDMS and gold electrodes	3.4×10^4	[152]
		Amperometry detection of 16S bacterial rRNA using a self-assembled monolayer (SAM) modified biosensor	PDMS, chromium, gold, platinum electrodes	4×10^5	[153]
		Multiplex (up to 16) amperometry detection of 16S bacterial rRNA using a SAM modified biosensor	Polymer, gold electrodes	4×10^4	[154]
		Electrochemical detection of biotinylated amplicons bound to streptavidin functionalised sensor	Reduced graphene sensor	N/A	[155]
		Electrochemical detection of immunocaptured bacteria	PDMS, gold electrodes	1×10^6	[156]
	AST	Impedance spectrometry detection of bacterial motility in a microfluidic channel	PDMS and glass	1×10^5	[157]
		Bacterial filtration via microbeads, bacterial capture and detection using resazurin and differential pulse voltammetry	PDMS and gold electrodes	1×10^5	[112]
Immunoassay	ID	Bacteria capture via antibody conjugated magnetic beads followed by colorimetric detection	Hydrophilic transparency, neodymium iron boron magnet	2.4×10^2	[158]
		Bacterial capture in microcapillary tubes followed by rapid optical sandwich fluorescent immunoassay	FEP-Teflon polymer	240	[159]
		Sandwich fluorescent immunoassay	PDMS	1.2×10^2	[160]
		Absorbent pads loaded with antibody conjugated particles for immunoagglutination quantified by angle-specific Mie scatter under ambient lighting conditions	Cellulose chromatography paper	10	[161]
Chemiluminescence	ID	Photodetection of luciferase-initiated ATP to ADP reaction using a graphene monolayer detector platform	Silicone, graphene	-	[162]
		Photodetection of ATP to ADP conversion in multiple spiral microchannels	Glass and silicon wafer	1×10^4	[163]
Raman spectroscopy	ID	Bacterial capture guided by a radial centrifugal field with Raman spectroscopy	PDMS and glass	2×10^7	[164]
Dual purpose devices	ID & AST	Microdroplet formation followed by labelling with a 16S rRNA probe and quantitative detection (Molecular)	Glass	1×10^5	[165]
		Centrifugal force-based collection and purification of bacteria, followed by bright field microscopy (direct quantification of bacterial growth).	VeroClear photopolymer	5×10^3	[166]
		Agglutination assay targeting 16S rRNA (molecular) followed by flow cytometry (direct quantification of bacterial growth)	Hydrophilic and light shielding tape laminate	100	[167]
		Microfluidic capillary tubes for bacterial capture, sequence specific molecular probes followed by single cell time lapse imaging (direct quantification of bacterial growth)	Glass	-	[168]
		Bacterial capture via antibodies (Immunoassay) in electrode chambers followed by an ATP chemiluminescence assay (chemiluminescence)	Polystyrene and fiberglass membrane filter	1×10^3	[169]
		Hybridization of molecular probes specific to 16S rRNA followed by fluorescence detection (Molecular)	PDMS	-	[170]
		Chromogenic agar combined with zones of inhibition type AST (colorimetric)	Paper	100	[171]

Electrochemical methods were presented in 7/45 articles with each using one of three approaches; 1) amperometry, which is the measurement of current, at a fixed potential, generated at the electrode [172]; 2) impedance, which is the measurement of resistance at the electrode at varying currents; 3) differential pulse voltammetry, which is used in the detection of reduction oxidation (redox) markers to determine cell viability [112]. Pertaining to the identification of bacteria, the electrochemical approach is remarkably similar to molecular-based methods. Cells are lysed, and the conserved regions of the genome, specifically 16S rRNA, are captured either in a chamber before the electrode chamber, or at the electrode itself. This enables a high degree of specificity and, thereby, accuracy in the identification of bacteria without the requirement for multiple amplification cycles or a thermal cycler. The use of a resazurin based electrochemical AST method was documented [112]. This type of methodological approach can be used with any bacteria that aerobically respires, enabling the method to be applied to a wide range of bacteria without the requirement for extensive modification to the electrochemical sensing platform. Given that UTIs are caused by a spectrum of different bacteria, the ability for a method to be used with all of the most common uropathogens is a highly desirable trait for a LOC based rapid AST platform. A review of resazurin based electrochemical biosensors is shown in **Section 2.1.3**.

Immunoassay based methodologies made up 4/45 articles, with the methods being restricted to bacterial identification only and not in AST or AMR. The high degree of specificity afforded by antibody-antigen interactions has made immunoassays an obvious choice for incorporation into LOC devices for UTI diagnostic systems. The disadvantage when using immunoassays is that antibodies can bind to analogues of the target analyte resulting in false positives [173].

A further 2/45 articles used **quantification of ATP chemiluminescence** based detection of viable bacteria and identifies the CFU/ml count without the requirement for prolonged culture by using calibration curves [162, 163]. However currently, the biggest limitation of using

chemiluminescence as a detection method is that various physicochemical factors can affect the selectivity and sensitivity of the analytical method [174].

The least used method accounting for 1/45 of the articles was **Raman spectroscopy**. Raman spectroscopy has seen several uses in biomedical applications, including the identification of bacteria [175]. The units that use Raman spectroscopy are compact and highly portable [164]. There however can be issues pertaining to sensitivity due to impurities interacting with the laser to produce unwanted photochemical effects [176], as well as background noise which can interfere with data collection [177].

The remaining 7/45 articles published discussed the use of **dual-purpose devices**. The ability to both identify and conduct AST of bacteria provides an advantage over current testing methods where the identification [100], and the AST [104, 105], of bacteria are conducted as two separate tests due to the requirement for the isolation of the pathogen first. By having both identification and AST occur on one device, both time and resources are saved. These articles demonstrate the ability of LOC devices to use multiple miniaturized processes that are usually conducted on the macroscale and conduct them on a single device [165-171].

The clinical CFU/mL count used in the diagnosis of a UTI is $\geq 1 \times 10^5$ CFU/mL [178] or $\geq 1 \times 10^6$ CFU/mL [179] depending on the literary source with the cut-off concentration being subjective to age, symptoms and urine collection method [180]. Therefore, for the purpose of the systematic review, a bacterial LOD of $\leq 1 \times 10^6$ CFU/mL was chosen for the assessment of the methodologies. Of the published methods, 43 of the 45 had a bacterial LOD equal to or below the clinically relevant CFU/mL LOD. Two papers did not meet this criterion, the first was the Kang *et al*. 2019 which tested a bacterial concentration range of 1×10^4 to 1×10^7 CFU/mL and had a bacterial LOD of 1×10^7. A lower LOD could not be achieved as a concentration of less than 1×10^7 CFU/mL due to issues with the encapsulation with bacteria in droplets that is required for the device to function [147]. The second was the Schroder *et al*. 2015 which tested a range of bacterial concentrations from 1×10^7 to 1×10^8 which had an LOD of 2×10^7. The underlying issue was a concentration less than 2×10^7 resulted it overall reduced integrated brightness of

fluorescence from within the chambers of the LOC device which made bacterial identification difficult [181]. Both of these methods could potentially benefit from a bacterial preconcentration step which would eliminate the bacterial LOD issues with minimal modification to the method as a whole.

1.6.2 Bacteria investigated

UTIs are caused by a spectrum of different bacteria with some being more prevalent than others [67] with differences in the percentage of the different causative uropathogenic bacteria found in uncomplicated and complicated UTIs. The bacteria investigated in the articles is detailed in **Figure 1.6A**. There are differences in the bacteria used in published articles versus the prevalence of the most common causative agents of UTIs as outlined in **Figure 1.6B**. Research-based methods are likely to be tested with bacteria that are common uropathogens and are also clinically relevant.

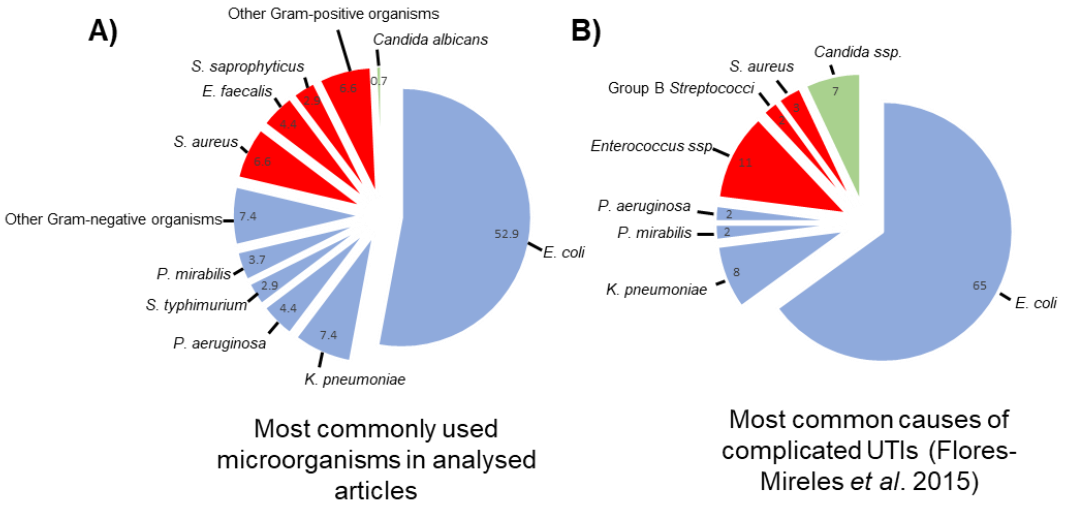

Figure 1.6: A) Shows the proportions of the Gram-negative (blue) and Gram-positive bacteria (red) used in all studies reviewed. "Other" Gram-negative and Gram-positive bacteria are the sum of bacteria in those categories that were used once only. For Gram-negative bacteria "other" constitutes *Salmonella enteritidis, Neisseria gonorrhoeae, Acinetobacter baumannii, Citrobacter freundii, Enterobacter cloacae, Enterobacter aerogenes, Citrobacter koseri, Serratia marcescens.* For Gram-positive, this constitutes, *Corynebacterium glutamicum, Staphylococcus haemolyticus, Staphylococcus epidermidis, Enterococcus faecium, Streptococcus viridans, Streptococcus pyogenes, Enterococcus spp.* **B)** Shows the proportion of the most common causative agents of UTIs pertaining to complicated UTIs including fungi (green) as reported in Flores-Mireles *et al*. 2015. [67]

E. coli was statistically the most used out of all of the bacteria investigated in the reviewed literature, (Kruskal test, p-value < 0.05) which further correlates with *E. coli* being the most common bacterial cause of UTIs [67, 74, 182, 183], followed by *K. pneumoniae* and *P. aeruginosa*. The emphasis on these latter two types of bacteria may in part be due to the MDR behaviour of *K. pneumoniae* found in UTIs [79], and the reported antibiotic resistance of *P. aeruginosa* found in intensive care units [184], the presence of which can lead to nosocomial infections of which UTIs make up 20 to 49% of the total number of all nosocomial infections [185, 186]. Of the Gram-positive bacteria, *S. aureus and E. faecalis* were both used more than eight other types of bacteria (Kruskal test, p-value < 0.05). The high usage correlates with the fact that both *S. aureus,* [84] and *E. faecalis,* [187] display MDR behaviour and, therefore, can prove difficult to treat with antibiotics. The high usage of these bacteria is because of the difficulty in treating MDR bacterial infections and the relative percentage of UTIs caused by each of the different types of bacteria in uncomplicated and complicated UTIs.

In the reviewed literature, the emphasis in testing was on Gram-negative bacteria which made up 78.7% of studies compared to Gram-positive bacteria which were used in 20.6% of studies with the remaining 0.7% being *C. albicans*. Currently, there is a definitive bias towards testing using Gram-negative organisms. In recent literature, the increased prevalence of MDR Gram-negative bacteria has been discussed, [49, 188-190] and with the risk of bacteraemia and urosepsis as a result of unchecked migration of bacteria in the urinary tract [67], a focus on Gram-negative bacteria is prudent. *E. coli* alone makes up 75% of uncomplicated and 65% of complicated UTIs [67, 72, 74, 182] with MDR *E. coli* also being documented in causing UTIs [191]. This is not to understate the importance of also testing methods with Gram-positive bacteria, some of which can also exhibit MDR behaviour such as the previously discussed *S. aureus* [21]. However, as the development of LOC-based methodologies specifically for UTIs are still a developing platform, a focus on the most common bacteria is not unexpected. Currently, the testing of Gram-negative and Gram-positive bacteria in the LOC devices used in UTI analysis is in keeping with current literature.

1.6.3 Biological sample types evaluated

Methods that work directly with human urine, as opposed to those that isolate the bacteria from the urine sample for resuspension in another medium face difficulties because of the inherent variability of urine. In urine, there is variation in the concentrations of proteins, endpoint metabolites such as creatine [192], pH [193], initial bacterial concentration [138], as well as trace elements [194] in human urine all of which could potentially affect the working principles of the applied method. It is necessary to test LOC based methods under lab conditions and sample types to demonstrate their effectiveness in a controlled environment and refine the techniques used. The way a method performs under lab conditions, is not always how it will perform in a clinical setting where there is more inherent variability. Artificially constructed samples are defined as those which are made up of stock bacteria such as those from culture collections or clinical isolates from diagnosed UTI infections (which have been identified) that are then spiked into a bacterial growth medium or another appropriate medium. Real clinical samples are defined as UTI urine samples acquired from clinical settings for testing purposes.

The use of artificially constructed samples and real clinical samples used as a function of the date published was observed to determine what trends were present in the tested sample types which is shown in **Figure 1.7**. The trend showed a more recent rapid increase in use of both artificial and real samples and there was a slight time lag in the use of real samples as compared to artificial samples. The probable cause of the delay in the uptake of testing using real samples is that is that microfluidic and LOC devices with an application towards UTIs are a developing technology which require testing with artificially constructed samples to assess the viability of the proposed system before further validation can be done using real clinical urine samples. Of the articles 10 of the 45 [129, 130, 138, 140, 143, 148, 164, 166, 168, 169] used artificially constructed samples to first test, and then further validated the proposed devices.

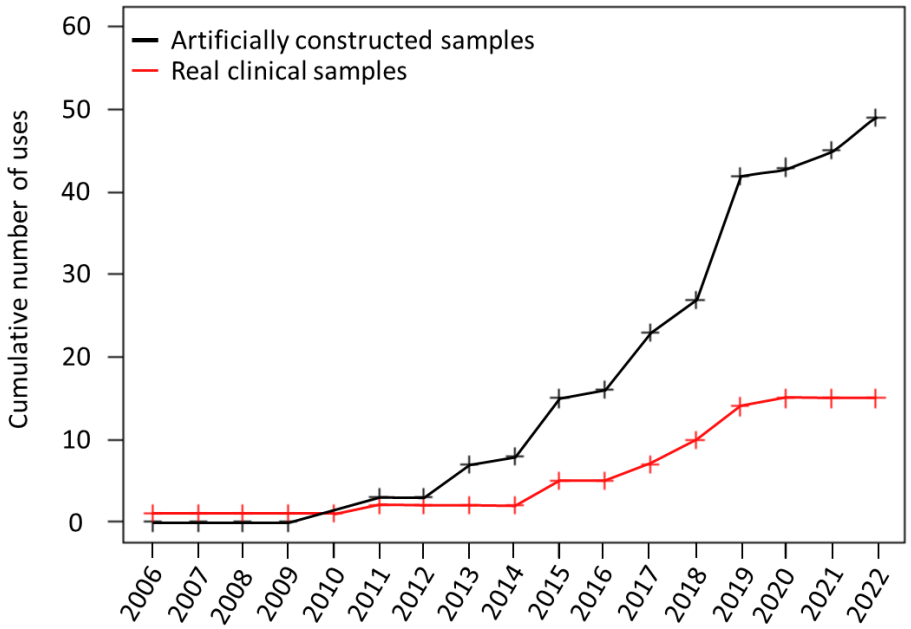

Figure 1.7: Shows the cumulative number of uses of artificially constructed samples and real clinical urine samples between 2006 and 2022

Situation permitting, if the proposed method is intended for commercial use blind testing with real clinical urine samples is necessary to ensure the proposed method works optimally outside of lab conditions where there are variables such as the differences in urine composition which may affect the different steps of the method.

The breakdown of the types of bacteria used in the artificially constructed samples is shown in **Figure 1.8 A**. The requirement for validation correlates with the fact a large proportion of the artificial samples were made up with stock bacteria. After initial validation with stock bacteria, the natural progression is to use clinical isolates to further validate the design of the method before moving onto real clinical urine samples. Two articles used no bacteria for the testing. One of the methodologies described used colorimetric reaction pads housed in a paper-based device which reacted to the presence of nitrites which can be taken to indicate the presence of uropathogenic bacteria [132]. The other article shared a similar mechanism having multiple reaction pads to detect nitrites, glucose, protein, occult blood, and leukocyte esterase with the reaction pads separated by hydrophobic channels [131].

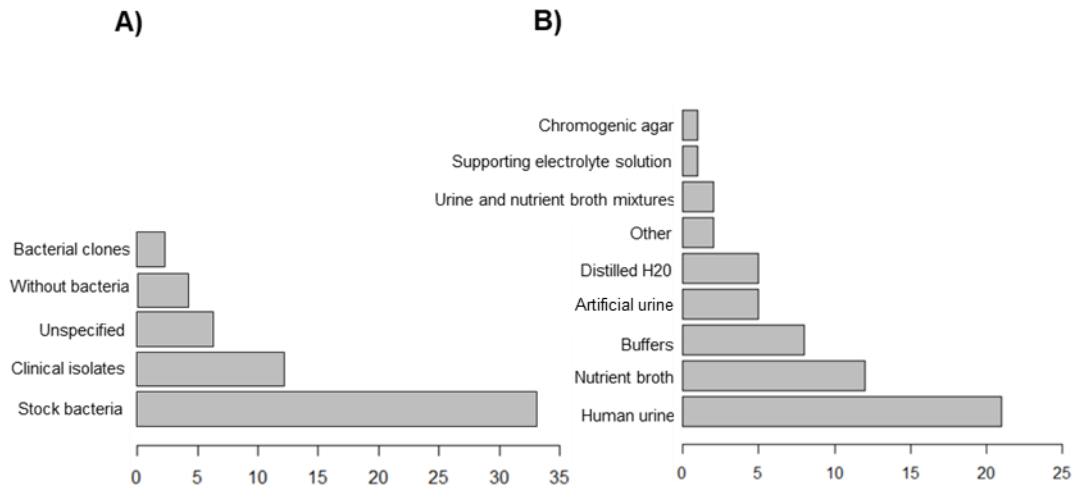

Figure 1.8: A) Shows the bacterial makeup of the artificially constructed samples. **B)** Shows the medium used in the artificially constructed samples. Nutrient broth refers to the use of Luria–Bertani, nutrient and Mueller–Hinton broth and Bacto brain heart infusion media. Buffers refers to the use of SELEX, phosphate buffered saline, luria broth and elution buffers. "Other" refers to mediums or solutions of unspecified makeup. Urine and nutrient broth mixtures refers to urine mixed with a type of nutrient broth at a 1:1 ratio.

Both articles are an excellent proof of concept for devices with a specific application for insertion into adult diapers as part of non-invasive testing for UTIs [131, 132], however, both would require testing with bacterial samples to validate the methodology proposed. Three articles did not specify the origin of the bacteria used, [155, 156, 171]. When testing a novel method with artificially constructed samples. The experimental setup must emulate the conditions of a UTI as closely as possible to see if the conditions of a UTI affect the proposed method in a negative way.

The media and solutions used in the reviewed articles are summarized in **Figure 1.8 B.** Of the articles, a number did not work directly with donated or artificial urine instead relying on another form of media [135-137, 153, 156]. The methods that use artificially constructed samples do not need to work with urine directly, this is demonstrated by instances wherein articles that used real clinical samples, or artificially constructed samples and real clinical samples first isolated the bacteria from the urine using a centrifuge, the bacteria were then resuspended in the media of choice [138, 140, 148, 164, 167, 168]. The rationale behind these experimental designs is that the media chosen for suspension of the bacteria had minor inherent variability when compared to urine enabling the chosen method to function without inhibition. Being able to

work directly from a urine sample is a desirable trait in a LOC device with a UTI application as it simplifies the method and reduces preparation time.

However, as mentioned previously working with urine comes issues, as urine is not homologous with differences in makeup and pH between [195] different people and of different health. Testing using artificial samples that do not use some form of urine as the media or solution are not necessarily neglecting the need to assess the proposed system with urine as the methods are not required to work with urine directly.

1.6.4 Antibiotics tested

Overall, when observing the use of antibiotics by group over time no one group of antibiotics were used significantly more than others (Kruskal test, p-value = 0.27). The antibiotics used in testing should reflect those that are used in clinical settings. However, these prescriptions are subjective to the country or region in which testing is conducted. One universal issue however is the overuse of broad-spectrum antibiotics, which contributes to antibiotic resistance [96]. The potential for rapid AST using LOC devices to identify effective narrow-spectrum antibiotics offers an excellent opportunity for tailored antibiotic treatments that will target the pathogen and minimize the chances of development of antibiotic resistance due to treatment with the incorrect antibiotic. This could also help to reduce the recurring UTIs that can occur due to prior antibiotic exposure [67, 180]. This opportunity, however, has yet to be fully explored. The use of broad-spectrum antibiotics made up 94.7% of the documented uses. The narrow-spectrum antibiotics used were mecillinam [115], oxacillin [115] and colistin [148]. Mecillinam is prescribed as part of international clinical practice for uncomplicated UTIs [196], and as a narrow-spectrum antibiotic, has minimal effect on intestinal microbiota [197]. Oxacillin is not usually used in the treatment of UTIs but is used to determine β-lactam antibiotic susceptibility in UTI causative bacteria [198]. Colistin is used for the treatment of drug-resistant bacteria, such as certain *Pseudomonas aeruginosa* strains [199]. The use of these narrow-spectrum antibiotics is in keeping with current literature. Testing rapid AST methods using broad-spectrum antibiotics however is still clinically important, if a broad-

spectrum antibiotic is prescribed UTI after rapid AST is conducted the probability of the pathogen surviving the treatment process is minimal. Additionally, as broad-spectrum antibiotics are commonly used in clinical settings then it is still important to test methods using broad-spectrum antibiotics to properly contrast and compare the proposed methods to those that are currently used. LOC devices aimed towards UTIs are still a developing diagnostic tool, in future work an effort should be made to conduct AST using more narrow-spectrum antibiotics to determine the viability of using the methods to conduct tailored antibiotic prescription.

1.6.5 Analysis time

One of the principal benefits of LOC based devices is that they offer a rapid time to analysis [200]. The summary of the time to analysis derived using the different analytical methods can be seen in **Figure 1.9,** showing no one method was significantly faster than the others (Pairwise Wilcoxon rank sum test, p-value > 0.05). On average immunoassay-based methodologies were the fastest method, which may be due, in part, to the application of the method with the application pertaining to the identification of bacteria [159-161, 169] rather than AST or AMR.

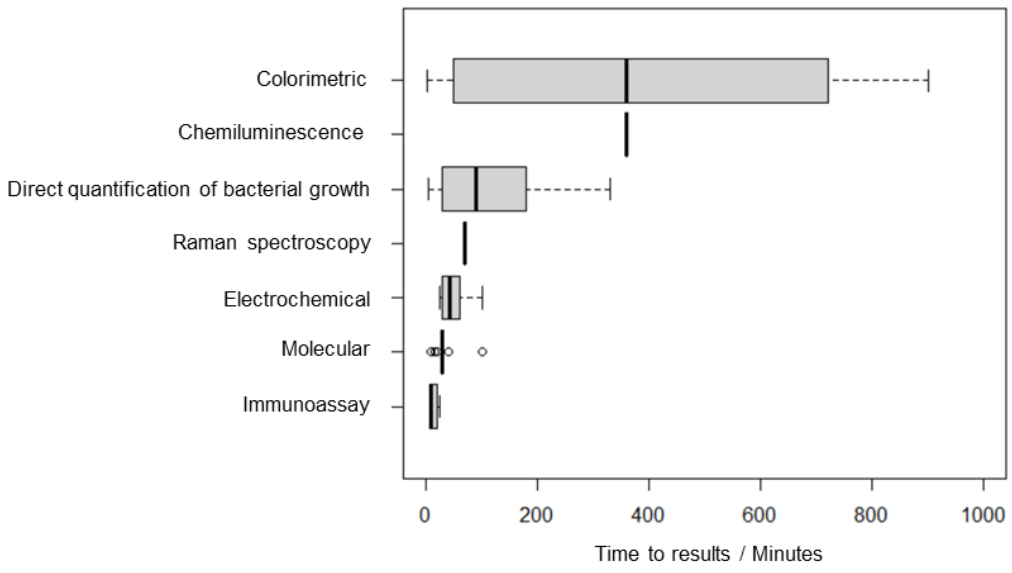

Figure 1.9: Time to analysis of the different detection methodologies employed in LOC devices.

There was no bacterial growth phase in the method and time-consuming genetic amplification methods were also not required which reduces the analysis time. The limitation however is it is likely that immunoassay-based methods will only be rapid when used for the identification of bacteria as using immunoassay-based methods for AST and AMR will most likely require a growth step in the method or time allowed for amplification which will increase the time to analysis. Molecular based methods are the second-fastest methods reported.

The overall singular fastest time to analysis was a colorimetric based method at two minutes. The proposed method used reaction pads which could detect nitrites which can be taken to identify the presence of a UTI [132]. The presence of nitrites can be taken to indicate a UTI as some uropathogens such as *E*. *coli* produce nitrites from the enzymatic conversion of nitrates as part of their metabolism [201]. The time to analysis of this method is dependent on how fast the reaction pads change colour in response to the introduction of nitrites. The LOC devices were designed to be inserted into adult diapers as a non-invasive UTI testing method for vulnerable people [132]. Although after urine is passed the pad takes two minutes to show a colour change, the time from the colour change occurring to the diaper being removed and the device inspected is a potentially random variable and may increase the time to analysis. Additionally, as the method in question was not tested with bacteria the validity of the time to analysis is yet to be established.

The overall second-fastest time to analysis, that was tested using bacteria was achieved using immunoassay-based methods and took a total of 6 minutes. The method utilized a smartphone-based detection system which could quantify the extent of the immunoagglutination of target bacteria versus capture antibodies which enabled the detection and identification of bacteria [161]. The immunoassay-based method is 4 minutes slower but the time to analysis is better defined as there is less potential for variability in the time between the result being made available and the result being recorded.

The slowest time to analysis was also demonstrated by a colorimetric method, media which had a time to analysis of 900 minutes (15 hours). This chromogenic media-based method could detect four different types of bacteria

without the requirement for specialized equipment [130]. In this niche use, devices relying on chromogenic media are excellent, but in comparison to the other methods, 900 minutes is slow.

Some of the articles did not specifically disclose a time to analysis but all of the methods found in the literature review that stated the time to analysis had a time to analysis faster than that of current culture-based bacterial identification and AST which takes 1440 minutes (24h) to complete [202]. Faster analytical methods will enable more rapid bacterial identification, AST and AMR testing which will help reduce the prescription of ineffective or partially ineffective antibiotics and extent the lifespan of currently used antibiotics.

1.6.6 Cost of analysis

Another defining feature of LOC devices is the low-cost nature of the methods as the material and consumable requirement is lower than with conventional lab-based methods. However, very few articles stated the cost of the testing unit. Of the articles, 25/45 [112, 129, 131-133, 135, 140, 141, 144, 146-151, 153, 158, 160-164, 166, 168] referred to the system being “Low-cost” or a synonym of the phrase. Two articles [159, 167] directly stated the cost of the device. The costs quoted in the studies that disclosed the exact cost were less than one cent (United States Dollars) for the materials per unit [159] and $0.27 [167]. One was reported as costly [143] due to the nature of the equipment involved in the method. The remaining articles made no reference to the cost of the device or method.

The least expensive method for conducting AST that is widely used is the “traditional” disk diffusion assay which costs $2.42 – 4.85 for the materials such as agar and antibiotics [203]. The longevity of techniques like the disk diffusion assay are in part due to their inexpensive nature, as well as versatility in dealing with multiple different types of bacteria. If LOC devices are to be implemented in a clinical setting, then the cost of the LOC unit and reagents should be comparable to or less expensive than the currently used methods. Some of the methods proposed by the articles have hidden costs. The hidden costs lie in the equipment required to facilitate the method. An example would

be the requirement for specialized equipment required for Raman spectroscopy that is quoted as ‘cost effective’ [164] or chemiluminescence detection that was quoted as a ‘low-cost solution process’ [162], as well as having no disclosed cost [169] and inferred lower cost due to lower material requirement [162, 163, 169]. Arguably the most cost-effective methods are those that require no equipment or use methods that utilise equipment that is already used in clinical settings. For example, PCR based diagnostic testing is currently carried out in healthcare organisations [204], thereby, PCR and other molecular based methodologies can be more readily implemented into healthcare systems.

1.6.7 Limitations & Recommendations

In the reporting of LOC devices aimed toward UTIs, there were several notable limitations in the presentation of information that have been reported. Firstly, the time to analysis of the LOC devices was sometimes either not clearly defined, or otherwise unspecified. A defining feature of LOC devices is the speed at which results can be gleaned [117] versus standard lab-based practices. Without a definitive disclosure of the analysis time, it becomes impossible to compare the relative speed of analysis. Secondarily, the presentation of costs was another limitation of the studies. Phrases such as “low-cost” or “inexpensive” were regularly used, however, these omissions in the literature yield no data for a proper comparison to the cost of the lab-based systems. Thirdly, there is a focus on testing methods using artificially constructed samples to emulate UTIs. Lastly, none of the LOC devices reported has been commercialised or implemented in a clinical setting despite some of the devices demonstrating a high degree of success using real clinical samples. Therefore, there is a need for translational research to expedite the use of these devices in clinical settings and, thereby, demonstrating their clear advantage over current methods.

Regarding the disclosure of the time taken to analysis; when a method is labelled as fast, or faster than another type of method the time to analysis should always be disclosed in the form of a total time taken for the method to be conducted or as a range of values should the analysis time differ with

different bacterial concentrations. Directly quantifying the costs of LOC devices may prove challenging, however, two of the other studies showed that it is possible as the material [159] and testing costs [167] were both quoted. It may be that the material costs per unit are negligible in most systems but reporting the cost as negligible as opposed to low cost when an exact figure is difficult to quantify gives a clearer indication that the system is indeed low cost in terms of material. When discussing consumables if the cost cannot be quoted the number of tests or runs that can be achieved using the device and the consumables used vs the lab-based methodological counterpart could be useful. One of the defining traits of microfluidic and LOC devices is their ability to reduce costs and consumables, to better determine the cost to benefit ratio of using LOC devices it would be good to see a clearer indication of exactly to what degree these devices can reduce costs. This in turn will enable a full cost-benefit style of analysis in future enabling a fair comparison of emerging technology to the gold standard methods. There is a cost difference associated with the devices made during research and development versus when the units can be mass-produced for commercial use. However, knowing the cost of the research and development units is still a beneficial figure to quote in the literature. There are different challenges presented in getting a methodological approach to work under lab conditions versus with a clinically acquired sample. In the future, increased use of real clinical samples would help further validate the concept of microfluidic and LOC based UTI analysis systems. Pertaining to commercialisation, a small consideration is further testing of a method would be required before commercialisation or use in a clinical setting which may already be underway. A much larger consideration however is determining how well the proposed method will integrate in healthcare systems.

This then brings up the topic of accessibility of the methods in a clinical setting such as the NHS. Ideally a LOC device should function as a “sample in, answer out” type of diagnostic device that operates independently of the equipment that may be used in clinical settings, thus enabling the efficient integration of the LOC device into the existing infrastructure. However, some methods may be supported by existing infrastructure. Therefore, in future publications a discussion on how easily a method could be implemented in a

clinical setting would be valuable in order to determine if it would be feasible to replace an existing method with a newly proposed method. The viability of the newly proposed methods could then be validated using blinded testing with clinical samples. This type of testing is crucial for establishing a new methodology as it enables direct comparison to the methods currently used in the clinical setting and, therefore, allows for an objective assessment of how well the proposed method performs, and whether it is feasible to replace the currently used methods with the proposed alternatives.

Although there are limitations with currently used culture-based AST one benefit of the system is the “One size fits all approach” which means that the same methods can be applied to a variety of bacterial infections, not just UTIs. However, the adaptability of microfluidic devices and the theory behind the mechanism are not restricted to just UTIs and could be adapted or used for other infectious bacterially induced diseases. Ultimately, microfluidic and LOC based devices may still be somewhat undergoing development, however, they do offer rapid, specific, and reliable tools for diagnostic, AST, and AMR testing for UTIs and potentially other infection types. There is a requirement for faster diagnosis, AST and AMR whilst maintaining a cost-effective approach while maintaining a high degree of accuracy, LOC devices have a great deal of potential to fit this function which will benefit patients, the workers in healthcare settings as well as work well with antibiotic stewardship schemes by helping to extend the longevity of clinically relevant antibiotics.

1.7 Thesis aims and objectives

The overall aim of this PhD project is to enable determination of antibiotic susceptibility of the bacteria causing UTI’s using a novel electrochemical LOC device. This will be achieved through completion of the objectives below:

1) To assess the sensitivity of electroanalytical methods in detecting the redox indicator resazurin and to assess the potential of binding resazurin to the surface of screen-printed macroelectrodes.

2) To assess the viability of using resazurin bulk modified macroelectrodes to conduct antibiotic susceptibility testing by determining how rapidly antibiotic susceptibility can be achieved using a model of *E. coli.*

3) To optimise the concentration of antibiotics loaded into hydrogels to achieve the determination of bacterial antibiotic susceptibility efficiently using models of *E. coli* and *K. pneumoniae* to emulate UTIs caused by common causative bacteria, as well as alter some key conditions to refine the methods.

4) To design a LOC device capable of housing screen-printed macroelectrodes and reagents by using computer-aided design that is then milled from polycarbonate using computer numerical control.

5) To assess the performance of the LOC devices used in combination with the resazurin bulk modified screen-printed macroelectrodes and antibiotic-loaded hydrogels as part of an electrochemically based antibiotic susceptibility testing method.

2. Chapter 2: Electrochemical Analysis

Elements of the work presented in this chapter has been published as Crane, B., Hughes, J.P., Rowley Neale, S.J., Rashid, M., Linton, P.E., Banks, C.E., Shaw, K.J., Rapid antibiotic susceptibility testing using resazurin bulk modified screen-printed electrochemical sensing platforms, Analyst, 146: 5574-5583 (2021).

Executive summary

In this chapter, we cover the electrochemical behaviour of resazurin using cyclic and differential pulse voltammetry (DPV) using carbon-graphite referenced screen-printed macroelectrodes (C-SPEs), and Ag|AgCl referenced screen-printed macroelectrodes (Ag-SPEs).

- At a physiological pH, electrochemical resazurin reduction was determined to be a diffusion-controlled reaction.
- C-SPEs produced a less stable potential but produced more consistent resazurin reduction peaks when compared to Ag-SPEs.
- All macroelectrodes were able to detect resazurin down to concentration of 0.00156 mM. The GC macroelectrode demonstrated the best resazurin limit of detection of 0.0096 mM when using DPV. C-SPEs were the second most sensitive at 0.012 mM with the Ag-SPEs being the least sensitive at 0.043 mM.
- C-SPEs were used as a template to produce resazurin bulk modified SPEs (R-SPEs) which reliably produced easily interpreted resazurin reduction peaks.

2.1 Introduction

Electrochemistry offers wide range of applicable techniques for qualitative and quantitative analysis of a target analyte. The breadth of the electroanalytical techniques available make electrochemistry incredibly versatile as a tool which can be effectively utilised in a biosensing platform [112, 152-154, 205]. An electrode system is made up of three individual parts which is shown in **Figure 2.1 A**:

1) The working electrode (WE), which acts as the conduit for the potential that is applied by the potentiostat and, thereby, carries out the principal step of electrochemical experimentation as reactions occur on the surface of the WE.
2) The counter electrode (CE), which completes the circuit formed when a potential is applied to the WE as shown in **Figure 2.1 B**. To ensure the kinetic reaction at the surface of the WE is not limited by the counter, the counter must have a larger working surface area than the WE.
3) The reference electrode (RE), which maintains a constant potential by providing a reference point to which potential applied to the WE can be compared. This type of electrode is referred to as a three-electrode setup. [205, 206].

The movement of an analyte to the surface of the WE is controlled by three types of mass transport namely convection, migration, or diffusion. Convection applies to analytes that move through the solution via mechanical means through stirring or vibrations.

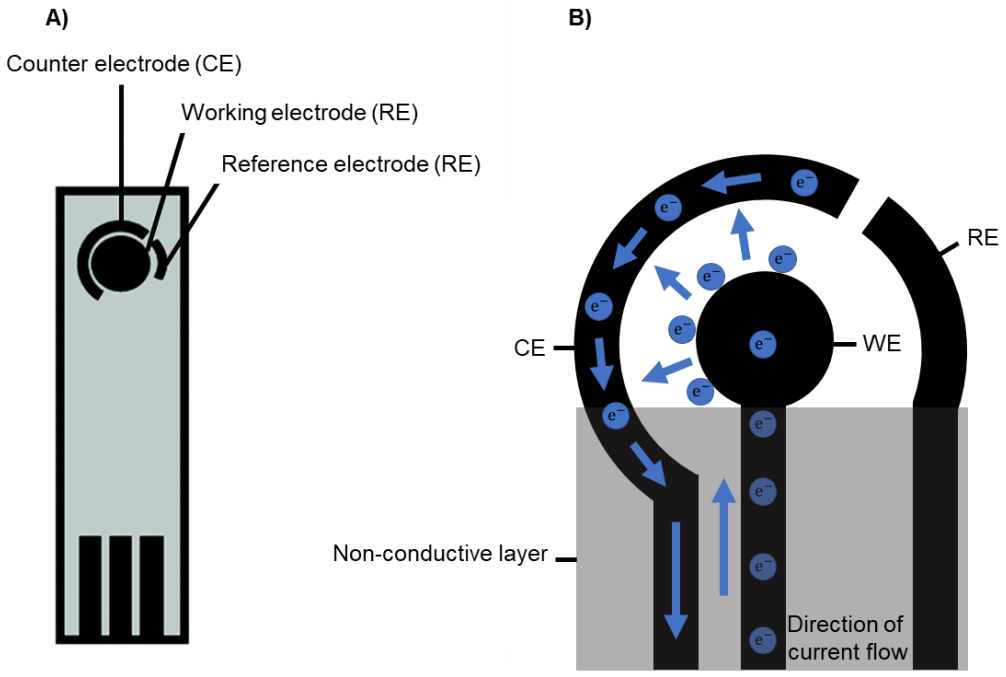

Figure 2.1. A) Schematic showing the three-electrode system of a carbon-based, screen-printed electrode. **B)** Schematic showing the flow of electrons through an SPE based three-electrode setup.

Migration applies to analytes that move through the action of an electric field through opposite polarities. Diffusion applies to analytes which move due to the formation of a concentration gradient between the WE and the rest of the solution [207]. Different factors can influence each mass transfer type, for example a lack of mechanical action will inhibit the electrochemical reduction of a convection-controlled analyte, or a low concentration gradient will inhibit a diffusion-controlled process [206, 207].

Recently the development of screen-printed macroelectrodes (SPEs) has provided a viable alternative to conventional macroelectrodes. SPEs have low cost due to their scales of economy and provide a highly reproducible one-shot sensor. The SPE printing process can be used to mass-produce SPEs compatible with miniaturised processes and methods. During or after the fabrication, SPEs can also be readily modified to fit a niche function which makes SPEs incredibly versatile. Conventional macroelectrodes on the other hand cannot be easily modified and, per unit, are more expensive than SPEs [208, 209] in addition to requiring more upkeep such as sonication to remove particulate matter between uses [210], electrochemically based cleaning [211], and mechanical polishing [206], which are not required when using SPEs. There are a range of electroanalytical techniques that can be used, discussed below are two of the most used techniques: cyclic voltammetry and differential pulse voltammetry.

2.1.1 Cyclic voltammetry

Cyclic voltammetry (CV) is an electroanalytical technique which is classically used to characterise the reduction oxidation (redox) behaviour of an electrochemically active analyte. To induce an electrochemically driven redox reaction, a potential is applied which starts at a more positive potential (E1), the applied potential is then swept negatively, this is called a cathodic trace. The applied potential is swept along a voltage range terminating at the switching potential (E2), whereafter the potential is then swept back towards a more positive potential terminating at E1, this is referred to as an anodic trace. This process is shown as a schematic in **Figure 2.2 A.** During the cathodic trace, electrochemical reduction occurs which is represented by a dip

in the current as shown by C1 in **Figure 2.2 B**. During the applied potential, a circuit forms between the WE and the CE, a reduction peak forms when electrons from this circuit reduce the analyte in solution, in this example potassium ferrocyanide, rather than completing the circuit, which induced the decrease in the current [206]. During an anodic sweep, the reduced form of the potassium ferrocyanide is oxidised, with the lost electrons becoming part of the circuit formed between the WE and the CE which is shown by an increase in the current as shown by A1 in **Figure 2.2 B**.

The oxidation and reduction peaks form due to development of a diffuse double layer, sometimes also referred to as an electrical double layer [212]. Using the formation of a reduction peak as the example, the diffuse double layer references the reduced form of the analyte that accumulates at the surface of the WE during an applied potential. This layer prevents the mass transport of the non-reduced form of the analyte to the surface of the WE. Additionally, a second layer also forms on top of the primary layer at the surface of the WE which is made up of the non-specifically absorbed unreduced form of the analyte which is attracted to the WE. Together these layers limit the rate of electrochemical reduction and, thereby, the current returns to a more neutral value resulting in the formation of a peak [206, 212].

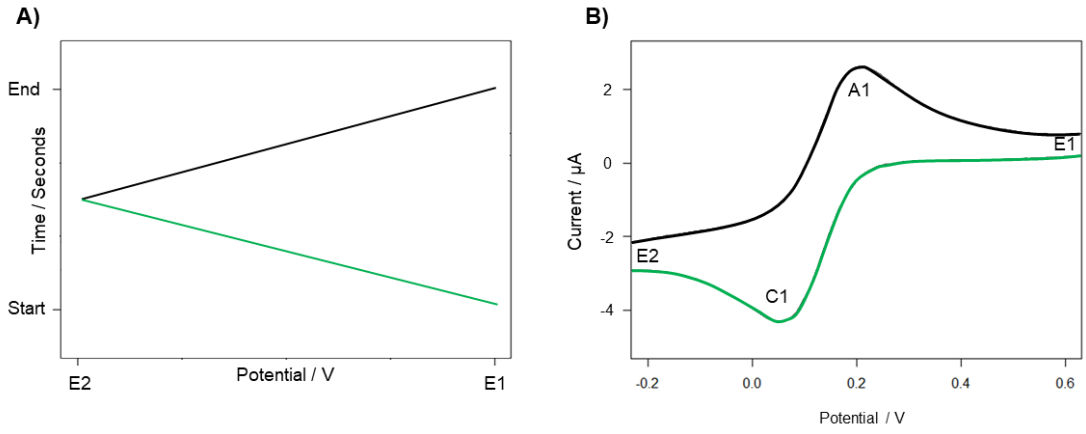

Figure 2.2. A) Shows the applied potential as a function of time in a cyclic voltammogram with E1 referencing the start of the cathodic sweep and where the anodic sweep returns too. E2 references the switching potential. **B)** Cyclic voltammogram of the reversible reduction of potassium ferrocyanide (1 mM) at a scanning rate of 0.05 Vs^{-1}.

The redox behaviour of a target analyte can be assessed after a cathodic and anodic trace has been applied. The height (I_p) and the position (E_p) of the peaks can be calculated using a three-point configuration as shown in **Figure 2.3**. The I_p of the reduction, and oxidation peaks is dependent on two variables, namely the concentration of the analyte and the applied scanning rate with an increase in either resulting in higher reduction and oxidation I_p values. The scanning rate is defined as the step size per second of the applied potential, i.e a scanning rate of 0.05 Vs^{-1} means for every second, the applied potential increased by 0.05 volts. The relationship between the I_p of the redox peaks and the applied scanning rate can identify the redox behaviour of a target analyte. For example, a linear relationship between a plot of the cathodic I_p versus the scanning rate would demonstrate that the reduction of an analyte is a absorption-controlled process, whereas, if the relationship in the plot of cathodic I_p versus the square root of the scanning rate is linear then the reduction of the analyte is a diffusion-controlled reaction. Additionally, the position of the redox peaks (E_p) can also be used to determine key characteristics about a target analyte. The distance between the cathodic E_p and the anodic E_p can be used to determine if a redox reaction is reversible. In a reversible redox reaction, the peak separation should be 57 mV at 25 °C, deviation from this enables the identification of non-reversible reactions.

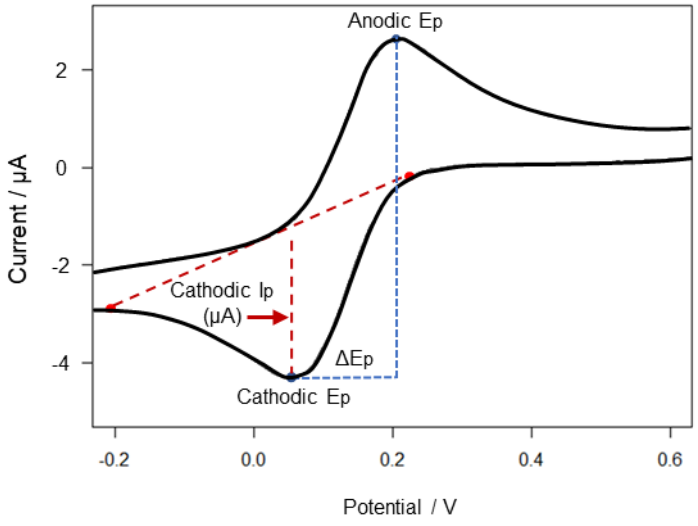

Figure 2.3. Voltammogram of the reversible reduction of potassium ferrocyanide (1 mM) at a scanning rate of 0.05 Vs^{-1}. Figure shows a three-point configuration for calculating I_p and E_p (Red) and the distance between the reduction and oxidation peaks (blue).

A non-reversible reaction is characterised by there being a high barrier to the electron transfer process, causing the cathodic E_p to shift to a more negative potential versus reversible reactions, as well as causing there to be a greater peak separation between the cathodic and anodic E_p values.

Therefore, CV is an excellent analytical tool for identifying the potential window in which electrochemical redox reactions occurs which is crucial for developing an electrochemically based AST system. Additionally, it enables the identification of the redox behaviour of an analyte in terms of the which method of mass transport occurs when the analyte is electrochemically reduced, if the analyte sensitive to changes in pH and the impact it has on the redox behaviour, as well as if the electrochemical reaction is reversible. However, the development of the double diffuse layer during the formation of a cyclic voltammogram limits reduces sensitivity of CV, thereby preventing CV from accurately determine small changes in the concentration of an analyte due to occlusion of the WE with the reduced form of the analyse. Additionally, CV has the issue of there being a background charging current throughout the experiment during the applied potential, which restricts the detection limit of CV further [213]. Therefore, for the sensitive detection of an analyte, a different electroanalytical method is required.

2.1.1 Differential pulse voltammetry

Differential pulse voltammetry (DPV) fulfils this requirement for a more sensitive electroanalytical technique. In DPV, a series of regular voltage pulses are superimposed on the applied linear potential as shown in **Figure 2.4 A**. The length of the pulsed potential is controlled by the E_{pulse}, the length of time the E_{pulse} is applied is controlled by the t_{pulse} which is visually characterised by the DPV staircase as shown in **Figure 2.4 B**. This helps to overcome the limitations of diffuse double layers as with the use of pulses the diffuse double layer takes longer to form which facilitates superior detection of an analyte [208, 214]. In using DPV, an analyte can be detected to a concentration of 10^{-7} to 10^{-8} mole/L under ideal conditions [214]. DPV however does have some limitations, DPV cannot be effectively used to determine the redox characteristics in terms of information derived from Ip versus scanning

rate and is less efficient at determining redox windows due to DPV being a more time consuming process when compared with CV [215]. Despite these limitations, DPV is vastly superior when the sensitive detection of an analyte is required, thereby DPV could be used as the basis for an electrochemically based AST platform.

Given the DPV uses pulses of potential rather than the constant application of a potential, the current generated in the circuit in calculated using the following formula:

$$I_{n2} - I_{n1} = \Delta I_{n,dp} \quad \textbf{Equation 2.1.}$$

where n is the number of the pulse, I_{n2} is the current generated after the pulse and In_1 is the current before the pulse, the method by which the I_{n1} *and* I_{n2} values are derived from the DPV staircase are shown in **Figure 2.4 B**. Therefore, a differential pulse voltammogram is made up of a series of discrete $\Delta I_{n,dp}$ data points, calculated from the current values at each differential pulse ($_{dp}$), plotted against the applied potential, a schematic of which is shown in **Figure 2.4 C**. This type of applied potential overcomes the limitations imposed by the diffuse double layer which enables the superior detection of an analyte when compared to CV.

In summary, although CV is an excellent analytical tool for determining the redox potential windows, and redox behaviour of an analyte, the diffuse double layer limits the ability of CV to enable the sensitive detection of an analyte. Although DPV is less well suited for determining the redox potential windows, and redox behaviour of an analyte, DPV is a much more sensitive electroanalytical technique for the detection of an analyte. In DPV, a series of regular voltage pulses are superimposed on the applied linear potential, visually characterised by the DPV staircase. This helps to overcome the limitations of diffuse double layers as with the use of pulses the diffuse double layer takes longer to form which facilitates superior detection of an analyte [208, 214].

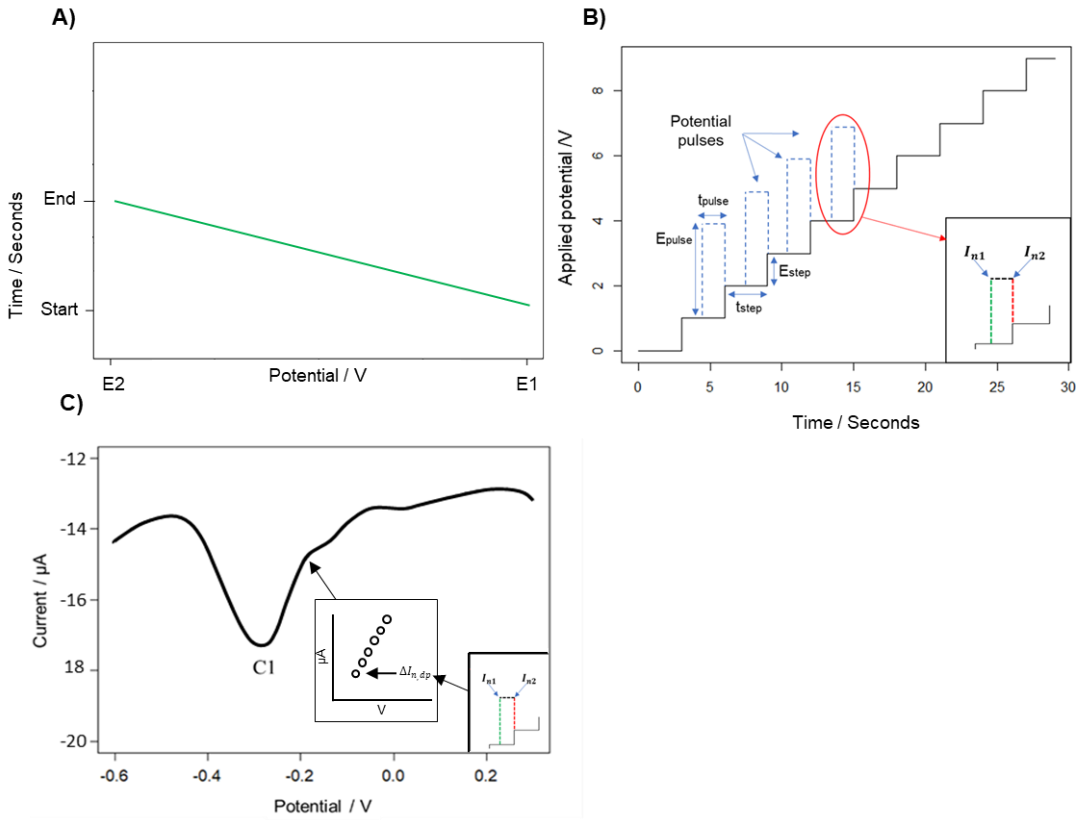

Figure 2.4. A) Shows the applied potential as a function of time in a cyclic voltammogram with E1 referencing the start of the cathodic sweep and E2 referencing the terminal potential. **B)** Example of a DPV staircase ramp showing the function of E_{step}, t_{step}, E_{pulse} and t_{pulse} [208, 214], as well as how I_{n1} and I_{n2} are derived from the staircase ramp which enables the current to be derived (**Equation 2.1**). E_{step} controls the size of the voltage increase across the applied potential range, t_{step} controls the time between the increases in the applied potential, E_{pulse} is the size of the current response to the application of the applied potential, and t_{pulse} controls how long the potential is applied to the WE. **C)** Shows how a differential pulse voltammogram is made up of discrete $\Delta I_{n,dp}$ data points derived from the equation $I_{n2} - I_{n1} = \Delta I_{n,dp}$.

2.1.2 Resazurin Based AST methodologies

Resazurin (7-Hydroxy-3H-phenoxazin-3-one 10-oxide), also known as alamar blue is a dye which is cell-permeable, non-toxic, and redox-sensitive. Resazurin has a nitrone group which can be reduced both electrochemically [216], and biologically [217], in a two-step, two-electron process. Resazurin is reduced to produce resorufin in an irreversible reaction, resorufin is then reduced to form dihydroresorufin as part of a reversible reaction as shown in **Figure 2.5** [216, 217].

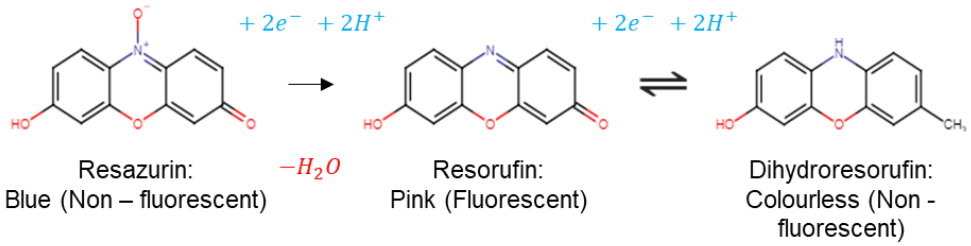

Figure 2.5. Simplified reduction pathway of resazurin to resorufin and resorufin to dihydroresorufin.

The location where resazurin is reduced in the bacterial cell was recently determined using *E. faecalis* as a model organism, which demonstrated that resazurin reduction occurs intracellularly and is most likely facilitated by dehydrogenase enzymes such as nicotinamide adenine dinucleotide dehydrogenase. Resorufin reduction, however, can occur either intra- or inter-cellularly [217]. Resazurin has a documented history of use in microbiology. The first documented use of resazurin was to detect the bacterial contamination of milk via a colorimetric assay whereby resazurin changed colour from blue to pink in the presence of bacteria [218].

Resazurin colorimetric based detection systems are, however, relatively slow as the method relies on the visual identification of the colour change. Resorufin is the fluorescent reduced form of resazurin, the detection of resorufin fluorescence can then be used to indicate metabolically active cells [219, 220]. Fluorescent based methods have successfully been used to rapidly identify antibiotic susceptibility [221] as well as having been used in minimum inhibitory concentration testing [222-224]. Although faster than colorimetric testing, there are disadvantages to using fluorescent-based detection. These methods rely on a sufficient concentration of resazurin being reduced for the fluorescence to increase beyond background levels. The time for this to be achieved is variable, with bacterial concentration and the medium being used both affecting the time to determine a significant change [225]. Additionally, resorufin can also be reduced to produce the colourless dihydroresorufin resulting in a loss of fluorescence [226, 227]. The loss of resorufin can cause misrepresentation of the number of metabolically active bacteria [228].

Electrochemical means of conducting AST eliminates the requirement for waiting for resorufin concentrations to reach detectable levels, instead, electrochemistry can be used to detect changes in the concentration of resazurin directly.

A summary of the published methods of electrochemical AST using resazurin and other electroactive analytes can be found in **Table 2.1.** Electrochemically based AST methods can be categorised as either label or label-free testing. Labelled testing methods use a label, in the form of an electrochemically active cell viability indicator such as resazurin [112, 205, 229], or another redox agent such as potassium ferrocyanide [230], which are absorbed at the WE. Label-free testing uses no form of label or dye, instead, these methods use impedance spectroscopy-based on bacterial capture [235, 236], or motility [157]. Alternatively, the bacterially induced pH change to the bulk solution was also used [234]. Each of these analysis times are faster than the 24 to 72 hours required for conducting culture-based disk diffusion assays. One of the primary advantages of label-free testing is that the is no dye used to interfere with the action of an antibiotic, or the cellular processes of the bacteria [234]. Despite the theoretical advantage posed by using label-free methods, the time to analysis demonstrated was, on average, similar to that of the labelled methods. Of the label-free method, two used bacterial capture through antibodies as part of the methodology [235, 236]. UTIs are caused by multiple different types of bacteria, a breakdown of which is covered in **Figure 1.4**. Methods that rely on antibody-based bacterial capture would require either extensive modification to the biosensor to enable the detection of all common causative types, or a series of specialised sensors for each of the different bacteria which complicates the setup of the method.

The use of a resazurin derived biosensor that could be used in combination with CV to detect changes in pH that infers the presence of metabolically active bacteria was also discussed [234]. Although *E. coli* K -12 can induce a significant change in pH, not all bacteria will have the same pH-based effect. Therefore, some modification of the method may be required to work ubiquitously with all uropathogenic bacteria. The method using the detection of motile bacteria presented a novel approach.

Table 2.1 Comparison of label free, labelled electrochemical AST, resazurin fluorescent assay and disk diffusion assays. The following abbreviations were used, working electrode (WE), counter electrode (CE), reference electrode (RE), cycle voltammetry (CV), differential pulse voltammetry (DPV), antibiotic susceptibility testing (AST), *Acinetobacter baumannii* (*A. baumannii*), *Burkholderia pseudomallei* (*B. pseudomallei*), *Citrobacter freundii* (*C. freundii*), *Escherichia coli* (*E. coli*), *Klebsiella pneumoniae* (*K. pneumoniae*), *Salmonella gallinarum* (*S. gallinarum*), *Staphylococcus aureus* (*S. aureus*), *Staphylococcus haemolyticus* (*S. haemolyticus*) [231].

Methodological approach	Electrode material	Method	Bacteria Tested	Antibiotics Tested	Time to Analysis (Minutes)	Advantages	Disadvantages
Disk diffusion assay	N/A	Zones of inhibition [104]	Any Isolates	Any	960 - 1440	Can be used with any bacterial isolates	Slow
Broth microdilution assay	N/A	Optical density changes [232]	Any Isolates	Any	960 - 1200	Can be used with any bacterial isolates	Slow
Real time quantitative PCR	N/A	Quantitative analysis of amplified gene [233]	Any Isolates	N/A	90	Can be used with any bacterial isolates	Bacterial specific
Microwell array resazurin assay	N/A	Fluorescent detection of resorufin [148]	Clinical isolates: *E. coli* *K. pneumoniae* *S. aureus* *A. baumannii* *C. freundii* *S. haemolyticus*	Freeze dried, multiplexed: Ampicillin Ciprofloxacin Colistin Erythromycin Gentamicin	330	High throughput	Slow relative to electrochemical methods
Label free	Planar pyrolytic graphite	Cyclic voltammetry detection of pH change via redox-active crystalline layer [234]	*E. coli* (K – 12)	Added to solution: Ampicillin Kanamycin	60	No dye	Extensive modification process
	Tantalum silicide	Impedance detection using bacterial capture [235]	*E. coli* ATCC 25922	Added to solution Ampicillin	60 - 120	High throughput	Specific to one bacterium
	N/A	Impedance detection of motile bacteria [157]	*E. coli* ATCC 25922 (Susceptible) & ATCC 700609 (Resistant)	Added to solution Nalidixic acid	N/A	Fastest AST method discussed	Requires adaptation for non-motile bacteria
	Silver interdigitated carbon WE, CE & RE	Impedance detection using bacterial capture [236]	*E. coli* K – 12 (ATCC 700891) Methicillin-resistant SRM551	Added to solution: Ampicillin Erythromycin Ciprofloxacin Methicillin Daptomycin Gentamicin	<90	No dye to interfere with cellular processes.	Specific to one bacterium
Labeled	Carbon WE, CE & RE (Published work of the thesis)	DPV detection of resazurin [231]	*E. coli* ATCC 25922	Added to solution Gentamicin	90	Single-step modification	Requires preincubation step.
	Gold WE &CE, silver RE	Impedance or DPV detection of oxidation using potassium ferrocyanide [230]	*S. aureus* (ATCC 29213) Methicillin-resistant S. aureus (ATCC 43300)	Added to hydrogel: Amoxicillin Oxacillin	<45	Low cost, reagents encapsulated in a hydrogel	Electrodes require maintenance
	Platinum WE, CE, Ag|AgCl RE	DPV detection of resazurin [205]	*E. coli* ATCC 25922 *K. pneumoniae* ATCC 700603	Added to solution: Ampicillin Kanamycin Tetracycline	180	Reusable biosensor	Electrode type incompatible with miniaturization
	Carbon WE & CE, Ag|AgCl RE	DPV detection of resazurin [237]	*S. gallinarum*	Added to solution: Ofloxacin Penicillin	60	Single-step modification	Modification process currently incompatible with bulk modification
	Gold WE, CE & RE.	DPV detection of resazurin [112]	*E. coli* ATCC 700928 *K. pneumoniae* ATCC 700603	Added to solution: Ciprofloxacin Ampicillin	30	High throughput	Reagents must be added to electrode chambers manually

A constant low amplitude voltage was passed across a microfluidic channel, motile bacteria that entered the channel induced a change in the current of the circuit induced by the applied voltage enabling determination of antibiotic susceptibility effectively instantaneously [157]. However, the method, in its current configuration is incompatible with non-motile bacteria and, therefore, cannot be effectively used for all bacteria. Within the confines of the identified articles, there is no significant advantage in using label-free over labelled electrochemical AST.

When comparing the labelled methods, the two methods using the smallest volumes of 1 nL (LOC device chamber) [112], and 160 µL were the fastest [229]. The benefit provided by working on the nano or micro scale is that heat and mass transfer occurs more rapidly leading to reduced analysis times [200]. Although different methodological setups were used, each of the studies used DPV as the electroanalytical technique for detecting changes in the peak current that indicate live bacteria versus antibiotic susceptible bacteria [112, 205, 229]. Pertaining to electrochemical AST, DPV is the best current electroanalytical technique for electrochemical resazurin AST, this is due to the sensitivity of DPV as an electroanalytical technique. Under ideal circumstances DPV can detect an analyte to a concentration of 10^{-7} to 10^{-8} mole/L [214], thus, enabling the detection of small changes in the concentration of resazurin enables rapid and accurate AST.

These studies show that the electrochemical detection of resazurin is a viable method for conducting rapid AST. Upon reviewing the literature, it is apparent that there is a timely requirement for a simple method of resazurin based electrochemical AST using SPEs. Modification of SPEs using screen printing in this type of application has also not been explored yet in the literature which offers a unique opportunity to explore a novel avenue of SPE modification. The integration of resazurin bulk modified SPEs into a LOC device offers a novel and simpler method of conducting electrochemical AST with fewer preparatory steps but retaining the fast time to analysis of the other electrode types.

2.1.3 Screen-printed macroelectrodes

A recent development in the electrochemical analysis is the use of SPEs which provide a series of benefits over conventional macroelectrode setups. SPEs were developed to fit a niche where inexpensive, single-use and reliable macroelectrodes could be used for *in situ* analysis [238]. The largest benefit of using SPEs over a comparable macroelectrode such as the glassy carbon macroelectrode is how modifiable SPEs are which allows them to fit a variety of applications. The ink composition from which the macroelectrodes are printed can be altered with the inclusion of polymers, metals, and enzymes to fit the desired function. Various metals can be printed onto the various macroelectrode elements such as platinum for the CE [239] or Ag|AgCl [211]. Carbon offers a reliable, cheap material for SPE composition and can be used as a reference material for SPEs [206]. Additionally, a benefit of carbon is the wide range of potentials that carbon will function at, with carbon operating at lower potentials than that of Ag|AgCl and platinum references [238]. SPEs can be modified with a variety of compounds including but not limited to; antibodies, aptamers, chemical ligands, nanoparticles and phages to facilitate AST and quantification of bacteria [240].

SPEs have been used to conduct AST independently of resazurin through the use of modifications and other electroanalytical techniques. For example, one such approach saw the use of silver interdigitated carbon-based SPEs assembled in plastic LOC type devices that captured bacteria using bacterial-surface-specific antibodies. Susceptibility was determined using impedance, which is an analogue of resistance, observed as a significant increase in impedance with the application of an effective antibiotic due to there being fewer bacteria receptor complexes formed at the surface of the electrode. This method could determine antibiotic susceptibility in <90 minutes [236].

Other examples include the use of a chitosan modified screen-printed carbon electrode array. The purpose of the modifications was to prevent antibiotic fouling of the electrodes. This method was used to identify aerobically respiring bacterial cells in response to the introduction of an antibiotic using amperometry to detect response currents using an oxidative

cocktail of ferricyanide and dichlorophenolindophenol. This could be used to identify antibiotic susceptibility in 20 minutes [241].

Other materials than carbon can be used for the fabrication of SPEs. Gold SPEs with Ag|AgCl references have been used in conjunction with agarose hydrogels loaded with the redox indicator potassium ferrocyanide mounted over the WE, CE, and RE. Both DPV and impedance were used to monitor bacterial growth in response to the inclusion of antibiotics in the hydrogel. DPV could be used to determine the extent of the reduction of potassium ferrocyanide by aerobically active bacteria. Impedance instead, as previously mentioned, could be used to monitor changes in the resistance of the circuit based on the electrode-electrolyte interface that is influenced by the aerobic respiration of bacteria [230].

Carbon-graphite SPEs (2mm WE) with a Ag|AgCl RE was modified via the addition of the redox indicator di-dodecyl dimethylammonium by drop-casting a 0.1 M concentration in chloroform onto the WE. Once the chloroform had evaporated, this facilitated the reading of the formal redox potential of the electron transfer process that occurred between the electrode of the SPE and the bacterial sample using CV. A higher current was indicative of high bacterial cell counts, the height of the current as a percentage after the introduction of an antibiotic could then be used to determine antibiotic susceptibility of bacteria in two to five hours [242].

SPEs are a versatile tool which are constantly evolving as an analytical platform with new modifications being made to improve upon the design [243]. SPEs have yet to be modified via the further screen printing of desired additive onto the WE of the SPE. This method of modification would enable the bulk modification of SPEs using pre-existing fabrication tools and only require a specialised mask for the printing process. In this thesis we report for the first time, the bulk modification of SPEs with resazurin by screen printing, and the integration of SPEs into LOC devices as part of a closed antibiotic testing system with an application aimed towards UTIs.

2.2 Aims and objectives

The main aim of this chapter is to electrochemically profile resazurin. This will be achieved through the completion of the objectives below:

- Using CV to determine the potential window where resazurin reduction occurs and whether the reduction of resazurin is diffusion or absorption controlled.
- Using DPV to determine the limit of detection of resazurin and assess the reproducibility of the reduction peak height produced by the SPEs with the different reference materials.
- Determine if the bulk modification of SPEs to incorporate resazurin is a viable delivery mechanism for the redox indicator into a solution.

2.3 Experimental

2.3.1 Fabrication of screen-printed macroelectrodes

Electrochemical profiling was conducted on resazurin using SPEs with two different RE materials. The SPE fabrication process started with the screen printing, as shown in **Figure 2.6 A**, of a carbon-graphite ink (product code: C2000802P2; Gwent Electronic Materials Ltd., U.K.) layer onto a polyester substrate (Autostat, 250 µm thickness) using a DEK 248 screen-printing unit (DEK, Weymouth, UK) to produce the macroelectrodes shown in **Figure 2.6 B**. This precursor layer was then cured at 60°C in a fan assisted oven for 30 minutes. After the first curing process, the connections were then sealed using a dielectric paste (product code: D2070423D5; Gwent Electronic Materials Ltd., U.K.) after which the SPEs are cured for a second time at 60ºC for 30 minutes, and the macroelectrodes were then ready for use. Two different generations of SPEs were fabricated with both types having a 3mm diameter WE but different overall geometries which are shown in **Figure 2.6 C**. Two different types of first-generation SPEs were fabricated, specifically, carbon-graphite paste referenced SPEs (C-SPEs) and Ag|AgCl referenced SPEs (Ag-SPEs). The WE of the unmodified first- and second-generation C-SPEs was modified to include resazurin (R-SPEs) by screen printing resazurin that had been mixed with carbon-graphite paste onto the WE as shown in **Figure 2.6**

C. The incorporation of resazurin was worked out using relative weight percentages of Mp to MI, where Mp is the mass of the particulate (resazurin) and MI is the mass of the ink used (carbon-graphite) [29-31]. Resazurin bulk modified macroelectrodes of 1%, 5% and 10% ((MP/MI) ×100)) were fabricated. After experimentation, a 10% wt. of resazurin was decided upon to ensure an even printing of resazurin and test the viability of the proposed method.

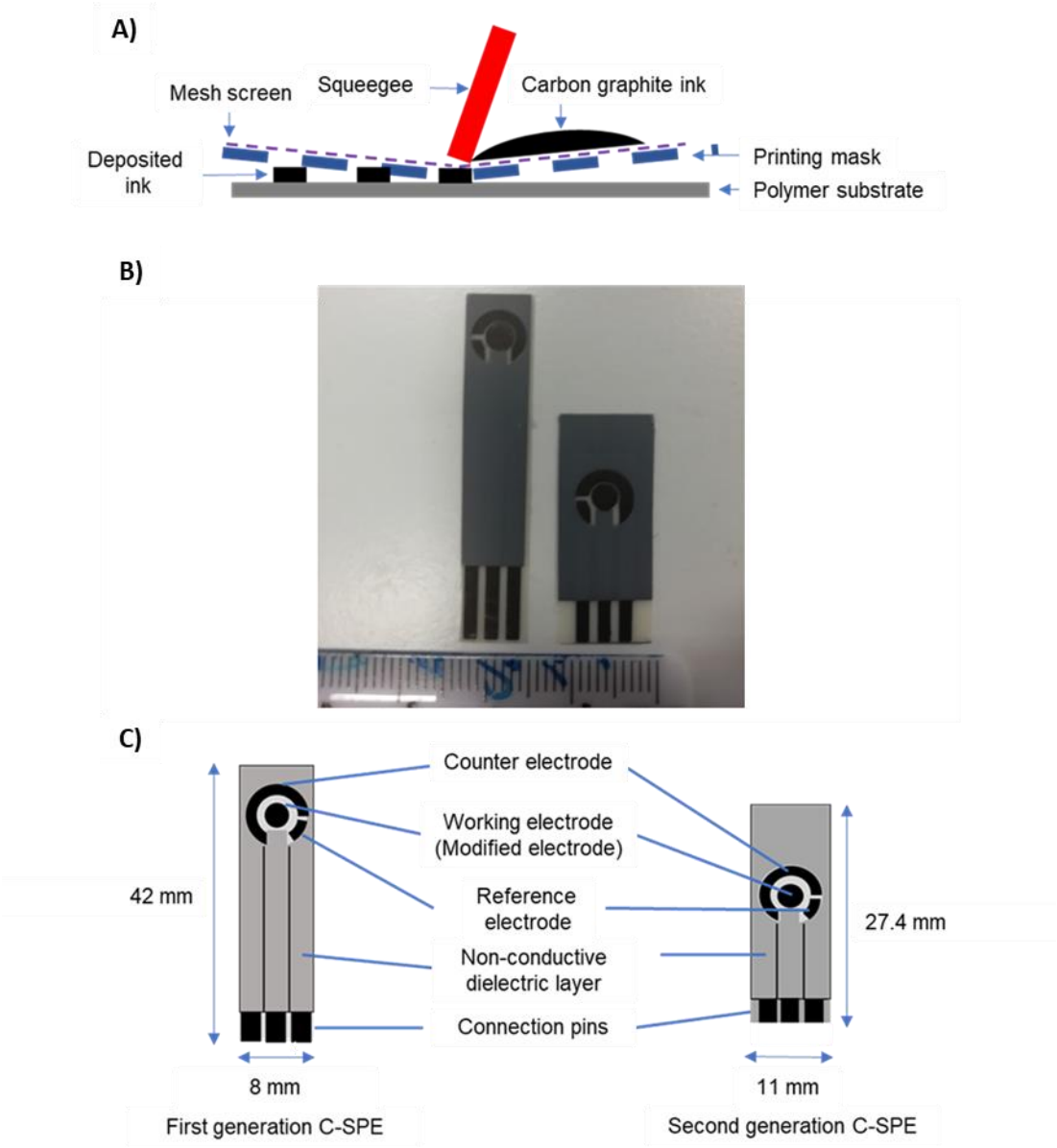

Figure 2.6. A) Shows a schematic of the screen-printed macroelectrode printing process. **B)** Shows a photograph of the first- (left) and second-generation (right) SPEs **C)** Shows a schematic for the screen-printed macroelectrode parts, dimensions, and resazurin modified region.

2.3.1 Sample drop covering (SDC)

To test the R-SPEs, and emulate the volumes used in the LOC devices for electrochemical experiments conducted off the LOC device, sample drop covering (SDC) was used. SDC was defined as pipetting a 60 µL volume of the chosen sample onto the SPE to cover the working, counter, and REs completely.

2.3.2 Reagents, solutions, and preparation

Surine artificial urine, potassium ferrocyanide, potassium phosphate monobasic, sodium hydroxide and resazurin were all obtained from Sigma-Aldrich (Gillingham, UK). Nutrient broth (SM0002) was obtained from Thermo Scientific (Oxoid, UK). Hydrochloric acid and a HI 2209 pH meter were obtained from Hanna instruments (Leighton Buzzard, UK). All of the following solutions were made up using purified water from a Millipore Milli-Q system. A buffered supporting electrolyte solution (BSES) was made up using 1.5 mM potassium phosphate monobasic with 0.1 M potassium chloride being added to act as the supporting electrolyte. BSES solutions (pH 2-10) were prepared using a HI 2209 pH meter with 10% hydrochloric acid and 0.1 mM sodium hydroxide solution to adjust the pH accordingly. Double strength nutrient broth (26 g/L) was also made up and sterilised using an autoclave set to 121°C for 20 minutes. Artificial urine was made up using equal volumes of surine artificial urine and double strength nutrient broth. The artificial urine was adjusted to pH 6 and sterilised using an autoclave set to 121°C for 20 minutes.

2.3.3 Electroanalytical setup

Electrochemical measurements were taken using C-SPEs, Ag-SPEs, R-SPEs and glassy carbon (GC) macroelectrode setup using CV and DPV. SPEs were interfaced with an EmStat3 potentiostat controlled by PSTrace 5.5 software using an EmStat three-pin screen-printed electrode connector (PalmSens, The Netherlands, Randhoeve). The PSTrace software was run using an ASUS E210M laptop. The macroelectrode setup was made up of a GC (1 mm) WE, platinum CE and Ag|AgCl (0.5 mm) RE (CH instruments Austin, Texas) set up

in the three-electrode configuration. The GC macroelectrode was maintained using mechanical polishing before experimentation, between readings and after experimentation using a figure of eight patterns on a cleaning cloth treated with a 1-micron and 0.1-micron alumina powder (CH instruments Austin, Texas) deposited on a cleaning cloth partially saturated with purified water. The GC three-electrode setup was interfaced using crocodile clips (PalmSens, The Netherlands, Randhoeve) and were attached to an electrochemical cell via a mounting bracket. CV was conducted using an E – step of 0.005 V. The following scanning rates were used; 0.005, 0.01, 0.015, 0.025, 0.050, 0.075, 0.100, 0.150 and 0.200 Vs^{-1}. Five replicates were done per applied scanning rate. DPV experiments utilised an E-step of 0.001 V, a T-pulse of 0.05 s, an E-pulse of 0.05 V and a scan rate of 0.01 V/s.

2.4 Statistical analysis

Statistical analysis was conducted using R (Version 3.5.3) with the R studio add-on (Version 1.2.5033) using 95% confidence limits. Normality of a dataset was assessed using a Shapiro-Wilk test, when comparing two data sets normally distributed data were analysed with a T-test or a Wilcoxon rank test if normality was not determined. If more than two datasets required comparison, an ANOVA was used for normally distributed data with a post hoc Tukey test to establish which data was and was not significant. For non-normal data sets a Kruskal Wallis test was used with a follow up pairwise Wilcoxon test to determine which data was and was not significant. Regression was used to establish if there was a cause-and-effect relationship between two variables.

2.5 Results and discussion

2.5.1 Determining the resazurin reduction potential window

The cyclic voltammograms of 1 mM resazurin in pH 6 BSES using C-SPEs are shown in **Figure 2.7 A**. The voltammogram show two I_{pc}s, C1 correlates to the reduction of resazurin to produce resorufin, C2 correlated with the reduction of resorufin to produce dihydroresorufin and A1 correlates to the oxidation of

dihydroresorufin to reform resorufin [216], the mechanism of which is shown in **Figure 2.7 B**. Repeated scans at a single scanning rate resulted in the peak height at C1, C2 and A1, being slightly reduced in height due to accumulation of reduction and oxidation products at the surface of the WE. An increase in the scan rate causes a decrease in the size of the diffusion layer produced which results in the production of higher currents as seen by the increase in the peak height at C1, C2 and A1 respectively.

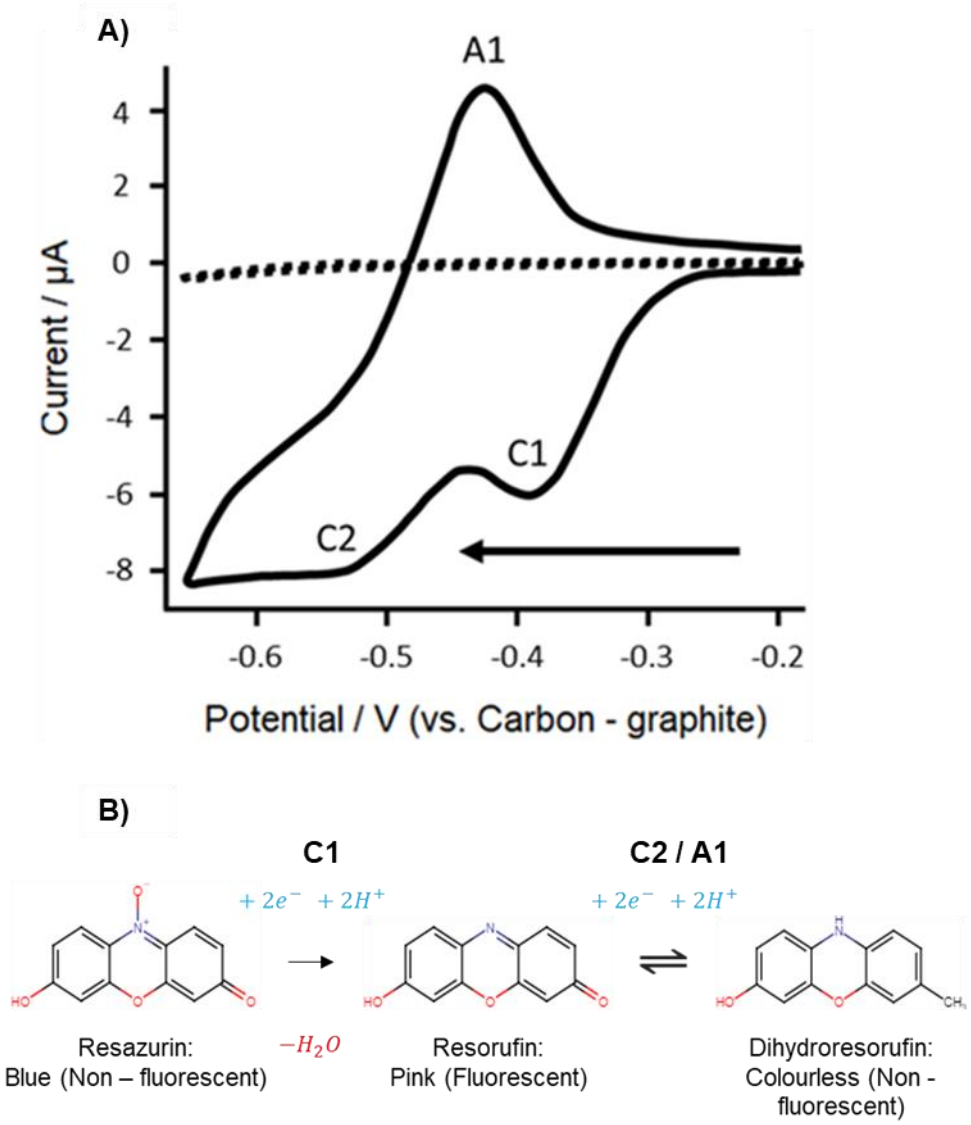

Figure 2.7 A) Typical cyclic voltammograms recorded in the presence (solid line) and absence (dashed line) of 1 mM resazurin in pH 6 BSES using a bare SPEs. Scan rate: 100 mVs^{-1}. The arrow indicates the direction of the voltammetric scan. N = 5. **B)** Simplified reduction pathway of resazurin to resorufin and resorufin to dihydroresorufin.

The resazurin reduction potential windows between pH 2 and pH 7 were -0.178 V to -0.475 V when using C-SPEs, between 0.105 V to -0.263 V when using Ag-SPEs and between 0.333 V to -0.425 V when using a GC macroelectrode. The identified reduction windows enabled the determination of the potential range wherein initial DPV experimentation is carried out and DPV based electrochemical AST would be conducted.

2.5.2 Investigating how resazurin reduction is controlled

To determine how resazurin reduction is controlled at the WE, the plot of the resazurin reduction I_{pc} at C1 was plotted against the square root of the scanning rate for pH 2-7 as shown in **Figure 2.8**. This was done in order to determine if the reduction of resazurin was diffusion controlled. The resulting trends produced in the plot show a linear relationship between I_{pc} at C1 and the square root of the scanning rate when infers that the process of resazurin reduction is diffusion controlled. Any absorption of resazurin at the surface of the WE was minimal, should significant absorption occurred, then the cathodic I_p value associated with resazurin reduction would undergo a greater decrease on subsequent CV scans due to the absorption of resazurin at the WE. Therefore, inside the physiological pH range of urine (normal range of pH 4 – 8) [193], resazurin reduction is a diffusion-mediated process with definable resazurin I_{pc} values that can be readily interpreted. The rate of diffusion and, thereby, the size of the resazurin reduction peak height correlated to the size of the diffusion gradient that forms between the WE and the concentration of resazurin in the bulk solution [207]. If the reduction process was diffusion and absorption controlled, or just absorption controlled the electroactive surface area of the WE could be a limiting factor in the detection of resazurin due to the inability to resolve small changes in the concentration of resazurin. With a diffusion-controlled process, there should be no loss of resolution as the electroactive surface area of the WE was high enough to enable uninhibited reduction of resazurin.

The I_{pc} values taken from the cyclic voltammograms showed a decrease in height as pH increased.

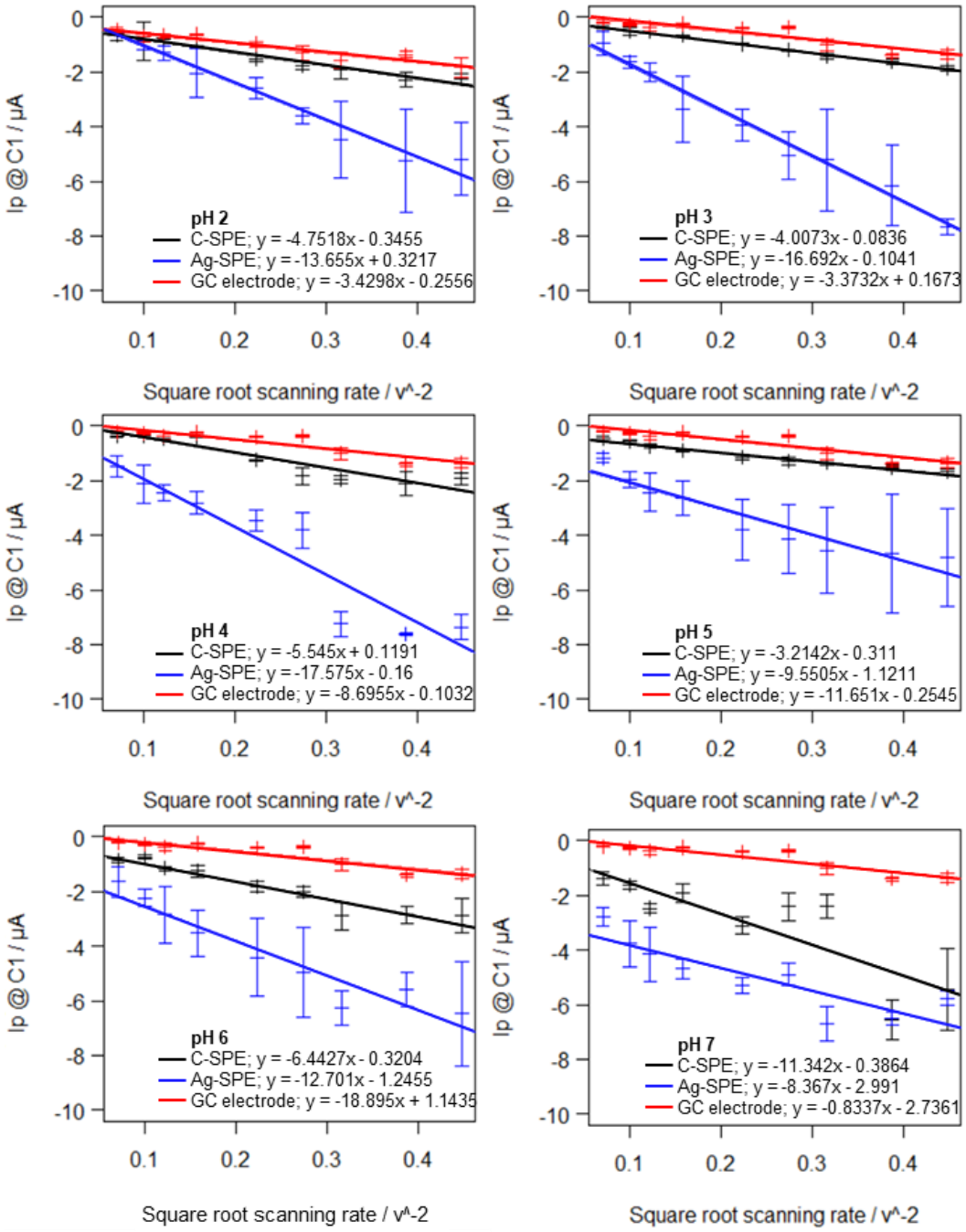

Figure 2.8. Plots of log resazurin reduction peak height (log (I_{pc} C1)) against the log of the scanning rate (log(*v*)) using resazurin (1 mM) in BSES set to pH 2 – 7 using C-SPE, Ag – SPEs and a GC electrode. N = 5.

This trend was expected, as when dissolved in an aqueous solution the anionic form of resazurin forms bonds with water molecules.The resazurin-water bonds become stronger as pH increases; in turn, this decreases the absorption of resazurin at the surface of the WE which reduces the height of the I_{pc}s produced [216]. The Ag-SPEs produced higher resazurin I_{pc} values on

average than the C-SPEs, however, there was a greater deviation in the height of the resazurin I_{pc} generated. This was in contrast to literature as Ag|AgCl references have a documented history of use as a reliable reference material and are commonly used as a material for the RE of SPEs [244]. The GC macroelectrode also produced higher resazurin I_{pc} values relative to the C-SPEs, however, the standard deviation was comparatively lower than the Ag-SPEs. Although Ag-SPEs and the GC macroelectrode setup both use a Ag|AgCl RE, the Ag-SPEs use a pseudo reference whereas the GC macroelectrode setup used a RE separated from the bulk solution by a porous frit. Therefore, the issue with the Ag-SPEs appears to be the contact of the RE with the resazurin bulk solution.

The RE helps to provide a consistent applied potential to the WE by providing a reference point to which potential applied to the WE can be compared [205, 206]. The RE, however, does not generate a current which prevents the reference from interfering with the electrochemical reaction [212]. Ag-SPEs are, in isolation from the data and discussion shown here, excellent analytical tools when used in specific applications where more conventional macroelectrodes cannot be used such as in miniaturised processes [245]. However, in this application the choice of a Ag|AgCl pseudo RE appears to have a negative impact, potentially due to fouling during the applied potential due to accumulation of redox products. This observation is, however, subjective to the work conducted in the thesis pertaining to the resazurin I_{pc} values. The performance of Ag|AgCl as a reference material was also assessed using DPV to determine if the variance was CV specific.

2.5.3 Characterisation using differential pulse voltammetry

The differential pulse voltammograms of resazurin (1 mM) in pH 6 BSES show one definable cathodic peak (C1) using C-SPEs, Ag-SPEs and the GC macroelectrode as shown in **Figure 2.9 A**, **B** and **C** respectively. The first cathodic peak (D1) generated using the C-SPEs can be discounted as the peak is an artefact produced as a result of the slightly less stable potential applied to the WE due to the carbon-graphite reference.

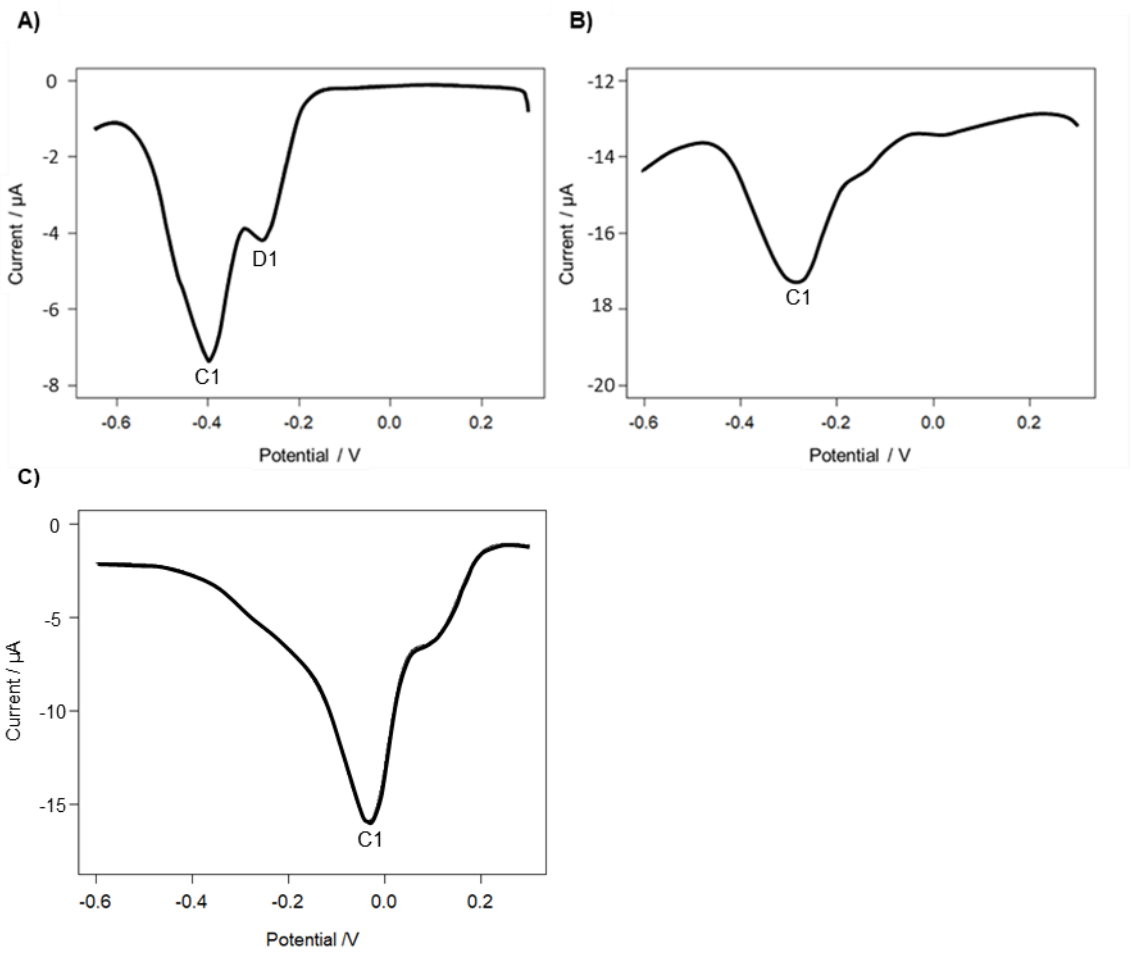

Figure 2.9. Differential pulse voltammograms of resazurin (1mM) in pH 6 BSES using **A)** C-SPE and **B)** Ag-SPEs **C)** and GC macroelectrode respectively. Scan rate: Scan rate 0.01 V/s. N = 5.

The resazurin reduction potential windows between pH 2 and pH 7 was -0.140 V to -0.364 V when using C-SPEs, between -0.021 V to -0.341V when using Ag-SPEs and between 0.166 V to -0.063 V when using a GC macroelectrode. Compared to CV, the potential window was shifted by approximately -0.1 V, thereby, no significant change in the applied potential would be required for DPV driven electrochemical AST testing. Differential pulse voltammograms of resazurin do not show the double cathodic peak as seen with CV. This caused the resorufin and resazurin I_{pc}s to become amalgamated which has also been previously observed when using DPV and gold WE, CE and REs to detect resazurin in artificial urine where the bulk of the I_{pc} corresponded to resazurin reduction [112].

The proposed method relies on the electrochemical detection of resazurin using DPV and does not rely on the detection of resorufin so the lack of a definitive resorufin reduction peak has no detrimental effect on the proposed electrochemical AST system.

Next, we determined the sensitivity of the C-SPEs, Ag-SPEs, and the GC macroelectrode setup in detecting resazurin using DPV. For this experiment resazurin concentrations of 1, 0.5, 0.25, 0.125, 0.0625, 0.0313 and 0.0156 mM were used. Plotting the differential pulse voltammogram resazurin I_p at C1 against the molar concentration shows a nonlinear, logarithmic trend as shown in **Figure 2.10A**, **B** and **C** for C-SPEs, Ag-SPEs and the GC macroelectrode respectively (Raw data for the resazurin LOD can be found in the **Appendix Section 7.1**, **Tables 7.1**, **7.2** and **7.3** for C-SPEs, Ag-SPEs and the GC macroelectrode respectively). The reduction of resazurin is a diffusion-controlled reaction, therefore, the height of the I_{pc} values derived at C1 correlated to the size of the diffusion gradient that formed between the WE and the concentration of resazurin in the bulk solution when a DPV scan was taken. In the trends shown by the C-SPE and the GC macroelectrode, the decrease in the I_{pc} values at C1 in the concentration range between 1 mM and 0.25 mM was smaller than the decrease in the concentration range of 0.125 mM to 0.0156 mM. The smaller decrease in the I_{pc} values would indicate that the decreased concentration of resazurin was insufficient to significantly reduce the concentration gradient that formed during the applied DPV scan, leading to a smaller drop in the height of the I_{pc} values. However, at a concentration of equal to, or less than 0.125 mM the decrease in the resazurin concentration was sufficient to significantly reduce the diffusion gradient as such that the decrease in the I_{pc} values resulted in discrete data points.

Additionally, as the concentration of resazurin was reduced the standard deviation associated with the I_{pc} values for the C-SPE and the GC electrode, on average, also decreased. The higher standard deviation at the higher concentrations of resazurin was likely caused by two factors. Firstly, there could have been some absorption of resazurin at the surface of the WE.

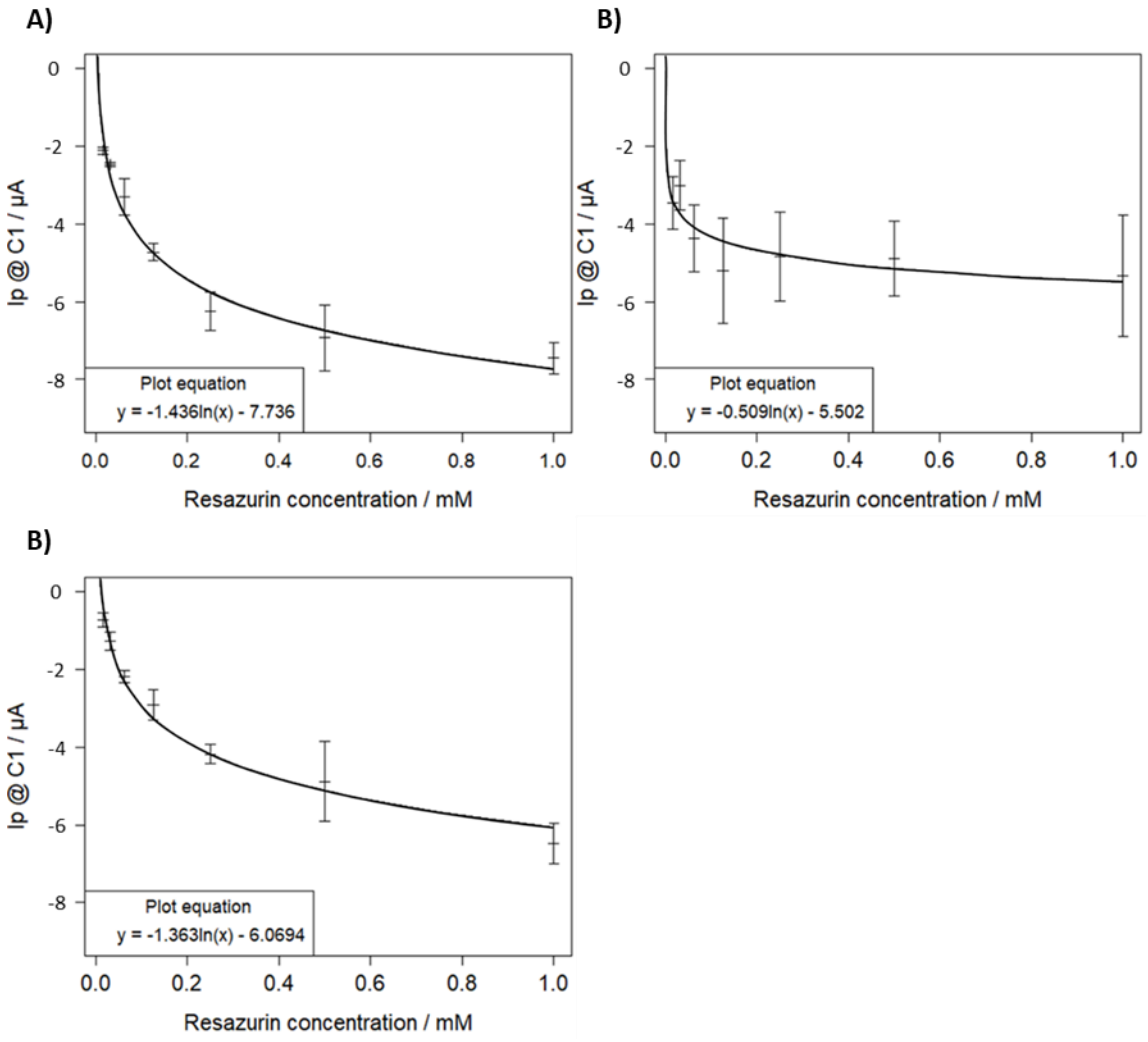

Figure 2.10. Plot of resazurin reduction peak height (Ip_c at C1) against resazurin concentration using DPV and **A)** C-SPE, **B)** Ag – SPEs and **C)** a GC WE with an Ag|AgCl RE. Scan rate: 0.01 V/s. N = 5, error bars represent standard deviation.

Some absorption of resazurin likely occurred during the CV based experimentation (**Figure 2.7 A**), although given that any absorption was minimal and that CV is less sensitive than DPV, the absorption did not significantly affect the ability of the cyclic voltammogram to consistently produce I_{pc} at C1 which is associated with resazurin reduction. However, as DPV is a more sensitive electroanalytical technique, any resazurin absorption at the WE decreased the sensitivity of the macroelectrodes. Therefore, at the higher concentrations of resazurin in the range of 1 mM to 0.125 mM the amount of resazurin that was absorbed at the surface of the WE was greater than at the lower concentrations, leading to a decreased electrochemically

active surface area of the WE over subsequent scans causing a greater variance in the I_{pc} values derived at C1 and, therefore, greater standard deviation.

All macroelectrode types were able to detect resazurin down to a concentration of 0.0156 mM using DPV. An issue presented with the Ag-SPEs is the large deviation in the I_{pc} value produced at each concentration. This distinct lack of a reproducible resazurin I_{pc} values was also observed when using CV as the electroanalytical technique. The C-SPEs and the GC macroelectrode setup produced a more consistent I_{pc} values than the Ag-SPEs which is observable in the smaller standard deviation. The consistency of the C-SPEs make them a notably better choice versus the Ag-SPEs for use in the electrochemical AST system and integration of resazurin via screen printing.

To determine the limit of detection (LOD), the following equation was used;

$$LOD = 3.3\ (\frac{\sigma}{S}) \qquad \textbf{Equation 2.2}$$

where σ is the standard deviation of the response of the curve, and S is the slope of the curve approximating the LOD at the x axis coordinate corresponding with the lowest tested concentration of resazurin (15.6µM). Using this formula, the GC macroelectrode demonstrated the best LOD of 0.0096mM, followed by the C-SPEs with 0.012 mM, and Ag-SPEs demonstrating the least sensitivity with a LOD of 0.043 mM. Although the GC macroelectrode outperformed the C-SPEs, the LODs were comparable with only a 0.0024mM difference in the calculated LOD values demonstrating the sensitivity of the C-SPEs. The C-SPEs however have demonstrated a superior LOD to a previously published system wherein the LOD was 0.125 mM using a thin platinum WE, CE and Ag|AgCl reference [205].

2.5.4 Effect of pH on resazurin reduction potential

Before discussing the use of DPV to detect resazurin in artificial urine it is worth discussing the relationship between resazurin E_p and pH. As previously stated, pH influences the reduction behaviour of resazurin. Noting that the *pKa* of resazurin is 6.71 (at 25 °C) [246], a linear trend was observed between the CV derived E_p value at C1 versus pH with an increase in pH causing a shift in E_p to a more negative value as shown in **Figure 2.11**. This is due to the participation of protons (H^+) in the electrochemical reduction of resazurin which can be described with the following;

$$E_p = E^0_{formal} - \frac{2.303RTm}{nF}pH \quad (1) \qquad \textbf{Equation 2.3}$$

where E_p [V] is the peak potential, E^0_{formal} [V] is the formal potential of the redox couple, *R* [J K^{-1}] is the universal gas constant, *T* [K] is the temperature (298 K), *m* and *n* are the number of protons and electrons involved in the redox process, and F is the faraday constant [247]. As protons (H^+) are required for the electrochemical reduction of resazurin to form resorufin, an increase in pH causes the abundance of hydrogen to drop which causes a shift in the E_p value to a more negative value [216].

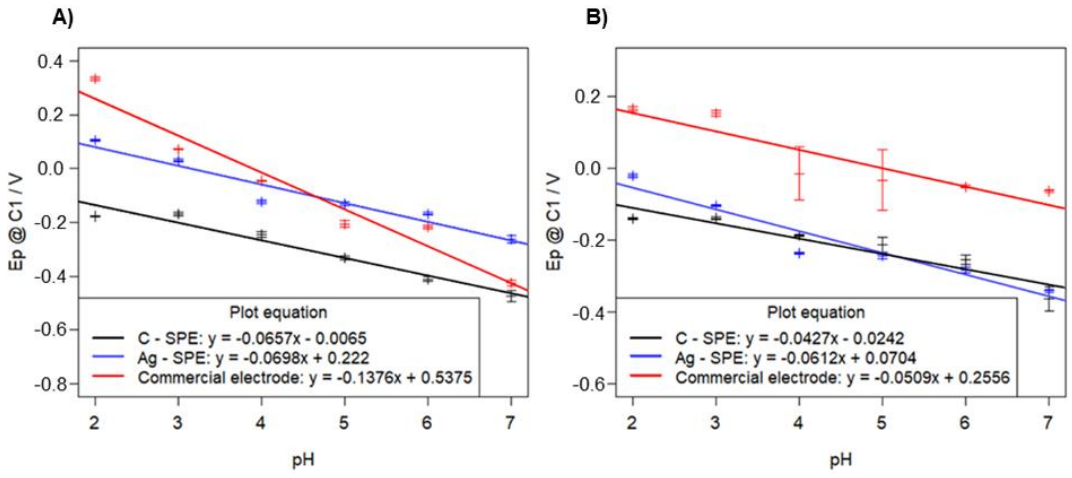

Figure 2.11. Plots of resazurin reduction peak position (E_p at C1) against pH using **A)** CV and **B)** DPV with C-SPE, Ag-SPEs and GC WE with a Ag|AgCl RE. CV scan rate =100 mV/s. DPV scan rate = 0.01 V/s**.** N = 5, error bars represent standard deviation.

Additionally, given that the reduction of resazurin to resorufin is a two proton, two-electron process, the gradient yielded by the C-SPEs of 65.7 mV/pH is the closest to the theoretically expected slope. This further demonstrates that in the niche application of resazurin detection in BSES without oxygen removal C-SPEs provide superior resolution to the Ag-SPEs and GC macroelectrode setup. Resazurin reduction peaks were successfully generated in BSES between a pH of 2 – 7. In CV and DPV based testing using a pH of greater than or equal to eight did not produce an easily definable resazurin reduction peak. As previously stated the normal urine pH range is 4 – 8 [193], the proposed system works at a pH range of 2 – 7. Buffers can be integrated to ensure the pH of the sample remains within the optimal range with the proposed system which eliminates the issue. The high sensitivity of the C-SPEs demonstrates the high resolution afforded in using SPEs even compared to the use of a more conventional GC macroelectrode. C-SPEs were chosen as the template for the fabrication of the first- and second-generation R-SPEs, based on the reproducibility of resazurin I_{pc} values in CV, and DPV as well as the superior LOD when using DPV. An assessment of the performance of the Ag-SPEs can be found in the **Appendix Section 7.2.**

2.5.5 Differential pulse voltammetry using artificial urine

Next, we repeated the previous experiment to determine the consistency of I_{pc} height and the sensitivity of the C-SPEs using artificial urine as the supporting electrolyte to better emulate the conditions of a urine sample. The concentrations of resazurin remained the same with 1, 0.5, 0.25, 0.125, 0.0625, 0.0313 and 0.0156 mM resazurin being dissolved in artificial urine. The SDC technique was used to emulate the small volumes used in a LOC device.

The differential pulse voltammogram of resazurin (1 mM) in pH 6 artificial urine is shown in **Figure 2.12 A** shows one definable cathodic peak (C1) with C1 corresponding with the reduction of resazurin to resorufin.

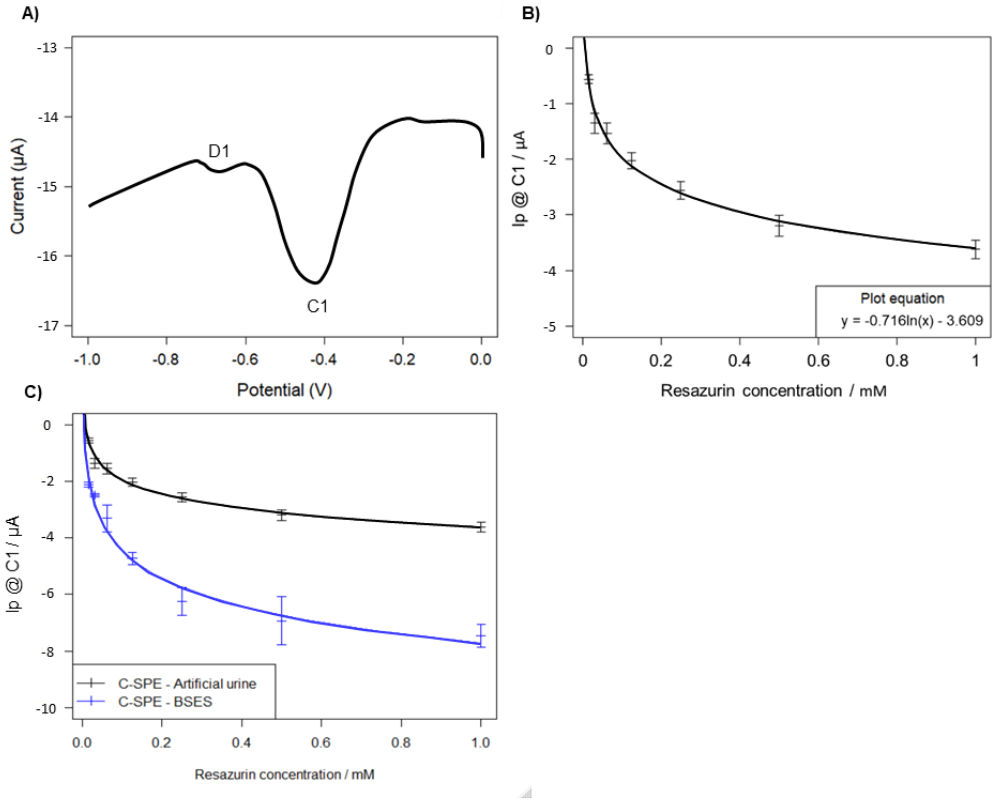

Figure 2.12. A) Differential pulse voltammogram of resazurin (1 mM) in pH 6 artificial urine and SDC using C - SPEs. **B)** Plot of resazurin reduction peak height (I_{pc} at C1) against resazurin concentration (Moles) in pH 6 artificial urine using SDC. Scan rate = 0.01 V/s**.** N = 5, error bars represent standard deviation. **C)** Overlap of the resazurin LOD plots from **Figure 2.10 A**, and **Figure 2.12 B**.

The reduction of resorufin is occluded by the double diffusion layer produced by the reduction of resazurin, therefore, there was no definable resorufin reduction peak which also occurred when using BSES. The cathodic peak at D1 can be discounted as an artefact. If there was a reduction double peak correlating to resazurin and resorufin reduction respectively, it would have also been presented when using the BSES solution and been a consistent trend. **Figure 2.12 B** shows the plot of resazurin I_{pc} at C1 against concentration produced a logarithmic trend. The use of DPV and C-SPEs enabled for reliable detection of resazurin down to a concentration of 0.0156 mM (Raw data for the resazurin LOD using C-SPEs can be found in the **Appendix Section 7.3 Table 7.4).**

The height of the resazurin I_{pc} values at each molar concentration were significantly smaller than their BSES counterparts (1, 0.5, 0.25, 0.125 0.0313 and 0.0156 mM - $W = 25$, $P < 0.05$ & 0.0625 mM – $T = 7.7339$, $df = 5.2374$, p

< 0.05) an overlap of which is shown in **Figure 2.12 C**. The artificial urine was used to emulate clinical urine samples as the salt concentration of urine will be less than that of a supporting electrolyte solution such as BSES. The lower concentration of the supporting electrolyte increases the internal resistance of the circuit which causes smaller resazurin I_{pc} values at a given concentration [206, 207, 239]. This data shows that when using artificial urine resazurin can still be reliably detected down to a concentration of 0.0156 mM with an estimated LOD of 0.0078 mM (Calculated using **Equation 2.2**) which shows the sensitivity DPV has as an electroanalytical tool in application with the proposed system which in turn will enable the detection of small changes in the concentration of resazurin.

2.5.6 Testing the resazurin bulk modified screen-printed macroelectrodes

Although SPEs have been used as part of a surface-modified resazurin based detection method [237], the use of SPEs as a platform for rapid electrochemical AST has yet to be fully explored. The novel use of bulk modified SPEs would reduce the time and complexity of fabrication, modification and reduce the number of steps required to produce a set of modified SPEs whilst maintaining a rapid time to analysis afforded in using an electrochemical method.

Resazurin bulk modified SPEs (R-SPEs) were produced using C-SPEs as the template. R-SPEs were tested using pH 6 artificial urine using SDC and a volume of 60 µL. Using pH 6 artificial urine and 1 mM resazurin with an applied potential of 0V to -1V. However, for the characterisation of the R-SPEs, the applied potential was lengthened by 0.4V to create a new applied potential of 0V to -1.4V. This longer applied potential was required to fully capture the resazurin I_{pc}s generated using R-SPEs. To determine the best percentage incorporation of resazurin to use R-SPEs with w/v ratios of 1, 5 and 10% were fabricated and tested using SDC and pH 6 artificial urine. To determine if the percentage w/v of the incorporated resazurin had a significant effect, the difference in the resazurin reduction peak height values was compared as shown in **Figure 2.13 A** wherein it is shown that each of the resazurin I_{pc}

values were significantly different (Raw data for the I_{pc} values derived when testing the R-SPEs can be found in the **Appendix Section 7.4 Table 7.5**). Halving the w/v ratio did not half the resazurin I_{pc} value when comparing 5% and 10% w/v with average I_{pc} values of -3.19 and -1.13 µA respectively. The difference in I_{pc} values between 1 and 5% w/v was, however, approximately half with average I_{pc} values of -0.65 and -1.13 µA respectively. This nonlinear relationship between concentration, in this instance pertaining to the percentage w/v and the height of the resazurin I_{pc} has been observed in the LOD based experimentation. The concentration of resazurin on the R-SPEs was estimated using the equation:

$$-0.716\ln(x) - 3.609 \qquad \textbf{Equation 2.4.}$$

which is derived from the plot in **Figure 2.12 B**, the resazurin I_{pc} values and the estimated resazurin concentrations were then plotted onto the LOD curve as shown in **Figure 2.13 B**.

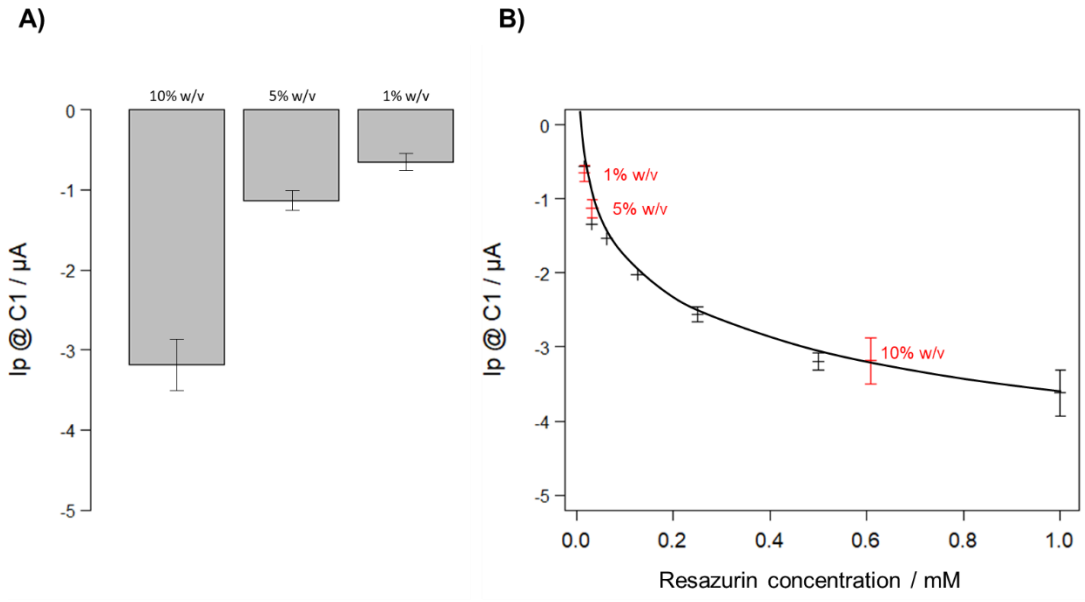

Figure 2.13. A) Plot of resazurin reduction I_{pc} derived using 1, 5 and 10% w/v R-SPEs using pH6 artificial urine and SDC. Scan rate = 0.01 V/s**.** N = 5, error bars represent standard deviation. **B)** Plot of resazurin reduction peak height (I_{pc} at C1) against resazurin concentration (Moles) in pH 6 artificial urine using SDC including annotated data points referencing the I_{pc} values derived from the 1, 5 and 10% w/v R -SPEs. N = 5, error bars represent standard deviation.

This enabled the determination of the best percentage w/v ratio for R-SPE fabrication. The derived molar concentrations for 10%, 5% and 1% w/v R-SPEs were 0.6271 mM, 0.03199 mM, and 0.0163 mM respectively. Given that the calculated LOD of resazurin when using C-SPEs which are used as the template for R-SPEs is 0.0078 mM, both 5 and 1% w/v R-SPEs molar concentrations are too close to the LOD. When conducting electrochemical AST, using an antibiotic concentration where the bacterial growth is inhibited rather than outright stopped thorough cell death, some biological reduction of resazurin will still occur. However, given the low molar concentrations shown by the 5% and 1% w/v R-SPEs, the extent of this biological reduction may decrease the concentration of resazurin in the bulk solution to be close to the LOD making determining antibiotic susceptibility difficult and potentially cause false-negative results. 10% w/v R-SPEs were then determined to be the optimal and used for electrochemical AST.

The differential pulse voltammogram produced by the first- and second-generation R-SPEs was compared to a concentration of 0.6271 mM resazurin using C-SPEs to determine if any significant differences were present in the voltammograms produced. The comparative concentration was derived from **Figure 2.12 B** using the plot of resazurin I_{pc} versus concentration to convert the I_{pc} values generated by the first-generation R-SPEs into a molar concentration. The differential pulse voltammograms produced by the R-SPEs and C-SPEs are shown in **Figure 2.14 A**. Each of the SPE types produced a single cathodic I_{pc} (C1), the profile of the differential pulse voltammograms were noticeably different from one another. The cathodic peak areas were all significantly different in size from one another (Pairwise Wilcox Test, p-value = 0.024) with second-generation R-SPEs showing the highest, followed by first-generation R-SPEs with C-SPEs showing the smallest area with averages of 3.984 (Standard deviation = 1.39), 1.546 (Standard deviation = 0.22) and 0.516 VμA (Standard deviation = 0.14) respectively. Additionally, the first-generation R-SPE E_p was significantly more negative relative to the C-SPEs ($t = -3.9056$, $df = 5.5054$, $p < 0.05$) with an average of -0.74V and -0.642V respectively. There was no significant difference in the I_{pc} values of the first-generation R-SPEs and the C-SPEs (Pairwise Wilcox Test, p-value = 1).

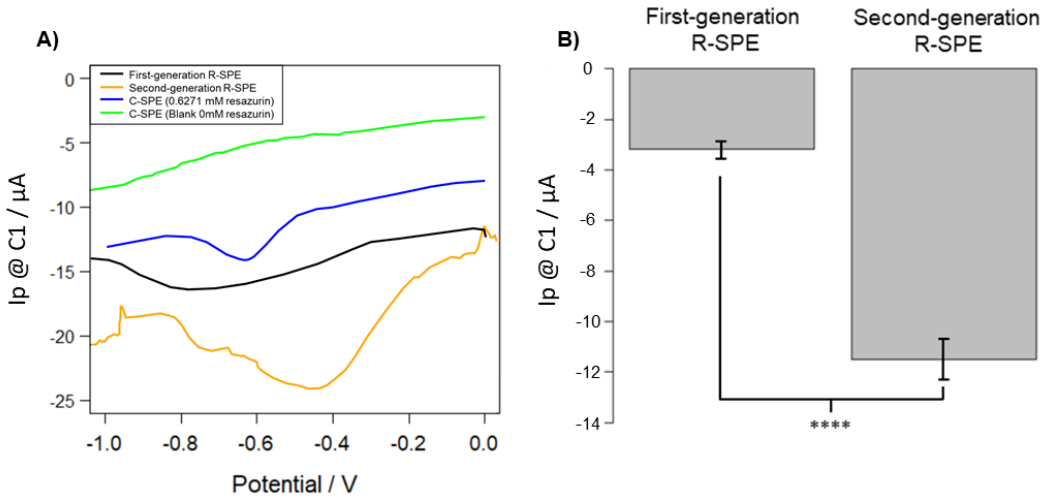

Figure 2.14. A) Differential pulse voltammogram of R – SPEs, C-SPE with 0.6271 mM resazurin, and C – SPE with 0 mM resazurin using pH 6 artificial urine and SDC. Scan rate = 0.01 V/s**.** N = 5. **B)** Comparison of the resazurin I_{pc} values derived using first- and second-generation R-SPEs. N = 5, error bars represent standard deviation, significance is indicated as follows; **** = p-value < 0.00005

However, the second-generation R-SPEs demonstrated a significantly higher resazurin I_{pc} value than the other SPE types (Pairwise Wilcox Test, p-value < 0.05), the difference in the I_{pc} values is shown in **Figure 2.14 B**. The w/v was the same as first-generation R-SPE at 10%, however, the length of the carbon paste that attaches to the WE, CE and RE of the second-generation R-SPEs was 19 mm shorter, thereby, reducing the overall length of the circuit, in turn reducing the internal resistance of the circuit during the applied potential enabling a higher peak current. These differences in the differential pulse voltammograms are attributable to the difference in the size of the WE of the R-SPEs and the C-SPEs. The R-SPE fabrication does increase the geometric size of the WE from ~7 mm to ~8 mm in diameter, however, to fully determine the extent of the differences in the C-SPEs and R-SPEs WE surface characteristics optical profilometry was carried out with the results being surmised in **Figure 2.15**.

The bulk modification of the C-SPEs to produce R-SPEs results in the following characteristic changes. Firstly, the mean maximum height significantly increases, this in conjunction with the significant increase of the mean height indicating that the R-SPEs WE are thicker but have a peak and trough type structure as shown in the 3D images.

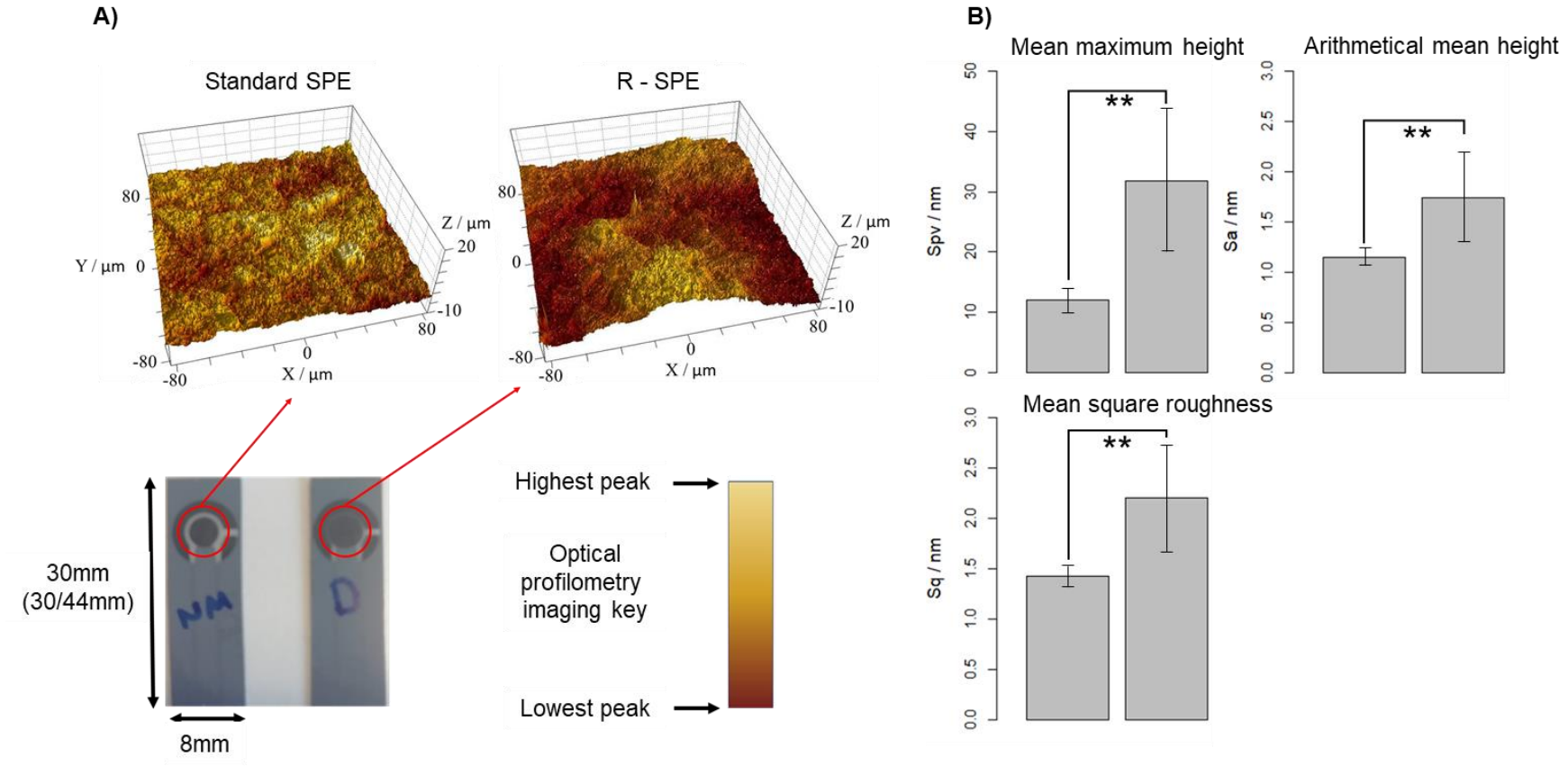

Figure 2.15. Schematic showing **A)** the surface characterisation of the C-SPE labelled as NM for not modified, and R-SPEs labelled with a D. And **B)** Barplots and statistical analysis of the different surface characteristics including mean maximum height (Spv), arithmetical mean height (Sa) and mean square roughness (Sq). Scan rate = 0.01 V/s**.** N = 9, error bars represent standard deviation, significance is indicated as follows: ** = p-value < 0.005.

Secondarily, the mean square roughness significantly increases, this is then product of the peak and trough structure which, in conjunction with the increased geometric area overall increases the electroactive surface area of the R-SPEs relative to the C-SPEs. This is advantageous as a greater surface area enables greater resazurin reduction, thus, theoretically enabling more sensitive detection. The difference in surface area is demonstrated in the differential pulse voltammograms in **Figure 2.14 A** wherein the resazurin I_{pc} profile showed a larger reduction area, with the diffusion layer taking longer to form as shown by the current increasing at a potential of -0.8 V as opposed to -0.7 V when using C-SPEs due to the larger electrochemically active surface area. Therefore, the screen-printing modification process gives the first- and second-generation R-SPEs surface characteristics that are beneficial for electroanalysis.

There is an advantage to using screen printing based bulk modification of WEs. Of the types of surface modification presented which are summarised in **Table 2.1**, some enable the method of electrochemical AST such as the fabrication of a pH-sensitive resazurin derived redox-active crystalline layer [234], the use of capture antibodies [235, 236] or increase the degree of sensitivity in the detection of resazurin such as the deposition of multiwalled carbon nanotubes and gold nanoparticles onto the WE of a carbon-based SPE [237]. Resazurin bulk modification, however, both enables the method of conducting electrochemical AST via delivery of a cell viability indicator into simulated LOC conditions and imparts surface characteristics onto the WEs that are beneficial for the sensitive detection of an analyte. This demonstrates the utility of using screen printing-based modification processes in the fabrication of simple, but effective, electrochemical AST platforms. Additionally, the modification process is both fast and simple enabling R-SPEs to be fabricated quickly while minimising the chances of errors in the fabrication process.

2.6 Conclusions

Using screen printing to incorporate resazurin onto C-SPEs was successful with the first- and second-generation R-SPEs producing strong and easily

interpreted resazurin I_{pc}s. C-SPEs were chosen as the template for R-SPE production due to the consistency of the resazurin I_{pc}s values that were generated using both CV and DPV when using carbon as the reference material versus AgAgCl. Using DPV resazurin can be reliably detected down to a concentration of 0.0156 mM using artificial urine as a supporting electrolyte solution. The high sensitivity of DPV allows for the detection of small changes in the concentration of resazurin in a bulk solution and, thereby, could be used to rapidly determine the response in bacterial growth to antibiotics.

3. Chapter 3: Antibiotic susceptibility testing

Elements of the work presented in this chapter have been published as Crane, B., Hughes, J.P., Rowley Neale, S.J., Rashid, M., Linton, P.E., Banks, C.E., Shaw, K.J., Rapid antibiotic susceptibility testing using resazurin bulk modified screen-printed electrochemical sensing platforms, Analyst, 146: 5574-5583 (2021).

Executive summary

This chapter will cover the AST conducted using the first-generation R-SPEs and antibiotic-loaded hydrogels conducted independently of the LOC devices. The main findings are:

- First-generation R-SPEs can be used to determine antibiotic susceptibility in a total of 70 minutes of testing time in *E. coli* versus gentamicin sulphate.
- Antibiotic-loaded polyvinyl alcohol hydrogels can be used to effectively deliver an inhibitory concentration of antibiotics within 15 minutes to *E. coli* and *K. pneumoniae* under simulated LOC conditions.
- *E. coli* ATCC 25922 and *K. pneumoniae* ATCC 700603 showed susceptibility to ceftriaxone, cephalexin, colistin, gentamicin, trimethoprim, and piperacillin antibiotic hydrogels while showing resistance to vancomycin hydrogels. *E. coli* NCTC 13351 showed resistance to ceftriaxone, cephalexin and vancomycin hydrogels while being susceptible to all other types as expected.

3.1 Introduction

3.1.1 Antibiotic selection

AST is one of the most important practices in any clinical setting pertaining to infectious diseases. The current gold standard for AST is the disk diffusion assay (see **Section 1.4**), where bacteria are cultured onto nutrient agar that has been treated with antibiotic coated disks [104, 105]. If a method is developed to be used in a specific application such as UTIs, it is important to test the method using the antibiotics that are prescribed in the clinical setting

that may also be used as part of culture-based AST. The antibiotics commonly used to treat UTIs in the UK are shown in **Table 3.1**. These antibiotics were chosen due to their relevance and use in the clinical setting in the context of treating UTIs. The proposed electrochemical method was tested against these antibiotics to demonstrate the ability of the electrochemical method to rapidly determine the susceptibility of the most common UTI causative bacteria to clinically relevant antibiotics. Should the proposed method be proven to work effectively using clinically relevant antibiotics, it serves to demonstrate that the proposed method could theoretically be used to replace culture-based testing.

3.1.2 Hydrogels

A hydrogel is a gel wherein most of the structure is made up of water with the rest being made up of a 3D matrix of a hydrophilic polymer. There are three classifications of hydrogel compositions; homopolymeric hydrogels which are made up of one type of monomer [248]; copolymeric hydrogels, which are comprised of two or more monomer types one of which is hydrophilic in an arrangement that can be alternating along the polymer length, or be fabricated in a random pattern [249]; and finally, multipolymer interpenetrating polymeric hydrogels, which are made up of two independently formed polymer networks which are then cross-linked [250]. Of these approaches, the homopolymeric hydrogels are the simplest owing to the fact they are made up of a single monomer, turned polymer after polymerisation. Hydrogels have a documented history of use as a delivery vector for drugs in oral cavities [251], the gastrointestinal tract [252], ocular areas [253], transdermally [254] and also for wound healing [255]. Hydrogels have also been used to deliver antibiotics, for example, where a copolymeric hydrogel was fabricated using poly (ethylene glycol) diacrylate and chitosan, this hydrogel precursor was then loaded with antibiotics after which polymerisation was induced using ultraviolet light (UV) [256]. Another example saw the use of a copolymeric hydrogel fabricated using a poly(2-(dimethylamino)ethylmethacrylate) and poly(acrylic acid), whereby polymerisation was induced by drying the copolymeric precursor at room temperature.

Table 3.1. Breakdown of the antibiotics name, antibiotic class, and use in the clinical setting within the UK

Antibiotic name	Antibiotic class	Use in a clinical setting	Mechanism of action	Side effects
Cephalexin	Cephalosporin	1) Lower UTI (Pregnant women after AST is conducted) - Oral second line 2) Lower UTI (Pregnant women) - Asymptomatic bacteriuria 3) Acute pyelonephritis (Non-pregnant persons) - Oral first line 4) Acute pyelonephritis (Pregnant women) – Oral first line 5) Recurring UTI – Oral second line 6) Catheter associated UTI (Upper UTI symptoms, pregnant and non-pregnant persons) – Oral first line [257]	Beta lactam ring binds to penicillin binding proteins stopping cell wall synthesis at the last stage of peptidoglycan synthesis [258].	Tendinopathy (rare) [259] Allergic reaction (If allergic to penicillins) [260]
Ceftriaxone	Cephalosporin	1) Acute prostatitis - Intravenous first line 2) Acute pyelonephritis (Non – pregnant persons) - Intravenous first line 3) Catheter-associated urinary-tract infection (Non – pregnant persons) - Intravenous first line [257] Resistant to the actions of beta lactamases including: cephalosporinases, extended-spectrum beta lactamases and penicillinase [258]	Beta lactam ring binds to penicillin binding proteins stopping cell wall synthesis at the last stage of peptidoglycan synthesis [258]. Inhibition of cell wall synthesis and cell division via inhibition of the enzymes carboxypeptidases, endopeptidases, and transpeptidases [261]	Allergic reaction (If allergic to penicillins) [260] Diarrhoea [262]
Colistin	Polymyxin	1) Used to treat MDR Gram-negative bacteria [263, 264]	Degradation of the cell membrane via displacement of magnesium and calcium ions from the phospholipid bilayer due to electrostatic interactions between the anionic lipopolysaccharide and the cationic polypeptide of the colistin [265, 266]	Skin rash & hives Generalised Itching Fever Mild gastrointestinal issues [267] Potential nephrotoxicity [267, 268]
Gentamicin sulphate	Aminoglycoside	1) Acute prostatitis – Intravenous first line 2) Acute pyelonephritis – Intravenous first line for non – pregnant people 3) – Catheter associated UTI - Intravenous first line for non – pregnant people [257]	Inhibition of protein synthesis via binding to 30S ribosomes, thereby, preventing mRNA translation, and leading to the formation of truncated or non-functional proteins [269]	Hearing loss [270] Nausea, vomiting, balance issues, and vertigo Mild proteinuria [271]
Piperacillin	Penicillin	Complicated UTIs caused by Gram – negative bacteria [272, 273]	Beta lactam ring binds to penicillin binding proteins stopping cell wall synthesis at the last stage of peptidoglycan synthesis [274]	Anaemia Candida infection; Constipation Gastrointestinal discomfort Headache; Insomnia [275]
Trimethoprim	Antifolate	1) Lower UTI (Non – pregnant persons) – Oral first line 2) Acute prostatitis – Oral first line 3) Acute pyelonephritis – Oral first line 4) Recurring UTI (Men and women) – trimethoprim 5) Catheter associated UTI (Non – pregnant persons) – oral first line	The reduction of dihydrofolate to tetrahydrofolate, which is the active from of folic acid is blocked [276]	Gastrointestinal intolerance Skin eruptions [276]
Vancomycin	Glycopeptide	Prescribed for Gram – positive infections by single or MDR organisms [277]	Crosslinking of the cell wall is prevented by vancomycin binding to D-alanyl D-alanine which induces inhibition of peptidoglycan synthase and the P-phospholipid carrier [278, 279].	Chills Fever Hypotension, Hypersensitivity reactions Interstitial nephritis Phlebitis, Nephrotoxicity Ototoxicity Neutropenia [280]

The poly(2-(dimethylamino)ethylmethacrylate) and poly(acrylic acid) hydrogel produced was able to secrete antibiotics based on environmental pH changes [281]. In the context of the proposed electrochemical AST method, however, both methods have limitations. The use of UV light-based polymerisation requires specific equipment such as a photosensitive crosslinker and specific wavelengths of UV to polymerise monomers to form a hydrogel. pH dependant release of an antibiotic is not suited for the AST method proposed as the consistent release of the antibiotic after the introduction of artificial urine or human urine to the hydrogel is desired.

Homopolymeric poly(vinyl alcohol) (PVA) based hydrogels have good mechanical properties, are stable at room temperature, have high water content and have no significant negative effect on the growth of bacteria [282]. Different w/v ratios of PVA have been evaluated, with the most frequently used being 10% [283-287], and a range from 15% [288] down to 3% [282, 289-292].

There are several methods of inducing polymer crosslinking to fabricate a hydrogel. Of the identified methods, freeze-thaw presents the most viable option for fabricating antibiotic-loaded hydrogels. The use of chemicals could potentially alter the pH or otherwise affect the electrochemical sensor if any residual chemicals were present in the hydrogel post-fabrication. Crosslinking via UV radiation requires both a photoinitiator and a radiation source to induce polymerisation [256]. There could be potential for residual photoinitiator to have an effect either on the electrochemical detection of resazurin or the growth of bacteria, although wash steps could be introduced.

Freeze-thaw based polymerisation was identified as a more cost-effective and simple means of fabricating a hydrogel as it required no additional equipment to enable the method to be undertaken in a laboratory. A schematic view of PVA hydrogel fabrication is shown in **Figure 3.1**. In the initial stage of the freeze-thaw method of gelation between PVA monomers, spinodal liquid-liquid phase separation occurs, which in turn develops a porous network of spaces. These spaces are mainly occupied by free water with the rest being made up of PVA and the water absorbed within the PVA based structures. The PVA rich region has crystalline structures which act as the crosslinking point between the monomers [293].

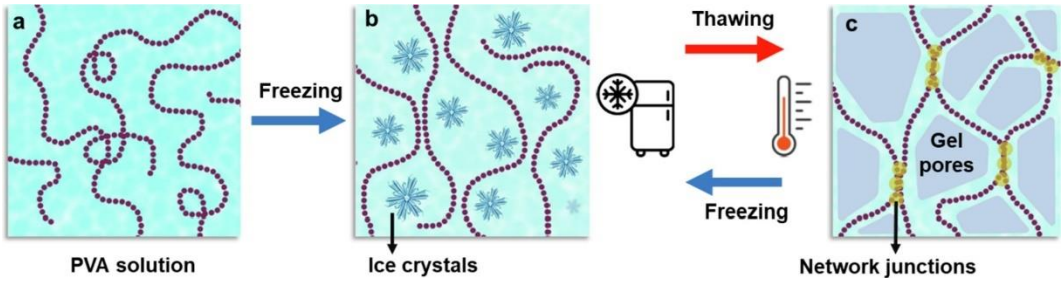

Figure. 3.1. Schematic view showing the formation of a PVA hydrogel via freeze thawing taken from Adelnia *et al*. 2022 [294]. **a)** shows PVA chains suspended in solution. **b)** shows the freezing step, wherein PVA chains are trapped between ice crystals due to phase separation. **c)** shows the thawing step, wherein the gel network is formed as hydrogen bonding links adjacent PVA chains [294].

Multiple freeze-thaw cycles result in a greater degree of crosslinking, thus, resulting in a denser hydrogel [295]. When using freeze thaw hydrogel fabrication, it is important to consider whether the antibiotic being loaded can tolerate the range of temperatures that are used in the fabrication process and no degradation will occur. The other limitation is that freeze thawing is a time intensive process due to the requirement for multiple freeze thaw cycles to form a useable hydrogel. Freeze thaw fabricated hydrogels however do not require the use of a crosslinking agents that may contaminate the hydrogel and affect either the three-electrode setup of the proposed electrochemical AST system, the action of the antibiotic, or the growth of the bacteria on a LOC device. Therefore, in the proposed application, freeze thaw fabricated hydrogels presented the best option for antibiotic delivery.

For the delivery of antibiotics into a solution, two methods of antibiotic loading of PVA hydrogels were presented; 1) To passively load the antibiotic into the PVA hydrogel precursor and then fabricate a hydrogel using freeze-thaw cycles [256, 284, 296]; 2) Saturate the fabricated hydrogel using an antibiotic solution [291]. Saturation loading is a good choice when the hydrogel fabrication process might reduce the efficacy of the antibiotic itself such as the use of acids or elevated temperature-induced monomer crosslinking as the antibiotic is introduced after the hydrogel is fabricated. The antibiotics used, however, were stable at temperatures in the range used during the freezing steps (-20°C), and the initial temperature which the antibiotics were loaded into the hydrogel precursor (50 °C). Based on the thermal tolerances of the antibiotics that were used, passive loading of the antibiotics was chosen as it

enabled the production of a usable antibiotic hydrogel quickly and with fewer overall steps when compared to saturation loading.

3.2 Aims and objectives

The main aim of this chapter is to test the efficacy of delivering resazurin, and antibiotics to simulated LOC conditions. This will be achieved through the completion of the following objectives:

- Assessment of the viability of conducting rapid AST using first-generation R-SPEs with a bacterial model of *E. coli* ATCC 25922 and example antibiotic gentamicin sulphate.

- Determine if PVA antibiotic-loaded hydrogels are a viable method of delivering a wide range of antibiotics at a concentration to inhibit the growth of *E. coli* ATCC 25922, *E. coli* NCTC 13351 and *K. pneumoniae* ATCC 700603.

3.3 Experimental

3.3.1 Standard bacterial preparation

Overnight cultures (ONCs) of *E. coli* ATCC 25922, *K. pneumoniae* ATCC 700603 and *E. coli* National Collection of Type Cultures (NCTC) 13351 were prepared by depositing one colony of bacteria from a stock plate into 10 mL of single strength nutrient broth which was then incubated overnight at 37°C. After incubation, the ONCs optical density was adjusted to a standard 0.7 at 600 nm using a spectrophotometer using nutrient broth as a diluting agent. For conducting experiments, a volume of the standard inoculum was added to the artificial urine produce an initial colony-forming unit count per mL (CFU/ml) of $1.76x10^{7}$.

3.3.2 Serial dilutions, and bacterial enumeration

Where bacterial enumeration was required, 10 µL samples, were taken and added to 90 µL of phosphate-buffered saline (PBS) (Sigma-Aldrich,

Gillingham, UK) to act as a 10^{-1} dilution. The samples were then further serially diluted using a 1 in 10 ratio to a factor of 10^{-5}. The 10^{-5} dilution factor was the used for bacterial enumeration wherein five nutrient agar (Oxoid, UK) spread plates were prepared using 20 µL aliquots.

3.3.3 Culture-based AST CFU/ml counts

An ONC of *E. coli* was prepared as described in **Section 3.3.1**, after which 125 µL of the standardised inoculum was added to 4875 µL of artificial urine for a total volume of 5000 µL in a universal. The inoculated artificial urine was then incubated for 70 minutes at 37°C on a shake plate producing a bacterial concentration of ~$1.75x10^{8}$.

A gentamicin sulphate (Sigma-Aldrich, Gillingham, UK) stock solution was prepared in sterile deionised water at a concentration of 50 mg/mL. An aliquot from the gentamicin sulphate stock solution was taken and diluted to a working concentration of 100 µg/ml using sterilised deionised water. Gentamicin sulphate from the 100 µg/ml stock solution was added (0.3 µl) to five of the wells of a flat bottomed 96 well plate (Sarstedt, Germany) so that the final working concentration of the antibiotic was 0.5 µg/ml, artificial urine was added to make a total volume of 60 µL in the well. An additional five wells were prepared without the antibiotic to act as a control. In the control wells, an equal volume of sterilised deionised water was added in place of the antibiotic stock solution (0.3 µl), artificial urine was then added to the well such that the total volume in the well was 60 µL. One 96 well plate was made for each of the incubation time points for a total of four 96 well plates.

The 96 well plates were incubated for one to four hours in increments of one hour. Samples were then analysed by bacterial enumeration, as described in **Section 3.3.2**, using a 10 µL sample taken from the 96 well plate chamber**.** Subsequent experiments used an incubation time of 80 minutes in 20-minute increments. The CFU/ml counts produced for each of the different tested variables were then compared to determine if there was a statistically significant difference in the CFU/ml values produced using the statistical tests as discussed in **Section 2.4**. This was conducted to determine if the

concentration of antibiotics used had a significant effect on the growth of the bacteria independently of the macroelectrode.

3.3.4 Broth microdilution assay

Minimum inhibitory concentration (MIC) values were derived using broth microdilution assays performed in triplicate using flat bottomed 96 well plates (Sarstedt, Germany). The following antibiotics were solubilised in sterile deionised water at a concentration of 50 mg/mL: ceftriaxone disodium salt (Sigma-Aldrich, Gillingham, UK), colistin sulphate (Sigma-Aldrich, Gillingham, UK), gentamicin sulphate (Sigma-Aldrich, Gillingham, UK), piperacillin sodium salt (Sigma-Aldrich, Gillingham, UK), and vancomycin hydrochloride (Sigma-Aldrich, Gillingham, UK). Cephalexin (Sigma-Aldrich, Gillingham, UK) was prepared at a concentration of 5 mg/mL in sterilised deionised water. Lastly, trimethoprim (Sigma-Aldrich, Gillingham, UK) was prepared at a concentration of 50 mg/mL in dimethyl sulfoxide (Sigma-Aldrich, Gillingham, UK). All antibiotics were filter sterilised using 45 nm syringe filter paper.

The initial concentration of antibiotics prepared in the first column of the 96 well plate was 1000 µg/ml and then serially diluted two-fold to a terminal concentration of 1.95 µg/ml in Mueller Hinton broth (Sigma-Aldrich, Gillingham, UK). *E. coli* ATCC 25922 (Susceptible), *K. pneumoniae* ATCC 700603 (Susceptible), and *E. coli* NCTC 13351 (Resistant to cephalexin and ceftriaxone) were prepared as described in **Section 3.3.1.** The OD, however, was standardised at 0.1 from which a 10 µL aliquot was deposited into each of the wells for an initial CFU/ml count of 2×10^6. The plates were read after 24 hours using a Multiscan GO 96 well plate reader set to a wavelength of 600 nm. The MIC value was taken as the lowest concentration which significantly inhibited bacterial growth after a 24-hour incubation when statistically compared to the antibiotic free control. Significance was determine using the tests discussed in **Section 2.4.**

3.3.5 Electrochemical determination of bacterial growth

E. coli ATCC 25922 was prepared as described in **Section 3.3.1**, after which 125 µL of the standardised inoculum was added to 4875 µL of artificial urine for a total volume of 5000 µL in a universal. After a 70-minute preincubation step, gentamicin sulphate was then added at concentrations of 0 to 1.4 µg/ml in increments of 0.1 µg/ml. The antibiotic-treated solution was then vortexed, then the SDC method was used to drop the inoculated artificial urine onto first-generation R-SPE.

An initial DPV scan was taken after the SDC step was carried out using the same parameters described in **Section 2.1.3** with some modifications to the applied potential. The applied potential started at 0 V and was swept to -1.4 V on the first scan, with sweeps from 0 V to -1 V for all subsequent scans. Subsequent readings were taken each hour for up to four hours. Between readings, the artificial urine was incubated at 37°C. The resazurin I_{pc} at each time point was calculated after the completion of the experiment. The height of the resazurin reduction peaks of the antibiotic-treated artificial urine were statistically compared to those of the artificial urine with no antibiotic, a significantly higher resazurin reduction peak height for the antibiotic-treated artificial urine is associated with significant inhibition of bacterial growth. Five replicates were carried out per incubation time point, significance was determined using the tests discussed in **Section 2.4.**

3.3.6 Hydrogel fabrication and antibiotic loading

The PVA (Mw 89,000 to 99,000, Sigma-Aldrich, Gillingham, UK) hydrogel precursor was made by adding 1g of PVA to 10 mL of deionised water to produce a weight to volume ratio of 10%. The precursor was then autoclaved for one hour [287] at 121°C to sterilise the PVA and dissolve it completely. The precursor was then moved to a heated magnetic stirring plate and stirred continuously for 30 minutes at 50°C. Any bubbles were then removed via ultrasonication [289] and a 1.662 mL volume of the precursor was cast into glass petri dishes and spread using an oscillating shake plate to create a 0.3 mm thick precursor. The precursor was then formed into a gel by using eight freeze-thaw cycles. The first cycle was made up of a -20°C freeze cycle

overnight followed by thawing at room temperature for 30 minutes. The remaining 7 cycles consisted of one hour of freezing at -20°C and then thawing for 30 minutes at room temperature [297]. After the last freeze-thaw cycle, the gel was then sectioned using a 2 mm diameter biopsy punch (Williams Medical, UK). Antibiotics were loaded when the precursor cooled down to 50°C [298] using antibiotic stock solutions as described in **3.3.4**. The end concentration for each antibiotic-loaded hydrogel respectively was 0.8 mg/mL ceftriaxone, 2.6 mg/mL cephalexin, 2.2 mg/mL colistin, 5.6mg/mL gentamicin sulphate, 4.2 mg/mL piperacillin sodium salt, 10.5 mg /mL trimethoprim and 45 mg/mL vancomycin.

3.3.7 Assessing the antimicrobial properties of the hydrogel

Hydrogels were fabricated and loaded with antibiotics as described in **Section 3.6.6**. The antibacterial properties of the antibiotic-loaded hydrogels were assessed using *E. coli* ATCC 25922, *K. pneumoniae* ATCC 700603, and *E. coli* NCTC 13351. Bacteria were prepared as described in **Section 3.3.1**, after which 125 µL of the standardised inoculum was added to 4875 µL of artificial urine for a total volume of 5000 µL in a universal. The inoculated artificial urine was then incubated for 70 minutes on a shake plate at 37°C. A V bottomed 96 well plate (Thermo Fisher Scientific, Leicestershire, UK) was set up to test the following parameters: 1) antibiotic-loaded hydrogels; 2) antibiotic-free hydrogels; 3) a volume of sterile water equal to the volume of the hydrogel (0.9425 µL); 4) antibiotic added in solution equivalent to the concentration of antibiotic, if the hydrogel achieved 100% antibiotic release. Four of these 96 well plates were made up with each being used to test a different incubation time period. The plates were incubated for 5, 10, 15 and 20 minutes respectively. After each incubation time, serial dilution followed by bacterial enumeration was carried out, as described in **Section 3.3.2**, using a 10 µL sample taken from the 96 well plate. To determine if significant inhibition of bacterial growth had occurred, the derived CFU/ml counts between the antibiotic hydrogel treated bacteria, and the antibiotic free controls were statistically compared using the statistical tests as discussed in **Section 2.4.**

3.4 Results and discussion

3.4.1 Confirmation of bacterial growth and the MIC of *gentamicin sulphate against E. coli* ATCC 25922

The work covered in **Chapter 2** demonstrated that first-generation R-SPEs reliably produce an easily interpreted resazurin I_{pc}, which is shown in **Figure 2.14 A**. Before conducting R-SPE based electrochemical AST, preliminary work was conducted to establish the growth of bacteria in the artificial urine, as well as confirm the MIC at which 50% (MIC 50) of bacterial growth is inhibited by gentamicin sulphate to determine how sensitive the R-SPEs can be in detecting significant inhibition of bacterial growth. A model of *E. coli* ATCC 25922 was used to determine bacterial growth in artificial urine. The CFU/ml counts of the bacteria grown without antibiotic treatment were compared to those treated with gentamicin sulphate, using the MIC 50 concentration of 0.5 µg/ml [299].

Figure 3.2 compares the growth of *E. coli* ATCC 25922 in artificial urine, with and without antibiotic present. The growth of the untreated bacteria increased in a linear trend demonstrating that artificial urine has no significant negative effect on bacterial growth. The antibiotic treated bacteria exhibited the same trend, however the growth was inhibited approximately 50% relative to the untreated bacteria confirming that a gentamicin sulphate concentration of 0.5 µg/ml is the MIC 50 value. This enabled a point of comparison for the electrochemical AST to which the sensitivity of the first-generation R-SPEs could be assessed relative to a culture-based AST method.

3.4.1 Long incubation first-generation R-SPE Electrochemical AST

Establishing the viability of first-generation R-SPEs as tools for conducting rapid AST was an imperative step in starting the development of a full LOC device. An overview schematic of the operating principles of the electrochemical AST can be seen in **Figure 3.3**. First-generation R-SPEs were then used to conduct electrochemical AST using a range of gentamicin sulphate concentrations from 0.1 to 1.4 µg/ml.

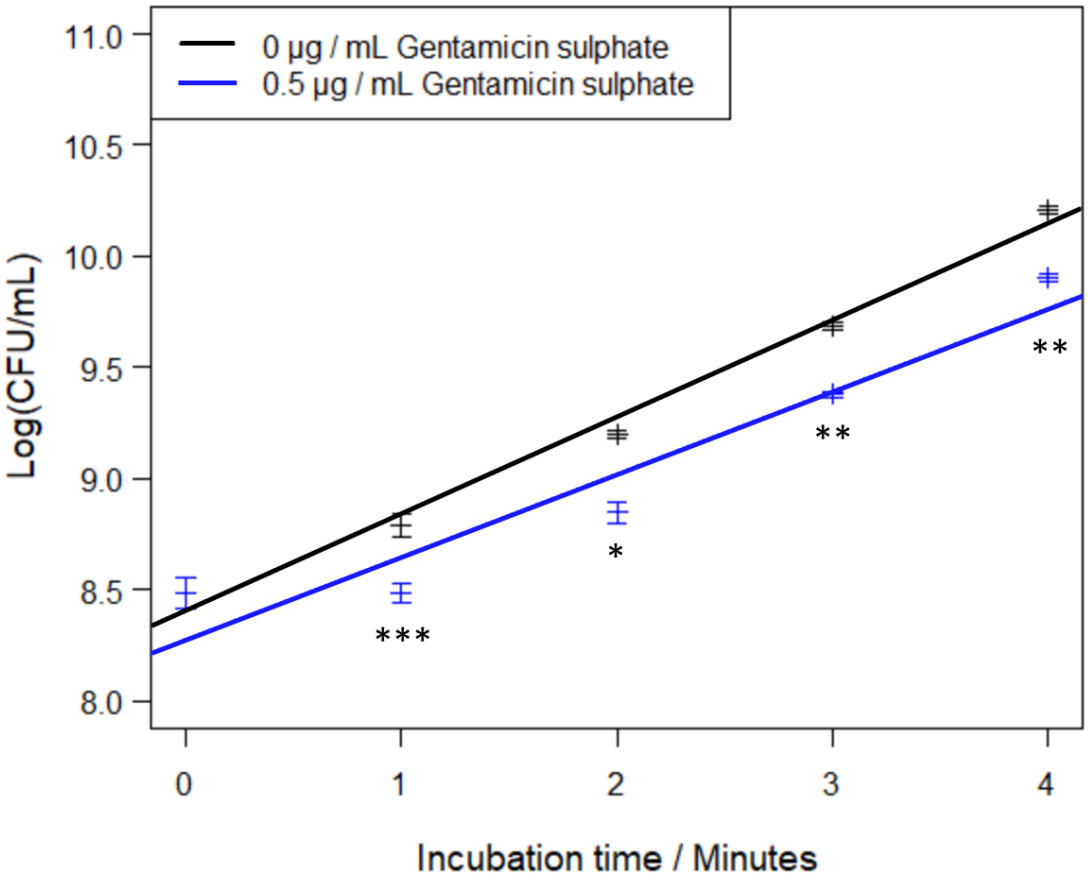

Figure 3.2 CFU/ml counts derived using concentrations of 0 and 0.5µg/ml gentamicin sulphate versus *E. coli* ATCC 259222. N = 5, error bars represent standard deviation, significance is indicated as follows: * = p-value < 0.05, ** = p-value < 0.005, *** = p-value < 0.0005.

By using a range of concentrations, including the MIC50 value of 0.5 µg/ml, it would determine how sensitive the first-generation R-SPEs are in detecting the change in resazurin concentration between the antibiotic-treated bacteria, and untreated control. The plot of the height of the resazurin I_{pc} at C1 (as shown in **Figure 2.14 A**) versus the incubation time for gentamicin sulphate concentrations of 0.5 and 0.7 µg/ml are shown in **Figure 3.4 A** and **B** respectively. In using a concentration of 0.5 µg/ml, the resazurin I_{pc} associated with antibiotic-treated bacteria was on average higher, however, it was not statistically significantly higher that the antibiotic free control which would the infer that the antibiotic was ineffective.

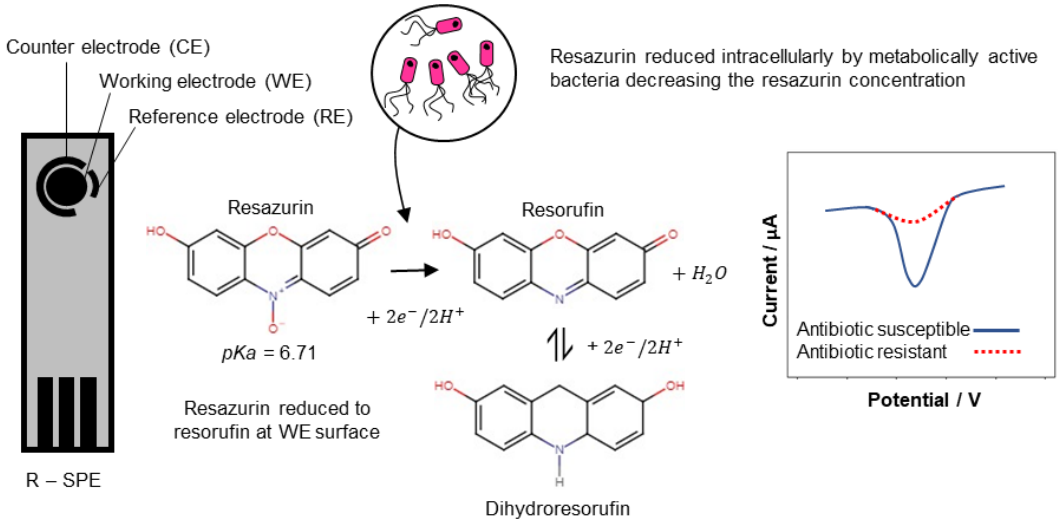

Figure 3.3. An overview schematic of phenotypic AST using an electrochemical based methodology. Resazurin can be reduced intracellularly by metabolically active bacteria or electrochemically at the surface of the working electrode which allows the antibiotic susceptible and antibiotic resistant bacteria to be determined [216, 217]

A higher concentration of 0.7 µg/ml, however, did yield a significantly higher resazurin I_{pc} value at each of the incubation points, which infers that a concentration of 0.7 µg/ml does effectively inhibit bacterial growth with antibiotic susceptibility of *E. coli* ATCC 25922 being determined in 130 minutes of total time (70-minute preincubation plus 60 minutes of testing). The first-generation R-SPEs could not resolve a statistically significant difference in the reduction peak height values derived at the MIC 50 concentration of 0.5 µg/ml. This indicates there is a loss in sensitivity in using first-generation R-SPEs versus culture-based CFU/ml count-based AST. Gentamicin sulphate is an aminoglycoside, mechanically it induces cell death by interrupting mRNA translation by binding to the 16S rRNA at the 30S ribosomal subunit, thus, any proteins synthesised are partially formed and non-functional [269]. Resazurin reduction occurs intracellularly with the reduction process being enabled by dehydrogenase enzymes such as nicotinamide adenine dinucleotide (NADH). The production of these enzymes is inhibited by gentamicin, however, NADH will still be produced by any metabolically active cells, additionally, some of the cells that have been killed by gentamicin will still be capable of resazurin reduction for a short time due to the continued presence of intracellular dehydrogenase enzymes.

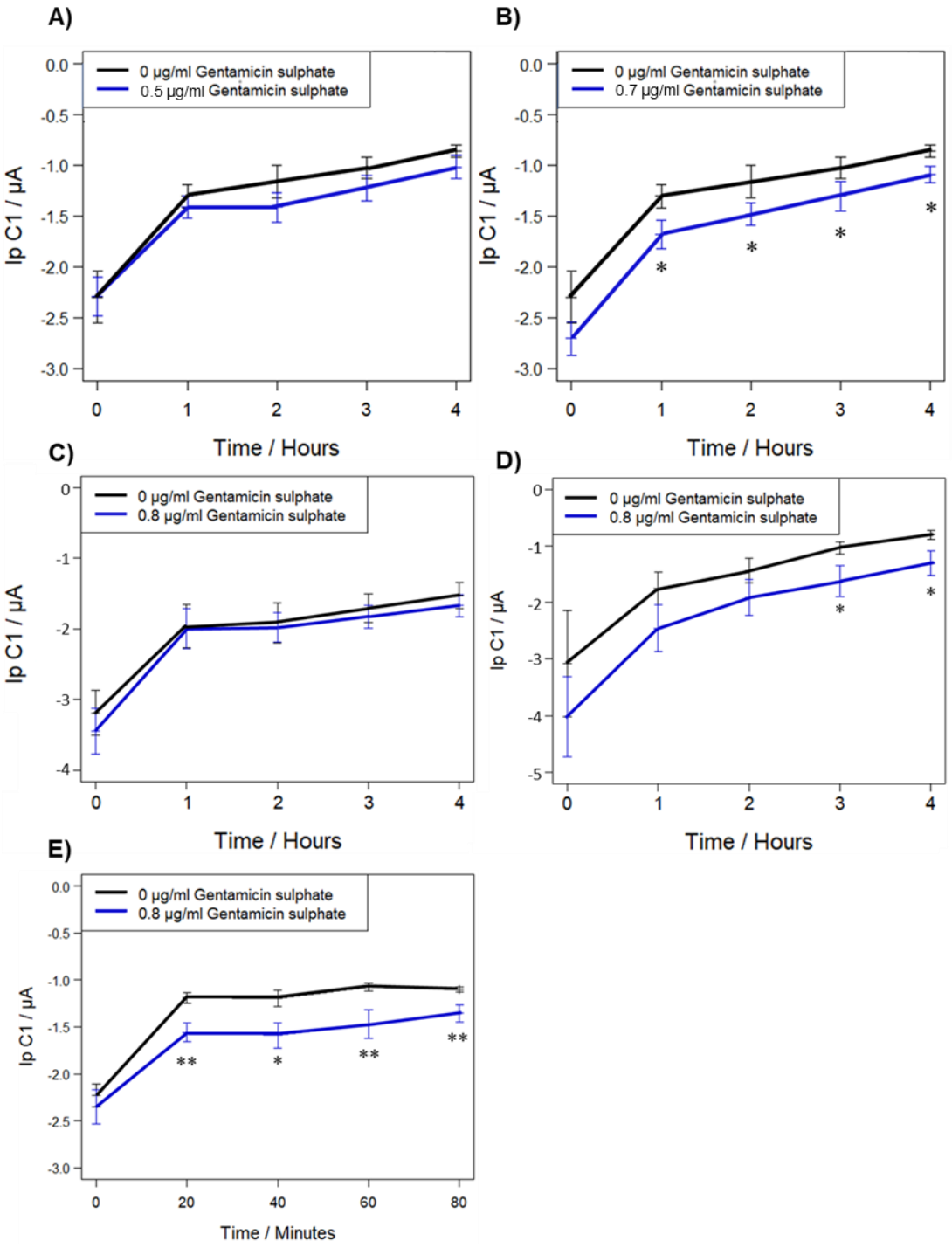

Figure 3.4 Figure sections **A** to **D** show resazurin I_{pc}s generated using DPV at time intervals of one hour using; **A)** Inoculated artificial urine, 0 (control) and 0.5 µg/ml concentrations of gentamicin sulphate and first-generation R-SPEs. **B)** Inoculated artificial urine, 0 (control) and 0.7 µg/ml concentrations of gentamicin sulphate and first-generation R-SPEs. **C)** Sterile artificial urine, 0 (control) and 0.8 µg/ml concentrations of gentamicin sulphate and first-generation R-SPEs. **D)** Inoculated artificial urine, 0 (control) and 0.8 µg/ml concentrations of gentamicin sulphate and C-SPEs. **E)** Shows resazurin I_{pc}s using DPV at time intervals of 20 minutes using inoculated artificial urine, 0 (control) and 0.8 µg/ml concentrations of gentamicin sulphate and first-generation R-SPEs. N = 5, error bars represent standard deviation, significance is indicated as follows: * = p-value < 0.05, ** = p-value < 0.005.

A concentration of gentamicin sulphate greater than that of the MIC 50 value was required to sufficiently inhibit cell growth so that first-generation R-SPEs could determine a significant difference in the concentrations of resazurin in the antibiotic-treated bacteria versus the antibiotic-free control in the time intervals that were used. To experiment with different time intervals and control testing, a gentamicin sulphate concentration of 0.8 µg/ml was used.

A consideration with the use of DPV based electrochemical detection of resazurin is that the sulphate group may be electrochemically active. To ensure that the significant difference that was found was a result of the difference in the bacterial growth rates between the control and antibiotic-treated bacteria, the experiment was conducted using sterile artificial urine and gentamicin sulphate concentrations of 0 and 0.8 µg/ml. The results are summarised in **Figure 3.4 C**, no significant difference was found between either of the concentrations at any of the time points. At a concentration of 0.8 µg/ml gentamicin sulphate has no significant effect on the electrochemical reduction of resazurin. Any significant difference that is determined to occur between the antibiotic-treated and antibiotic-free *E. coli* ATCC 25922 is due to the significant biological reduction of resazurin by the antibiotic-free bacteria. The simple single-step bulk modification process used to fabricate first-generation R-SPEs produced a viable single use analytical tool that could determine the susceptibility of *E. coli* ATCC 25922 to gentamicin sulphate within 130 minutes, thereby, the analytical potential of the first-generation R-SPEs has been demonstrated.

To justify the use of the modified SPEs, the experiment was repeated using unmodified C-SPEs and resazurin dissolved in solution. The plot of the resazurin I_{pc} using C-SPEs at each incubation point is shown in **Figure 3.4 D**. Relative to the first-generation R-SPEs counterpart as shown in **Figure 3.4 B** there was a greater standard deviation in the resazurin I_{pc}s values with susceptibility being determined after 250 minutes of total testing time (70-minute preincubation and 180 minutes of testing time). C-SPEs yield a slower time to analysis than first-generation R-SPEs validating the use of the bulk modification step and the use of first-generation R-SPEs over unmodified C-SPEs to conduct electrochemical AST. This also indicates that the potentially

beneficial surface characteristics of the first-generation R-SPEs WE did have a positive effect on the detection of resazurin enabling more consistent production of resazurin I_{pc} values.

Shorter time intervals were then used to determine whether the time to analysis could be reduced. The overall method of conducting electrochemical AST remained the same, however, the time between DPV readings was reduced to 20 minutes. The plot of the resazurin I_{pc} using first-generation R-SPEs, and 20-minute time intervals is shown in **Figure 3.4 E**. The same trend was shown in **Figure 3.4 B** wherein the resazurin I_{pc} produced by antibiotic-treated bacteria was on average higher, however, susceptibility of *E. coli* ATCC 25922 to gentamicin sulphate was determined in 90 minutes of total testing time (70-minute preincubation plus 20 minutes of testing time). This demonstrates that the time to analysis could be reduced enabling more rapid determination of antibiotic susceptibility. Additionally, by reducing the time between DPV reading the effect of the residual dehydrogenase enzymes belonging to dead bacteria was less pronounced, reducing the deviation in the resazurin reduction peak height values derived from the voltammograms.

When developing a new method, it is important to consider the advantages and disadvantages of the method relative to its contemporaries. A breakdown of the different electrochemical and some conventional AST methods and the advantages and disadvantages they pose is covered in **Table 2.1.** The distinction between labelled and label-free is discussed in **Section 2.1.3** The proposed method demonstrates a significantly faster time to analysis than the gold standard disk diffusion assay as well as the broth microdilution assay, both of which are culture-based AST methods. The speed at which antibiotic susceptibility is established is also faster, or comparable in speed, to other labelled or label-free methods. Although slightly slower than some of its electrochemical contemporaries, the advantage of using a resazurin based electrochemical AST method is that it is compatible with any bacteria that can synthesise dehydrogenase enzymes which are found in both aerobic and anaerobic bacteria [300]. Therefore, the method can be used with a range of different bacterial organisms making it versatile. The proposed method offers an inexpensive and simpler alternative to other resazurin based

electrochemical detection systems for AST with an application towards urinary tract infections. This proposed system utilises 10% wt. R-SPEs, the percentage of which can be varied to potentially further decrease the time taken to achieve statistical significance to further optimise the system and reduce cost. Therefore, it has been demonstrated that the use of single-step bulk modified first-generation R-SPEs are a viable means of conducting rapid AST in isolation, and when compared with similar methods.

3.4.2 Preliminary antibiotic-loaded hydrogel testing

The delivery of resazurin was accomplished by bulk modifying C - SPEs by screen printing resazurin loaded ink onto the WE to fabricate R-SPEs. The next step was to devise a method of delivering antibiotics into the chambers containing the macroelectrodes. To fulfil this requirement, antibiotic hydrogels were fabricated, and their antimicrobial effects quantified.

Broth microdilution assays for each of the antibiotic that were used were prepared starting at an initial antibiotic concentration of 1000 µg/ml, serial dilution was prepared from this initial concentrating using a dilution ratio of 1:2 terminating in a concentration of 1.95 µg/ml. The results of the broth microdilution assay with annotations are available in **Table 3.3** for *E. coli* ATCC 25922, *E. coli* NCTC 13351 and *K. pneumoniae* 700603 (A full breakdown can be found in the **Appendix Section**, **Figure 7.3, 7.4** and **7.5** respectively)**.**

Table 3.3 Breakdown of the results derived from a broth microdilution assay to determine the MIC for a suite of antibiotics. N = 8

	MIC (µg/ml)		
Antibiotic	***E. coli* ATCC 25922**	***E. coli* NCTC 13351**	***K. pneumoniae* ATCC 700603**
Ceftriaxone	≤ 1.95	N/A – resistant	≤ 1.95
Cephalexin	≤ 1.95	62.5 – resistant	≤ 3.91
Colistin	≤ 3.91	≤ 3.91	≤ 1.95
Gentamicin	≤ 32	≤ 16	≤ 1.95
Piperacillin	≤ 1.95	≤ 1.95	≤ 1.95
Trimethoprim	≤ 1.95	≤ 1.95	≤ 1.95
Vancomycin	≤ 250	≤ 250	≤ 250

After the determination of the MIC values, the next step was to load a hydrogel with gentamicin sulphate at a concentration that would induce significant inhibition of bacterial growth. This experiment served to determine whether pure PVA hydrogels were a viable means of delivering antibiotics under simulated LOC device conditions. The predicted release rate of the antibiotic from a 10% w/v PVA based hydrogel was 40% in ~36 minutes [291].Continuing the use of gentamicin as the model antibiotic, the PVA hydrogel was loaded with 2.6 mg/mL of gentamicin sulphate, if 100% of the gentamicin sulphate diffused out of the hydrogel, the concentration of gentamicin sulphate in the simulated macroelectrode chamber volume on the 96 well plate would equal 160 µg/ml. Working under the assumption of the predicted release rate the concentration in the tested volume should reach 64 µg/ml in ~36 minutes, thereby, a concentration of 32 µg/ml in approximately 15 minutes. Using this predicted release rate, after an incubation period of 20 minutes the cell growth of *E. coli* ATCC 25922 and *K. pneumoniae* ATCC 700603 was expected to be significantly inhibited.

The efficacy of the antibiotic release can be seen in **Figure 3.5** where in statistically significant inhibition of bacterial growth was determined to occur in 40 minutes for *E. coli* ATCC 25922 and 60 minutes for *K. pneumoniae* ATCC 700603.

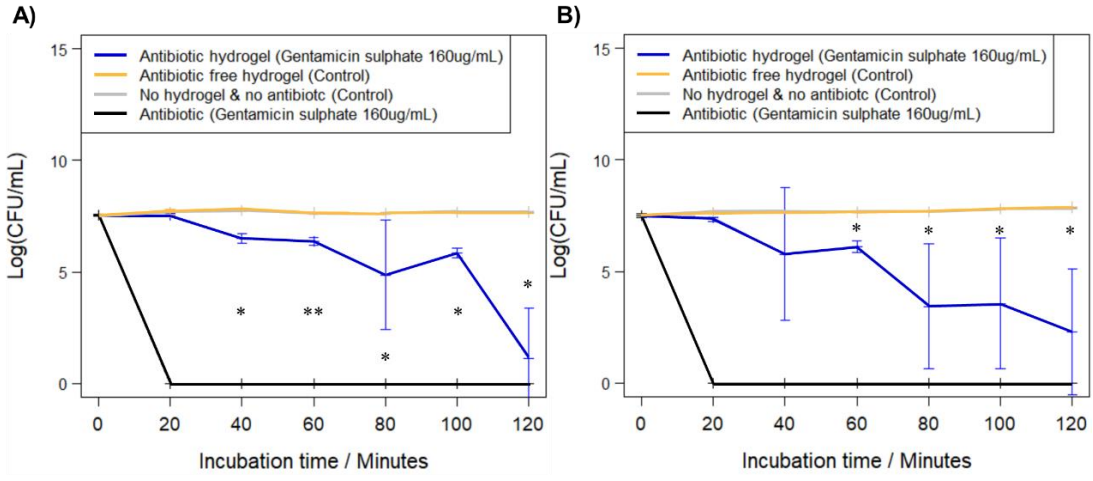

Figure 3.5 Bacterial growth of **A)** *E. coli*, **B)** *K. pneumoniae* as shown by the change in CFU/ml. N = 5, error bars represent standard deviation, significance is indicated between the CFU counts associated with the two controls, significance is indicated as follows: * = p-value < 0.05, ** = p-value < 0.005.

The release of the antibiotic was slower than expected as theoretically a concentration of 32 µg/ml of gentamicin sulphate should have been released in approximately 15 minutes which was not reflected in the trends exhibited by the growth of either bacterium. Due to the slower than predicted antibiotic release, the concentration of the antibiotic in the hydrogel precursor was increased to 5.2 mg/mL, double of what was originally used, for a 100% release concentration of 320 µg/ml to induce the desired inhibitory effect.

Further testing used shorter time intervals of 5 minutes to a total of 20 minutes in order to determine if the increased antibiotic concentration was sufficient to induce significant inhibition of bacterial growth in ≤ 20 minutes. The bacterial growth rates in response to the antibiotic hydrogels are shown in **Figure 3.6 A** and **B** for *E. coli* ATCC 25922 and *K. pneumoniae* ATCC 700603 respectively. The growth of both *E. coli* ATCC 25922 and *K. pneumoniae* ATCC 700603 were significantly inhibited after 10 minutes using both the gentamicin sulphate. An increased concentration of the antibiotic loaded into the hydrogel precursor produced the desired inhibitory effect. The inhibitory effect of the hydrogels was not instantaneous, with the antibiotic loaded hydrogels showing a steady release over time.

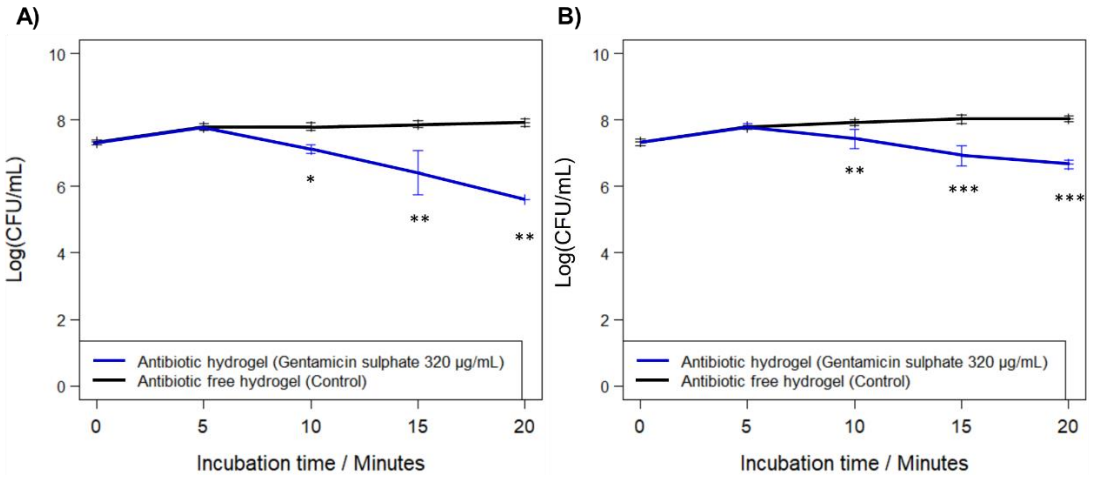

Figure 3.6 Bacterial growth of **A)** *E. coli*, **B)** *K. pneumoniae* in response to gentamicin sulphate hydrogels as shown by the change in CFU/ml. N = 5, error bars represent standard deviation, significance is indicated as follows: * = p-value < 0.05, ** = p-value < 0.005, *** = p-value < 0.0005.

Therefore, when moving onto the electrochemical AST an important consideration was the readings must be taken in a time frame of 15 to 20 minutes as the release of the antibiotic was sufficient to inhibit the growth of bacteria, but not released in a concentration so high that it would overcome the breakpoint of the resistance mechanism of a bacterium to give a false-positive result. After the effectiveness of using gentamicin sulphate hydrogels was determined, a suite of antibiotic-loaded hydrogels were fabricated and tested versus *E. coli* ATCC 25922, *K. pneumoniae* ATCC 700603 and *E. coli* NCTC 13351 which is summarised in **Figure 3.7** (**Appendix Section 7.6**, **Table 7.6** contains a full statistical breakdown). The concentrations of the antibiotics loaded into the hydrogel precursor followed the same formula as what was used for gentamicin sulphate after the initial testing of the gentamicin sulphate hydrogels using long incubation points as discussed in **Section 4.3.4**. Each of the bacteria tested demonstrated the same susceptibility profiles to the antibiotics used as was shown during the broth microdilution assay results which are shown in **Table 3.3**, with *E. coli* ATCC 25922 and *K. pneumoniae* ATCC 25922 showing susceptibility to all antibiotics except vancomycin. Whereas *E. coli* ATCC 13351 showed susceptibility to all antibiotics except cephalexin, ceftriaxone, and vancomycin.

The inhibition of bacterial growth via the use of vancomycin hydrochloride was part of the suite of antibiotics tested. Vancomycin is significantly less effective versus Gram-negative bacteria [301, 302] when compared to Gram-positive bacteria due to the mechanism of action of vancomycin in bacterial growth inhibition [278, 279]. The purpose of the inclusion of vancomycin was to determine whether an antibiotic which should not significantly inhibit bacterial growth of *E. coli* or *K. pneumoniae* would induce significant inhibition of growth when used at the same upscale factor as antibiotics of similar solubility (gentamicin sulphate, piperacillin sodium salt, ceftriaxone disodium salt). During this experimental setup, vancomycin hydrochloride at a 100% release concentration of 1.3 mg/mL did not significantly inhibit the bacterial growth of either *E. coli* or *K. pneumoniae* at any time point between 5 and 20 minutes.

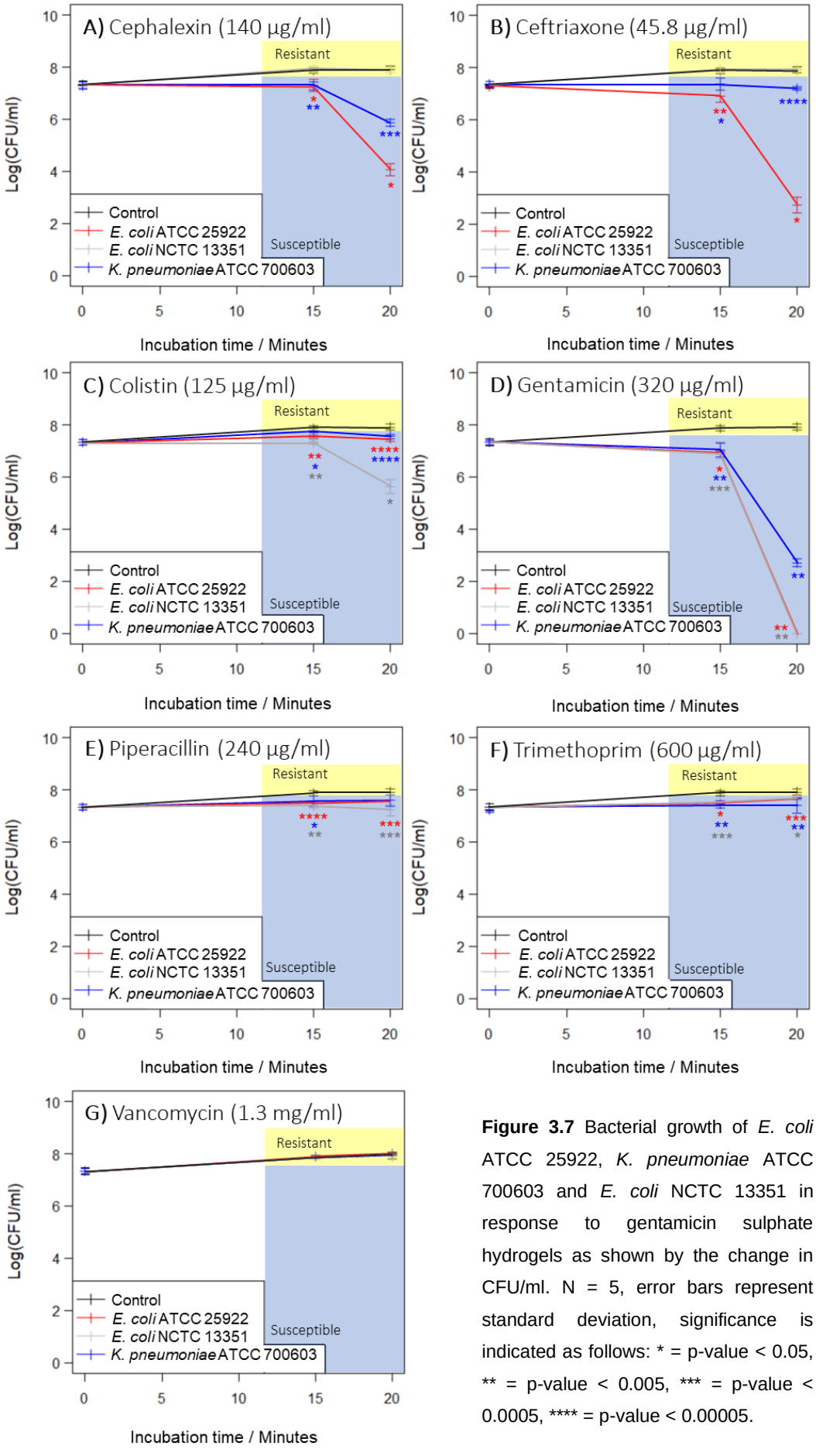

Figure 3.7 Bacterial growth of *E. coli* ATCC 25922, *K. pneumoniae* ATCC 700603 and *E. coli* NCTC 13351 in response to gentamicin sulphate hydrogels as shown by the change in CFU/ml. N = 5, error bars represent standard deviation, significance is indicated as follows: * = p-value < 0.05, ** = p-value < 0.005, *** = p-value < 0.0005, **** = p-value < 0.00005.

The antibiotic hydrogels were able to deliver a significant inhibiting concentration after 15 minutes which is the timeframe that is compatible with the speed at which antibiotic susceptibility could be determined electrochemically as demonstrated in **Figure 3.4 E**. The efficacy of the antibiotic release from the hydrogels was less than expected. This was due to the method by which the hydrogels were loaded with antibiotics. The hydrogel precursor was loaded with antibiotics in their solubilised forms before being mixed thoroughly, polymerisation was then induced using multiple freeze-thaw cycles. The gels used in the AST had a diameter of 2 mm, a height of 0.3 mm and an overall volume of 0.9425 µL, therefore, the secretion of the antibiotic from the hydrogels should have been efficient.

However, in using a w/v volume ratio of 10% and multiple freeze-thaw cycles it is likely that the matrix of PVA making up the solid element of the hydrogel is significantly denser than the surrounding media used in the AST. This caused the diffusion of the antibiotics from the gel to be slower than expected. As the antibiotic is released most rapidly from the most external elements of the hydrogel first, this increases the concentration of the antibiotic in the surrounding media, thus decreasing the concentration gradient. The decreased concentration gradient, in combination with the high density of the PVA hydrogel, is likely to result in slow release of the antibiotic.

The least efficient release was of the antibiotic trimethoprim, as it required an upscale factor of 8, from the initially predicted concentration, to induce significant inhibition of bacterial growth within 15 to 20 minutes. This coincides with the fact that trimethoprim is also the least water-soluble of the antibiotics used at < 1 mg/mL in water. Trimethoprim was solubilised in DMSO for addition to the hydrogel precursor. Note all AST using trimethoprim used DMSO in the antibiotic-free hydrogel controls at an equivalent concentration to what was used in the trimethoprim loaded antibiotic hydrogels to ensure the DMSO concentration used did not have a significant negative effect on the growth of both *E. coli* strains and *K. pneumoniae*.

3.5 Conclusions

First-generation R-SPEs have been used to conduct AST and identify antibiotic susceptibility within 90 minutes (70-minute preincubation and 20 minutes of testing time). In comparison, using unmodified C-SPEs antibiotic susceptibility can be determined within 250 minutes of total elapsed time (70-minute preincubation and 180 minutes of testing time) demonstrating that first-generation R-SPEs can enable more rapid electrochemical AST, therefore validating the use of the bulk modification of SPEs using screen printing.

Pure PVA based hydrogels had no significant negative effect on the growth of *E. coli* or *K. pneumoniae* making PVA ideal for use for antibiotic loading. Antibiotic-loaded PVA based hydrogels induce significant inhibition of bacterial growth after 15 minutes of testing time. The antibiotic load of the PVA hydrogel precursor was doubled and increased by a factor of eight for trimethoprim beyond the initially conceived loaded concentration, to overcome the limitation in the release rate of the antibiotic from the hydrogel.

The R-SPEs and the antibiotic loaded hydrogels could detect significant inhibition of bacterial growth and induce significant inhibition of bacterial growth within the desired time frame. Chapter 4 will now focus on the LOC devices that were designed to enable the integration of both the R-SPEs and the hydrogel into a single unit to enable parallelised multiplexed electrochemical AST.

4. Chapter 4: Lab on a Chip Testing

Executive summary

In this chapter, we cover the testing of the Lab on a Chip (LOC) devices and the testing of the complete electrochemical LOC based AST system.

- The LOC design was optimised to create an effective multiplexed system. Bacteria was delivered to first- and second-generation LOC devices using a flow rate of 10 µl per min and manual hydrodynamic filling using a syringe respectively.
- Second-generation R-SPEs and antibiotic hydrogels were integrated into first- and second-generation LOC devices. Using this combined approach, antibiotic susceptibility could be determined within 85 minutes (70-minute preincubation and 15-minute testing time).
- Proof-of-concept was demonstrated using spiked human urine samples on second-generation LOC devices wherein the most effective antibiotic for treating simulated urinary tract infections can be determined within 85 minutes (70-minute preincubation and 15-minute testing time) at pH values of 5.4, 5.8 and 7.4 respectively.

4.1 Introduction

This chapter covers the consolidation of all the previously conducted works covered in **Chapters 2** and **3** onto the LOC devices, which were designed such that they could house R-SPEs, and the antibiotic hydrogels to enable parallelised multiplexed electrochemical AST.

4.1.1 LOC device material composition

A breakdown of the percentage frequency of the materials used in LOC devices for UTIs between 2006 and 2022 is shown in **Figure 4.1.** Looking into the literature surrounding LOC devices for UTIs two material choices were the most frequently used: polydimethylsiloxane (PDMS) and poly(methyl methacrylate) (PMMA). PDMS based LOC devices have been used in bacterial identification [152, 153, 156] and for AST [112, 157].

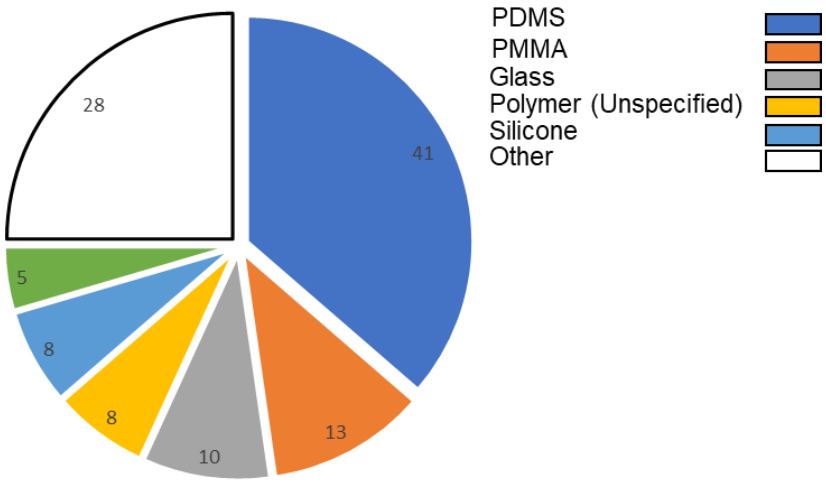

Figure 4.1. Shows the percentage breakdown of the use of different LOC device materials between 2006 and 2022 as a percentage value taken from **Table 1.1**. Material name abbreviations were as follows were as follows: poly(methyl methacrylate) (PMMA) polydimethylsiloxane (PDMS) and other which included materials used only once including polycarbonate, propylene co-polymer FEP-Teflon, hydrophilic and light shielding tape, polystyrene, nicrocellulose paper, tetradecane, hydrophilic sheets, photopolymer, Fluorinated ethylene propylene and borosilicate.

The advantage of using PDMS is that the material can be gas permeable, depending on the constitution of the precursor, enabling samples to remain oxygenated during testing [303] so unless there are nutritional issues within the system, bacteria can grow unimpeded. The fabrication methods are also straightforward, as the PDMS polymer can be added to a mould before being subjected to heat or UV treatment to initiate polymerisation to fabricate a solid PDMS based LOC device [152]. The use of PDMS has two disadvantages. Firstly, that it is not an easy material to work with for mass production. Secondarily, bonding the PDMS microfluidic layers whilst also integrating an macroelectrode layer would be challenging. PMMA can be injection moulded or hot-embossed. LOC devices fabricated using PMMA have been used in applications for bacterial identification [131, 135, 136, 150] and AMR [142] testing. PMMA, however, cannot be sterilised using an autoclave as the glass transition temperature is too low, which will cause the structure of the PMMA based LOC device to distort which in turn will render any microfluidics inoperable, and prevent the assembly of the LOC device, therefore, preventing multiple uses. Polycarbonate based LOC devices have been used for AMR

testing [143]. Polycarbonate is a solid polymer and does not require moulding to form a LOC device, instead, polycarbonate is procured as sheets for either manual or computer-aided milling to produce the desired shape and size. This creates robust, reusable LOC devices which is a distinct advantage over PDMS and PMMA. A disadvantage of polycarbonate is that it is not air-permeable and oxygen availability could be a limiting factor in bacterial growth. Under the current method, the bacteria are initially cultured off the LOC device to bring them to the lag phase of growth before they are introduced onto the LOC device. Using first-generation R-SPEs antibiotic susceptibility could be determined electrochemically within 20 minutes of testing, given that this is a very short time frame in which the oxygen concentration could become a limiting factor for bacterial growth, it unlikely that oxygen will become a limiting factor for bacterial growth inside the LOC devices. However, this parameter will still require investigation before electrochemical AST is conducted. A significant advantage of using polycarbonate LOC devices is that they can be autoclaved, enabling multiple uses of a single LOC device making it an ideal material for the research and design stage an LOC based electrochemical AST platform.

4.1.2 Microfluidic flow

There are several different types of microfluidic flow or analyte manipulation that can be used in a LOC device. Magnetic forces can be used to selectively capture and move specific magnet nanoparticle conjugated targets such as specific bacteria such as *E. coli* [152] or specific elements of the bacterial genome like the blaCTX-M-15 gene [141]. A LOC-based diagnostic platform for UTIs should be able to be used ubiquitously with all the common causative types of bacteria. UTIs have many causative types of bacteria as is shown in **Figure 1.4**, therefore if a magnetic-based transport system was used in the LOC device then multiple types of magnetic particles bound with bacterial specific antigens would be required for the method to function. This would increase the complexity of the LOC device and is, therefore, impractical in this application. Hydrodynamic flow, also known as hydrodynamic pumping enables the passage of a liquid through a microfluidic channel through the

application of pressure via gravity [135], hydrostatic forces, centrifugal forces, or by mechanical means such as a syringe pump [304]. Given that hydrodynamic flow-based approaches can be applied to all bacterial samples while suspended in a liquid medium, hydrodynamic flow was chosen as the method by which the LOC were filled.

4.2 Aims and objectives

The main aim of this chapter is a consolidation of all of the work conducted in **Chapters 3** and **4** to produce proof-of-concept LOC devices for electrochemical antibiotic susceptibility. This will be achieved through the completion of the objectives below:

- To determine the optimal design for the LOC devices and ensure even distribution of flow into macroelectrode chambers.
- To determine if bacterial growth can occur within the macroelectrode chambers on the LOC device.
- To determine whether second-generation R-SPEs and antibiotic hydrogels can successfully be integrated into LOC devices
- To evaluate if electrochemical antibiotic susceptibility could be determined using spiked human urine samples.

4.3 Experimental

4.3.1 LOC design

LOC devices were designed with the following considerations: the macroelectrode chambers had to be able to store all the reagents required for electrochemical AST; the microfluidic channels and inlets/outlets needed to enable even sample delivery to macroelectrode chambers; and an macroelectrode recess was required to integrate the R-SPEs with the LOC device.

The design of the LOC devices was done using AutoDesk Inventor 2019 (San Rafael, CA, USA) computer-aided design software. The LOC devices were fabricated using precision computerised numerical control (CNC) machining controlled using Datron CNC V9.108 software running on a

Datron M7 milling machine. The LOC devices were milled from polycarbonate with each chip being made of three individual layers as shown in **Figure 4.2**. The bottom layer had recesses for the integration of SPEs as well as the bolts to hold the device together. The middle layer was milled with the microfluidic channels with a width of 0.5 mm and a depth of 0.3 mm, the macroelectrode integration chambers, and a recess for the O-ring used to seal the LOC device chambers. The first- and second-generation LOC devices used O-rings with an internal diameter of 10.5 mm and a 1 mm cross-section (Polymax, Bordon, UK). The top layer was a single block of polycarbonate with holes milled for the inlet and outlet ports which connected with the microfluidics of the middle layer. The middle and top layers were aligned and then fusion bonded using a DrCollin P200 hot press.

Figure 4.3 A shows the first-generation of the LOC devices the macroelectrode chambers were rhomboid-shaped to enable consistent microfluidic flow from the inlet to the outlet channels. The chambers as an overall width of 0.7 cm, a length of 1.3 cm and a height of 0.3 mm with the internal volume being 16.5 µL. **Figure 4.3 B** shows the second-generation LOC devices which have been expanded to incorporate eight macroelectrodes/chambers.

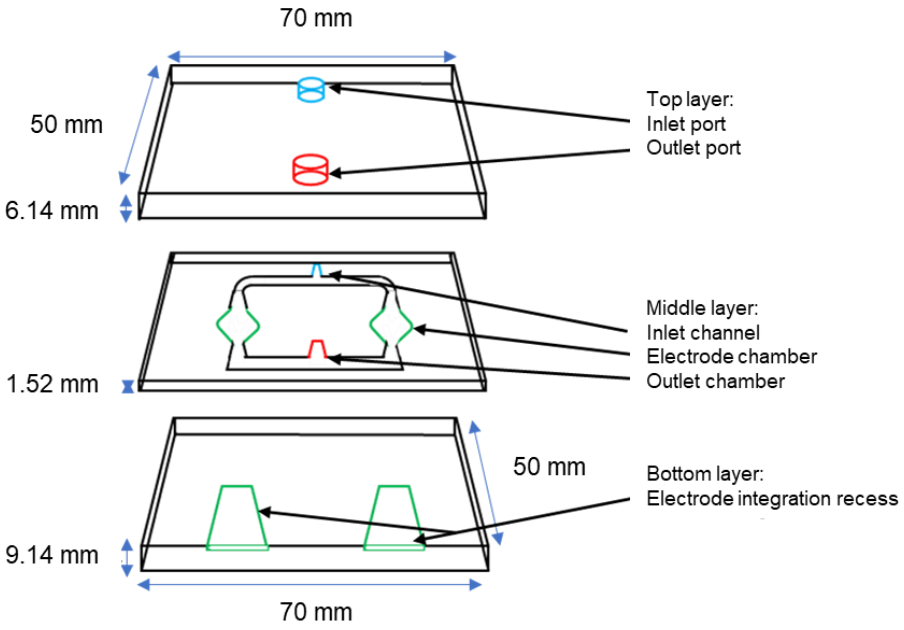

Figure 4.2 Exploded view of the three layers that make up a first-generation LOC device. Areas highlighted with colour indicate areas of the LOC device that overlap.

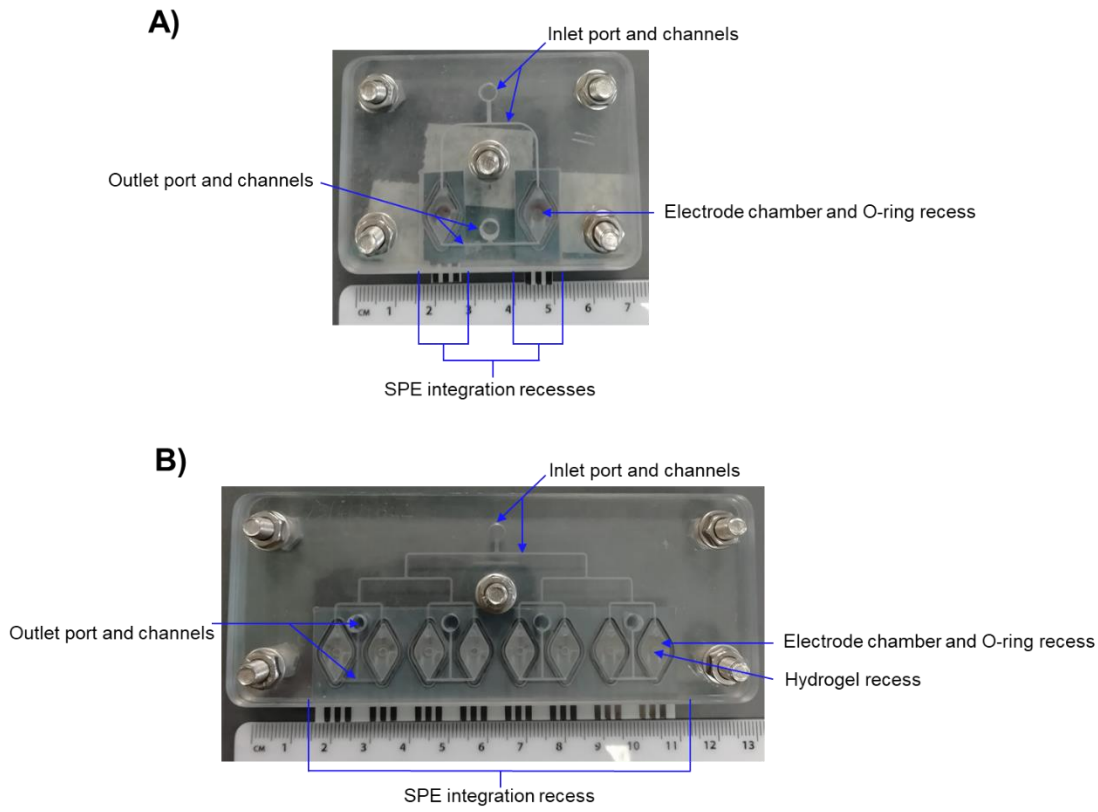

Figure 4.3. A) First and **B)** second-generation LOC devices.

The device was designed with one inlet port and a series of branching microfluidic channels designed such that each chamber was equidistant from the inlet port. Additionally, it was designed with one outlet port per pair of macroelectrode integration chambers.

4.3.2 LOC device preparation

Prior to any LOC based experimentation, the devices were first flushed through and then submerged in 70% ethanol solution (Sigma-Aldrich, Gillingham, UK) for 10 minutes before being moved to a drying rack. Additionally, O-rings were subjected to the same ethanol-based cleaning. The 3 layers of the LOC were then attached together. The LOC devices were filled using a model MD-1001 syringe pump (Bioanalytical Systems, West Latayette, USA). The pump used 5 mL syringes (Sarstedt, Numbrecht, Germany) to which a 50 mm length of silicone tubing (Gardiflex, Hertfordshire, UK) with an internal diameter of 3mm was attached. The tip of a 1 mm syringe was

removed (Sarstedt, Numbrecht, Germany) and attached to the terminal end of the tubing to act as the interface between the pump and the LOC devices.

4.3.3 Obstruction removal

The microfluidic outlet channels of the LOC devices could become obstructed by PVA hydrogels that migrated out of the LOC device chambers. Obstruction removal was carried out by first disassembling the LOC device and autoclaving the middle plate containing the LOC chambers and channels for 20 minutes at 121°C to degrade the PVA hydrogel. The device was then flushed with distilled water by manually exerting maximal pressure via a 5 mL syringe to flush out the remains of the hydrogel. The device was then prepared using the method in **Section 4.3.2** for experimental use.

4.3.4 Microfluidic flow testing

Optimal flow rates for the LOC devices were determined to enable quick and efficient filling without leaks or any issues with the filling of the LOC chambers. To visualise the movement of solutions through the LOC devices, phosphate buffered saline (PBS) was mixed with blue food dye (Sainsburys, UK) at a ratio of 1:6, the mixture was filter sterilised before use, using a 45nm syringe filter (Sarstedt, Numbrecht, Germany). First and second-generation LOC devices were tested using flow rates of 8, 10 and 20 µL per minute. The syringe pump as setup as described in **Section 4.3.2** The success rate of having all the chambers fill was recorded per LOC device individually with each device being tested three times per flow rate. The success rates were then converted into percentages for assessing the performance of each of the LOC devices.

4.3.5 Confirmation of bacterial delivery

After the syringe pump was turned off, the LOC device was opened, serial dilution followed by bacterial enumeration was carried out, as described in **Chapter 3 Section 3.2.2,** using 10 µl samples taken from each of the deposits of artificial urine left by the macroelectrode chambers on the second-generation R-SPEs. Second-generation LOC devices were filled using manual

hydrodynamic filling with a 1 mL syringe. After filling, the same method of preparing spread plates was applied as previously described. The CFU/ml counts derived from each chamber from each flow rate were then statistically compared using the statistical tests as discussed in **Section 2.4.**

4.3.6 Bacterial growth on the LOC devices

As the LOC is a closed system there was a possibility that oxygen could be a limiting factor in bacterial growth, therefore, bacterial growth on the LOC in the absence of antibiotics was examined. Bacterial growth was assessed using *E. coli* ATCC 25922 and *K. pneumoniae* ATCC 700603 which were prepared and standardised as discussed in **Section 3.2.1**, after which the standardised inoculum was then diluted by a factor if 40 in artificial urine for a total volume of 5000 µL in a universal. The inoculated artificial urine was then incubated for 70 minutes at 37°C, after which the preincubated sample was pumped into the LOC devices at a flow rate of 10 µL per minute. Post filling, incubation times of 0, 1, 2, 3 and 4 hours were used to quantify bacterial growth on the LOC devices. After a given incubation time, the LOC device was opened, and serial dilution followed by bacterial enumeration, as described in **Section 3.2.2**. The experiment was repeated three times per LOC device. Running in parallel, the same experimental setup was conducted using 96 well plates into which five rows of five wells were filled with a total of 16.5 µL of inoculated artificial urine using both *E. coli* ATCC 25922 *and K. pneumonia* ATCC 700603 independently. The CFU/ml counts were calculated and statistically compared, using the statistical tests discussed in **Section 2.4,** to the LOC derived counterparts to determine if there was a significant effect on bacterial growth conducted on the LOC devices.

4.3.7 Electrochemical LOC antibiotic susceptibility testing

The next step in the testing was to combine all the individual elements detailed in **Sections 3.3.2** and **3.3.3** (initial electrochemical AST and hydrogel testing) to evaluate the electrochemical AST platform as a whole. First-generation LOC devices were used to test one type of antibiotic-loaded hydrogel against an

antibiotic-free hydrogel to determine if antibiotic susceptibility could be determined within the time it had taken for the antibiotic-loaded hydrogels to induce significant inhibition of bacterial growth. The antibiotic-loaded hydrogels were placed on top of second-generation SPEs, which were then integrated into the first-generation LOC devices as seen in **Figure 4.4**.

E. coli ATCC 25922 and *K. pneumoniae* ATCC 700603 were prepared and standardised as discussed in **Section 3.2.1**, after which the standardised inoculum was then diluted by a factor if 40 in artificial urine for a total volume of 5000 µL in a universal. The first-generation LOC devices were then spiked with the prepared diluted inoculum using a syringe pump and a flow rate of 10 µL per minute. An initial electrochemical reading was taken immediately after the filling step using DPV using the same parameters described in **Section 2.3.4**, with an applied voltage of 0.1 to -1.1V. The LOC devices were then incubated at 37°C for 15 minutes before a second DPV reading was taken. To confirm that any significance in the resazurin I_{pc}s was due to significant inhibition of the bacteria by the antibiotic hydrogels, after the incubation period, the LOC device was opened, and serial dilution followed by bacterial enumeration was carried out, as described in **Section 3.2.2**.

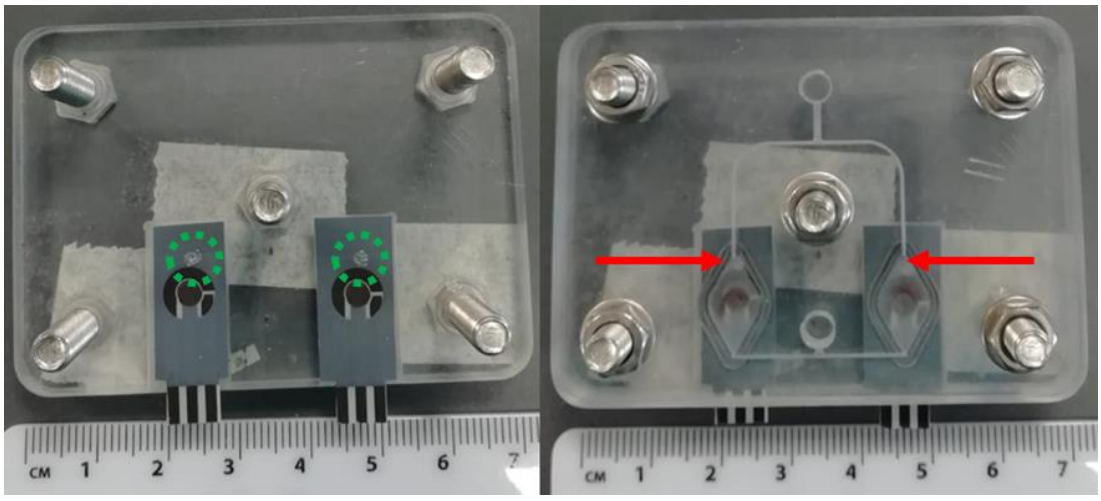

Figure. 4.4. Shows the loading of the antibiotic hydrogels onto first-generation SPEs before (Left) where the hydrogels are highlighted in the green circles, and after (right) device assembly where the position of the hydrogels are highlighted with red arrows.

Both the resazurin I_{pc}s and the CFU/ml counts from the antibiotic-loaded hydrogel chamber counts were compared, using the statistical tests as discussed in **Section 2.4,** to the values derived from the antibiotic-free hydrogel chambers at each incubation time to determine if the antibiotic-loaded hydrogel had a significant effect on the bacterial growth in the LOC devices.Ideally, however, a LOC device should be capable of testing multiple antibiotics on a single device. Second-generation LOC devices were used to test seven antibiotic-loaded hydrogels and an antibiotic-free control. The following hydrogels were loaded into chambers one through eight respectively as shown in **Figure 4.5**: antibiotic-free hydrogel, piperacillin, gentamicin, vancomycin, ceftriaxone, trimethoprim, cephalexin, colistin. The order was based on the effectivity of the antibiotic hydrogels as demonstrated in **Section 3.3.3** with the antibiotic hydrogels that inhibited bacterial growth the least positioned so that the macroelectrode chambers would be the first to be read using DPV, with the exception of vancomycin as it is ineffective versus Gram-negative bacteria and so was read last. *E. coli* ATCC 25922, *K. pneumoniae* ATCC 700603 and *E. coli* NCTC 13351 were prepared discussed in **Section 3.2.1***,* after which 125 µL of the standardised inoculum was added to 4875 µL of artificial urine for a total volume of 5000 µL in a universal.

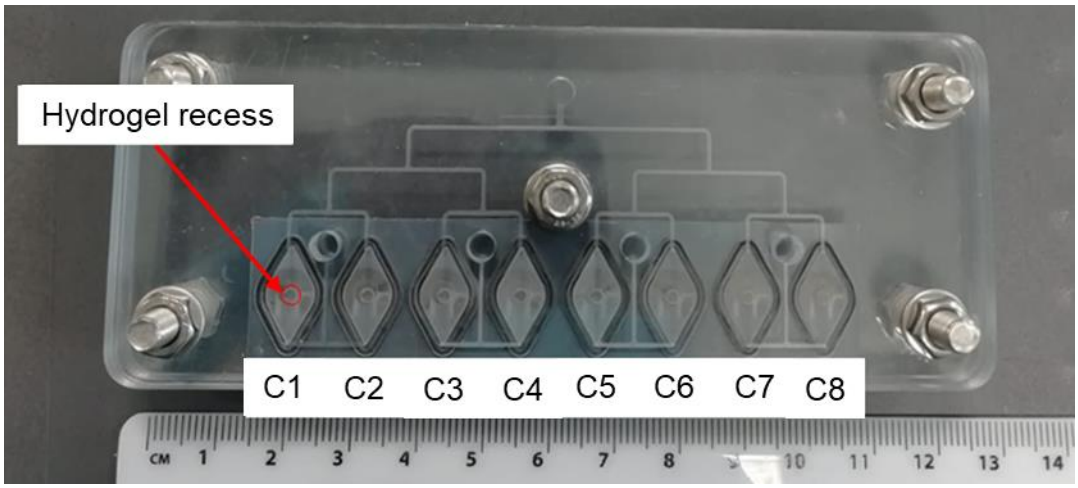

Figure 4.5. LOC device hydrogel loading into Second-generation LOC devices. The position of the antibiotic-free hydrogel is highlighted with a red arrow and circle. Each subsequent hydrogel was sequestered in the same position in subsequent macroelectrode chambers one through to eight (C1 – C8).

Second-generation LOC devices were spiked with a bacterial sample using manual hydrodynamic filling with a 1 mL syringe, DPV measurements and statistical testing was carried out using the same parameters and method as the first-generation LOC devices. To ensure that DPV readings were taken quickly, two potentiostats were used simultaneously to take readings. DPV recordings were taken in pairs from the following chambers: C1 and C5; C2 and C6; C3 and C7; and C4 and C8. The LOC devices were then incubated at 37°C for 15 minutes after which another reading was taken using DPV. In using two potentiostats simultaneously the time taken to complete all eight chambers was ~3 minutes. This initial 3-minute reading time was subtracted from the total 15-minute incubation time.

4.3.8 Electrochemical LOC antibiotic susceptibility testing using urine

Urine samples were donated by volunteers (ethical approval was granted by the Faculty of Science and Engineering Ethics and Research Governance Committee (EthOS reference 2021-1838-26841)). The donated urine was sterilised via autoclave after it was received and after use, any remaining urine was destroyed in accordance with the Human Tissues Act 2004. Prior to autoclaving, the pH of the urine was recorded, then unfiltered human urine was mixed at a 1:1 ratio with double strength nutrient broth the pH of which was adjusted to match the pH of the urine. The bacterial preparations of *E. coli* ATCC 25922, *K. pneumoniae* ATCC 700603 and *E. coli* NCTC 13351 used the same method as described in **Section 3.2.1**, with the OD being standardised at 0.7 at 600 nm. After this step, 125 µL of the standardised inoculum was added to 4875 µL of artificial urine for a total volume of 5000 µL in a universal.

The solution was then put into a centrifuge at 5000 rpm for 10 minutes to form bacterial pellets, the supernatant was discarded carefully and replaced with a 5000 µL volume of human urine mixed in a one-to-one ratio with double strength nutrient broth. The spiked mixture was then introduced into second-generation LOC devices using manual hydrodynamic filling and electrochemical AST was conducted as described in **Section 4.2.7**.

4.4 Results and discussion

4.4.1 Microfluidic flow testing

The shape of the macroelectrode chamber was an important consideration as any issues in microfluidic flow across the macroelectrode chamber could cause filling issues or formation of air bubbles which would interfere with electrochemical readings due to occlusion of the macroelectrodes. The optimal chamber shape that was conceived featured a rhomboid-shaped design, as shown in **Figure 4.3**, which enabled consistent flow across the chamber by promoting contact between the media, the surface of the macroelectrode and the top of the chamber simultaneously. The macroelectrode chamber filling success rate of the first-generation LOC devices was tested and demonstrated a 66% success rate in filling both the left and right chambers using flow rates of 8, 10 or 20 µL per minute.

The second-generation LOC devices shared the same chamber design as the first-generation LOC devices but featured eight chambers in parallel with one inlet port and one outlet port per two chambers as shown in **Figure 4.3 B**. Initially the flow testing of the second-generation LOC devices presented some minor difficulties. Firstly, up to a maximal flow rate of 100 µL/minute as provided by the syringe pump, the macroelectrode integration chamber would fill improperly or not fill at all due to insufficient pressure. **Figure 4.6 A** demonstrates the secondary issue in that there would be leakage from the chambers due to insufficient pressure being applied to the O-rings to form a watertight seal. This methodological limitation was rectified by installing a metal bracket onto the second-generation LOC devices to achieve a more consistent application of pressure to the O-ring, thus, preventing leakage. The outlet ports were installed with sterile filters to decrease the speed at which air escaped, thereby, increasing the internal pressure on the device during the introduction of a liquid forcing the dye into filling each of the chambers. Thirdly, to generate greater pressure when the dye was introduced, manual hydrodynamic filling using a 1mL syringe was used in place of a syringe pump. This change to the setup resulted in 100% filling of all eight chambers with no leaks occurring in 85% of cases, an example is demonstrated in **Figure 4.6 B.**

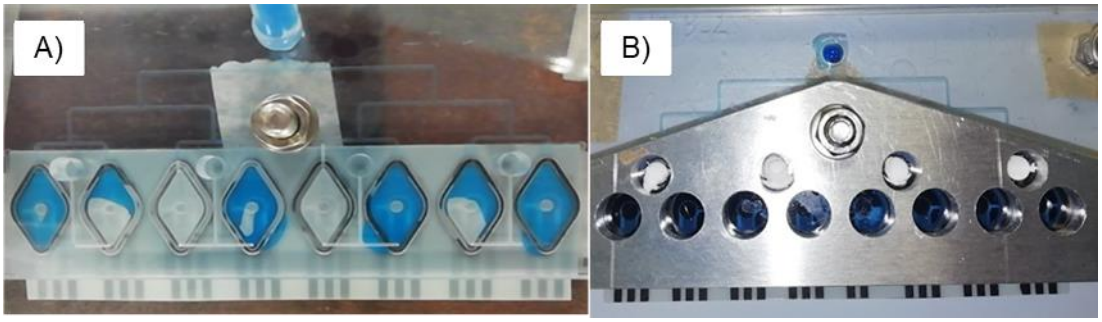

Figure 4.6. A) Shows the delivery of dye to the eight chambers of the Second-generation LOC device at a flow rate of 100 µL per minute. B) Shows the delivery of dye to the eight chambers of the Second-generation LOC device using manual hydrodynamic filling using a 1mL syringe and a metal bracket.

4.4.2 Confirmation of bacterial delivery

The delivery of bacteria to the different chambers of the LOC devices is imperative for the proper working of the electrochemical AST methodology as the method relies on determining changes in the concentration of resazurin, given that the extent of the biological reduction occurring being dependent on the concentration of bacteria in a media, any significant differences in the bacterial concentration across the different macroelectrode integration chambers could result in false-positive or negative results. The bacterial delivery to the two chambers of the first-generation LOC devices was assessed first, CFU/ml counts delivered to the two chambers hereafter referred to as the left and right chambers were statistically compared to determine if there was a significant difference in bacterial delivery. Flow rates of 8, 10, and 20 µl/mL were tested to determine if there would be a significant change when using different flow rates. The end CFU/mL counts derived from the left and the right chambers was also compared to bacteria grown outside of the LOC device but under the same conditions to assess if the microfluidic channels of the LOC device had a significant effect on the delivery of the bacteria. Each of the six first-generation LOC devices was tested to examine inter-chip variability and numbered one through to six for point of reference.

The CFU/ml counts delivered to the left and right chambers respectively for flow rates of 8, 10 and 20 µL/min is shown in **Figures 4.7 A**, **B** and **C** respectively with each LOC device being tested three times. There was no significant difference observed in the majority of flow rates and devices. The bacteria delivered to device number 3 had significantly different bacterial

concentrations in the left and right chambers respectively with the left chamber having a significantly higher bacterial load delivered (Paired t-test, t = 2.8141, df = 4, p-value = 0.04812) at a flow rate of 20 µl/min which is shown in **Figure 4.7 A**. In future experimentation a flow rate of 10 µL/min was used to fill the first-generation LOC devices. The experiment was repeated with the second-generation LOC devices, although the overall dimensions of the chambers and the microfluidic channels did not change between the first- and second-generation LOC device designs the network of channels in the second-generation LOC devices was longer overall and with more microfluidic junctions.

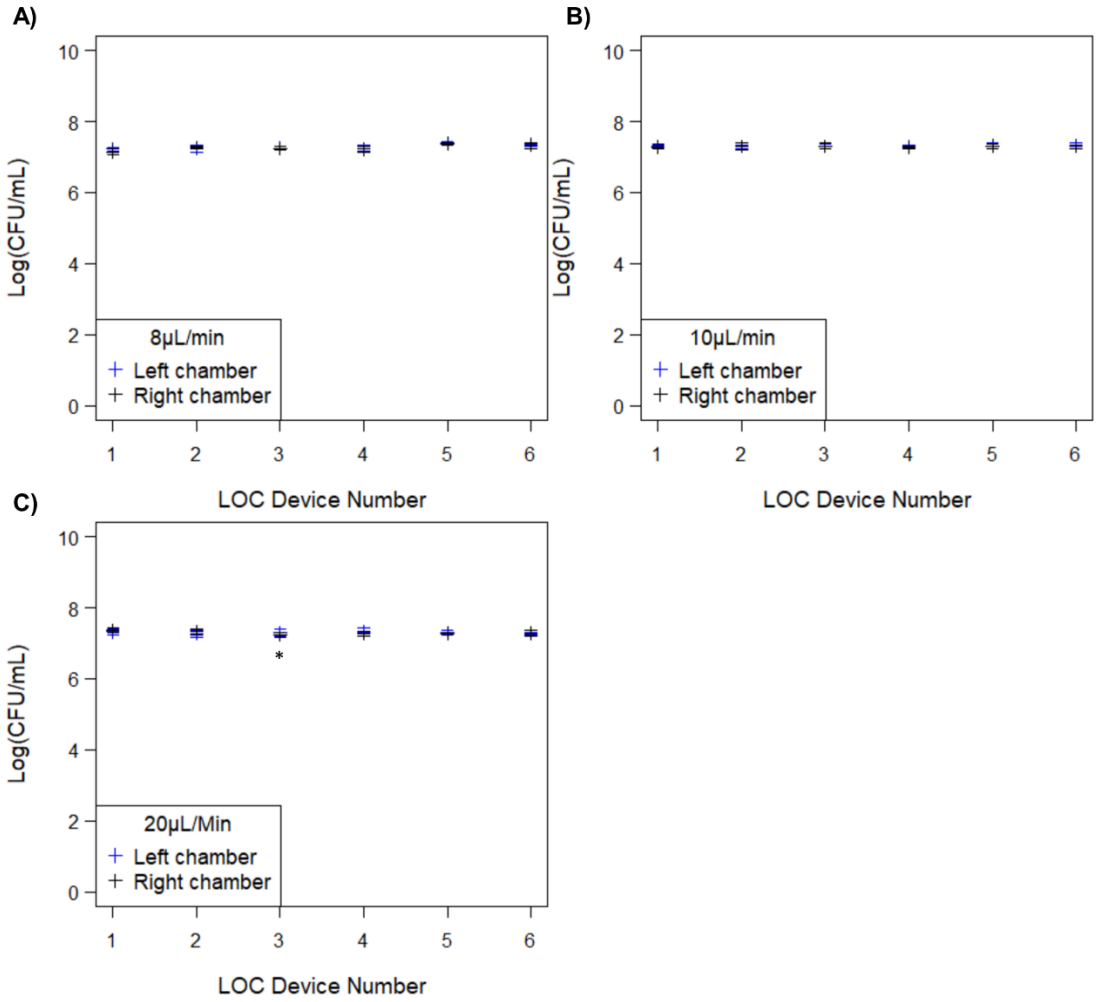

Figure 4.7. Shows the bacterial CFU/ml count derived from the left (Black) and the right (Blue) chambers of first-generation LOC devices when using a flow rate of **A)** 8, **B)** 10, **C)** and 20 µl per minute. N = 15, three repeats per LOC device, error bars represent standard deviation, significance is indicated as follows: * = p-value < 0.05.

The chambers were designated as one through to eight from left to right, and the devices one and two for point of reference. As mentioned in **Section 5.2.1** the filling of the second-generation LOC devices was carried out using manual hydrodynamic filling with a 1 mL syringe. This was done as using up to a maximal flow rate of 100 µL/min using the syringe pump resulted in improper macroelectrode chamber filling. Contributing factors to this were dimensional channel differences, or partial blockages in the inlet or outlet channels resulting in the uneven flow of liquid. Some issues were encountered attempting to take samples from the second-generation LOC devices for the purposes of bacterial enumeration. When separating the top and bottom plates of the second-generation LOC devices, the nutrient broth that was deposited from the macroelectrode chambers onto the second-generation R-SPEs from adjacent macroelectrode chambers could spread out and mix together. These nutrient broth deposits were then deemed unsuitable sources to take samples from for serial dilution and the preparation of spread plates. To gather data, multiple repeats were required to gain a full dataset. When samples were taken, only isolated deposits of nutrient broth were used, whereas deposits from adjacent chambers that had spread out and run together were ignored. This ensured that viable data would be gathered pertaining to the bacterial delivery to each of the macroelectrode chambers.

The CFU/ml counts derived from each of the chamber of the second-generation LOC devices is shown in **Figure 4.8**. The CFU/mL that were derived from each of the macroelectrode chambers were not statistically significant for second-generation LOC device number one (Kruskal-Wallis chi-squared = 10.407, df = 10, p-value = 0.4055) or number two (Kruskal-Wallis chi-squared = 11.996, df = 8, p-value = 0.1514). Manual hydrodynamic filling using a 1 mL syringe was then used for all second-generation LOC device-based experimentation.

4.4.3 Bacterial growth inside the LOC device

As mentioned previously, the biological reduction of resazurin is dependent on the concentration of the bacteria, as the bacterial population size dictates the extent of the biological reduction of the resazurin.

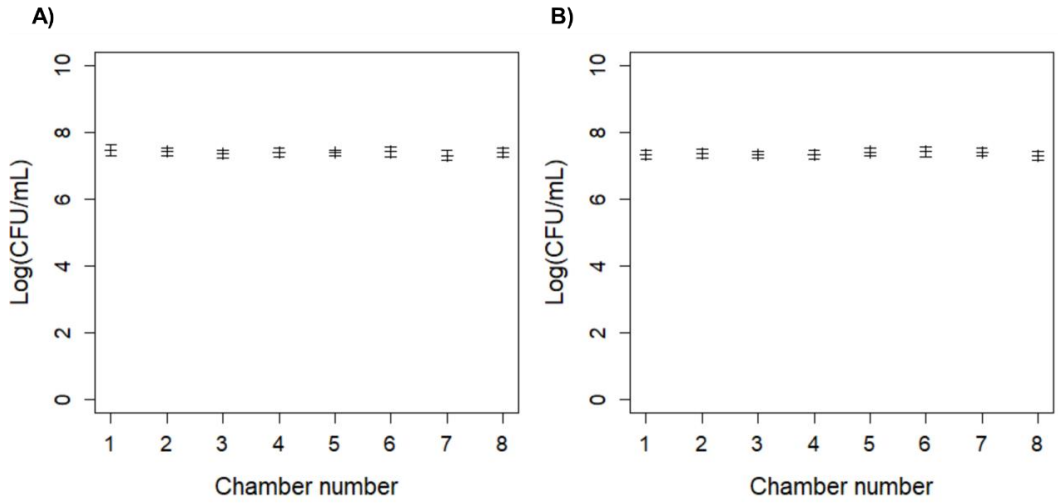

Figure 4.8. Shows the bacterial CFU/ml count derived from chambers one through to eight of the second-generation LOC devices **A)** one and **B)** two using manual hydrodynamic filling using a 1 mL syringe. N = 15, three repeats per LOC device, error bars represent standard deviation.

If the bacterial growth on the LOC devices was significantly inhibited due to nutritional or oxygen deficiency, the biological reduction of resazurin would therefore also be inhibited which in turn would increase the time to analysis as more time would be required for to electrochemically determine whether there is a significant difference in the resazurin concentrations between the antibiotic free, and antibiotic treated bacteria.

To determine if the conditions inside the LOC device affected bacterial growth, *E. coli* ATCC 25922 was spiked into first-generation LOC devices which were then incubated. Serial dilution followed by bacterial enumeration was carried out as described in **Section 3.2.2**, using 10 µl samples taken from the LOC chambers after each incubation point (up to 4 hours). The CFU/ml counts of bacteria cultured from samples were taken from the first-generation LOC device chambers and statistically compared to those taken from a 96 well plate which acted as a reference point and control as shown in **Figures 4.9 A** and **B** respectively. The growth of *E. coli* showed a significant decrease in growth versus the control after three hours of growth on the LOC device (T-test, t = 8.9242, df = 4, p-value = 0.0008717), whereas *K. pneumoniae* deviated after four hours of growth (T-test, t = -4.644, df = 4, p-value = 0.009705).

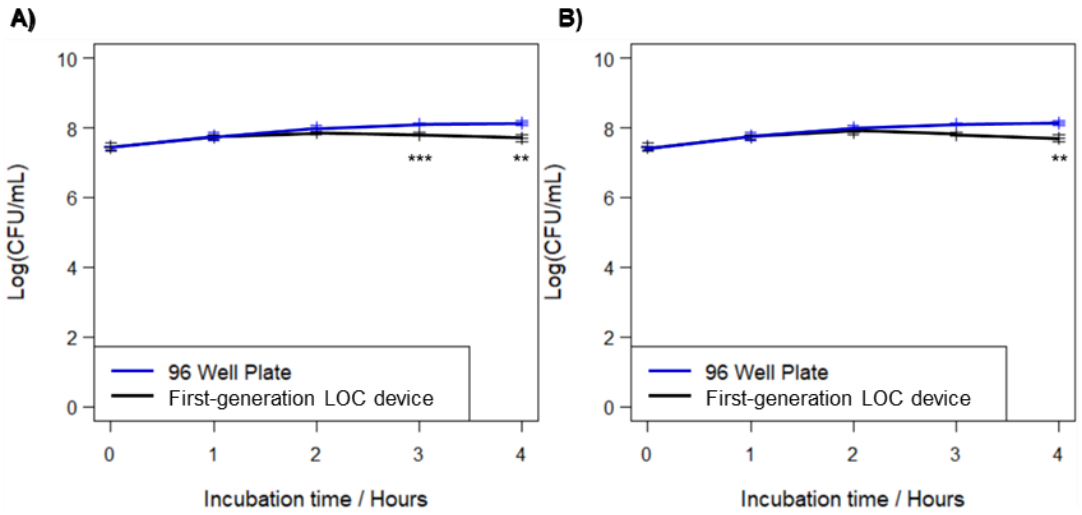

Figure 4.9. Shows the growth of **A)** *E. coli* and **B)** *K. pneumoniae* cultured in the first-generation LOC device and a 96 well plate. N = 15, three repeats per LOC device, error bars represent standard deviation, significance is indicated as follows: ** = p-value < 0.005, *** = p-value < 0.0005.

E. coli is a facultative anaerobic bacteria [305], thus, not requiring oxygen to proliferate. If the growth issues pertained to nutritional deficiency or an accumulation of toxic metabolic end products both of which can negatively affect bacterial growth [306], then the same decrease in growth would be reflected in the 96 well plate as the same volumes and incubation times were used. The only significant difference in the setups was the availability of oxygen to the bacterial populations with the bacteria spiked into the LOC devices being in a sealed chamber with significantly less ventilation relative to a 96 well plate. As previously stated *E. coli* is a facultative anaerobe, however the bacteria usually have a lower growth rate when undergoing anaerobic respiration [305].

Despite the characteristics of the bacteria that enable growth under unideal conditions, when incubated for a time greater than two-hours on the first-generation LOC devices the growth of *E. coli* ATCC 25922 is significantly inhibited. This, however, should not have a negative affect the electrochemical AST method as it is made up of a 70-minute preincubation off the LOC device, followed by a 20-minute interval of on-LOC device testing (making a total time of 90 minutes (**Chapter 4**) which is a substantially shorter time frame than the two hours of incubation required for bacterial growth on the first-generation LOC devices to become inhibited.

4.4.4 Electrochemical AST using first-generation LOC devices

Currently, it has been established that bacterial delivery to the different chambers on the first-generation LOC and second-generation LOC devices are not statistically significantly different and that the growth of bacteria on the devices are sufficient for the determination of antibiotic susceptibility. The next step was to establish how quickly AST could be determined using the second-generation R-SPEs in combination with the first-generation LOC devices and the antibiotic hydrogels using pH 6 artificial urine. The independent time points for the second DPV scan used to determine susceptibility were set at 10, 15 and 20 minutes to determine if a significant difference could be determined in a time ≤ 20 minutes. To validate the electrochemically determined AST results, serial dilution followed by bacterial enumeration was carried out, as described in **Section 3.2.2**, using 10 µl samples that were taken the macroelectrode chambers. The CFU/ml counts from the macroelectrode chamber with the antibiotic-loaded hydrogel were then statistically compared to the CFU/ml counts from the antibiotic-free control to determine if significant inhibition of bacterial growth had occurred. The reduction in the resazurin reduction peak height values derived after exposure to gentamicin sulphate hydrogels and the CFU/ml counts can be seen in **Figures 4.10 A** and **B** respectively. Electrochemical susceptibility could be determined at time points of 15 ($t = -2.8022$, $df = 4.4284$, p-value = 0.0434) and 20 minutes ($t = -9.8868$, $df = 3.9482$, p-value = 0.0006265). Under this experimental setup electrochemically antibiotic susceptibility can be determined five minutes faster than that indicated in **Section 4.3.1**, demonstrating a small but not insignificant improvement in the time to analysis. The electrochemical determination of susceptibility was verified from the CFU/ml counts derived from the second-generation LOCs chambers which showed significant inhibition at time points of 15 (T-test, $t = 4.727$, $df = 4.0661$, p-value = 0.008765) and 20 minutes (T-test, $t = 9.2554$, $df = 4.1999$, p-value = 0.0005999).

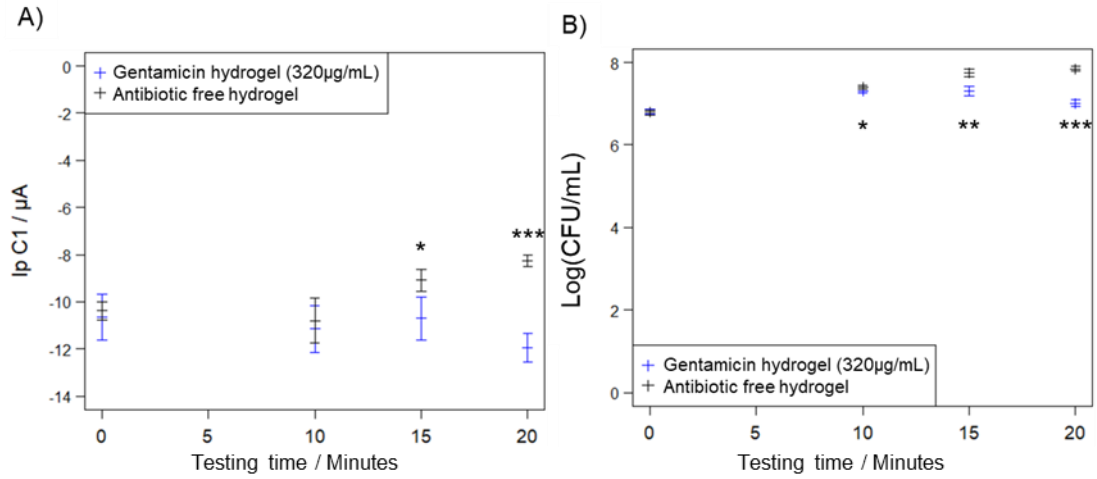

Figure 4.10. A) Resazurin reduction peak height at time intervals of 10, 15 and 20 minutes. DPV was conducted using second-generation R-SPEs. N = 4, error bars represent standard deviation. **B)** CFU/ml counts derived from first-generation LOC devices post electrochemical AST. N = 5, error bars represent standard deviation, significance is indicated as follows: * = p-value < 0.05, ** = p-value < 0.005, *** = p-value < 0.0005.

Significant inhibition of bacterial growth was determined, via CFU counts, to occur after 10 minutes of incubation (t = 2.8691, df = 5.9358, p-value = 0.0288), however, this was not detected electrochemically. Although technically the bacterial growth had been significantly inhibited, the overall change in the concentration of resazurin after 10 minutes was insufficient for electrochemical detection. For subsequent tests using the antibiotic hydrogels a time point of 15 minutes was used for the second DPV scan with the continued CFU/ml-based verification of the electrochemical determination of bacterial growth being run in parallel.

The results from electrochemical AST using the second-generation LOCs, antibiotic hydrogels, and the bacteria *E. coli* ATCC 25922 and *K. pneumoniae* ATCC 700603 are shown in **Figure 4.11** (**Appendix Section 7.7**, **Table 7.7** contains a full statistical breakdown of the resazurin I_{pc} values and CFU/ml validation). Both species of bacteria showed susceptibility to all antibiotics except for vancomycin within 15 minutes. These results were then validated via the use of CFU/ml counts derived from the macroelectrode integration chambers which showed that all antibiotics except for vancomycin, showed significant inhibition of bacterial growth relative to the antibiotic-free control.

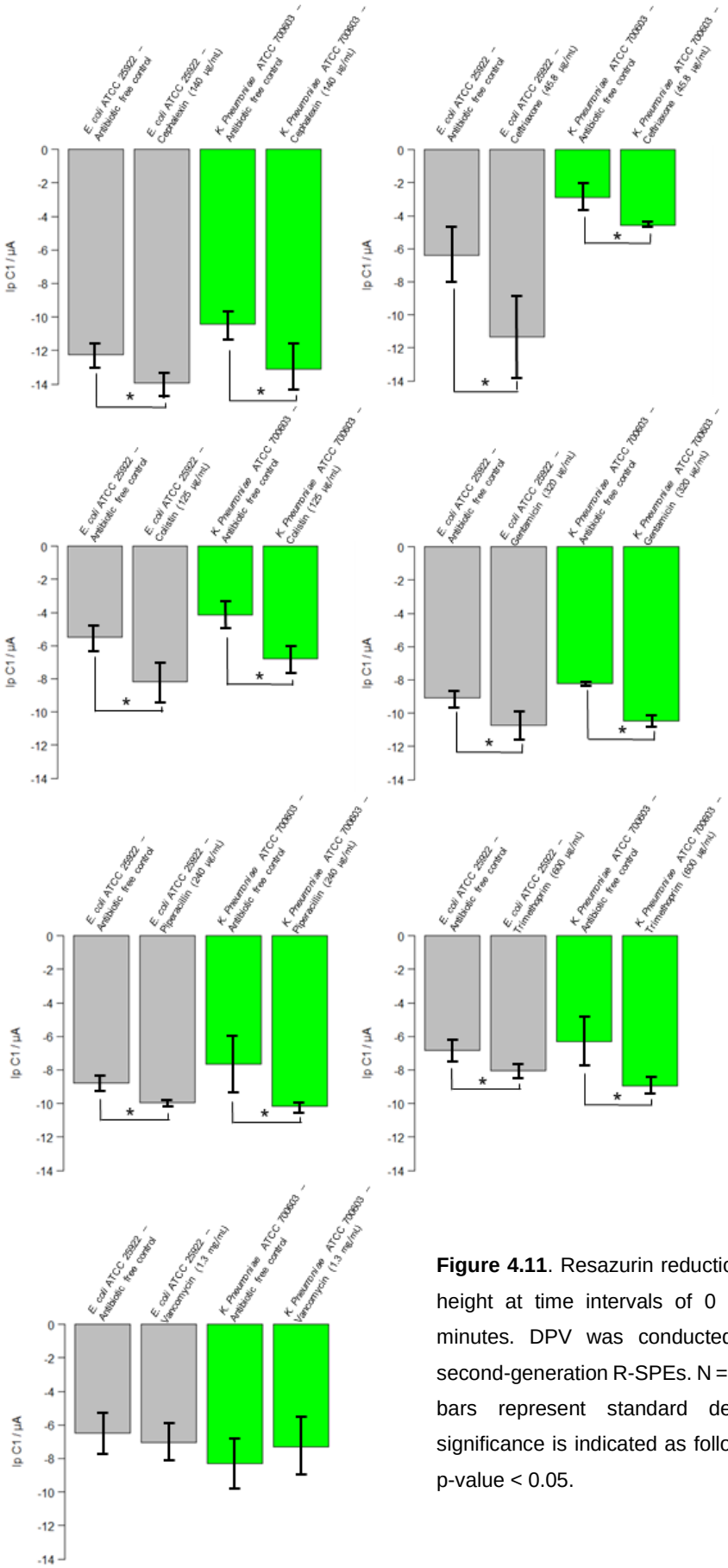

Figure 4.11. Resazurin reduction peak height at time intervals of 0 and 15 minutes. DPV was conducted using second-generation R-SPEs. N = 4, error bars represent standard deviation, significance is indicated as follows: * = p-value < 0.05.

It has already been discussed previously in **Section 3.4.4** that vancomycin is ineffective versus Gram-negative bacteria due to its mechanism of action [301, 302]. This demonstrated that the electrochemical AST method could differentiate between effective and ineffective antibiotics. The antibiotic hydrogels were then combined with second-generation R-SPEs and second-generation LOC devices to determine the viability of conducting parallelised electrochemical AST using seven different antibiotics and an antibiotic-free control.

4.4.5 Electrochemical AST using second-generation LOC devices

The second-generation LOC devices were first tested using pH 6 artificial urine to determine if the same success could be replicated as with the first-generation LOC devices. CFU/ml counts were not taken when conducting AST using the second-generation LOC devices as issues pertaining to the mixing of media from adjacent chambers continued. However, electrochemically determined AST results had already been validated using CFU/ml counts for each of the antibiotics used. **Figure 4.12 A** shows the I_{pc}s derived from the second-generation LOCs after 15 minutes of incubation using *E. coli* ATCC 25922 with versus the full suite of antibiotics. The susceptibility profile was the same as was observed using first-generation LOCs demonstrating that there were no significant negative effects with the change in the methodological setup. The experiment was then repeated using *K. pneumoniae* ATCC 700603 and *E. coli* NCTC 13351 as shown in **Figure 4.12 B** and **C** respectively (**Appendix Section 7.7**, **Table 7.8 contains** a full statistical breakdown of the p-values). In **Section 4.3.3** it was established using both broth microdilution assays and hydrogel 96 well plate assays that *E. coli* NCTC 13351 was resistant to both cephalexin and ceftriaxone with vancomycin being ineffective due to *E. coli* being Gram-negative. In terms of use for electrochemical AST, this served as a means of evaluating whether the method could determine antibiotic resistance.

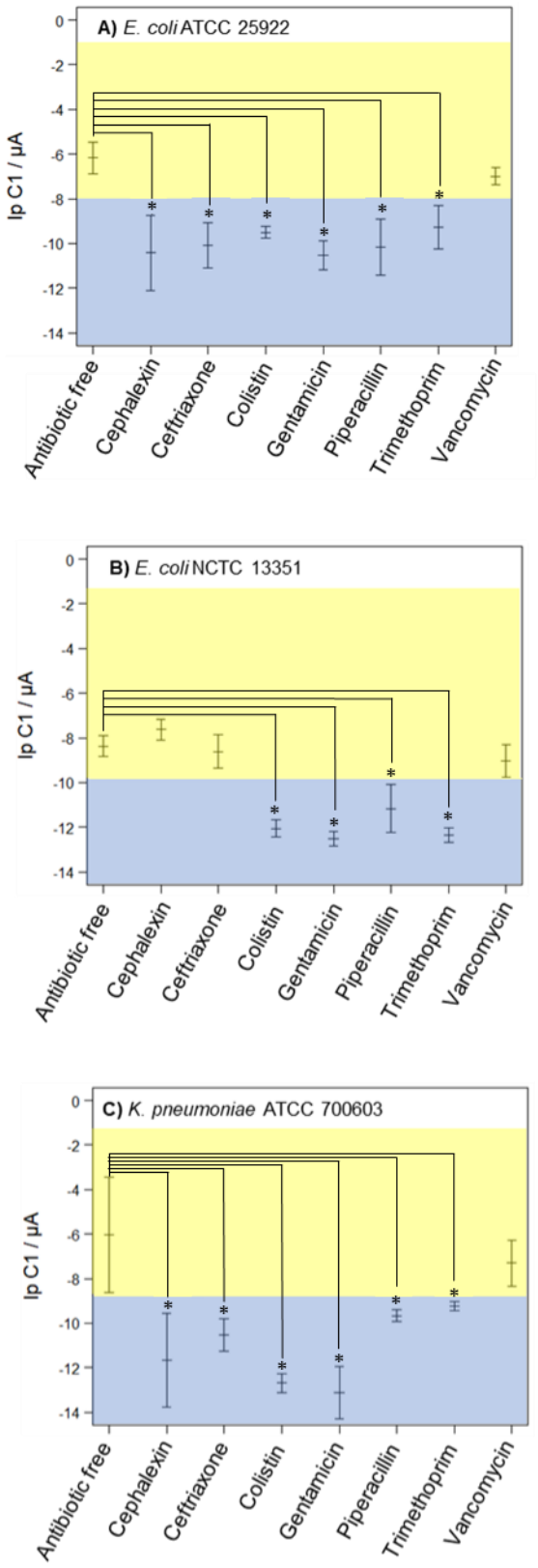

Figure 4.12. Resazurin I_{pc}s derived from the antibiotic-free control versus antibiotic hydrogels after 15 minutes of incubation for **A)** *E. coli* ATCC 25922, **B)** *E. coli* NCTC 13351, **C)** *K. pneumoniae* ATCC 700603. DPV was conducted using second-generation R-SPEs. N = 4, error bars represent standard deviation, significance is indicated as follows: * = p-value < 0.05.

The electrochemical antibiotic susceptibility profiles of both *K. pneumoniae* and *E. coli* NCTC 13351 were demonstrated to be the same as that established during the initial AST using 96 well plate hydrogel assays, as shown in **Figure 3.7**, and electrochemical AST with first-generation LOC devices. Therefore, the electrochemical AST method can differentiate between antibiotic susceptible and non-susceptible bacteria. The methodology was then tested using donated human urine. Working with real urine presents more variables that cannot be adequately accounted for when using artificial urine. Depending on the hydration status, diet, and the types of medication an individual may be on there will be variation in the elemental traces [194], metabolites [192], salts such as sodium chloride [307, 308], and pH variance [193], all of which could potentially interfere with either the mechanism of action of the antibiotic or the reduction of resazurin at the surface of the WE. Testing the proposed method with donated urine is a crucial step in determining how well the method can tolerate variation in the urinary constituents as described above and determine what if any limitations the method may have when dealing with actual patient specimens.

Urine samples ranging from pH 5.4 to 7.4 were tested. **Figure 4.13** shows the resazurin I_{pc}s derived from the second-generation LOCs after 15 minutes of incubation (**Appendix Section 7.7**, **Table 7.9** contains a full statistical breakdown of the p-values). *E. coli* ATCC 25922 demonstrated that it is the same as that determined using artificial urine as shown previously, effectively showing that antibiotic susceptibility can be determined electrochemically when using real urine and at a pH less than that which was used for the initial testing (pH of 5.8 and 6 respectively). *K. pneumoniae* ATCC 700603 is susceptible to all antibiotics except for vancomycin. The susceptibility profile remained consistent with previous findings. *E. coli* NCTC 13351, however, only showed susceptibility to two of the seven antibiotics, colistin and piperacillin, whereas previously it had shown susceptibility to the expected four of out of seven. It was established previously that the antibiotic hydrogels definitively induce significant inhibition of *E. coli* NCTC 13351 growth within 15 minutes of incubation on the LOC devices.

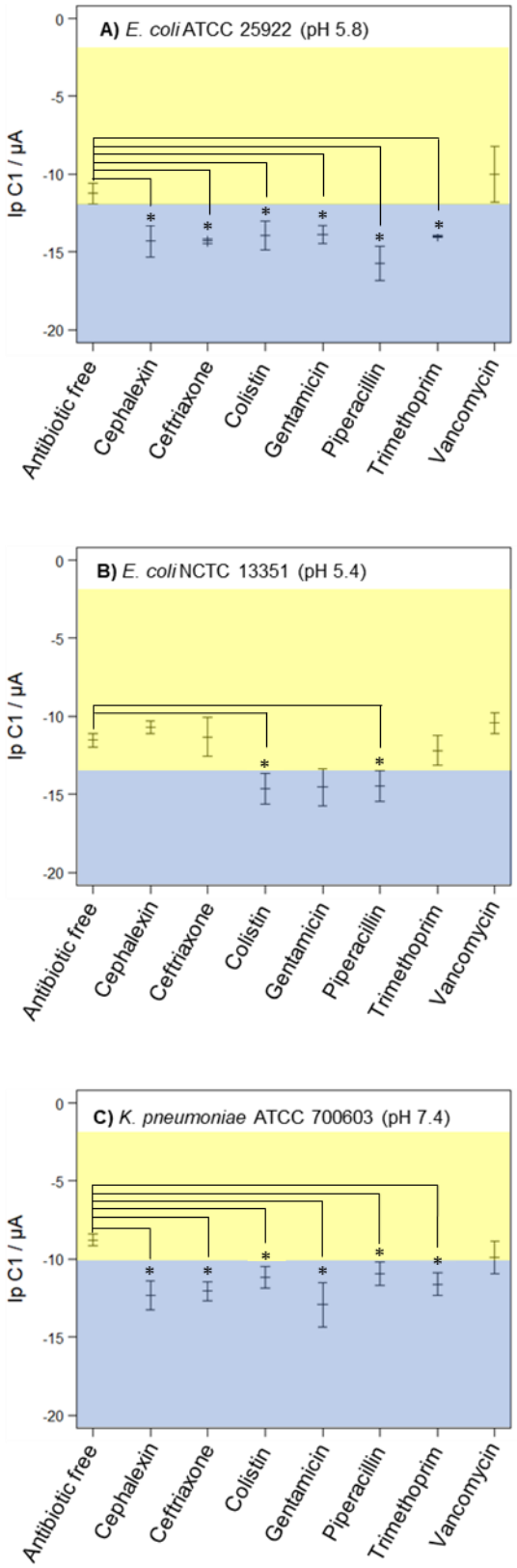

Figure 4.13. Resazurin reduction peak heights derived from the antibiotic-free control versus antibiotic hydrogels after 15 minutes of incubation using donated urine. DPV was conducted using second-generation R-SPEs. N = 4, error bars represent standard deviation, significance is indicated as follows: * = p-value < 0.05.

Although the growth of the bacteria was significantly inhibited by the antibiotic hydrogels, a significant change in the concentration of resazurin in the gentamicin and trimethoprim chambers could not be determined electrochemically. Human urine is not an ideal supporting electrolyte solution due to the inherent variation in the salt concentration that occurs due to hydration levels [309] as well as potential fluid and salt supplementation that a person may take [310]. When adding a supporting electrolyte to a solution the concentration of the salt must be higher than the concentration of the analyte, otherwise the conductivity of the solution will be low, thereby, the solution will be resistive to the charge transfer [206] that is required for electrochemical reduction. To be an effective supporting electrolyte solution, BSES used in **Chapter 3 Section 3.2.1** used a potassium chloride concentration of 0.1 M which was significantly higher than the concentration of resazurin used (1 mM), therefore, eliminating the potential for conductivity issues.

The salt concentration of the donated urine was unknown; however, the urine was mixed with double strength nutrient broth (Oxoid CM0001) which when mixed with urine at a one-to-one ratio resulted in a sodium chloride concentration of 0.86 M. Given that the concentration of resazurin that was released from the R-SPEs was 0.6271 mM, a supporting electrolyte concentration of 0.86 M should be sufficient to enable the balance of charge without any significant limitations. Therefore, although urine itself is not an ideal supporting electrolyte solution, the addition of nutrient broth creates a solution that functions as a supporting electrolyte solution for the purposes of electrochemical AST. Hence it is unlikely that there was an insufficient salt concentration for efficient electrochemical reduction and the determination of the change in the concentration of resazurin, especially given that the susceptibility profiles of *E. coli* ATCC 25922 and *K. pneumoniae* ATCC 700603 did not change when moving between testing with artificial urine and donated urine.

In terms of the constituent elements of urine, there are some which can become absorbed at the surface of the WE such as albumin [311, 312], or those with electroactive properties, such as citrate which can interfere with

electrochemical resazurin reduction [313]. Other examples are creatinine [314], histidine [315], lactate [316, 317], phenylalanine [318], threonine [319], tryptophan [320], tyrosine [321] and glutamate [322] which are electrochemically active and formate [323] which can be absorbed at the WE. These metabolites are present at concentrations on average much less than that of resazurin and may additionally require a modified electrode and a higher applied potential for the metabolite to be electrochemically reduced. However, given that each of the listed metabolites is present in urine, the total concentration they present may have a negative effect on detection of resazurin due to absorption of other electrochemically active substances at the surface of the WE, therefore, reducing the resolution of the WE. However, the method presented here was still able to identify the two most effective antibiotics in treating a hypothetical antibiotic-resistant *E. coli* (NCTC 13351) driven UTI with the antibiotics being piperacillin and colistin respectively.

4.5 Conclusions

Ultimately, the objective of this work was to develop a method of rapidly determining the most effective antibiotic to treat a UTI caused by Gram-negative bacteria, there is a technical limitation insofar that certain urinary metabolites may interfere with resazurin reduction, however, despite this, effective antibiotics can still be rapidly identified. However, the electrochemical determination of antibiotic susceptibility using first- and second-generation R-SPEs have been well demonstrated as a proof of concept for rapid AST in a clinically relevant way of susceptibly testing, for an issue that affects thousands of people per year.

5. Chapter 5: Conclusions and Future work

5.1 Conclusions

The overall aim of the work conducted was to develop a new method of conducting rapid AST using a LOC based electrochemical method utilising to address the essential clinical need for faster determination of antibiotic susceptibility in UTIs.

First, the feasibility of using resazurin as a redox indicator in combination with screen-printed macroelectrodes was assessed as presented in **Chapter 2**. The resazurin LOD of the macroelectrodes was assessed using DPV wherein it was determined that the GC macroelectrode was the most sensitive in terms of resazurin LOD, followed closely be C-SPEs and with Ag-SPEs being the least sensitive. This demonstrated that in this given application, C-SPEs can perform comparably to a GC macroelectrode, supporting the use of SPEs as analytical tools In comparing the reproducibility in terms of CV resazurin I_{pc} and DPV resazurin I_{pc} values, C-SPEs outperformed the Ag-SPEs.

Due to these properties, C-SPEs were chosen for the R-SPE template. Using SDC and DPV, first-generation R-SPEs produced stable, easily interpreted and reproducible resazurin I_{pc}s. Second-generation R-SPEs produced a significantly larger resazurin I_{pc} value than both C-SPEs and first-generation R-SPEs. This difference was caused by the second-generation R-SPEs having a lower internal resistance due to an overall shorter circuit length. The modification process to fabricate R-SPEs imparted beneficial surface characteristics onto the WE. Using optical profilometry, it was determined that the mean square roughness of R-SPEs was significantly higher than that of the C-SPEs, therefore, the R-SPEs had a greater electrochemically active surface area enabling more sensitive detection of resazurin than C-SPEs. Therefore, it was concluded that using resazurin as a redox indicator in combination with screen-printed macroelectrodes was a viable means of delivering a cell viability indicator into a simulated LOC sample volume.

Preliminary electrochemical AST was carried out using the first-generation R-SPEs to assess whether they were a viable means of conducting

rapid AST. The susceptibility of *E. coli* ATCC 25922 to gentamicin sulphate was assessed using first-generation R-SPEs. The fastest time in which susceptibility was determined was 90 minutes (70-minute preincubation + 20 minutes of testing time) using a gentamicin concentration of 0.8 µg/ml. First-generation R-SPEs demonstrated slightly less sensitivity than what could be expected when using a disk diffusion or broth microdilution assay, however, the faster time to analysis derived from using first-generation R-SPEs demonstrated that they were a viable means of conducting rapid AST.

Part of the design considerations for the proposed LOC devices was that the macroelectrode chambers would contain all the reagents required for electrochemical AST, therefore, a method of delivering antibiotics into the LOC devices was required. PVA based hydrogels were fabricated, tested and then optimised. The optimised hydrogels were tested against *E. coli* ATCC 25922, *E. coli* NCTC 13351 (cephalexin and ceftriaxone resistant) and *K. pneumoniae* ATCC 700603. In using the antibiotic hydrogels, the susceptibility profiles of each of the bacteria could be determined in 15 to 20 minutes of testing time. This demonstrated, as summarised **Chapter 4**, that PVA hydrogels can be used to deliver a concentration of an antibiotic which induced inhibition of bacterial growth in susceptible bacteria and none for resistant types enabling differentiation between susceptible and non-susceptible types. The second-generation R-SPEs were then combined with the antibiotic hydrogels within a LOC device to test the method as a whole.

The first sets of testing conducted with the first- and second-generation LOC devices was to determine whether the delivery of bacteria to the macroelectrode chamber was consistent. Initial testing determined that the delivery of bacteria to the chambers of both generations of LOC devices was statistically even, with the conditions within the macroelectrode chambers suitable for two hours of bacterial growth on the LOC devices. Initial testing was conducted using first- and second-generation LOC devices and artificial urine. In this testing, the susceptibility, or non-susceptibility of *E. coli* ATCC 25922, *E. coli* NCTC 13351 and *K. pneumoniae* ATCC 700603 could be derived within 85 minutes of testing time (15-minute testing time + 70-minute preincubation) as shown in **Chapter 5**. The next experimental step was to use

second-generation LOC devices to assess whether electrochemical AST could be conducted using donated urine samples as part of a simulated UTI. In the subsequent testing, the susceptibility profiles of *E. coli* ATCC 25922 and *K. pneumoniae* ATCC 600703 remained consistent with previous findings showing susceptibility to all antibiotics with the exception of vancomycin. The susceptibility profile of *E. coli* NCTC 13351, however, differed from its previously defined profile with it only showing susceptibility to colistin and piperacillin, and none to gentamicin and trimethoprim which had been demonstrated previously. This lack of reproducibility was attributed to the different constituents of urine, of which some of the endpoint metabolites can be slightly electrochemically active and, thereby, interfere with the detection of resazurin.

Ultimately, however, the proposed method of rapid electrochemical AST did identify the most effective antibiotics to treat the simulated UTIs, which in turn could be prescribed to a patient suffering from a UTI. The fact that multiple antibiotics could be identified as effective would enable more tailored prescription to work with patient allergies and enable the use of an antibiotic that would have the least negative side effects, and also reduce the risk of recurring UTIs from occurring due to antibiotic-related disturbance of the gastrointestinal tract [67].

5.2 Future work

An investigation into different percentage incorporations of resazurin in the second-generation R-SPEs would enable the determination of whether a lower percentage would function better as an electrochemical AST tool. The issue with percentage incorporations of 1% and 5% with first-generation R-SPEs was that the resazurin I_{pc} value produced was too close to the estimated LOD. However, the second-generation R-SPEs demonstrated a significantly higher resazurin I_{pc} value at the same 10% resazurin incorporation as the first-generation R-SPEs. Thus, at a percentage incorporation of 1% and 5% the second-generation R-SPEs should also produce significantly higher resazurin I_{pc} value. Therefore, lower percentage incorporation of resazurin could be tested to determine whether antibiotic susceptibility could be detected faster,

as the bacterially induced changes in the concentration of resazurin should be more apparent due to the lower concentrations of resazurin in the bulk solution.

The method as a whole could also be tested using a range of initial bacterial concentrations, specifically 1.76×10^2 to 1.76×10^7 CFU/ml in increments of 10^1. This testing would enable the determination of the bacterial LOD of the method at concentrations less than the initial CFU/ml that was used of 1.76×10^8 post preincubation. Further tests using donated urine from a spectrum of volunteers would enable an assessment of how the system as a whole would perform on a broad-spectrum of sample types due to the inherent variation in biological samples and enable further refinement of the method.

Future work on the antibiotic hydrogels would focus on the efficient delivery of antibiotics and the addition of a buffer to the LOC macroelectrode chambers. A more efficient release of the antibiotic could be achieved via reduction of the w/v ratio of PVA added to the precursor creating a more porous polymer enabling greater diffusion of antibiotics from the hydrogel into the macroelectrode chamber. The method of fabricating PVA hydrogels would require modification for the release of a buffer. During the stage where the hydrogel precursor was produced, the PVA would be suspended in PBS instead of purified water before being autoclaved to dissolve the PVA. The hydrogel produced would be capable of releasing the buffer solution into the macroelectrode chamber which would prevent significant pH variance from the pH values that are optimal for electrochemical AST enabling the reliable production of resazurin I_{pc}s. The long-term potency of the antibiotics loaded into the hydrogels could also be explored. Antibiotic-loaded hydrogels would be stored frozen, with the frozen hydrogels being subjected to only seven freeze-thaw cycles before long term storage. Another set of antibiotic hydrogels would then be refrigerated after all eight freeze thaw cycles, with both sets being stored for six months with testing conducted each month to determine if the potency of the antibiotics degraded over time and which method would be better for storage.

The long-term goal for the proposed methodology is to produce an automated version of the LOC device that can be used without the requirement

of specialist knowledge of electrochemical procedures. The conceptual schematic for the automated design is shown in **Figure 5.1**. The operating system would be compatible with the second-generation LOC devices, each of which would be loaded with a different series of antibiotics to enable versatile electrochemical AST depending on the type of infection that was presented. UTI samples would be introduced to the single-use LOC devices, which would then be sealed to prevent leaks or contamination and then integrated into the automated LOC device reader. This type of system would be used as a point of care diagnostic tool to rapidly prescribe antibiotics for complicated UTIs, or any UTI that threatened complications for the patient due to immunosuppression, age, or other prevailing illnesses.

The reagent cost per use of the second-generation LOC devices was low. It is too early to be able to state a definitive cost of the research endpoint LOC devices as the design and method will be refined and changed, and economies of scale would need to be evaluated. The proposed method shows promise, and after further refinement, through the described future works the method could then be validated in a research laboratory. To do this clinical UTI samples would be requested, then tested on the proposed system as part of blinded testing. The electrochemical AST results would then be compared to the AST results produced in the clinical setting using gold standard tests. The results could then be compared and the viability of the proposed method could be determined, in addition to a cost-benefit analysis to ensure the method is objectively assessed.

The conservation of effective antibiotics is crucial for the long-term treatment of bacterial infections. UTIs are one of the most common types of bacterial infection in the world and given the increased rates of MDR behaviour in Gram-negative bacteria which make up the majority of uropathogens, UTIs pose a significant healthcare threat as antibiotic treatment options become increasingly limited. The ability to conduct rapid AST as part of point-of-care testing such as the proposed electrochemical method would greatly help in the quick and efficient prescription of appropriate antibiotics. This in turn would extend the longevity of antibiotics that are currently used in clinical settings, and any antibiotics introduced in the future.

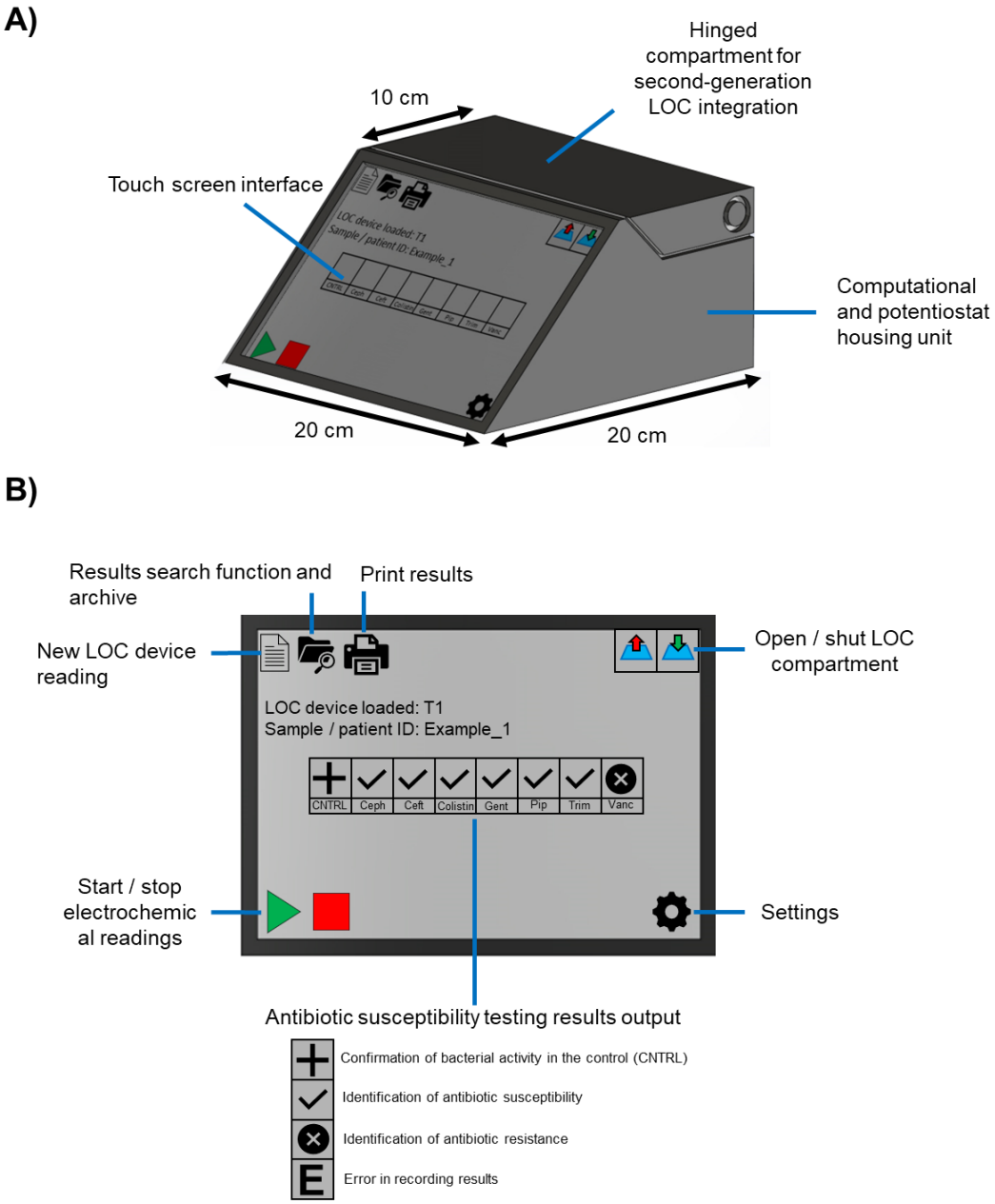

Figure 5.1 Schematic showing; **A)** Computational until that is compatible with second-generation LOC devices to enable rapid AST with minimal setup and training requirements; **B)** Touch screen interface that would be used on the computational unit, currently showing the theoretical output for *E. coli* ATCC 25922**.**

6. Publications and presentations

6.1 Presentations

Molecular Microbial Ecology Group (MMEG) 2018 – Oral presentation “A novel means of determining an effective antibiotic to treat urinary tract infections”

Early career scientist research symposium 2019 – Poster presentation “Determination of antibiotic susceptibility of bacteria causing urinary tract infections using a novel electrochemical lab on a chip design”

Microbiological society annual conference 2022 – Oral presentation “Determination of antibiotic susceptibility of bacteria causing urinary tract infections using a novel lab-on-a-chip electrochemical device”

6.2 Publications

Crane *et al.* (2021) “Rapid antibiotic susceptibility testing using resazurin bulk modified screen-printed electrochemical sensing platforms”. *Analyst*. 8(146), pp. 5574-5583. doi: 10.1039/D1AN00850A.

Crane *et al.* (2022). “Lab on a Chip devices for Urinary Tract Infection diagnostics”. Journal of Medical Microbiology. Submitted February 2022.

7. Appendix

7.1 Resazurin LOD raw data sets (BSES)

Table 7.1 – 3 (Figure 2.10). Raw data sets for the resazurin LOD experiment using C-SPEs, Ag-SPEs and the GC macroelectrode with pH 6 BSES.

	C-SPE						
Resazurin concentration (Mm)	Ipc_1 (µA)	Ipc_2 (µA)	Ipc_3 (µA)	Ipc_4 (µA)	Ipc_5 (µA)	Average Ipc (µA)	Ipc_SD
1	-6.916	-7.981	-7.651	-7.448	-7.271	-7.45E	4.00E-01
0.5	-8.095	-7.414	-6.801	-6.352	-5.978	-6.93E	8.44E-01
0.25	-6.812	-6.729	-5.824	-5.723	-6.155	-6.25E	5.03E-01
0.125	-4.661	-4.683	-4.513	-4.669	-5.095	-4.72E	2.18E-01
0.0625	-4.011	-3.566	-3.068	-2.917	-2.952	-3.30E	4.74E-01
0.03125	-2.51	-2.523	-2.439	-2.513	-2.399	-2.48E	5.48E-02
0.015625	-1.987	-2.095	-2.207	-2.201	-2.066	-2.11E	9.35E-02

	Ag-SPE						
Resazurin concentration (Mm)	Ipc_1 (µA)	Ipc_2 (µA)	Ipc_3 (µA)	Ipc_4 (µA)	Ipc_5 (µA)	Average Ipc	Ipc_SD
1	-6.546	-6.803	-5.939	-4.195	-3.232	-5.343	1.557903
0.5	-6.228	-5.481	-4.693	-4.131	-3.905	-4.8876	0.964963
0.25	-6.443	-5.371	-4.696	-4.271	-3.39	-4.8342	1.150913
0.125	-7.397	-5.467	-4.86	-4.343	-3.958	-5.205	1.350054
0.0625	-5.602	-4.764	-4.234	-3.84	-3.388	-4.3656	0.856838
0.03125	-3.864	-3.391	-2.945	-2.54	-2.303	-3.0086	0.632345
0.015625	-4.363	-3.781	-3.466	-3.06	-2.618	-3.4576	0.668472

	GC macroelectrode						
Resazurin concentration (Mm)	Ipc_1 (µA)	Ipc_2 (µA)	Ipc_3 (µA)	Ipc_4 (µA)	Ipc_5 (µA)	Average Ipc	Ipc_SDD
1	-6.838	-6.396	-5.685	-6.45	-7.014	-6.4766	0.513138188
0.5	-5.029	-3.361	-5.604	-5.983	-4.456	-4.8866	1.03076491
0.25	-4.434	-4.382	-3.794	-4.168	-4.11	-4.1776	0.254622858
0.125	-2.91	-3.155	-3.317	-2.272	-2.9135	-2.9135	0.397702464
0.0625	-2.332	-2.295	-1.981	-2.276	-2.081	-2.193	0.153380246
0.03125	-1.475	-1.371	-0.896	-1.238	-1.373	-1.2706	0.225684071
0.015625	-0.799	-1.012	-0.561	-0.629	-0.667	-0.7336	0.178151059

7.2 Ag-SPE performance assessment

Ag-SPEs produced inconsistent resazurin I_{pc} values for CV and DPV based experiments. To determine if the inconsistency was due to the choice of reference material, Ag-SPEs were tested using 1 mM potassium ferrocyanide dissolved in pH 6 BSES and CV. For comparative purposes C-SPEs were also tested under the same parameters. The cyclic voltammograms for both Ag-SPEs and C-SPEs show one cathodic and one anodic peak (C1 and A1 respectively) with C1 correlating with the reduction of potassium ferrocyanide and A1 correlating with the oxidation of the reduced form of potassium ferricyanide as shown in **Figure 7.1 A & B**.

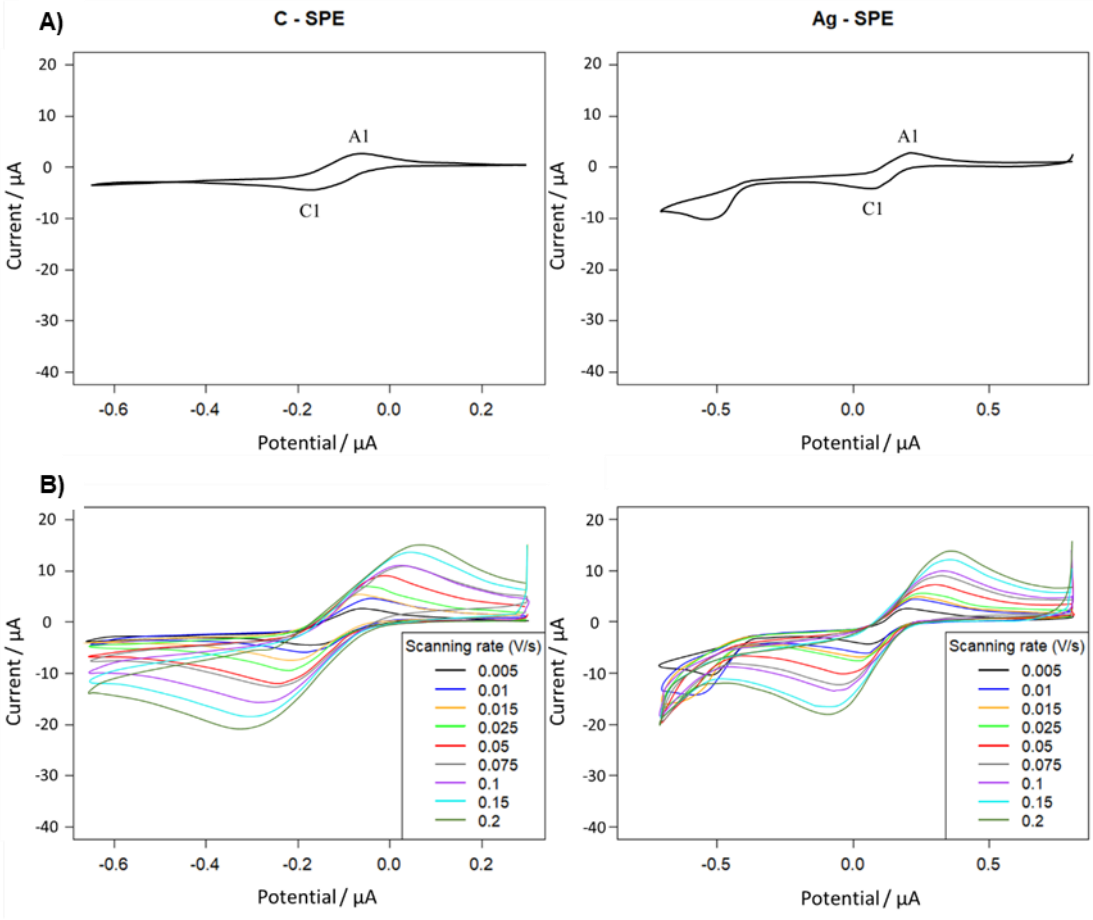

Figure 7.1. **Row A)** Cyclic voltammogram potassium ferrocyanide (1 mM) in pH 6 BSES using C-SPE, Ag-SPEs and a GC macroelectrode setup respectively: Scan rate 0.05V/s. **Row B)** Cyclic voltammogram potassium ferrocyanide (1mM) in pH 6 BSES using C-SPE, Ag-SPEs respectively and a GC macroelectrode setup: Scan rates 0.005 – 0.2 V/s. N = 5

To determine if the reduction of potassium ferrocyanide is diffusion or absorption mediated as a plot of log I_{pc} at C1 against the log of the scanning rate was plotted as shown in **Figure 7.2**. The gradients for both Ag-SPEs and C-SPEs were both less than 0.5 indicating diffusion mediated reduction [216]. Additionally, the standard deviation of the I_{pc} values derived from the Ag-SPEs are notably smaller than the standard deviation seen in the resazurin I_{pc} values of the equivalent pH which were shown in **Figure 2.12**. Other than the difference in the applied potential window the principal difference was the redox indicator, therefore, it seems likely that the electrochemical reduction reaction between Ag-SPEs and resazurin produces inconsistent resazurin I_{pc} values. Ordinarily Ag|AgCl is an excellent choice for a reference material and is commonly used in electrochemical experiments that use both aqueous and non-aqueous solutions [206, 207, 239]. A major consideration for choosing the reference material, however, is the potential for any reactions between the material of the reference and the analyte which is being detected [207].

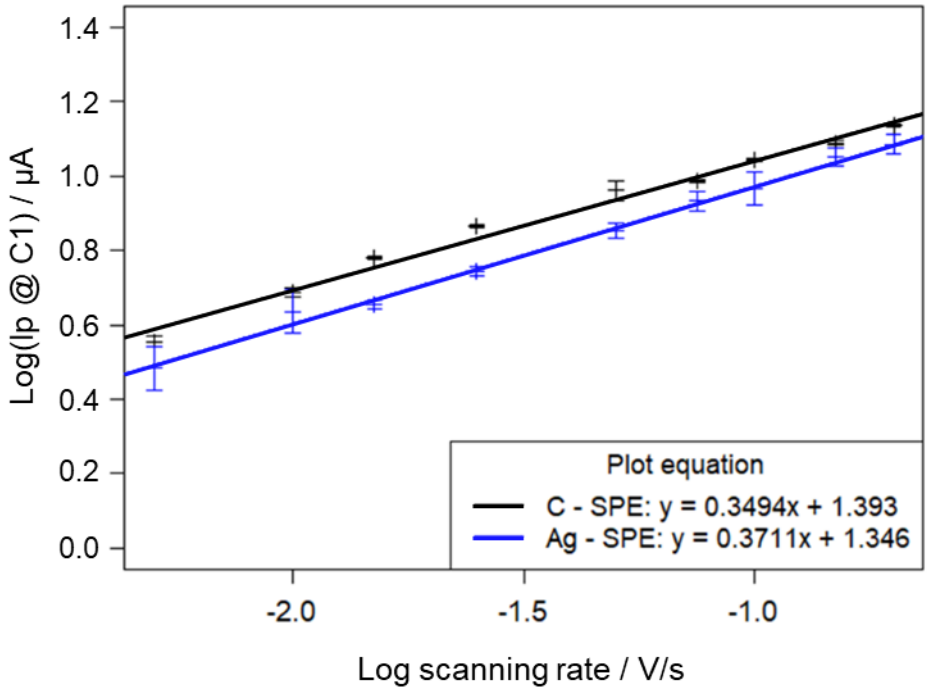

Figure 7.2. Plot of log potassium ferrocyanide reduction peak height (log (I_{pc} at C1)) against log scanning rate (log(*v*)) using potassium ferrocyanide (1 mM) in BSES set to pH 6. N = 5, error bars represent standard deviation, significance is indicated with an appropriate * symbol.

As mentioned in the literature review resazurin is a phenoxazine-3-one dye which has a distinctly blue colour when in its non-reduced form [216, 217]. The resazurin could potentially be either staining the Ag|AgCl references or be partially absorbed at the surface of the reference during an applied potential which in turn causes a large degree of deviation in the resazurin reduction peak I_{pc} values which were produced. Another slight drawback in using Ag|AgCl is if the reference suffers damage which compromises the surface the silver ions (Ag^{+}) can leak from the reference material and interfere with electrochemical readings [211]. This combination of factors makes Ag|AgCl referenced SPEs an unsuitable template for the fabrication of R-SPEs.

7.3 R-SPE resazurin incorporation raw data (Artificial urine)

Table 7.4 (Figure 2.12). Raw data sets for the resazurin LOD experiment using C-SPEs, with pH 6 artificial urine.

	C-SPE						
Resazurin concentration (Mm)	Ipc_1 (µA)	Ipc_2 (µA)	Ipc_3 (µA)	Ipc_4 (µA)	Ipc_5 (µA)	Average Ipc	Ipc_SDD
1	-3.79E-06	-3.71E-06	-3.68E-06	-3.57E-06	-3.36E-06	-3.62E+00	1.68E-07
0.5	-3.43E-06	-3.34E-06	-3.20E-06	-2.99E-06	-3.02E-06	-3.19E+00	1.92E-07
0.25	-2.72E-06	-2.69E-06	-2.48E-06	-2.34E-06	-2.56E-06	-2.56E+00	1.60E-07
0.125	-1.87E-06	-2.18E-06	-2.12E-06	-1.87E-06	-2.09E-06	-2.02E+00	1.46E-07
0.0625	-1.69E-06	-1.75E-06	-1.39E-06	-1.31E-06	-1.56E-06	-1.54E+00	1.89E-07
0.03125	-1.47E-06	-1.45E-06	-1.49E-06	-1.27E-06	-1.07E-06	-1.35E+00	1.79E-07
0.015625	-5.72E-07	-6.87E-07	-4.64E-07	-5.01E-07	-5.65E-07	-5.58E-01	8.51E-08

7.4 R-SPE resazurin incorporation raw data

Table 7.5 (Figure 2.13). Raw data sets for the I_{pc} values for the different w/v incorporations of resazurin.

Resazurin concentration (Mm)	Ipc_1 (µA)	Ipc_2 (µA)	Ipc_3 (µA)	Ipc_4 (µA)	Ipc_5 (µA)	Average Ipc	Ipc_SD
10	-2.735	-3.253	-3.495	-3.535	-2.921	-3.1878	0.314763657
5	-1.297	-1.176	-1.205	-0.979	-1.015	-1.1344	0.119632103
1	-0.644	-0.646	-0.827	-0.492	-0.665	-0.6548	0.106258929

7.5 *MIC graphical data*

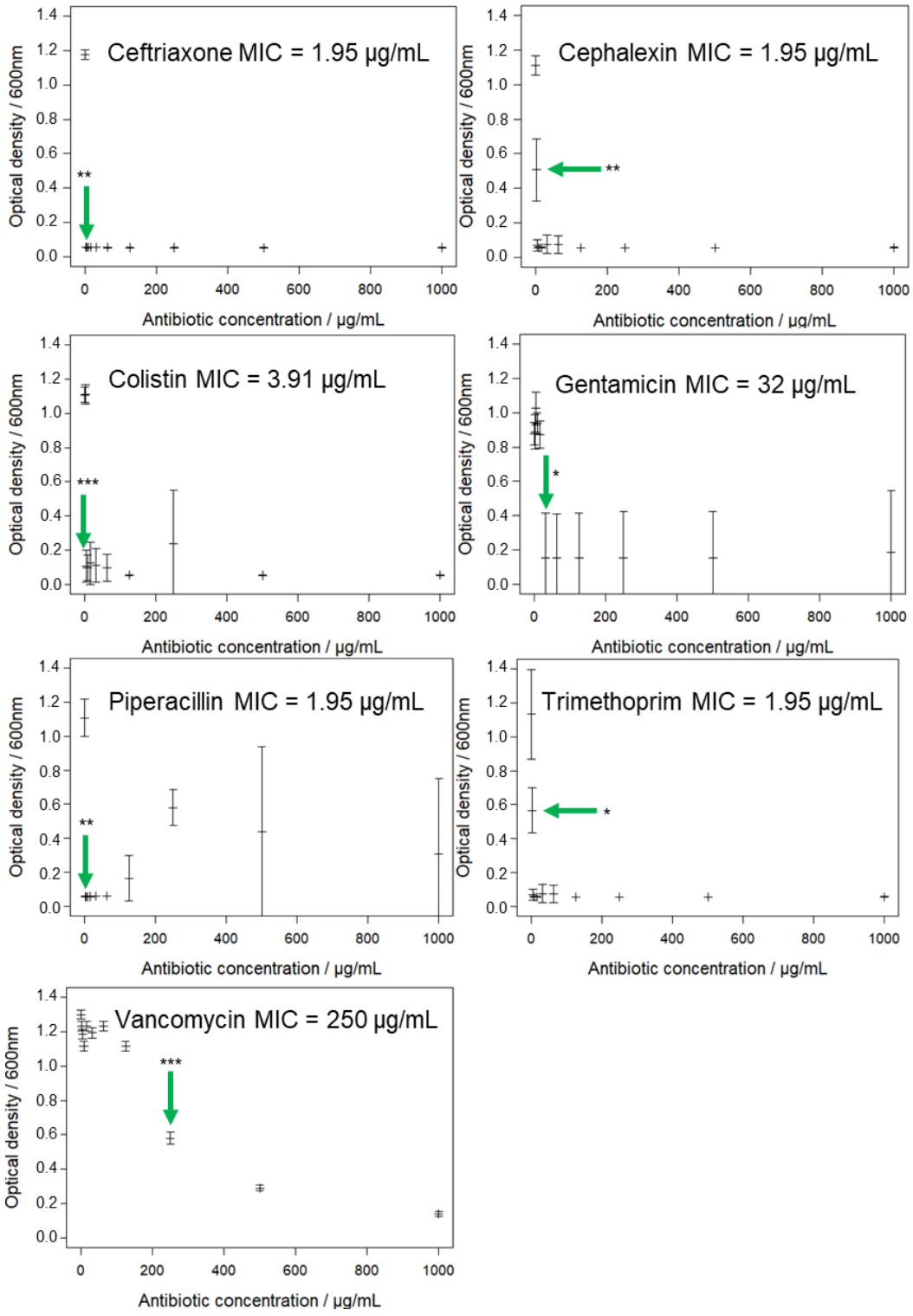

Figure 7.3 (Table 3.3). Full breakdown of the results derived from a broth microdilution assay to determine the MIC for a suite of antibiotics including 1.95 to 1000 µg/ml antibiotic concentrations for *E. coli* ATCC 25922. MIC results are highlighted in green. N = 8, error bars represent standard deviation, significance is indicated as follows: * = p-value < 0.05, ** = p-value < 0.005, *** = p-value < 0.0005, **** = p-value < 0.00005

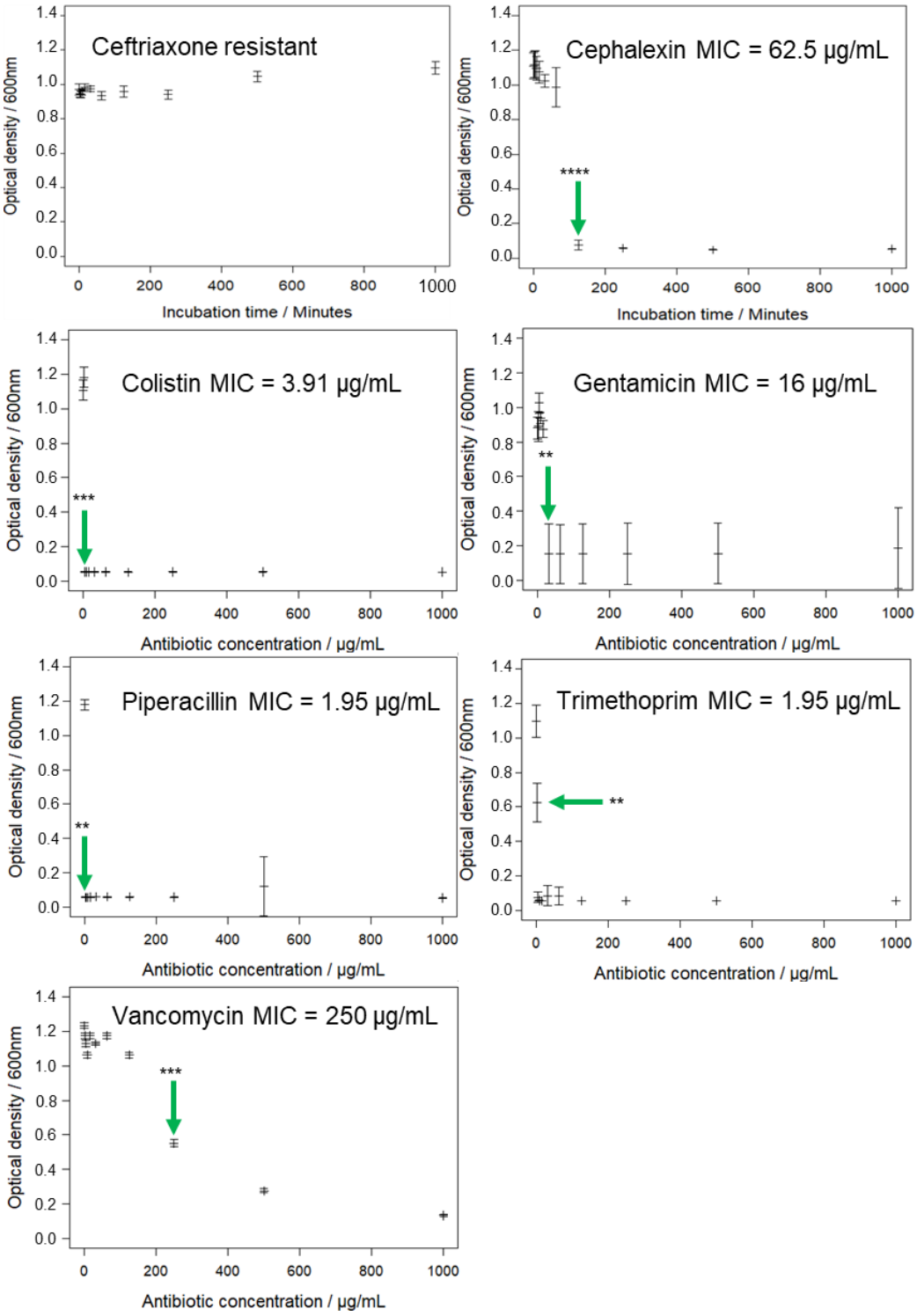

Figure 7.4 (Table 3.3). Full breakdown of the results derived from a broth microdilution assay to determine the MIC for a suite of antibiotics including 1.95 to 1000 µg/ml antibiotic concentrations for *E. coli* NCTC 13351. MIC results are highlighted in green. N = 8, error bars represent standard deviation, significance is indicated as follows: ** = p-value < 0.005, *** = p-value < 0.0005, **** = p-value < 0.00005

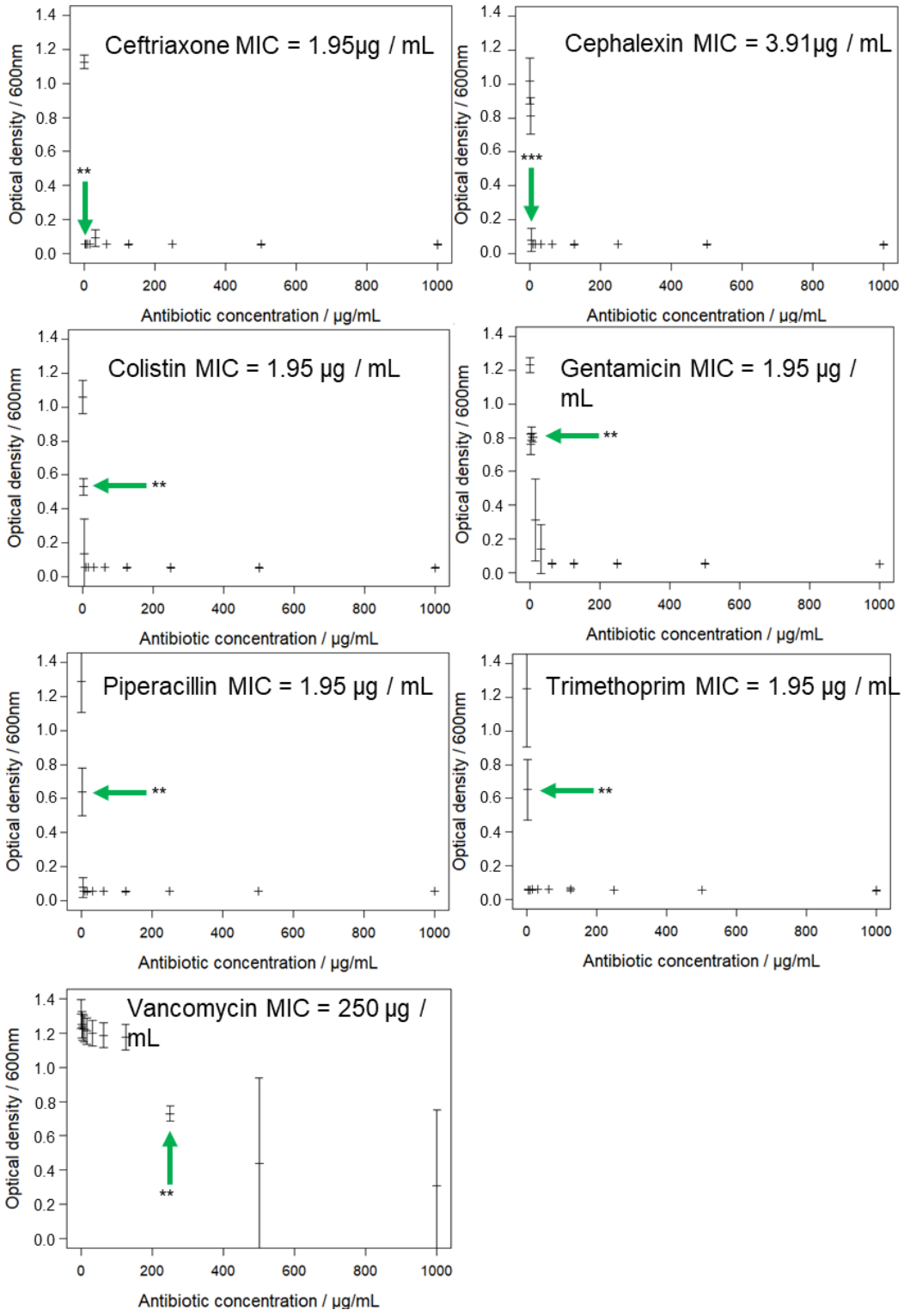

Figure 7.5 (Table 3.3). Full breakdown of the results derived from a broth microdilution assay to determine the MIC for a suite of antibiotics including 1.95 to 1000 µg/ml antibiotic concentrations for *E. coli* ATCC 25922, *E. coli* NCTC 13351 and *K. pneumoniae* ATCC 700603. MIC results are highlighted in green. N = 8, error bars represent standard deviation, significance is indicated as follows: ** = p-value < 0.005, *** = p-value < 0.0005.

7.6 Hydrogel AST statistical analysis

Table 7.6 (Figure 3.7). Full statistical comparison of the CFU/ml counts derived using antibiotic loaded hydrogels, and antibiotic free hydrogels after 15 and 20 minutes of incubation. Results wherein there was significant inhibition of bacterial growth are highlighted in green. Results wherein antibiotic resistance was demonstrated are highlighted in yellow N = 5.

		Incubation Time / Minutes	
	Antibiotic	**15**	**20**
***E. coli* ATCC 25922**	Ceftriaxone (45.8 µg/ml)	t = -6.5779, df = 5.215, p-value = 0.001036	W = 0, p-value = 0.01116
	Cephalexin (140 µg/ml)	t = -3.2942, df = 7.9731, p-value = 0.01101	W = 0, p-value = 0.01141
	Colistin (125 µg/ml)	t = -4.5395, df = 4.7285, p-value = 0.007064	t = -11.7, df = 7.557, p-value = 4.13e-06
	Gentamicin (320 µg/ml)	W = 0, p-value = 0.01167	W = 0, p-value = 0.007495
	Piperacillin (240 µg/ml)	t = -8.1019, df = 7.9167, p-value = 4.232e-05	t = -6.0501, df = 7.9724, p-value = 0.0003101
	Trimethoprim (600 µg/ml)	W = 0, p-value = 0.01091	t = -6.919, df = 5.9044, p-value = 0.0004834
	Vancomycin (1.3 mg/mL)	t = 1.4606, df = 7.2569, p-value = 0.186	W = 8, p-value = 0.3947
***E. coli* NCTC 13351**	Ceftriaxone (45.8 µg/ml)	t = 0.65991, df = 7.7838, p-value = 0.5283	t = 0.55328, df = 6.9544, p-value = 0.5974
	Cephalexin (140 µg/ml)	t = 0.37578, df = 7.3289, p-value = 0.7177	t = 0.35852, df = 7.4567, p-value = 0.7299
	Colistin (125 µg/ml)	t = -6.1263, df = 4.2243, p-value = 0.003004	W = 0, p-value = 0.01193
	Gentamicin (320 µg/ml)	t = -7.1042, df = 7.543, p-value = 0.0001352	W = 0, p-value = 0.00729
	Piperacillin (240 µg/ml)	W = 14.5, p-value = 0.008032	W = 4.5, p-value = 0.000612
	Trimethoprim (600 µg/ml)	t = -6.919, df = 5.9044, p-value = 0.0004834	t = -3.5014, df = 4.4675, p-value = 0.02076
	Vancomycin (1.3 mg/mL)	t = -0.74536, df = 5.3505, p-value = 0.4875	t = 0.43529, df = 6.7439, p-value = 0.6769
***K. pneumoniae* ATCC 700603**	Ceftriaxone (45.8 µg/ml)	W = 0, p-value = 0.01141	t = -9.7913, df = 6.063, p-value = 6.127e-05
	Cephalexin (140 µg/ml)	t = -4.9015, df = 5.4959, p-value = 0.003453	t = -7.6428, df = 5.9706, p-value = 0.0002682
	Colistin (125 µg/ml)	W = 1.5, p-value = 0.02733	t = -8.8561, df = 8, p-value = 2.086e-05
	Gentamicin (320 µg/ml)	t = -10.12, df = 3.4609, p-value = 0.001085	t = -6.6667, df = 3.0803, p-value = 0.006332
	Piperacillin (240 µg/ml)	t = -2.7586, df = 4.9745, p-value = 0.04012	t = -0.80888, df = 5.7351, p-value = 0.4508
	Trimethoprim (600 µg/ml)	t = -5.1465, df = 5.0131, p-value = 0.003598	t = -5.0675, df = 6.8127, p-value = 0.001574
	Vancomycin (1.3 mg/mL)	t = 1.4606, df = 7.2569, p-value = 0.186	t = -1.0512, df = 7.5343, p-value = 0.3257

7.7 LOC AST statistical analysis

Table 7.7 (Figure 4.11). Full statistical comparison of the resazurin I_{pc} values and CFU/ml values derived when using antibiotic loaded hydrogels, and antibiotic free hydrogels with first-generation LOC devices using *E. coli* ATCC 25922 and *K. pneumoniae* ATCC 700603. Results wherein there was significant inhibition of bacterial growth are highlighted in green. Results wherein antibiotic resistance was demonstrated are highlighted in yellow, N = 4

Bacteria	**Antibiotic**	**CFU/ml hydrogel AST assay - Statistical significance in CFU/ml counts after 15 minutes**	**First-generation LOC: Electrochemical AST - Statistical significance in resazurin reduction peak height values after 15 minutes**
E. coli ATCC 25922	Ceftriaxone (45.8 µg/ml)	t = -6.5779, df = 5.215, p-value = 0.001036	t = -2.8623, df = 5.3458, p-value = 0.0327
	Cephalexin (140 µg/ml)	t = -3.2942, df = 7.9731, p-value = 0.01101	t = -2.9031, df = 5.9985, p-value = 0.02723
	Colistin (125 µg/ml)	T = -4.5395, df = 4.7285, p-value = 0.007064	t = -3.2877, df = 5.1413, p-value = 0.02089
	Gentamicin Sulphate (320 µg/ml)	W = 0, p-value = 0.01167	t = -2.8022, df = 4.4284, p-value = 0.0434
	Piperacillin (240 µg/ml)	t = -8.1019, df = 7.9167, p-value = 4.232e-05	t = -3.9576, df = 4.1183, p-value = 0.01579
	Trimethoprim (600 µg/ml)	W = 0, p-value = 0.01091	t = -2.5149, df = 5.8296, p-value = 0.04674
	Vancomycin (1.3mg/mL)	t = 1.4606, df = 7.2569, p-value = 0.186	t = -0.56646, df = 5.9252, p-value = 0.5919
K. pneumoniae ATCC 700603	Ceftriaxone (45.8 µg/ml)	t = -13.558, df = 7.3631, p-value = 1.792e-06	W = 0, p-value = 0.02857
	Cephalexin (140 µg/ml)	t = -4.9015, df = 5.4959, p-value = 0.003453	t = -2.8864, df = 4.5215, p-value = 0.03865
	Colistin (125 µg/ml)	t = -3.329, df = 4.195, p-value = 0.02711	t = -4.0359, df = 5.9876, p-value = 0.006864
	Gentamicin Sulphate (320 µg/ml)	t = -6.2267, df = 4.4494, p-value = 0.002361	t = -10.12, df = 3.4609, p-value = 0.001085
	Piperacillin (240 µg/ml)	t = -2.7586, df = 4.9745, p-value = 0.04012	W = 0, p-value = 0.02857
	Trimethoprim (600 µg/ml)	t = -5.1465, df = 5.0131, p-value = 0.003598	t = -2.9291, df = 3.6991, p-value = 0.04718
	Vancomycin (1.3mg/mL)	t = 1.9959, df = 5.9584, p-value = 0.09328	t = 0.76531, df = 5.8474, p-value = 0.4738

Table 7.8 (Figure 4.12). Full statistical comparison of the resazurin I_{pc} values derived when using antibiotic loaded hydrogels, and antibiotic free hydrogels with second-generation LOC devices using *E. coli* ATCC 25922, *E. coli* NCTC 13351 and *K. pneumoniae* ATCC 700603. Results wherein there was significant inhibition of bacterial growth are highlighted in green. Results wherein antibiotic resistance was demonstrated are highlighted in yellow, N = 4

Bacteria	Antibiotic	Second-generation LOC: Electrochemical AST - Statistical significance in resazurin reduction peak height values after 15 minutes
***E. coli* ATCC 25922**	Ceftriaxone (45.8 µg/ml)	t = 5.5467, df = 5.4182, p-value = 0.002025
	Cephalexin (140 µg/ml)	t = 4.0408, df = 4.0305, p-value = 0.01536
	Colistin (125 µg/ml)	t = 7.6922, df = 3.7334, p-value = 0.002023
	Gentamicin (320 µg/ml)	t = 7.8421, df = 5.9575, p-value = 0.0002353
	Piperacillin (240 µg/ml)	t = 4.8096, df = 4.7485, p-value = 0.005543
	Trimethoprim (600 µg/ml)	t = 4.4524, df = 5.4757, p-value = 0.005384
	Vancomycin (1.3mg/mL)	t = 1.7853, df = 4.646, p-value = 0.1387
***E. coli* NCTC 13351**	Ceftriaxone (45.8 µg/ml)	t = 0.39161, df = 3.3972, p-value = 0.7186
	Cephalexin (140 µg/ml)	t = -1.5425, df = 3.9985, p-value = 0.1978
	Colistin (125 µg/ml)	t = 8.524, df = 3.7876, p-value = 0.001319
	Gentamicin (320 µg/ml)	t = 10.023, df = 3.5543, p-value = 0.0009893
	Piperacillin (240 µg/ml)	t = 3.3429, df = 2.7613, p-value = 0.04004
	Trimethoprim (600 µg/ml)	t = 9.7577, df = 3.4536, p-value = 0.001238
	Vancomycin (1.3mg/mL)	t = 1.06, df = 3.4509, p-value = 0.3576
***K. pneumoniae* ATCC 700603**	Ceftriaxone (45.8 µg/ml)	t = 2.8927, df = 3.4665, p-value = 0.04281
	Cephalexin (140 µg/ml)	t = 2.9134, df = 5.7586, p-value = 0.02817
	Colistin (125 µg/ml)	t = 4.388, df = 3.1598, p-value = 0.01967
	Gentamicin (320 µg/ml)	t = 4.3084, df = 4.2038, p-value = 0.01127
	Piperacillin (240 µg/ml)	W = 16, p-value = 0.02857
	Trimethoprim (600 µg/ml)	W = 16, p-value = 0.02857
	Vancomycin (1.3mg/mL)	W = 9, p-value = 0.8857

Table 7.9 (Figure 4.13). Full statistical comparison of the resazurin I_{pc} values derived when using antibiotic loaded hydrogels, and antibiotic free hydrogels with second-generation LOC devices using *E. coli* ATCC 25922, *E. coli* NCTC 13351 and *K. pneumoniae* ATCC 700603 using donated urine. Results wherein there was significant inhibition of bacterial growth are highlighted in green. Results wherein antibiotic resistance was demonstrated are highlighted in yellow, N = 4

Bacteria	Antibiotic	Second-generation LOC: Electrochemical AST - Statistical significance in resazurin reduction peak height values after 15 minutes using donated urine
***E. coli* ATCC 25922 pH 5.8**	Ceftriaxone (45.8 µg/ml)	t = 6.294, df = 2.1862, p-value = 0.01946
	Cephalexin (140 µg/ml)	t = 3.5408, df = 3.4795, p-value = 0.03018
	Colistin (125 µg/ml)	t = 3.2691, df = 3.6008, p-value = 0.03594
	Gentamicin Sulphate (320 µg/ml)	t = 4.228, df = 3.9118, p-value = 0.01404
	Piperacillin (240 µg/ml)	t = 4.8594, df = 3.2892, p-value = 0.0134
	Trimethoprim (600 µg/ml)	t = 5.7598, df = 2.047, p-value = 0.02734
	Vancomycin (1.3mg/mL)	t = -0.90341, df = 2.5475, p-value = 0.4435
***E. coli* NCTC 13351 pH 5.4**	Ceftriaxone (45.8 µg/ml)	t = -0.2284, df = 2.5252, p-value = 0.8365
	Cephalexin (140 µg/ml)	t = -1.9215, df = 3.9578, p-value = 0.1278
	Colistin (125 µg/ml)	t = 4.003, df = 2.8284, p-value = 0.03117
	Gentamicin Sulphate (320 µg/ml)	t = 3.312, df = 2.5766, p-value = 0.05646
	Piperacillin (240 µg/ml)	t = 3.8925, df = 2.8745, p-value = 0.03246
	Trimethoprim (600 µg/ml)	t = 0.83841, df = 2.8406, p-value = 0.4665
	Vancomycin (1.3mg/mL)	t = -1.9549, df = 3.5553, p-value = 0.1311
***K. pneumoniae* ATCC 700603 pH 7.4**	Ceftriaxone (45.8 µg/ml)	t = -0.2284, df = 2.5252, p-value = 0.0365
	Cephalexin (140 µg/ml)	t = 4.9752, df = 2.643, p-value = 0.02094
	Colistin (125 µg/ml)	t = 4.003, df = 2.8284, p-value = 0.03117
	Gentamicin Sulphate (320 µg/ml)	t = 3.312, df = 2.5766, p-value = 0.05646
	Piperacillin (240 µg/ml)	t = 3.8925, df = 2.8745, p-value = 0.03246
	Trimethoprim (600 µg/ml)	t = 0.83841, df = 2.8406, p-value = 0.0465
	Vancomycin (1.3mg/mL)	t = -1.9549, df = 3.5553, p-value = 0.1311

8. References

1. Fleming, A., *On the Antibacterial Action of Cultures of a Penicillium, with Special Reference to their Use in the Isolation of B. influenzæ.* British journal of experimental pathology, 1929. **10**(3): p. 226-236.
2. CDCP. *Antibiotic / Antimicrobial Resistance (AR / AMR)*. Office of Infectious Disease Antibiotic resistance threats in the United States 2013 [cited 2019 January 5th]; Available from: http://www.cdc.gov/drugresistance/threat-report-2013.
3. Chopra, I., L. Hesse, and A. O'Neill, *Discovery and development of new anti-bacterial drugs*, in *Pharmacochemistry Library*, H. van der Goot, Editor. 2002, Elsevier. p. 213-225.
4. Doi, Y., J.-I. Wachino, and Y. Arakawa, *Aminoglycoside Resistance: The Emergence of Acquired 16S Ribosomal RNA Methyltransferases.* Infectious disease clinics of North America, 2016. **30**(2): p. 523-537.
5. Ventola, C., *The Antibiotic Resistance Crisis: Part 1: Causes and Threats.* Pharmacy and Theraputics, 2015. **40**(4): p. 277 - 283.
6. Hutchings, M.I., A.W. Truman, and B. Wilkinson, *Antibiotics: past, present and future.* Current Opinion in Microbiology, 2019. **51**: p. 72-80.
7. Pettit, J.H. and R.J. Rees, *Sulphone resistances in leprosy. An experimental and clinical study* Lancet, 1964. **2**(7361): p. 673-4.
8. Kwon, J.H., *141 - Macrolides, Ketolides, Lincosamides and Streptogramins*, in *Infectious Diseases (Fourth Edition)*, J. Cohen, W.G. Powderly, and S.M. Opal, Editors. 2017, Elsevier. p. 1217-1229.e1.
9. David, H.L., *Resistance to D-cycloserine in the tubercle bacilli: mutation rate and transport of alanine in parental cells and drug-resistant mutants.* Applied microbiology, 1971. **21**(5): p. 888-892.
10. Lesher, G.Y., et al., *1,8-Naphthridine derivatives. A new class of chemotherapeutic agents.* Journal of Medicinal Chemistry, 1962. **91**: p. 1063-5.
11. Hooper, D.C. and G.A. Jacoby, *Mechanisms of drug resistance: quinolone resistance.* Annals of the New York Academy of Sciences, 2015. **1354**(1): p. 12-31.
12. Howard, S.J., et al., *Frequency and evolution of Azole resistance in Aspergillus fumigatus associated with treatment failure.* Emerging infectious diseases, 2009. **15**(7): p. 1068-1076.
13. Hassett, D.J., et al., *Response of Pseudomonas aeruginosa to pyocyanin: mechanisms of resistance, antioxidant defenses, and demonstration of a manganese-cofactored superoxide dismutase.* Infection and Immunity, 1992. **60**(2): p. 328-36.
14. Codjoe, F.S. and E.S. Donkor, *Carbapenem Resistance: A Review.* Medical sciences (Basel, Switzerland), 2017. **6**(1): p. 1.
15. Orrett, F.A., *The emergence of mupirocin resistance among clinical isolates of methicillin-resistant Staphylococcus aureus in Trinidad: a first report.* Japanese Journal of Infectious Diseases, 2008. **61**(2): p. 107-10.
16. Friedman, L., J.D. Alder, and J.A. Silverman, *Genetic changes that correlate with reduced susceptibility to daptomycin in Staphylococcus aureus.* Antimicrobial agents and chemotherapy, 2006. **50**(6): p. 2137-2145.
17. Fischer, J. and C. Ganellin, *Analogue-based drug discovery*. 2006, Wiley-VCH: Weinheim

p. 495.

18. Ventola, C.L., *The antibiotic resistance crisis: part 1: causes and threats.* P & T : a peer-reviewed journal for formulary management, 2015. **40**(4): p. 277-283.

19. Lesher, G.Y., et al., *1,8-Naphthridine derivatives. A new class of chemotherapeutic agents.* J Med Pharm Chem, 1962. **91**: p. 1063-5.
20. Magiorakos, A.P., et al., *Multidrug-resistant, extensively drug-resistant and pandrug-resistant bacteria: an international expert proposal for interim standard definitions for acquired resistance.* Clinical microbiology and infection, 2012. **18**(3): p. 268 - 81.
21. Kaur, D.C. and S.S. Chate, *Study of Antibiotic Resistance Pattern in Methicillin Resistant Staphylococcus Aureus with Special Reference to Newer Antibiotic.* Journal of Global Infectious Diseases, 2015. **7**(2): p. 78-84.
22. Vila, J., et al., *Escherichia coli: an old friend with new tidings.* FEMS Microbiology Reviews, 2016. **40**: p. 437 – 463.
23. Levy, S.B. and B. Marshall, *Antibacterial resistance worldwide: causes, challenges and responses.* Nature Medicine Supplement, 2004. **10**(12): p. 122-129.
24. *Antibiotic prescribing*. Evidence for better health care 2021 [cited 2022 31/01]; Available from: https://www.nuffieldtrust.org.uk/resource/antibiotic-prescribing.
25. *English surveillance programme for antimicrobial utilisation and resistance (ESPAUR)*. 2021, UK Health Security Agency: GOV.UK.
26. NICE, *Antimicrobial stewardship: systems and processes for effective antimicrobial medicine use*. 2015, NICE. p. 1 - 25.
27. DHSC, *Tackling antimicrobial resistance 2019–2024 The UK's five-year national action plan*, D.o.H.a.S. Care, Editor. 2019: GOV.UK.
28. Ashiru-Oredope, D. *What is antimicrobial resistance and why do we need to take action against it?* 2021 [cited 2022 18/01]; Available from: https://ukhsa.blog.gov.uk/2021/11/17/what-is-antimicrobial-resistance-and-why-do-we-need-to-take-action-against-it/.
29. Bush, K. and G.A. Jacoby, *Updated Functional Classification of beta-Lactamases.* Antimicrobial Agents and Chemotherapy 2010. **54**(3): p. 969 - 976.
30. Queenan, A.M. and K. Bush, *Carbapenemases: the Versatile β-Lactamases.* Clinical Microbiology Reviews, 2007. **20**(3): p. 440 - 458.
31. WHO. *Antibiotic Resistance*. 2020 [cited 2021 26/06

]; Available from: https://www.who.int/news-room/fact-sheets/detail/antibiotic-resistance.
32. Davies, J. and D. Davies, *Origins and Evolution of Antibiotic Resistance.* Microbiology and Molecular Biology Reviews, 2010. **74**(3): p. 417-433.
33. Munita, J.M. and C.A. Arias, *Mechanisms of Antibiotic Resistance.* Microbiology Spectrum, 2016. **4**(2): p. 1 - 37.
34. Reygaert, W.C., *An overview of the antimicrobial resistance mechanisms of bacteria.* AIMS microbiology, 2018. **4**(3): p. 482-501.
35. Martinez, J.L., *General principles of antibiotic resistance in bacteria.* Drug Discovery Today: Technologies, 2014. **11**: p. 33-9.
36. Cox, G. and G.D. Wright, *Intrinsic antibiotic resistance: mechanisms, origins, challenges and solutions.* International Journal of Medical Microbiology, 2013. **303**(6-7): p. 287-92.
37. Fajardo, A., et al., *The neglected intrinsic resistome of bacterial pathogens.* PLoS One, 2008. **3**(2): p. e1619.
38. Jeltsch, A., *Maintenance of species identity and controlling speciation of bacteria: a new function for restriction/ modification systems?* Gene, 2003. **317**: p. 13–16.
39. Boyd, E., et al., *Mosaic structure of plasmids from natural populations of Escherichia coli.* Genetics, 1996. **143**: p. 1091–1100.

40. Haase, J., M. Kalkum, and E. Lanka, *TrbK, a small cytoplasmic membrane lipoprotein, functions in entry exclusion of the IncP alpha plasmid RP4.* Journal of Bacteriology, 1996. **178**: p. 6720–6729.
41. Progue, J.M., D.A. Cohen, and D. Marchaim, *Editorial commentary: Polymyxin-resistant Acinetobacter baumannii: urgent action needed.* Clinical Infectious Diseases, 2015. **60**(9): p. 1304 - 1307.
42. Irrgang, A., et al., *Prevalence of mcr-1 in E. coli from Livestock and Food in Germany, 2010-2015.* PloS One, 2016. **11**(7): p. e0159863.
43. Coculescu, B.I., *Antimicrobial resistance induced by genetic changes.* Journal of Medicine and Life, 2009. **2**(2): p. 114-23.
44. Denamur, E. and I. Matic, *Evolution of mutation rates in bacteria.* Molecular Microbiology, 2006. **60**(4): p. 820 - 827.
45. Imhof, M. and C. Schlotter, *Fitness effects of advantageous mutations in evolving Escherichia coli populations* Proceedings of the National Academy of Sciences of the United States of America, 2001. **98**: p. 1113 - 1117.
46. Boe, L., et al., *The frequency of mutators in populations of Escherichia coli* Mutat Res, 2000. **448**: p. 47 - 55.
47. Wang, J. and P. Levin, *Metabolism, cell growth and the bacterial cell cycle.* Nature Reviews Microbiology, 2010. **7**(11): p. 822 - 827.
48. Fossum, S., E. Crooke, and K. Skarstad, *Organisation of sister origins and replisomes during multifork DNA replication in Escherichia coli.* The EMBO Journal, 2007. **26**(21): p. 4514 - 4522.
49. Exner, M., et al., *Antibiotic resistance: What is so special about multidrug-resistant Gram-negative bacteria?* GMS hygiene and infection control, 2017. **12**: p. Doc05-Doc05.
50. Cowan, S.W., et al., *Crystal structures explain functional properties of two E. coli porins.* Nature, 1992. **358**(6389): p. 727 - 733.
51. Kamio, Y. and H. Nikaido, *Outer Membrane of Salmonella typhimurium: Accessibility of Phospholipid Head Groups to Phospholipase C and Cyanogen Bromide Activated Dextran in the External Medium*.* Biochemistry, 1976. **15**(12): p. 2561 - 2570.
52. Silhavery, T.J., D. Kahne, and S. Walker, *The Bacterial Cell Envelope.* Additional Perspectives on Cell Biology of Bacteria, 2010. **2**(5): p. a000414.
53. Mullineaux, C.W., et al., *Diffusion of green fluorescent protein in three cell environments in Escherichia coli.* Journal of Bacteriology, 2006. **188**(10): p. 2442 - 2448.
54. Silhavery, T.J., D. Kahne, and S. Waler, *The Bacterial Cell Envelope.* Cold Spring Harb Perspect, 2010. **2**: p. a000414.
55. Breijyeh, Z., B. Jubeh, and R. Karaman, *Resistance of Gram-Negative Bacteria to Current Antibacterial Agents and Approaches to Resolve It.* Molecules, 2020. **25**(6).
56. Abbas, S., et al., *Frequency of Extensively Drug-Resistant Gram-Negative Pathogens in a Tertiary Care Hospital in Pakistan.* Cureus, 2020. **12**(12): p. e11914.
57. Dramsi, S., et al., *Covalent attachment of proteins to peptidoglycan.* FEMS Microbiology Reviews, 2008. **32**(2): p. 307 - 320.
58. Vollmer, W., D. Blanot, and M.A. de Pedro, *Peptidoglycan structure and architecture.* FEMS Microbiology Reviews, 2008. **32**(2): p. 147- 167.
59. Vollmer, W., *Structural variation in the glycan strands of bacterial peptidoglycan.* FEMS Microbiology Reviews, 2008. **32**(2): p. 287 - 306.
60. Ton-That, H., et al., *Anchor structure of staphylococcal surface proteins. III. Role of the FemA, FemB, and FemX factors in anchoring surface proteins to the bacterial cell wall.* The Journal of biological chemical, 1998. **273**(44): p. 29143 - 29149.

61. Rohrer, S. and B. Berger-Bachi, *FemABX peptidyl transferases: a link between branched-chain cell wall peptide formation and beta-lactam resistance in gram-positive cocci.* Antimicrobial agents and chemotherapy, 2003. **47**(3): p. 837 - 46.
62. Pratt, R.F., *Substrate specificity of bacterial DD-peptidases (penicillin-binding proteins).* Cellular and Molecular Life Sciences, 2008. **65**(14): p. 2138 - 2155.
63. NICE, *Urinary tract infection (catheterassociated): antimicrobial prescribing*, N.I.f.H.a.C. Excellence, Editor. 2018, NICE. p. 1 - 23.
64. Smith, D.R.M., et al., *Epidemiology and health-economic burden of urinary-catheter-associated infection in English NHS hospitals: a probabilistic modelling study.* Journal of Hospital Infection, 2019. **103**(1): p. 44-54.
65. Hooton, T., *Uncomplicated urinary tract infection.* The New England Journal of Medicine, 2012. **366**(11): p. 1028–1037.
66. Lichtenberger, P. and T. Hooton, *Complicated urinary tract infections.* Current Infectious Disease Reports, 2008. **10**(6): p. 499–504.
67. Flores-Mireles, A.L., et al., *Urinary tract infections: epidemiology, mechanisms of infection and treatment options.* Natural Reviews Microbiology, 2015. **13**(5): p. 269-284.
68. Khandelwal, P., S. Abraham, and G. Apodaca, *Cell biology and physiology of the uroepithelium.* The American Journal of Renal Physiology, 2009. **297**: p. F1477–F1501.
69. Alqarni, A., et al., *Clinical characteristics and prognosis of bacteraemia during postoperative intraabdominal infections* Critical Care, 2018. **22**(175): p. e1 - e10.
70. Peach, B.C., et al., *Risk Factors for Urosepsis in Older Adults.* Gerontology and Geriatric Medicine, 2016. **2**(1): p. 1 - 7.
71. Lo, E., et al., *Strategies to prevent catheter-associated urinary tract infections in acute care hospitals: 2014 update.* Infection Control & Hospital Epidemiology, 2014. **35**: p. 464-479.
72. Foxman, B., *Urinary tract infection syndromes: occurrence, recurrence, bacteriology, risk factors, and disease burden.* Infectious Disease Clinics of North America, 2014. **28**(1): p. 1-13.
73. Nielubowicz, G.R. and H.L. Mobley, *Host-pathogen interactions in urinary tract infection.* Nat Rev Urol, 2010. **7**(8): p. 430-41.
74. Kline, K.A., et al., *Immune activation and suppression by group B streptococcus in a murine model of urinary tract infection.* Infection and Immunity, 2011. **79**(9): p. 3588-95.
75. Levison, M.E. and D. Kaye, *Treatment of complicated urinary tract infections with an emphasis on drug-resistant gram-negative uropathogens.* Current Infectious Disease Reports, 2013. **15**(2): p. 109-15.
76. Fisher, J.F., et al., *Candida urinary tract infection: pathogenesis.* Clinical Infectious Diseases, 2011. **52 Suppl 6**: p. S437-51.
77. Chen, Y.H., W.C. Ko, and P.R. Hsueh, *Emerging resistance problems and future perspectives in pharmacotherapy for complicated urinary tract infections.* Expert Opinion on Pharmacotherapy, 2013. **14**(5): p. 587-96.
78. Ramírez-Castillo, F.Y., et al., *An evaluation of multidrug-resistant Escherichia coli isolates in urinary tract infections from Aguascalientes, Mexico: cross-sectional study.* Ann Clin Microbiol Antimicrob, 2018. **17**(1): p. 34.
79. Yasin, F., et al., *Combination Therapy for Multidrug-Resistant Klebsiella Pneumoniae Urinary Tract Infection.* Cureus, 2017. **9**(7): p. e1503-e1503.
80. Hashemzadeh, M., et al., *Study of biofilm formation, structure and antibiotic resistance in Staphylococcus saprophyticus strains causing urinary tract infection in women in Ahvaz, Iran.* New Microbes New Infect, 2021. **39**: p. 100831.

81. Swaminathan, S. and G.J. Alangaden, *Treatment of resistant enterococcal urinary tract infections.* Curr Infect Dis Rep, 2010. **12**(6): p. 455-64.
82. Cohen-Nahum, K., et al., *Urinary tract infections caused by multi-drug resistant Proteus mirabilis: Risk factors and clinical outcomes.* Infection, 2010. **38**(1): p. 41-6.
83. Takeyama, K., et al., *Multidrug-resistant Pseudomonas aeruginosa isolated from the urine of patients with urinary tract infection.* J Infect Chemother, 2002. **8**(1): p. 59-63.
84. Chambers, H.F. and F.R. Deleo, *Waves of resistance: Staphylococcus aureus in the antibiotic era.* Nature reviews. Microbiology, 2009. **7**(9): p. 629-641.
85. Anderson, G., et al., *Intracellular bacterial biofilm-like pods in urinary tract infections.* Science (New York N.Y.), 2003. **301**(5629): p. 105 - 107.
86. Hannan, T., et al., *Early severe inflammatory responses to uropathogenic E. coli predispose to chronic and recurrent urinary tract infection.* PloS pathogens, 2010. **6**(8): p. e1001042.
87. Hannan, T., et al., *Host-pathogen checkpoints and population bottlenecks in persistent and intracellular uropathogenic Escherichia coli bladder infection.* FEMS microbiology reviews, 2012. **36**(3): p. 616 - 648.
88. Schwartz, D., et al., *Population dynamics and niche distribution of uropathogenic Escherichia coli during acute and chronic urinary tract infection.* Infection and immunity, 2011. **79**(10): p. 4250-4259.
89. Gerlach, G., S. Clegg, and B. Allen, *Identification and characterization of the genes encoding the type 3 and type 1 fimbrial adhesins of Klebsiella pneumoniae.* Journal of Bacteriology, 1989. **171**(3): p. 1262–1270.
90. Murphy, C., et al., *Role of Klebsiella pneumoniae type 1 and type 3 fimbriae in colonizing silicone tubes implanted into the bladders of mice as a model of catheter-associated urinary tract infections.* Infection and Immunity, 2013. **81**(8): p. 3009 - 3017.
91. Struve, C., M. Bojer, and K. Krogfelt, *Characterization of Klebsiella pneumoniae type 1 fimbriae by detection of phase variation during colonization and infection and impact on virulence.* Infection and immunity, 2008. **76**(9): p. 4055-4065.
92. BAUS. *Urinary Infection (Adults)*. 2019 [cited 2019 02/08/19].
93. Schmiemann, G., et al., *The Diagnosis of Urinary Tract Infection.* Deutsches Ärzteblatt International, 2010. **107**(21): p. 361 - 367.
94. Bent, S. and S. Saint, *The optimal use of diagnostic testing in women with acute uncomplicated cystitis.* The American Journal of Medicine, 2002. **113**: p. 20S - 28S.
95. Smith, H., et al., *Antecedent antimicrobial use increases the risk of uncomplicated cystitis in young women.* Clinical Infectious Diseases, 1997. **25**(1).
96. Wagenlehner, F.M.E., et al., *Epidemiology, treatment and prevention of healthcare-associated urinary tract infections.* World Journal of Urology, 2012. **30**(1): p. 59 - 67.
97. Karve, S., et al., *The impact of initial antibiotic treatment failure: Real-world insights in patients with complicated urinary tract infection.* Journal of Infection, 2018. **76**(2).
98. Raman, G., et al., *Appropriate initial antibiotic therapy in hospitalized patients with gram-negative infections: systematic review and meta-analysis.* BMC Infectious Diseases, 2015. **15**: p. 395.
99. D'Costa, V., et al., *Sampling the antibiotic resistome.* Science, 2006. **311**(5759): p. 374 - 377.
100. Davenport, M., et al., *New and developing diagnostic technologies for urinary tract infections.* Nature Reviews Urology, 2017. **14**(5): p. 296-310.

101. Fünfstück, R., *C. M. Kunin (ed.)Urinary Tract Infections: Detection, Prevention, and Management.* Infection, 1998. **26**(3): p. 183-183.
102. NICE. *UTI (lower): antimicrobial prescribing*. 2018 [cited 2020 20/11

]; Available from: https://bnf.nice.org.uk/treatment-summary/urinary-tract-infections.html.
103. Pfaller, M.A. and R.N. Jones, *Performance Accuracy of Antibacterial and Antifungal Susceptibility Test Methods: Report From the College of American Pathologists Microbiology Surveys Program (2001–2003).* Archives of Pathology & Laboratory Medicine, 2006. **130**(6): p. 767 - 778.
104. Arena, F., et al., *Antibiotic Susceptibility Testing: Present and Future.* The Pediatric Infectious Disease Journal, 2015. **34**(10): p. 1128-30.
105. Khan, Z.A., M.F. Siddiqui, and S. Park, *Current and Emerging Methods of Antibiotic Susceptibility Testing.* Diagnostics (Basel, Switzerland), 2019. **9**(2): p. 49.
106. Perreten, V., et al., *Microarray-based detection of 90 antibiotic resistance genes of gram-positive bacteria.* Journal of Clinical Microbiology, 2005. **43**(5): p. 2291 - 2302.
107. Strommenger, B., et al., *Multiplex PCR assay for simultaneous detection of nine clinically relevant antibiotic resistance genes in Staphylococcus aureus.* Journal of Clinical Microbiology, 2003. **41**(9): p. 4089 - 4094.
108. Garibyan, L. and N. Avashia, *Polymerase chain reaction.* The Journal of investigative dermatology, 2013. **133**(3): p. 1-4.
109. VanGuilder, H.D., K.E. Vrana, and W.M. Freeman, *Twenty-five years of quantitative PCR for gene expression analysis.* Biotechniques, 2008. **44**(5): p. 619-26.
110. Eigner, U., et al., *Analysis of the comparative workflow and performance characteristics of the VITEK 2 and Phoenix systems.* Journal of clinical microbiology, 2005. **43**(8): p. 3829-3834.
111. Thomson, K.S., et al., *Comparison of Phoenix and VITEK 2 extended-spectrum-beta-lactamase detection tests for analysis of Escherichia coli and Klebsiella isolates with well-characterized beta-lactamases.* Journal of clinical microbiology, 2007. **45**(8): p. 2380-2384.
112. Besant, J.D., E.H. Sargent, and S.O. Kelley, *Rapid electrochemical phenotypic profiling of antibiotic-resistant bacteria.* Lab on a Chip, 2015. **15**(13): p. 2799 - 2807.
113. Roberts, M.C., S. Schwartz, and H.J.M. Aarts, *Erratum: Acquired antibiotic resistance genes: an overview.* Frontiers in Microbiology, 2012. **3**(1): p. 1 - 17.
114. Moher, D., et al., *Preferred reporting items for systematic reviews and meta-analyses: the PRISMA statement.* BMJ, 2009. **339**: p. b2535.
115. Baltekin, Ö., et al., *Antibiotic susceptibility testing in less than 30 min using direct single-cell imaging.* Proceedings of the National Academy of Sciences, 2017. **114**: p. 201708558.
116. Mohan, R., et al. *Microfluidic platform for rapid antibiotic susceptibility testing of polymicrobial communities*. in *17th International Conference on Miniaturized Systems for Chemistry and Life Sciences, MicroTAS 2013*. 2013.
117. Convery, N. and N. Gadegaard, *30 years of microfluidics.* Micro and Nano Engineering, 2019. **2**: p. 76-91.
118. Nabovati, G., et al., *Towards High Throughput Cell Growth Screening: A New CMOS 8 × 8 Biosensor Array for Life Science Applications.* IEEE Transactions on Biomedical Circuits and Systems, 2017. **11**(2): p. 380-391.
119. Hebert, P.D.N., et al., *Biological identifications through DNA barcodes.* Proceedings of the Royal Society of London. Series B: Biological Sciences, 2003. **270**(1512): p. 313-321.

120. Ozhikandathil, J., S. Badilescu, and M. Packirisamy, *Gold nanoisland structures integrated in a lab-on-a-chip for plasmonic detection of bovine growth hormone.* Journal of Biomedical Optics, 2012. **17**(7): p. 077001.
121. Chin, C.D., V. Linder, and S.K. Sia, *Lab-on-a-chip devices for global health: past studies and future opportunities.* Lab on a Chip, 2007. **7**(1): p. 41-57.
122. Amjad, M., *An Overview of the Molecular Methods in the Diagnosis of Gastrointestinal Infectious Diseases.* International Journal of Microbiology, 2020. **2020**: p. 8135724.
123. Franco-Duarte, R., et al., *Advances in Chemical and Biological Methods to Identify Microorganisms-From Past to Present.* Microorganisms, 2019. **7**(5): p. 130.
124. Grover, A. and P.C. Sharma, *Development and use of molecular markers: past and present.* Critical Reviews in Biotechnology, 2016. **36**(2): p. 290-302.
125. Cabada, M.M., et al., *Recombinase Polymerase Amplification Compared to Real-Time Polymerase Chain Reaction Test for the Detection of Fasciola hepatica in Human Stool.* The American journal of tropical medicine and hygiene, 2017. **96**(2): p. 341-346.
126. Fuchs, B.M., et al., *Flow cytometric analysis of the in situ accessibility of Escherichia coli 16S rRNA for fluorescently labeled oligonucleotide probes.* Applied and Environmental Microbiology Journal, 1998. **64**(12): p. 4973-82.
127. Wassenegger, M., *Advantages and disadvantages of using PCR techniques to characterize transgenic plants.* Molecular Biotechnology, 2001. **17**(1): p. 73-82.
128. Allen, R.J. and B. Waclaw, *Bacterial growth: a statistical physicist's guide.* Rep Prog Phys, 2019. **82**(1): p. 016601.
129. Huang, T., et al., *Rapid identification of urinary tract infections based on ultrasensitive bacteria detection using volumetric bar-chart chip.* Sensors and Actuators B: Chemical, 2019. **298**: p. 126885.
130. Wen, X.-X., et al., *Rapid Identification of Multiple Bacteria on a Microfluidic Chip.* Chinese Journal of Analytical Chemistry, 2014. **42**(6): p. 791-798.
131. Couto, A. and D. Tao, *Design of a microfluidic paper-based device for analysis of biomarkers from urine samples on diapers.* Conference proceedings IEEE engineering in medicine and biology society, 2017. **2017**: p. 181-184.
132. Chaohao, C. and D. Tao, *Microfluidic paper-based analytical devices for colorimetric detection of urinary tract infection biomarkers on adult diapers.* Conference proceedings IEEE engineering in medicine and biology society, 2015. **2015**: p. 5892-5.
133. Kadlec, M.W., et al., *A Cell Phone-Based Microphotometric System for Rapid Antimicrobial Susceptibility Testing.* Journal of Laboratory Automation, 2014. **19**(3): p. 258-66.
134. Devillé, W.L., et al., *The urine dipstick test useful to rule out infections. A meta-analysis of the accuracy.* BMC Urology, 2004. **4**: p. 4.
135. Cho, B., et al., *Nanophotonic Cell Lysis and Polymerase Chain Reaction with Gravity-Driven Cell Enrichment for Rapid Detection of Pathogens.* ACS Nano, 2019. **13**(12): p. 13866-13874.
136. Chen, J., et al., *Sensitive and rapid detection of pathogenic bacteria from urine samples using multiplex recombinase polymerase amplification.* Lab on a Chip, 2018. **18**(16): p. 2441-2452.
137. Dao, T.N.T., et al., *Rapid and sensitive detection of Salmonella based on microfluidic enrichment with a label-free nanobiosensing platform.* Sensors and Actuators B: Chemical, 2018. **262**: p. 588-594.

138. Bercovici, M., et al., *Rapid detection of urinary tract infections using isotachophoresis and molecular beacons.* Analytical chemistry, 2011. **83**(11): p. 4110-4117.
139. Rolando, J.C., et al., *Real-Time, Digital LAMP with Commercial Microfluidic Chips Reveals the Interplay of Efficiency, Speed, and Background Amplification as a Function of Reaction Temperature and Time.* Analytical Chemistry, 2019. **91**(1): p. 1034-1042.
140. Schoepp, N.G., et al., *Rapid pathogen-specific phenotypic antibiotic susceptibility testing using digital LAMP quantification in clinical samples.* Science Translational Medicine, 2017. **9**(410).
141. Kalsi, S., et al., *Sample pre-concentration on a digital microfluidic platform for rapid AMR detection in urine.* Lab on a Chip, 2019. **19**(1): p. 168-177.
142. Valiadi, M., et al., *Simple and rapid sample preparation system for the molecular detection of antibiotic resistant pathogens in human urine.* Biomedical Microdevices, 2016. **18**(1): p. 18.
143. Li, N., et al., *A self-contained and fully integrated fluidic cassette system for multiplex nucleic acid detection of bacteriuria.* Lab on a Chip, 2020. **20**(2): p. 384-393.
144. Kim, W., et al., *Rapid and accurate nanoelectrokinetic diagnosis of drug-resistant bacteria.* Biosens Bioelectron, 2022. **213**: p. 114350.
145. Chen, C.H., et al., *Antimicrobial Susceptibility Testing Using High Surface-to-Volume Ratio Microchannels.* Analytical Chemistry, 2010. **82**(3): p. 1012-1019.
146. Sabhachandani, P., et al., *Integrated microfluidic platform for rapid antimicrobial susceptibility testing and bacterial growth analysis using bead-based biosensor via fluorescence imaging.* Microchimica Acta, 2017. **184**(12): p. 4619-4628.
147. Kang, W., et al., *Ultrafast Parallelized Microfluidic Platform for Antimicrobial Susceptibility Testing of Gram Positive and Negative Bacteria.* Analytical Chemistry, 2019. **91**(9): p. 6242-6249.
148. Avesar, J., et al., *Rapid phenotypic antimicrobial susceptibility testing using nanoliter arrays.* Proceedings of the National Academy of Sciences, 2017. **114**(29): p. E5787.
149. Needs, S.H., H.M.I. Osborn, and A.D. Edwards, *Counting bacteria in microfluidic devices: Smartphone compatible 'dip-and-test' viable cell quantitation using resazurin amplified detection in microliter capillary arrays.* J Microbiol Methods, 2021. **187**: p. 106199.
150. Iseri, E., et al., *Digital dipstick: miniaturized bacteria detection and digital quantification for the point-of-care.* Lab on a Chip, 2020. **20**(23): p. 4349-4356.
151. Liu, X., et al., *Formation and Parallel Manipulation of Gradient Droplets on a Self-Partitioning SlipChip for Phenotypic Antimicrobial Susceptibility Testing.* ACS Sensors, 2022. **7**(7): p. 1977-1984.
152. Yang, Y., S. Kim, and J. Chae, *Separating and Detecting Escherichia Coli in a Microfluidic Channel for Urinary Tract Infection Applications.* Journal of Microelectromechanical Systems, 2011. **20**: p. 819-827.
153. Sin, M.L., et al., *A Universal Electrode Approach for Automated Electrochemical Molecular Analyses.* Journal of Microelectromechanical Systems, 2013. **22**(5): p. 1126-1132.
154. Liao, J.C., et al., *Use of electrochemical DNA biosensors for rapid molecular identification of uropathogens in clinical urine specimens.* Journal of Clinical Microbiology, 2006. **44**(2): p. 561-70.

155. Kaprou, G., et al. *Lab-on-PCB platform for the sensitive and rapid detection of urinary tract infections*. in *23rd International Conference on Miniaturized Systems for Chemistry and Life Sciences*. 2019. Basel, Switzerland.
156. Fu, Y., et al., *Rapid urinary bacteria detection using DEP- enhanced microfluidic immunocapture assay* in *19 th International Conference on Miniaturized Systems for Chemistry and Life Sciences*. 2015: Gyeongju, KOREA. p. 894 - 896.
157. Kara, V., et al., *Microfluidic detection of movements of Escherichia coli for rapid antibiotic susceptibility testing.* Lab on a Chip, 2018. **18**(5): p. 743-753.
158. Call, Z.D., et al., *Progress toward a Simplified UTI Diagnostic: Pump-Free Magnetophoresis for E. coli Detection.* Analytical Chemistry, 2022. **94**(21): p. 7545-7550.
159. Alves, I.P. and N.M. Reis, *Microfluidic smartphone quantitation of Escherichia coli in synthetic urine.* Biosensors & bioelectronics, 2019. **145**: p. 111624.
160. Olanrewaju, A.O., et al., *Microfluidic Capillaric Circuit for Rapid and Facile Bacteria Detection.* Analytical Chemistry, 2017. **89**(12): p. 6846-6853.
161. Cho, S., et al., *Smartphone-based, sensitive µPAD detection of urinary tract infection and gonorrhea.* Biosensors and Bioelectronics, 2015. **74**: p. 601-11.
162. Li, Z. and T. Dong. *High-sensitive hybrid photodetector based on CdSe quantum dots and graphene for detecting ATP bioluminescence on lab-on-chip devices*. in *2015 IEEE Biomedical Circuits and Systems Conference (BioCAS)*. 2015.
163. Feng, S., T. Dong, and Z. Yang, *Detection of urinary tract infections on lab-on-chip device by measuring photons emitted from ATP bioluminescence.* Conference proceedings IEEE Engineering in Medicine and Biology Society, 2014. **2014**: p. 3114-7.
164. Schröder, U.-C., et al., *Rapid, culture-independent, optical diagnostics of centrifugally captured bacteria from urine samples.* Biomicrofluidics, 2015. **9**(4): p. 044118.
165. Hsieh, K., et al., *Combating Antimicrobial Resistance via Single-Cell Diagnostic Technologies Powered by Droplet Microfluidics.* Acc Chem Res, 2022. **55**(2): p. 123-133.
166. Shumeiko, V., et al., *BactoSpin: Novel Technology for Rapid Bacteria Detection and Antibiotic Susceptibility Testing.* Sensors (Basel), 2021. **21**(17).
167. Wu, T.-F., et al., *A Rapid and Low-Cost Pathogen Detection Platform by Using a Molecular Agglutination Assay.* ACS Central Science, 2018. **4**(11): p. 1485-1494.
168. Gao, J., et al., *Nanotube assisted microwave electroporation for single cell pathogen identification and antimicrobial susceptibility testing.* Nanomedicine, 2019. **17**: p. 246-253.
169. Dong, T. and X. Zhao, *Rapid identification and susceptibility testing of uropathogenic microbes via immunosorbent ATP-bioluminescence assay on a microfluidic simulator for antibiotic therapy.* Analytical Chemistry, 2015. **87**(4): p. 2410-8.
170. Kaushik, A., et al., *Rapid Pathogen Detection and Antimicrobial Susceptibility Assessment from Urine Samples Via Amplification-Free Detection of Ribosomal RNA of Single-Bacteria.* Conference proceedings IEEE Engineering in Medicine and Biology Society, 2019: p. 566-569.
171. He, P., et al., *Bacterial pathogens detection and antimicrobial resistance testing using paper-based devices for urinary tract infections (UTI)*, in *23rd International Conference on Miniaturized Systems for Chemistry and Life Sciences*. 2019: Basel, SWITZERLAND. p. 837 - 838.
172. Kotanen, C.N., et al., *Implantable enzyme amperometric biosensors.* Biosensors and Bioelectronics, 2012. **35**(1): p. 14-26.

173. Gee, S.J., B.D. Hammock, and J.M. Van Emon, *Section 1 - Introduction*, in *Environmental Immunochemical Analysis Detection of Pesticides and Other Chemicals*, S.J. Gee, B.D. Hammock, and J.M. Van Emon, Editors. 1996, William Andrew Publishing: Westwood, NJ. p. 1-6.
174. Baeyens, W.R., et al., *Chemiluminescence-based detection: principles and analytical applications in flowing streams and in immunoassays.* Journal of Pharmaceutical and Biomedical Analysis, 1998. **17**(6-7): p. 941-53.
175. Krafft, C. and J. Popp, *The many facets of Raman spectroscopy for biomedical analysis.* Analytical and Bioanalytical Chemistry, 2015. **407**(3): p. 699-717.
176. Carey, P., *Biochemical Appliances of Raman and Resonance Raman Spectroscopies*. 1982, London: Academic Pres, INC.
177. Ramos, P. and I. Ruisánchez, *Noise and background removal in Raman spectra of ancient pigments using wavelet transform.* Journal of Raman Spectroscopy, 2005. **36**: p. 848-856.
178. Wilson, M.L. and L. Gaido, *Laboratory Diagnosis of Urinary Tract Infections in Adult Patients.* Clinical Infectious Diseases, 2004. **38**(8): p. 1150-1158.
179. Coulthard, M.G., et al., *Redefining urinary tract infections by bacterial colony counts.* Pediatrics, 2010. **125**(2): p. 335-41.
180. Grabe, M., et al., *Guidelines on Urological Infections*, E.A.o. Urology, Editor. 2015, EAU: Arnhem, The Netherlands. p. 1 - 85.
181. Schröder, U.-C., et al., *Rapid, culture-independent, optical diagnostics of centrifugally captured bacteria from urine samples.* Biomicrofluidics, 2015. **9**(4): p. 044118-044118.
182. Nielubowicz, G.R. and H.L. Mobley, *Host-pathogen interactions in urinary tract infection.* Nature Reviews Urology, 2010. **7**(8): p. 430-41.
183. Foxman, B., *The epidemiology of urinary tract infection.* Nature Reviews Urology, 2010. **7**(12): p. 653-60.
184. Pachori, P., R. Gothalwal, and P. Gandhi, *Emergence of antibiotic resistance Pseudomonas aeruginosa in intensive care unit; a critical review.* Genes & diseases, 2019. **6**(2): p. 109-119.
185. Maki, D.G. and P.A. Tambyah, *Engineering out the risk for infection with urinary catheters.* Emerging Infectious Diseases, 2001. **7**(2): p. 342-7.
186. Donlan, R.M., *Biofilms and device-associated infections.* Emerging Infectious Diseases, 2001. **7**(2): p. 277-81.
187. Arias, C.A., G.A. Contreras, and B.E. Murray, *Management of multidrug-resistant enterococcal infections.* Clinical microbiology and infection : the official publication of the European Society of Clinical Microbiology and Infectious Diseases, 2010. **16**(6): p. 555-562.
188. Pop-Vicas, A., et al., *Multidrug-resistant gram-negative bacteria among patients who require chronic hemodialysis.* Clinical journal of the American Society of Nephrology : CJASN, 2008. **3**(3): p. 752-758.
189. Nagvekar, V., S. Sawant, and S. Amey, *Prevalence of multidrug-resistant Gram-negative bacteria cases at admission in a multispeciality hospital.* Journal of Global Antimicrobial Resistance, 2020. **22**: p. 457-461.
190. Bassetti, M., et al., *Treatment of Infections Due to MDR Gram-Negative Bacteria.* Frontiers in Medicine, 2019. **6**: p. 74.
191. Mutters, N.T., et al., *Treating urinary tract infections due to MDR E. coli with Isothiocyanates – a phytotherapeutic alternative to antibiotics?* Fitoterapia, 2018. **129**: p. 237-240.
192. Saude, E., et al., *Variation of metabolites in normal human urine.* Metabolomics, 2007. **3**: p. 439-451.

193. Bono, M.J. and W.C. Reygaert, *Urinary Tract Infection*, in *In: StatPearls [Internet]*. 2020, StatPearls Publishing: Treasure Island (FL).
194. Moore, R.E.T., et al., *Determination of major and trace element variability in healthy human urine by ICP-QMS and specific gravity normalisation.* RSC Advances, 2018. **8**(66): p. 38022-38035.
195. Rose, C., et al., *The Characterization of Feces and Urine: A Review of the Literature to Inform Advanced Treatment Technology.* Critical reviews in environmental science and technology, 2015. **45**(17): p. 1827-1879.
196. Gupta, K., et al., *International Clinical Practice Guidelines for the Treatment of Acute Uncomplicated Cystitis and Pyelonephritis in Women: A 2010 Update by the Infectious Diseases Society of America and the European Society for Microbiology and Infectious Diseases.* Clinical Infectious Diseases, 2011. **52**(5): p. e103-e120.
197. Zykov, I.N., et al., *Efficacy of mecillinam against clinical multidrug-resistant Escherichia coli in a murine urinary tract infection model.* International Journal of Antimicrobial Agents, 2020. **55**(2): p. 105851.
198. Ferreira, A.M., et al., *Oxacillin resistance and antimicrobial susceptibility profile of Staphylococcus saprophyticus and other staphylococci isolated from patients with urinary tract infection.* Chemotherapy, 2012. **58**(6): p. 482-91.
199. Sorlí, L., et al., *Colistin for the treatment of urinary tract infections caused by extremely drug-resistant Pseudomonas aeruginosa: Dose is critical.* Journal of Infection, 2019. **79**(3): p. 253-261.
200. Anderson, H. and A.v.d. Berg, *Microfluidic devices for cellomics: a review.* Sensors and Actuators, 2003(92): p. 315 - 325.
201. Honrado, C. and T. Dong, *A capacitive touch screen sensor for detection of urinary tract infections in portable biomedical devices.* Sensors (Basel, Switzerland), 2014. **14**(8): p. 13851-13862.
202. Giuliano, C., C.R. Patel, and P.B. Kale-Pradhan, *A Guide to Bacterial Culture Identification And Results Interpretation.* P & T : a peer-reviewed journal for formulary management, 2019. **44**(4): p. 192-200.
203. Reller, L.B., et al., *Antimicrobial Susceptibility Testing: A Review of General Principles and Contemporary Practices.* Clinical Infectious Diseases, 2009. **49**(11): p. 1749-1755.
204. Moloney, E., et al., *A PCR-based diagnostic testing strategy to identify carbapenemase-producing Enterobacteriaceae carriers upon admission to UK hospitals: early economic modelling to assess costs and consequences.* Diagnostic and Prognostic Research, 2019. **3**(1): p. 8.
205. Mishra, P., et al., *Rapid antibiotic susceptibility testing by resazurin using thin film platinum as a bio-electrode.* Journal of Microbiological Methods, 2019. **162**: p. 69-76.
206. Elgrishi, N., et al., *A Practical Beginner's Guide to Cyclic Voltammetry.* Journal Of Chemical Education, 2018. **95**(1): p. 197 - 206.
207. Bard, A.J. and L.R. Faulkner, *Electrochemical Methods: Fundamentals and Applications*, ed. E. Swain. 2001: JOHN WILEY & SONS, INC.
208. Stojek, Z., *Pulse Voltammetry*, in *Electroanalytical Methods*, F. Scholz, Editor. 2010, Springer-Verlag Berlin Heidelberg: Springer, Berlin. p. 107.
209. Li, M., et al., *Recent developments and applications of screen-printed electrodes in environmental assays--a review.* Analytica Chimia Acta, 2012. **734**: p. 31 - 44.
210. Ranganathan, S., T.-C. Kuo, and R.L. McCreery, *Facile Preparation of Active Glassy Carbon Electrodes with Activated Carbon and Organic Solvents.* Analytical chemistry, 1999. **71**(16): p. 3574 - 3580.

211. McCarthy, B., et al., *Electrochemical reduction of Brønsted acids by glassy carbon in acetonitrile-implications for electrocatalytic hydrogen evolution.* Inorganic chemistry, 2014. **53**(16): p. 8350 - 8361.
212. Wang, J., *Analytical Electrochemistry*. Practical considerations. 2006, Hoboken, N.J: John Wiley & Sons, Inc.
213. Bilal, S., *Cyclic Voltammetry*, in *Encyclopedia of Applied Electrochemistry*, G. Kreysa, K.-i. Ota, and R.F. Savinell, Editors. 2014, Springer New York: New York, NY. p. 285-289.
214. Scholz, F., *Voltammetric techniques of analysis: the essentials.* ChemTexts, 2015. **1**(17): p. 1 - 24.
215. Kaczmarska, K., et al., *Differential pulse voltammetric determination of an immunosuppressive drug teriflunomide on an edge plane pyrolytic graphite electrode.* RSC Advances, 2017. **7**(42): p. 26028-26036.
216. Khazalpour, S. and D. Nematollahi, *Electrochemical study of Alamar Blue (resazurin) in aqueous solutions and room-temperature ionic liquid 1 butyl-3-methylimidazolium tetrafluoroborate at a glassy carbon electrode.* Royal Society Of Chemistry, 2013. **4**(1): p. 8431 - 8438.
217. Chen, J.L., T.W.J. Steele, and D.C. Stuckey, *Metabolic reduction of resazurin; location within the cell for cytotoxicity assays.* Biotechnology and bioengineering, 2017. **115**(2): p. 351 - 358.
218. McKenzie, D.A., *Milk Testing - A Forward Look.* International Journal of Dairy Technology, 1962. **15**(4): p. 207 - 212.
219. Khalifa, R.A., et al., *Resazurin Microtiter Assay Plate method for detection of susceptibility of multidrug resistant Mycobacterium tuberculosis to second-line anti-tuberculous drugs.* Egyptian Journal of Chest Diseases and Tuberculosis, 2013. **62**(2): p. 241-247.
220. Palomino, J.-C., et al., *Resazurin Microtiter Assay Plate: Simple and Inexpensive Method for Detection of Drug Resistance in Mycobacterium tuberculosis.* Antimicrobial Agents and Chemotherapy, 2002. **46**(8): p. 2720 - 2722.
221. Foerster, S., et al., *A new rapid resazurin-based microdilution assay for antimicrobial susceptibility testing of Neisseria gonorrhoeae.* The Journal of antimicrobial chemotherapy, 2017. **72**(7): p. 1961-1968.
222. Schmitt, D.M., et al., *Antibacterial activity of resazurin-based compounds against Neisseria gonorrhoeae in vitro and in vivo.* International Journal of Antimicrobial Agents, 2016. **48**(4): p. 367-72.
223. Elshikh, M., et al., *Resazurin-based 96-well plate microdilution method for the determination of minimum inhibitory concentration of biosurfactants.* Biotechnology letters, 2016. **38**(6): p. 1015-1019.
224. Mann, C.M. and J.L. Markham, *A new method for determining the minimum inhibitory concentration of essential oils.* Journal of Applied Microbiology, 1998. **84**(4): p. 538-44.
225. Riss, T.L., et al., *Cell Viability Assays*, in *Assay Guidance Manual*. 2004, Eli Lilly & Company and the National Center for Advancing Translational Sciences: Bethesda (MD).
226. O'Brien, J., et al., *Investigation of the Alamar Blue (resazurin) fluorescent dye for the assessment of mammalian cell cytotoxicity.* European Journal of Biochemistry, 2000. **267**(17): p. 5421 - 5426.
227. Zalata, A.A., et al., *The correlates and alleged biochemical background of the resazurin reduction test in semen.* International Journal of Andrology, 1998. **21**(5): p. 289-94.

228. Uzarski, J.S., et al., *Essential design considerations for the resazurin reduction assay to noninvasively quantify cell expansion within perfused extracellular matrix scaffolds.* Biomaterials, 2017. **129**: p. 163-175.
229. Ren, Y., et al., *Rapid detection of antibiotic resistance in Salmonella with screen printed carbon electrodes.* Journal of Solid State Electrochemistry, 2020. **24**.
230. Hannah, S., et al., *Rapid antibiotic susceptibility testing using low-cost, commercially available screen-printed electrodes.* Biosensors and Bioelectronics, 2019. **145**: p. 111696.
231. Crane, B., et al., *Rapid antibiotic susceptibility testing using resazurin bulk modified screen-printed electrochemical sensing platforms.* Analyst, 2021. **146**: p. 5574-5583.
232. Bueno, J., *Chapter 2 - Antimicrobial Models in Nanotechnology: From the Selection to Application in the Control and Treatment of Infectious Diseases*, in *Nanotechnology in Diagnosis, Treatment and Prophylaxis of Infectious Diseases*, M. Rai and K. Kon, Editors. 2015, Academic Press: Boston. p. 19-38.
233. Böckelmann, U., et al., *Quantitative PCR monitoring of antibiotic resistance genes and bacterial pathogens in three European artificial groundwater recharge systems.* Applied and environmental microbiology, 2009. **75**(1): p. 154-163.
234. Bolotsky, A., et al., *Organic redox-active crystalline layers for reagent-free electrochemical antibiotic susceptibility testing (ORACLE-AST).* Biosensors and Bioelectronics, 2021. **172**: p. 112615.
235. Brosel-Oliu, S., et al., *3D impedimetric sensors as a tool for monitoring bacterial response to antibiotics.* Lab on a Chip, 2019. **19**(8): p. 1436-1447.
236. Safavieh, M., et al., *Rapid Real-Time Antimicrobial Susceptibility Testing with Electrical Sensing on Plastic Microchips with Printed Electrodes.* ACS Applied Materials & Interfaces, 2017. **9**(14): p. 12832-12840.
237. Ren, Y., et al., *Rapid detection of antibiotic resistance in Salmonella with screen printed carbon electrodes.* Journal of Solid State Electrochemistry, 2020. **24**(7): p. 1539-1549.
238. Dominguez Renedo, O., M. Alonso-Lomillo, and M. Arcos Mart´ınez, *Recent developments in the field of screen-printed electrodesand their related applications.* Talanta, 2007. **15**(2): p. 202 - 219.
239. Zoski, C., *Handbook of Electrochemistry*. 1st ed, ed. C. Zoski. 2007, Amsterdam: Elsevier Science. 879.
240. Munteanu, F.-D., et al., *Detection of Antibiotics and Evaluation of Antibacterial Activity with Screen-Printed Electrodes.* Sensors, 2018. **19**(901): p. 1 - 26.
241. Mann, T.S. and S.R. Mikkelsen, *Antibiotic Susceptibility Testing at a Screen-Printed Carbon Electrode Array.* Analytical Chemistry, 2008. **80**(3): p. 843-848.
242. Chalenko, Y., et al., *Electrochemistry of Escherichia coli JM109: Direct electron transfer and antibiotic resistance* Biosensors and Bioelectronics, 2012. **32**(1): p. 219 - 223.
243. Mohamed, H.M., *Screen-printed disposable electrodes: Pharmaceutical applications and recent developments.* TrAC Trends in Analytical Chemistry, 2016. **82**: p. 1-11.
244. Honeychurch, K.C. and J.P. Hart, *Screen-printed electrochemical sensors for monitoring metal pollutants.* TrAC Trends in Analytical Chemistry, 2003. **22**(7): p. 456-469.
245. Sophocleous, M. and J.K. Atkinson, *A review of screen-printed silver/silver chloride (Ag/AgCl) reference electrodes potentially suitable for environmental potentiometric sensors.* Sensors and Actuators A: Physical, 2017. **267**: p. 106-120.
246. *Resazurin | 550-82-3*. 2021 [cited 2021 16/02/2021]; Available from: https://www.chemicalbook.com/ChemicalProductProperty_EN_CB5733831.htm.

247. Compton, R.G. and C.E. Banks, *Understanding Voltammetry*. 2017: WORLD SCIENTIFIC (EUROPE). 456.
248. Iizawa, T., et al., *Synthesis of porous poly (N-isopropylacrylamide) gel beads by sedimentation polymerization and their morphology.* Journal of applied polymer science, 2007. **104**(2): p. 842-850.
249. Yang, L., J.S. Chu, and J.A. Fix, *Colon-specific drug delivery: new approaches and in vitro/in vivo evaluation.* International journal of pharmaceutics, 2002. **235**(1-2): p. 1-15.
250. Maolin, Z., et al., *The swelling behavior of radiation prepared semi-interpenetrating polymer networks composed of polyNIPAAm and hydrophilic polymers.* Radiation Physics and Chemistry, 2000. **58**(4): p. 397-400.
251. Peppas, N.A., et al., *Hydrogels in pharmaceutical formulations.* European Journal of Pharmaceutics and Biopharmaceutics, 2000. **50**(1): p. 27-46.
252. Lowman, A.M., et al., *Oral delivery of insulin using pH-responsive complexation gels.* Journal of Pharmaceutical Sciences, 1999. **88**(9): p. 933-937.
253. Cohen, S., et al., *A novel in situ-forming ophthalmic drug delivery system from alginates undergoing gelation in the eye.* Journal of Controlled Release, 1997. **44**(2): p. 201-208.
254. Nnamani, O., *Characterization and controlled release of gentamicin from novel hydrogels based on Poloxamer 407 and polyacrylic acids.* African Journal of Pharmacy and Pharmacology, 2013. **7**: p. 2540-2552.
255. Boddé, H.E., E.A. Van Aalten, and H.E. Junginger, *Hydrogel patches for transdermal drug delivery; in-vivo water exchange and skin compatibility.* Journal of Pharmacy and Pharmacology, 1989. **41**(3): p. 152-5.
256. Huang, L., et al., *Antibacterial poly (ethylene glycol) diacrylate/chitosan hydrogels enhance mechanical adhesiveness and promote skin regeneration.* Carbohydrate Polymers, 2019. **225**: p. 115110.
257. NICE. *Urinary-tract infections*. 2021 [cited 2021 29/08/21]; Available from: https://bnf.nice.org.uk/treatment-summary/urinary-tract-infections.html.
258. Pandey, N. and M. Cascella, *Beta Lactam Antibiotics*, in *StatPearls*. 2021, StatPearls Publishing

259. Cohen, P.R., *Cephalexin-associated Achilles Tendonitis: Case Report and Review of Drug-induced Tendinopathy.* Cureus, 2018. **10**(12): p. e3783.
260. Pichichero, M.E., *Cephalosporins can be prescribed safely for penicillin-allergic patients.* The Journal of Family Practice, 2006. **55**(2): p. 106-12.
261. Rawls, S.M., *Antibiotics, β-Lactam*, in *Encyclopedia of the Neurological Sciences (Second Edition)*, M.J. Aminoff and R.B. Daroff, Editors. 2014, Academic Press: Oxford. p. 207-209.
262. Scholar, E., *Ceftriaxone*, in *xPharm: The Comprehensive Pharmacology Reference*, S.J. Enna and D.B. Bylund, Editors. 2007, Elsevier: New York. p. 1-7.
263. Karakkattu, J., et al., *Effectiveness and Safety of Colistin in Multi Drug Resistant Urinary Tract Infections.* Journal of Applied Pharmaceutical Science, 2017. **7**: p. 148-152.
264. Sorlí, L., et al., *Colistin for the treatment of urinary tract infections caused by extremely drug-resistant Pseudomonas aeruginosa: Dose is critical.* J Infect, 2019. **79**(3): p. 253-261.
265. Schindler, M. and M.J. Osborn, *Interaction of divalent cations and polymyxin B with lipopolysaccharide.* Biochemistry, 1979. **18**(20): p. 4425-30.
266. Newton, B.A., *The properties and mode of action of the polymyxins.* Bacteriology Reviews, 1956. **20**(1): p. 14-27.

267. Koch-Weser, J.A.N., et al., *Adverse effects of sodium colistimethate: manifestations and specific reaction rates during 317 courses of therapy.* Annals of internal medicine, 1970. **72**(6): p. 857-868.
268. Brown, J.M., D.C. Dorman, and L.P. Roy, *Acute renal failure due to overdosage of colistin.* Medical Journal of Australia, 1970. **2**(20): p. 923-4.
269. Beganovic, M., et al., *A Review of Combination Antimicrobial Therapy for Enterococcus faecalis Bloodstream Infections and Infective Endocarditis.* Clinical Infectious Diseases, 2018. **67**(2): p. 303-309.
270. Fausti, S.A., et al., *High-frequency audiometric monitoring for early detection of aminoglycoside ototoxicity.* The Journal of Infectious Diseases, 1992. **165**(6): p. 1026-32.
271. Kahlmeter, G. and J.I. Dahlager, *Aminoglycoside toxicity - a review of clinical studies published between 1975 and 1982.* Journal of Antimicrobial Chemotherapy, 1984. **13 Suppl A**: p. 9-22.
272. Seo, Y.B., et al., *Randomized controlled trial of piperacillin-tazobactam, cefepime and ertapenem for the treatment of urinary tract infection caused by extended-spectrum beta-lactamase-producing Escherichia coli.* BMC Infectious Diseases, 2017. **17**(1): p. 404.
273. Nowé, P., *Piperacillin/tazobactam in complicated urinary tract infections.* Intensive Care Medicine, 1994. **20**(3): p. S39-S42.
274. Castle, S.S., *Piperacillin*, in *xPharm: The Comprehensive Pharmacology Reference*, S.J. Enna and D.B. Bylund, Editors. 2007, Elsevier: New York. p. 1-5.
275. NICE. *Piperacillin with tazobactam*. 2021 [cited 2021 07/12]; Available from: https://bnf.nice.org.uk/drug/piperacillin-with-tazobactam.html.
276. Gleckman, R., N. Blagg, and D.W. Joubert, *Trimethoprim: Mechanisms of Action, Antimicrobial Activity, Bacterial Resistance, Pharmacokinetics, Adverse Reactions, and Therapeutic Indications.* Pharmacotherapy: The Journal of Human Pharmacology and Drug Therapy, 1981. **1**(1): p. 14-19.
277. Patel, S., C. Preuss, and F. Bernice. *Vancomycin*. 2021 [cited 2021 29/08/21

]; Available from: https://www.ncbi.nlm.nih.gov/books/NBK459263/.
278. Lee, T., et al., *Antimicrobial-resistant CC17 Enterococcus faecium: The past, the present and the future.* Journal of Global Antimicrobial Resistance, 2019. **16**: p. 36-47.
279. Bartoletti, M., et al., *Multidrug-Resistant Bacterial Infections in Solid Organ Transplant Candidates and Recipients.* Infectious Disease Clinics of North America, 2018. **32**(3): p. 551-580.
280. Bruniera, F.R., et al., *The use of vancomycin with its therapeutic and adverse effects: a review.* European Review for Medical and Pharmacological Sciences, 2015. **19**(4): p. 694-700.
281. Zhentan, L., et al., *pH-Triggered hydrogel degradation for the smart release of antibiotic aiming at bacterial infection.* New Journal of Chemistry, 2016. **41**(2).
282. Ricciardi, R., et al., *Structural Organization of Poly(vinyl alcohol) Hydrogels Obtained by Freezing and Thawing Techniques: A SANS Study.* Chemistry of Materials, 2005. **17**(5): p. 1183-1189.
283. Shah, S., et al., *Fluorescence properties of doxorubicin in PBS buffer and PVA films.* Journal of Photochemistry and Photobiology B, 2017. **170**: p. 65-69.
284. Fathollahipour, S., et al., *Erythromycin Releasing PVA/sucrose and PVA/honey Hydrogels as Wound Dressings with Antibacterial Activity and Enhanced Bio-adhesion.* Iranian Journal of Pharmaceutical Research, 2020. **19**(1): p. 448-464.

285. Oliveira, R.N., et al., *Mechanical properties and in vitro characterization of polyvinyl alcohol-nano-silver hydrogel wound dressings.* Interface Focus, 2014. **4**(1): p. 20130049.
286. Ghasemzadeh, H. and F. Ghanaat, *Antimicrobial alginate/PVA silver nanocomposite hydrogel, synthesis and characterization.* Journal of Polymer Research, 2014. **21**(3): p. 355.
287. Imtiaz, N., et al., *Fabrication of an Original Transparent PVA/Gelatin Hydrogel: In Vitro Antimicrobial Activity against Skin Pathogens.* International Journal of Polymer Science, 2019. **2019**: p. 7651810.
288. Otsuka, E. and A. Suzuki, *A simple method to obtain a swollen PVA gel crosslinked by hydrogen bonds.* Journal of Applied Polymer Science, 2009. **114**(1): p. 10-16.
289. Ma, S., et al., *A Novel Method for Preparing Poly(vinyl alcohol) Hydrogels: Preparation, Characterization, and Application.* Industrial & Engineering Chemistry Research, 2017. **56**(28): p. 7971-7976.
290. Mohammadi, S., et al., *Preparation and characterization of zinc and copper co-doped WO3 nanoparticles: Application in photocatalysis and photobiology.* Journal of Photochemistry and Photobiology B: Biology, 2016. **161**: p. 217-221.
291. Manju, S., M. Antony, and K. Sreenivasan, *Synthesis and evaluation of a hydrogel that binds glucose and releases ciprofloxacin.* Journal of Materials Science, 2010. **45**(15): p. 4006-4012.
292. Jiang, S., S. Liu, and W. Feng, *PVA hydrogel properties for biomedical application.* Journal of the Mechanical Behavior of Biomedical Materials, 2011. **4**(7): p. 1228-1233.
293. Nakano, T. and T. Nakaoki, *Coagulation size of freezable water in poly(vinyl alcohol) hydrogels formed by different freeze/thaw cycle periods.* Polymer Journal, 2011. **43**(11): p. 875-880.
294. Adelnia, H., et al., *Freeze/thawed polyvinyl alcohol hydrogels: Present, past and future.* European Polymer Journal, 2022. **164**: p. 110974.
295. Stauffer, S.R. and N.A. Peppast, *Poly(vinyl alcohol) hydrogels prepared by freezing-thawing cyclic processing.* Polymer, 1992. **33**(18): p. 3932-3936.
296. Sundara Rajan, S., et al., *Polyethylene Glycol-Based Hydrogels for Controlled Release of the Antimicrobial Subtilosin for Prophylaxis of Bacterial Vaginosis.* Antimicrobial Agents and Chemotherapy, 2014. **58**(5): p. 2747.
297. Cascone, M.G., et al., *Morphological evaluation of bioartificial hydrogels as potential tissue engineering scaffolds.* Journal of Materials Science: Materials in Medicine, 2004. **15**(12): p. 1309-13.
298. Shukla, S. and A. Shukla, *Tunable antibiotic delivery from gellan hydrogels.* Journal of Materials Chemistry B, 2018. **6**(40): p. 6444-6458.
299. Andrews, J.M., *Determination of minimum inhibitory concentrations.* Journal of Antimicrobial Chemotherapy, 2001. **48**: p. 5 - 16.
300. Maier, R.M. and T.J. Gentry, *Chapter 11 - Physiological Methods*, in *Environmental Microbiology (Third Edition)*, I.L. Pepper, C.P. Gerba, and T.J. Gentry, Editors. 2015, Academic Press: San Diego. p. 213-243.
301. Herzog, T. and W. Uhl, *Chapter 4 - Multidrug-Resistant Bacteria in Pancreatic Surgery*, in *Microbiology for Surgical Infections*, K. Kon and M. Rai, Editors. 2014, Academic Press: Amsterdam. p. 61-76.
302. *6 - Practical Antimicrobial Therapeutics*, in *Veterinary Medicine (Eleventh Edition)*, P.D. Constable, et al., Editors. 2017, W.B. Saunders. p. 153-174.
303. Lamberti, A., S.L. Marasso, and M. Cocuzza, *PDMS membranes with tunable gas permeability for microfluidic applications.* RSC Advances, 2014. **4**(106): p. 61415-61419.

304. Burger, R. and J. Ducrée, *Handling and analysis of cells and bioparticles on centrifugal microfluidic platforms.* Expert Review of Molecular Diagnostics, 2012. **12**(4): p. 407-421.
305. Unden, G., et al., *Oxygen regulated gene expression in facultatively anaerobic bacteria.* Antonie Van Leeuwenhoek, 1994. **66**(1-3): p. 3-22.
306. Hershey, A.D. and J. Bronfenbrenner, *Factors limiting bacterial growth : III. Cell size and "physiological youth" in bacterium coli cultures* The Journal of general physiology, 1938. **21**(6): p. 721-728.
307. Sherman, R.A. and R.P. Eisinger, *The Use (and Misuse) of Urinary Sodium and Chloride Measurements.* JAMA, 1982. **247**(22): p. 3121-3124.
308. Lucko, A.M., et al., *Percentage of ingested sodium excreted in 24-hour urine collections: A systematic review and meta-analysis.* The Journal of Clinical Hypertension (Greenwich), 2018. **20**(9): p. 1220-1229.
309. Balcı, A.K., et al., *General characteristics of patients with electrolyte imbalance admitted to emergency department.* World journal of emergency medicine, 2013. **4**(2): p. 113-116.
310. Zorbas, Y.G., et al., *Fluid and salt supplementation effect on body hydration and electrolyte homeostasis during bed rest and ambulation.* Acta Astronaut, 2002. **50**(12): p. 765-74.
311. Hiraoka, R., et al., *Paper-Based Device for Naked Eye Urinary Albumin/Creatinine Ratio Evaluation.* ACS Sensors, 2020. **5**(4): p. 1110-1118.
312. Guo, B., J. Anzai, and T. Osa, *Adsorption behavior of serum albumin on electrode surfaces and the effects of electrode potential.* Chemical and Pharmaceutical Bulletin (Tokyo), 1996. **44**(4): p. 800-3.
313. Azzouzi, S., et al., *Citrate-selective electrochemical μ-sensor for early stage detection of prostate cancer.* Sensors and Actuators B: Chemical, 2016. **228**: p. 335-346.
314. Gao, X., et al., *Creatinine-induced specific signal responses and enzymeless ratiometric electrochemical detection based on copper nanoparticles electrodeposited on reduced graphene oxide-based hybrids.* Sensors and Actuators B: Chemical, 2019. **285**: p. 201-208.
315. Xu, C., et al., *A simple and facile electrochemical sensor for sensitive detection of histidine based on three-dimensional porous Ni foam.* International Journal of Electrochemical Science, 2018. **13**: p. 9794-9802.
316. Malon, R.S.P., et al., *Cotton fabric-based electrochemical device for lactate measurement in saliva.* Analyst, 2014. **139**(12): p. 3009-3016.
317. Manivel, P., et al., *A novel electrochemical sensor based on a nickel-metal organic framework for efficient electrocatalytic oxidation and rapid detection of lactate.* New Journal of Chemistry, 2018. **42**(14): p. 11839-11846.
318. Saha, M. and S. Das, *Electrochemical detection of l-serine and l-phenylalanine at bamboo charcoal–carbon nanosphere electrode.* Journal of Nanostructure in Chemistry, 2014. **4**(2): p. 102.
319. Saranya, S., et al., *Simultaneous detection of glutathione, threonine, and glycine at electrodeposited RuHCF/rGO–modified electrode.* Ionics, 2019. **25**(11): p. 5537-5550.
320. Szunerits, S., et al., *Preparation of boron-doped diamond nanowires and their application for sensitive electrochemical detection of tryptophan.* Electrochemistry Communications, 2010. **12**(3): p. 438-441.
321. Wang, Q., et al., *Simultaneous electrochemical detection of tryptophan and tyrosine using boron-doped diamond and diamond nanowire electrodes.* Electrochemistry Communications, 2013. **35**: p. 84-87.

322. Shadlaghani, A., et al., *Direct Electrochemical Detection of Glutamate, Acetylcholine, Choline, and Adenosine Using Non-Enzymatic Electrodes.* Sensors, 2019. **19**(3).
323. Grozovski, V., et al., *Adsorption of Formate and Its Role as Intermediate in Formic Acid Oxidation on Platinum Electrodes.* ChemPhysChem, 2011. **12**(9): p. 1641-1644.